INVESTIGATION OF REGULATORY FUNCTIONS OF MICRORNAS IN SKIN AND HAIR FOLLICLE DEVELOPMENT AND CYCLING

A role of microRNA-214 in skin and hair follicle homeostasis

Majid Ali ALAM

Submitted for the degree

of Doctor of Philosophy

Medical Biosciences

School of Life Sciences

University of Bradford

2014

Abstract

Investigation of regulatory functions of microRNAs in skin and hair follicle development and cycling

Majid Ali ALAM

Keywords: skin, hair follicle, microRNA, miR-214, gene expression

miRNAs are important post-transcriptional regulators of gene expression which play vital roles in the arrays of physiological processes, including skin and hair follicle (HF) development. In this study, the role for miR-214 in the skin and HF development and their postnatal physiological regeneration was investigated. miR-214 exhibits discrete expression patterns in the epidermis and HF in developing and postnatal skin, and is highly expressed in the epithelial stem cells and their lineage-committed progenies. The effects of miR-214 on HF morphogenesis and cycle progression were evaluated by using doxycycline-inducible miR-214 transgenic mice (K14-rtTA/TRE-miR-214). Keratinocyte specific miR-214 overexpression during skin embryogenesis resulted in the partial inhibition of HF induction and formation of the HF reduced in size producing thinner hair. Overexpression of miR-214 in telogen skin caused retardation of the anagen progression and HF growth. Inhibitory effects of miR-214 on HF development and cycling were associated with supressed activity of stem cells, reduced proliferation in the hair matrix, and altered differentiation. miR-214 induced complex changes in gene expression programs in keratinocytes, including inhibition of cyclins and cyclin-dependent kinases and several essential components of Wnt, Edar, Shh and Bmp signalling pathways,

whereas β-catenin acts as a novel conserved miR-214 target. Indeed, the inhibitory effects of miR-214 on HF development were rescued by intracutaneous delivery of pharmacological Wnt activator.

Thus, this study demonstrated that by targeting β-catenin and, therefore, interfering with Wnt signalling activity miR-214 may act as one of the upstream effectors of the signalling cascades which govern HF morphogenesis and cycling.

Acknowledgments

Firstly, I would like to extend my deepest gratitude to my supervisor Dr Natasha Botchkareva for her support, help, patience and guidance throughout my PhD studies. I would also like to thank Prof Vladimir Botchkarev for his words of wisdom and advice.

I would like to thank Dr Mohammed Ahmed for his help and support during the beginning of my PhD and would also like to thank Dr Andrei Mardaryev for his advice and sharing of his technical expertise.

I would like to thank Dr Andrey Sharov and Dr Andrei Marydaryev for their help with mice, Dr Mohammed Ahmed for designing transgene construct and Dr Krystof Poterlowicz for all bioinformatics analysis.

Lastly, I would like to thank my beloved parents and family for their unfaltering love and support.

Dedicated to my parents whose sacrifices made me the person I am today

Verily, in the creation of the heavens and the earth, and in the succession of night and day, there are indeed signs for those of understanding.

Qu'ran 3:190

Contents

List of Tables

List of Figures

Abbreviations

Ago	Argonaute
BCIP	5-Bromo-4-chloro-3-indolyl phosphate
BIO	6-bromoindirubin-3'-oxime
BMP	Bone morphogenetic protein
BMPR1A	Bone morphogenetic protein receptor 1a
cDNA	Complimentary DNA
Ct	Threshold cycle
Ctnnb1	β-catenin
DAPI	4,' 6-diamidino-2-phenylindole
DEPC	Diethyl-pyrocarbonate
DGRC8	DiGeorge Syndrome Critical Region Gene 8
DIG	Digoxygenin
Dkk	Dickkopf
DMEM	Dulbeccos modified eagle's medium
Dox	Doxycyclin
DP	Dermal Papilla
DTG	Double transgenic
ECM	Extracellular Matrix
Eda	Ectodysplasin
Edar	Ectodysplasin receptor
EGF	Epidermal growth factor
EMEM	Eagles minimum essential media
Exp5	Exportin 5
FGF	Fibroblast Growth Factor
GFP	Green fluorescent protein
GTP	Guanosine triphosphate
GSK	Glycogen synthase kinase
HF	Hair follicle
HFSC	Hair follicle stem cells

HGF	Hepatocyte Growth Factor
Hrr	Hairless gene
IGF	Insulin growth factor
IRS	Inner Root Sheath
ISH	In-situ hybridisation
KGF	Keratinocyte Growth Factor
LEF	Lymphoid enhancer factor
LNA	Locked Nucleic Acid
LRCs	Label retaining cells
miR	MicroRNA
miRNA	MicroRNA
mRNA	Messenger RNA
NBT	4-Nitro blue tetrazolium chloride
ORS	Outer root sheath
PBS	Phosphate saline buffered solution
PDGF-A	Platelet derived growth factor-A
Pol II	RNA polymerase II
Pri-miRNA	Primary-microRNA
Pre-miRNA	Precursor-microRNA
PMEKs	Primary mouse epidermal keratinocytes
qRT-PCR	Real-Time Quantitative Reverse Transcription PCR
RISC	RNA induced silencing complex
SD	Standard deviation
SHG	Secondary hair germ
Shh	Sonic hedgehog
TGF	Transforming growth factor
TNF	Tumour necrosis factor
TRBP	The human immunodeficiency virus trans-activation response RNA- binding protein
UTR	Untranslated region
VDR	Vitamin D receptor
WT	Wild type

1.0 INTRODUCTION

1.1 Structure and Functions of Skin

The skin has long captivated scientists dating back to the beginning of the 19th century. Studies carried out by Hermann Rein first demonstrated the presence of a barrier between the stratum corneum and viable epidermis based on the physiological behaviour of isolated human skin (Menon et al., 2012; Rein, 1924). In recent years the structure and biochemistry of skin has been greatly elucidated, revealing how the skin is a multifaceted organ (Blanpain and Fuchs, 2009; Fuchs, 2007; Tobin, 2006).

The largest organ of the body (~15% of total body weight in adult humans) (Healy, 2005) the skin provides an indispensable barrier. It carries out a variety of complex roles required for the body to survive and function properly. It acts as the first line of defence against the environment, providing a physical barrier preventing dehydration, entry of microbes, mechanical and chemical stress. In addition, the skin can regenerate after injury, participates in immune responses and through its pigment producing melanocytes, it protects against harmful ultra-violet radiation (Costin and Hearing, 2007; Proksch et al., 2008; Slominski and Wortsman, 2000; Tobin, 2006). The skin is considered to have two distinct layers, the epidermis and dermis with an underlying connective tissue the subdermis. The epidermis is the outermost constituent of the skin, consisting of a stratified, multilayered epithelium between 75 and 100μm thick and up to 600μm thick on the palms and soles (Tobin, 2006).

Underneath the epidermis is the dermis, which is a two to four-mm thick layer of connective tissue and fibroblasts that accommodate the neural, vascular, lymphatic and secretory apparatus of the skin. Separating the two layers is the

basement membrane, a highly specialised layer of extracellular matrix (Fuchs and Raghavan, 2002; Tsuruta et al., 2011).

The two main types of human skin are glabrous, non-hairy skin and hair bearing skin. Glabrous skin which is found on the palms and soles is characterised by a thick epidermis and lack of hair follicles and sebaceous glands.

The skin houses several appendages which include the pilosebaceous unit consisting of the hair follicle and sebaceous gland, mammary glands, nails and teeth **(Figure 1.1)** (Eckert et al., 2013; Fuchs, 2007).

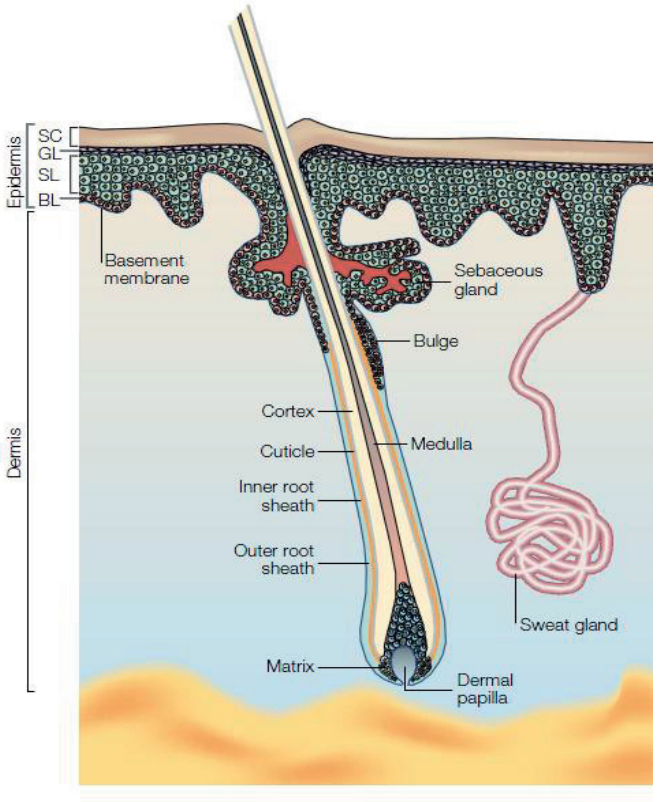

Figure 1.1 The skin and its appendages. The skin consists of the epidermis and dermis, separated by a basement membrane. The epidermis is stratified sqaumous epithelia generally consisting of four layers. Also shown is a cross-section the hair follicle, the sebaceous glands and sweat glands. BL, basal layer; SL, spinous layer; Gl, granular layer; SC, stratum corneum. Adapted from Fuchs and Raghavan 2002

1.2 Epidermis

The epidermis is stratified epithelium that originates from a single layer of ectodermal cells that are specified to the epidermal lineage. In mouse epidermis, a single layer of epidermal cells forms and persists from embryonic day 9.5 (E9.5) to embryonic day 12 (E12) when keratinocytes begin to stratify and form the multiple layers of the epidermis (Eckert et al., 1997). As the skin becomes populated by mesenchymal cells, signals transmitted instruct the stratification of the epidermis and initiate the positioning of down growths that mark the induction of hair follicle morphogenesis (Blanpain and Fuchs, 2006; Blanpain and Fuchs, 2009; Koster and Roop, 2007).

In humans, at approximately three weeks of embryonic life, the epidermis consists of no more than a single layer of undifferentiated cells. At four weeks the epidermis begins to stratify. The ectoderm initially gives rise to the periderm, a superficial layer of cells that is a purely embryonic structure. This forms a transient covering for the epidermis, which is ultimately lost as the epidermis keratinises beneath it. As epidermal differentiation and stratification progress, cells of the periderm are sloughed off into the amniotic fluid and contribute to the vernix caseosa that covers the foetal skin (McGrath et al., 2010).

The epidermis is composed of epithelial cells that differ from each other both structurally and functionally. The epidermis generally consists of 4 layers, which are the basal, spinosum, granular layers and the outermost stratum corneum **(Figure 1.2)**. There is an additional layer, the stratum lucidum in the palms and soles. It contains no blood vessels and varies in thickness from less than 0.1mm on the eyelids to approximately 1mm on the palms and soles. The main cell type that makes up the epidermis is the keratinocyte, which make up

approximately 95% of the epidermal cellular content. One of the main functions of the keratinocyte is to synthesise the keratin protein, which forms the intermediate filament system in epithelial cells, and are connected by protein bridges call desmosomes (Kolarsick P. A. J., 2011; Proksch et al., 2008; Tobin, 2006)

1.2.1 Basal Layer

The innermost layer of the epidermis above the dermis is the basal layer. Rapidly proliferating keratinocytes within the basal layer continually renew the epidermis throughout a lifetime. Basal cells within the interfollicular epidermis represent a unique population of stem cells and transiently amplifying (TA) progenitor cells that can produce daughter cells or initiate a program of terminal differentiation, generating the suprabasal layers of the epidermis (Alonso and Fuchs, 2003; Fuchs and Horsley, 2008). Cell in the basal layer are polarised with their lower surface anchored to the basement membrane by integrins such as α6 and β4 (Margadant et al., 2010) These integrins play an important role in organising hemidesmosomes, which anchor the basal keratinocytes to the basement membrane (Tsuruta et al., 2011). Cells in the basal layer are characterised by expression of keratin 5 (K5) and keratin 14 (K14). As basal cells divide and migrate up to form the suprabasal layers there is a down-regulation of K5 and K14 expression and an increase in expression of keratins 1 (K1) and 10 (K10) (Blanpain and Fuchs, 2006).

In addition, two different cell types are present in the basal layer; Merkel cells and melanocytes. Merkel cells function as mechanoreceptors and transmit tactile sensation. They are neuroendocrine cells concentrated in touch-sensitive

areas of glabrous, hairy skin and some mucosa (Lumpkin and Caterina, 2007; Polakovicova et al., 2011). Initially Merkel cells were thought to originate from neural crest cells; however lineage tracing experiments using epidermal and neural crest specific promoters showed that Merkel cells actually arise from epidermal cells (Morrison et al., 2009; Van Keymeulen et al., 2009).

Melanocytes are pigment producing cells derived from the neural crest. Melanocytes are responsible for producing the pigment melanin and transferring it to keratinocytes. Melanin-containing granules known as melanosomes, which are membrane-bound organelles, is where melanin production predominantly occurs. Melanosomes protect the epidermis by transferring melanin through their dendrites to keratinocytes, where they produce supranuclear melanin caps that reduce damage caused by harmful UV radiation (Costin and Hearing, 2007; Lin and Fisher, 2007; Tobin, 2006).

1.2.2 Spinosum Layer

As basal cells reproduce and mature, they move towards the outer layer of skin, initially forming the stratum spinosum (‘spiny’ layer). The stratum spinosum contains between 8-10 sheets of irregular polyhedral keratinocytes with some limited capacity for cell division. As cells enter the spinous layer they switch off the expression of K5 and K14 and switch expression to K1 and K10, forming a robust intermediate filament network interlinked with desmosomes (Blanpain and Fuchs, 2009; Fuchs and Green, 1980).The upper most cells of the spinous layer consist of additional structural proteins such as involucrin and loricrin (Baroni et al., 2012). Also found in the spiny layer are Langerhans cells, which are immunologically active cells, derived from the bone marrow. They are

crucial for the immune barrier of the skin, acting as antigen-presenting cells and play a vital role in immunological reactions such as allergic contact dermatitis (Baroni et al., 2012; Moll et al., 2008). Langerhans cells are characterised by the presence of cytoplasmic organelles named Birbeck granules (Romani et al., 2012). Birbeck granules contain langerin, a pattern recognition receptor which allows Langerhans cells to detect and respond to pathogens (Valladeau et al., 2000; van der Vlist and Geijtenbeek, 2010)

1.2.3 Granulosum Layer

The granular layer consists of 3-5 sheets of non-dividing keratinocytes. Keratins 1 and 10 which are initially synthesised in the stratum spinosum become the predominant keratins in the granular layer (Fuchs, 1990). It contains flattened, polyhedral non-dividing keratinocytes that produce granules of a protein called keratohyaline. The keratohyaline granules represent a mixture of smaller proteins containing keratohyaline and filaggrin (Matoltsy and Matoltsy, 1970). The lamellated granules are specialised secretory granules, which contain lipids and their extracellular processing enzymes. The granules increase in number and size and as the cell nuclei breakdown, their cell membrane increasingly becomes impermeable. These cells flatten as dividing cells underneath them progressively push them toward the skin surface (Costin and Hearing, 2007; Tobin, 2006).

1.2.4 Stratum Corneum

The stratum corneum is the outermost layer of the epidermis consisting of 15-30 sheets of keratinocytes, which are terminally differentiated (non-viable) but biochemically-active cells called corneocytes. The corneocytes are connected

by corneo-desmosomes and embedded in a lipid-rich matrix containing specialised proteins and lipids (Elias, 2005; Lee et al., 2006; Menon et al., 2012; Tobin, 2006). Keratinocytes of the stratum corneum release lysosomal enzymes that degrade organelles leading to the formation of a tightly cross-linked squamous layer completing the cutaneous layer. The final stages of keratinocyte differentiation are linked to dramatic changes in the structure of keratins, leading to the transformation of these cells into flat and anucleated corneocytes, surrounded by a cell envelope. The terminal differentiation of basal layer cells leads to the formation of anucleated cells which form the epidermal barrier until they are shed and are replaced by the inner cells migrating upward. This occurs continually throughout a lifetime with cells migrating upwards in a synchronised manner. This program of migration and shedding occurs every two weeks in human epidermis, with each transit amplifying basal cell dividing three to six times before differentiating (Alonso and Fuchs, 2003). During the latter stages of differentiation, keratins are organised into condensed arrays. Filaggrin, a matrix protein, aggregates keratin filaments into tight bundles, which promotes the flattening of keratinocytes, which is characteristic of corneocytes in the stratum corneum (Menon et al., 2012; Proksch et al., 2008). Over time, these cells slough off and are replaced by underlying differentiating keratinocytes (Proksch et al., 2008).

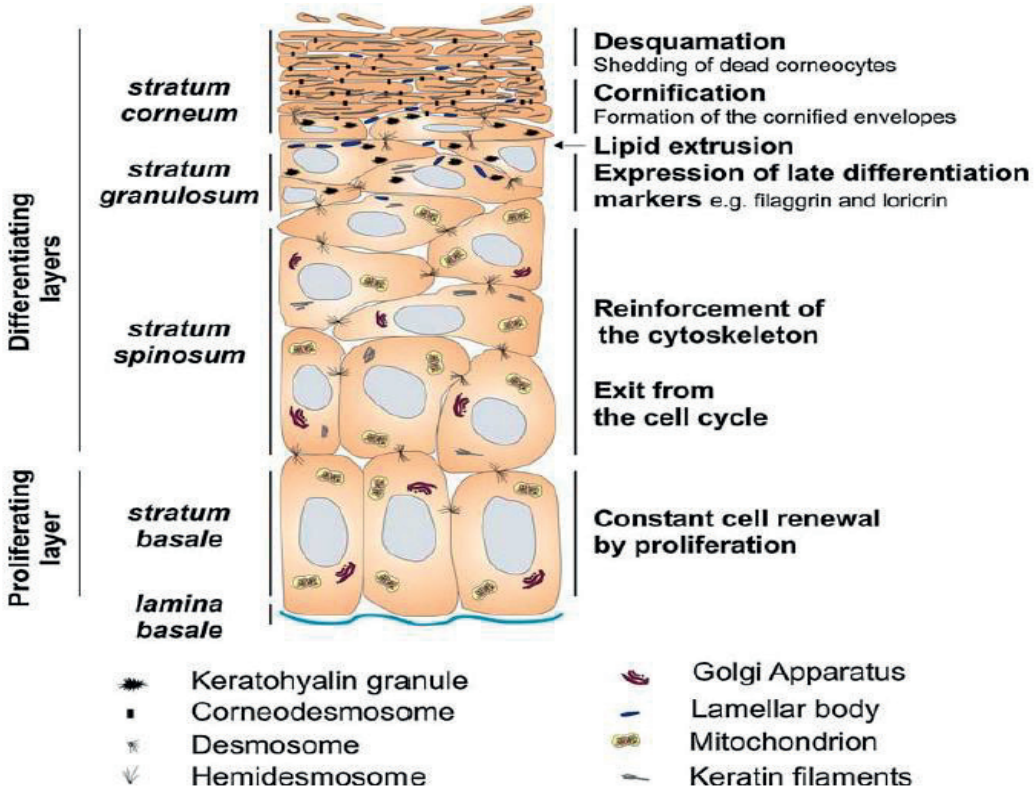

Figure 1.2. Illustration of the epidermis. The epidermis generally consists of four layers based on the characteristics of the keratinocytes of each layer. The basal layer is a monolayer of mitotically active cells that gives rise to the suprabasal layers. The stratum spinosum (spinous layer) lies above the basal layer and consists of several stratified layers. The stratum granulosum (granular) layer consists of three to four flattened layers of anucleated cells. Keratinocytes in this layer express proteins such as filaggrin and loricrin, which aggregate to form keratohyalin granules. In addition, lipids are produced and stored in lamellar bodies. The outermost layer is the stratum corneum, a cornified layer consisting of 15-30 sheets of terminally differentiated keratinocytes called corneocytes. The epidermis is separated from the underlying dermis by the basement membrane (lamina basale). Adapted from Lippens et al 2009.

1.2.5 Dermis

Underneath the epidermis is the dermis, a 2 to 4mm thick layer of connective tissue and fibroblasts that accommodate the neural, vascular, lymphatic and

secretory apparatus of the skin (Costin and Hearing, 2007; Sorrell and Caplan, 2004; Tobin, 2006). The main cell type of the dermis is the fibroblast, a migratory cell that synthesises and organises the extracellular matrix (Chang et al., 2002; Costin and Hearing, 2007). The superficial papillary layer of the dermis is arranged into ridge-like structures, containing microvascular and neural components that maintain the epidermis (Sorrell and Caplan, 2004). The reticular layer of the dermis extends from the papillary layer to the deeper vascular plexus and makes up approximately 80% of the thickness of the dermis (Sorrell and Caplan, 2004). Collagen is the major constituent and provides the skin with great tensile strength and tissue integrity, whereas elastin maintains elasticity and resiliency. The dermis also accommodates multifunctional cells of the immune system such as mast cells, Langerhans cells and macrophages (McGrath and Uitto, 2010; Tobin, 2006).

Mast cells are specialised secretory cells originating from bone marrow. They are present in the papillary dermis and also in subcutaneous fat. The characteristic feature of mast cells is the presence of dense cytoplasmic granules that contain histamine, heparin, serine proteases and cytokines (Kolarsick P. A. J., 2011). They can be identified by their characteristic cell surface markers such as CD1a antigen and MHC class II antigens (Mizumoto and Takashima, 2004). Mast cells function as an immune response, releasing inflammatory mediators such as histamine to protect the body from pathogens (Kolarsick P. A. J., 2011; Prussin and Metcalfe, 2006).

1.2.6 Skin Appendages

The skin contains appendages such as nails, hair follicles and a number of glands which includes sweat, sebaceous and mammary glands. Although fully formed skin appendages differ greatly in their shape, number, functions and regenerative capacity, they are extraordinarily similar in the early stages of their development at both the morphogenetic and molecular levels (Mikkola, 2007; Mikkola and Millar, 2006). The development of skin appendages involves reciprocal and sequential interactions between the ectodermal epithelium and the mesenchyme (Jahoda et al., 1996; Oliver and Jahoda, 1988). The appendages of the skin can originate from either the ectoderm and mesoderm (hair and mammary gland) or the neural crest (tooth, vibrissae and cranial hair). The epithelial-mesenchymal interactions are mediated by a number of signalling pathways which includes: Wnt, bone morphogenetic proteins (BMPs), sonic hedgehog (Shh), ectodysplasin (EDA), fibroblast growth factors (FGFs) and transforming growth factor-β (TGF-β) families and their downstream transcription factors that are required for the development of these skin appendages (Fuchs, 2009; Mikkola, 2007). The molecular signals of growth and transcription factors are widely conserved across many species as well as across distinct appendages (Fuchs, 2009; Mikkola, 2007; Mikkola and Millar, 2006).

1.3 The Hair Follicle

The hair follicle is a dynamic mini-organ found in mammals. Humans possess over two million hair follicles, with approximately two percent located on the scalp. The significance of hair has long been associated with health, culture and

identity dating back to the days of ancient Egypt, to modern day society with hair products and services now a multi-billion pound industry. Although human hair plays an important role in life, its physiological importance is inversely related to the psychological impact it has, however disorders such as alopecia and hirsutism cause great psychological distress to those affected (Blume-Peytavi and Hahn, 2008; Cotsarelis, 2012; Krause and Foitzik, 2006; Vogt et al., 2008). The main function of the hair follicle is to produce the visible hair shaft/fibre. The skin of mammals is covered in hair except the glabrous skin of the lips, palms and soles. The visibility of hair is clear in the majority of mammals, however for humans, hair growth is extremely reduced in most areas with small vellus hairs making them virtually invisible to the human eye (Botchkareva, 2009; Stenn and Paus, 2001). In mammals, the hair follicles encompass several functions, which includes protection (thermoregulation, camouflage, protection against UV) and adaptation to seasonal changes (shedding, social and sexual communication) (Stenn and Paus, 2001; Wu et al., 2008).

1.3.1 Hair Follicle Anatomy

The hair follicle is one of the most complex and highly organised mini-organs of the human body. Composed of several distinct layers, it is one of many appendages residing in the skin and is the only mammalian organ that possesses the extraordinary capability to self-renew throughout a lifetime **(Figure 1.3)**. This capability of self-renewal is based on epithelial-mesenchymal interactions that control the activity of several stem cell populations within this mini-organ. The hair follicle plays a role in many aspects of mammalian biology including organogenesis, cell-cell interactions, tissue growth, regeneration and

aging (Botchkarev and Paus, 2003; Jahoda et al., 2001; Krause and Foitzik, 2006; Stenn and Paus, 2001).

The mature hair follicle is a highly organised, cylindrical structure, separated from the dermis by the dermal sheath. At the centre of the follicle is the hair shaft, which is surrounded by the inner root sheath, the companion layer and the outer root sheath (Langbein et al., 2004; Schneider et al., 2009). The hair follicle can be divided into three regions: the infundibulum, isthmus and inferior segment. The infundibulum and isthmus of the hair follicle are known as the 'permanent' upper region, whereas the lower inferior segment is known as the 'cycling' region, which is continuously remodelled in each hair cycle. The infundibulum region of the hair follicle extends from the surface of the skin to the sebaceous gland duct opening to the hair canal. The region between the sebaceous gland duct opening and the arrector pili muscle site is known as the isthmus. The inferior segment extends from the bulge to the base of the hair follicle bulb **(Figure 1.3)** (Paus and Foitzik, 2004; Schneider et al., 2009). The hair bulb can be divided into two parts, with the lower consisting of actively proliferating keratinocytes and the upper portion containing differentiating keratinocytes. The boundary at which these regions are divided is referred to as the 'critical line of Auber' (Auber, 1956; Aubin-Houzelstein, 2012) .

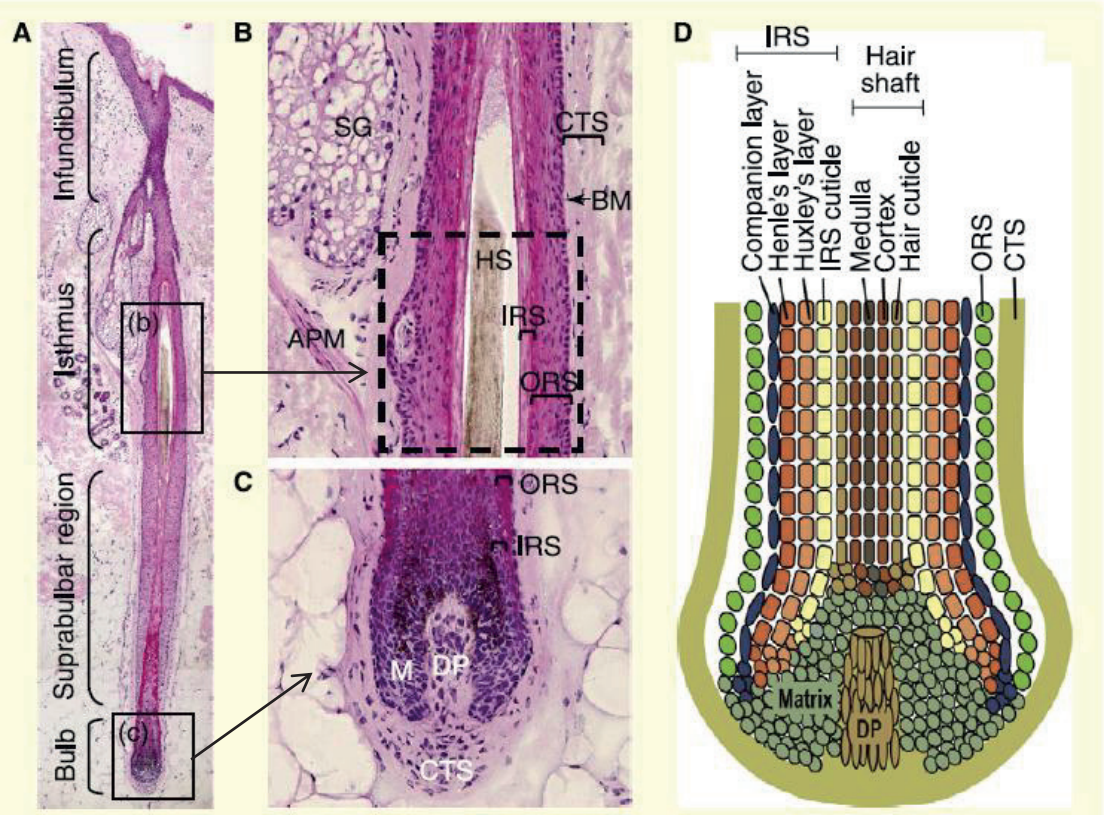

Figure 1.3. Hair Follicle Morphology. **(A)** Image of longitudinal section of human anagen scalp follicle **(B)** Magnified image of the isthmus. Dashed box indicates approximate location of the bulge **(C)** Magnified image of the hair bulb portion **(D)** Schematic drawing illustrating the concentric layers of the ORS, IRS and hair shaft in the bulb. IRS is made up of four layers: Companion layer, Henle's layer, Huxle's layer and the inner root sheath cuticle. Cells of the companion layer are tightly bound to Henle's layer, but to the ORS allowing the companion layer to function as a slippage plane between the stationary ORS and the upwards moving IRS. Further inwards the IRS cuticle is composed of scales that interlock with the scales of the hair shaft cuticle, anchoring the shaft in the follicle**,** allowing both layers to jointly move during hair follicle growth. SG, sebaceous gland; APM, arrector pili muscle; DP, dermal papilla; CTS, connective tissue sheath; BM, basal membrane; M, matrix; IRS, inner root sheath; ORS, outer root sheath; HS, hair shaft. Adapted from Schneider et al 2009.

1.3.2 Hair Shaft

The hair shaft or fibre is the visible product generated by the hair follicle and is formed by keratin proteins. The hair shaft of terminal hair follicles consists of three layers: an outer cuticle, central cortex and a medulla. The cortex is the main structure of the shaft, forming the bulk and strength of the hair shaft and is made up of long keratinised cells, which are formed into long fibres (Harkey, 1993) . The hair shaft cuticle covers the hair and is formed by layers, which interlock with opposing layers of the inner root sheath, allowing the hair shaft and the inner root sheath to move upwards together (Rogers, 2004). During hair shaft growth, cortical cells emerging from the proliferative keratinocytes rapidly undergo a differentiation program and begin to synthesise large amounts of hair-specific keratin proteins. Some of these hair specific proteins include four type I keratins which are K25, K26, K27 and K28 and four type II keratins which are K71, K72, K73 and K74 (Langbein and Schweizer, 2005).

Several transcription factors have been identified to be crucial for hair shaft differentiation. For example the *homeobox C13* (*Hoxc13*) gene is expressed primarily in the upper bulb region in hair follicles of all hair types in mice (Godwin and Capecchi, 1998) and also in human hair follicles (Jave-Suarez et al., 2002). The expression of *Hoxc13* is initiated at the early stages of hair follicle differentiation, during both hair follicle morphogenesis and the anagen phase during the hair cycle and its expression continues in the proximal-most region of catagen follicles during regression (Shang et al., 2002). In anagen follicles, the *Hoxc13* expression domain encompasses distinct subpopulations of cells primarily in the matrix and the three cylindrical layers of the differentiating hair shaft, including cuticle, cortex, and medulla (Jave-Suarez et

al., 2002; Potter et al., 2006). Two independent studies employing loss- and gain-of-function of Hoxc13 demonstrated the crucial role for this gene in hair shaft differentiation (Godwin and Capecchi, 1998; Tkatchenko et al., 2001). In Hoxc13-null mice external hairs failed to grow, thus resulting in a completely nude appearance and defective nail development (Godwin and Capecchi, 1998). In transgenic mice overexpressing Hoxc13, there is a delayed formation of a thin and 'rough' hair coat during postnatal development and progressive alopecia during adulthood (Tkatchenko et al., 2001).

The transcription factor Foxn1 is another important regulator of hair shaft differentiation (Nehls et al., 1994). Mutation of Foxn1 leads to the development of the nude phenotype in severely immunocompromised nude mice (Flanagan, 1996; Nehls et al., 1994). Whereas wild type and heterozygous animals start to develop a dense hair coat around postnatal day 5 (Flanagan, 1966), hairs do not emerge from the dorsal skin of mice homozygous for any of the reported allelic mutations in the Foxn1 gene. The hair shafts in nude mice were found to bend and coil as soon as they enter the hair canal (Flanagan, 1966). Foxn1 was found to control the expression of keratins in the cortex of the hair shaft and is responsible for broken hair shafts being produced (Schlake et al., 2000).

1.3.3 Inner Root Sheath

The inner root sheath is adjacent and bound to the growing hair shaft and is responsible for guiding the hair shaft in its passage outward (Rogers, 2004; Stenn and Paus, 2001). It is made up of three layers which are the cuticle, Huxley's and Henle's layers. It functions as a physical barrier that separates the hair shaft from the outer root sheath, which creates the external concentric layer of epithelial cells (Schlake, 2007; Stenn and Paus, 2001). The inner root sheath

ensures the maintenance of a constant desmosomal anchorage of the companion layer which is required for an optimal moulding and guidance of the growing hair (Rogers, 2004; Stenn and Paus, 2001). The inner root sheath and hair shaft are tied together by their interlocked cuticle structures. The inner root sheath packaged shaft uses the innermost, companion layer of the outer root sheath as a slippage plane for orientation to move straight forward the skin surface (Krause and Foitzik, 2006; Stenn and Paus, 2001). The lineages of the inner root sheath have shown to express a variety of structural keratins, which are required for its mechanical strength. Cells of the inner root sheath produce keratins 1 & 10 and trichohyalin which collectively provide strength to the inner root sheath to support and guide its upward movement (Botchkareva and Randall 2009).

The establishment of the inner root sheath cell lineage is dependent on the activities of several factors which include GATA3 and Cut1 (Ellis et al., 2001; Kaufman et al., 2003). The Cutl1 gene encoding CDP is a transcription repressor in diverse processes. CDP is expressed in progenitors and cell lineages of the inner root sheath. Cutl1 deficiency leads to the reduction in size of the growing inner root sheath, accompanied by deregulated transcription of Shh, followed by cyst formation (Ellis et al., 2001). GATA-3 is a transcription factor, which is expressed in the Huxley and Cuticle layers of the inner root sheath (Kaufman et al., 2003). Ablation of GATA-3 expression has been shown to lead to structural changes in the inner root sheath. GATA-3 deficient follicles are no longer spatially aligned and the hair shaft develops as an overdeveloped mass of irregular medulla, cortical and cuticle cells. This demonstrates the importance of GATA-3 in these two layers of the inner root sheath, which are critical for the proper differentiation and/or organisation of the hair shaft

(Kaufman et al., 2003). A recent study by Kim et al found that the transcription factor Dlx3 is downregulated by the overexpression of the hairless (Hr) transcription factor leading to abnormal formation of the inner toot sheath (Kim et al., 2012). Kim et al reported that through the overexpression of the hairless gene in transgenic mice, the formation of the inner root sheath was abnormal and the expression of Dlx3 and inner root sheath keratins were suppressed. They showed that Hr downregulated Dlx3 mRNA expression through suppression of Dlx3 promoter activity. In addition, they found that Dlx3 regulated the expression of inner root sheath keratins, thus regulation of Dlx3 by Hr affects inner root sheath keratin expression, modulating the formation of the inner root sheath (Kim et al., 2012).

1.3.4 The Outer Root Sheath

The outer root sheath is a non-keratinising proliferative cellular layer of the hair follicle, which surrounds the inner root sheath and is continuous with the basal layer of the epidermis (Tanaka et al., 1998). The outer root sheath emerges proximally in the middle of the anagen bulb and continues distally to combine with the infundibulum. The outer root sheath is established during the early stages of anagen by the downward migration of the regenerating epithelium and then sustains itself independent of the bulbar matrix by basal cell growth (Reynolds and Jahoda, 1991). It displays a curved extension below the sebaceous gland known as the bulge, a stem cell niche where relatively undifferentiated stem cells reside for keratinocytes and melanocytes. The outer root sheath contains progenitor cells originating from the bulge that deliver into the matrix of the bulb. The progeny of keratinocytes and melanocytes migrate down from the bulge to the matrix of the hair bulb before differentiating.

(Botchkareva et al., 2001; Cotsarelis et al., 1990). In addition to epithelial cells, other cell types are also present in the outer root sheath. In human hair follicles, Langerhans cells have been found in the infundibular epithelium, including the follicular bulge and rarely in the epithelium below the entry of sebaceous glands (Langbein et al., 2004). It has been shown that Sox9 is essential for outer root sheath differentiation and formation of the hair follicle stem cell compartment (Vidal et al., 2005).

1.3.5. Hair Bulb

The hair bulb comprises of keratinocytes and melanocytes cells that envelop the mesenchymal cells that make up the dermal papilla. The matrix is divided into two regions, the lower region consisting of rapidly proliferating keratinocytes and the upper region consisting of differentiating keratinocytes with limited proliferative activity (Legue and Nicolas, 2005; Schneider et al., 2009). The hair matrix also contains melanocytes which migrate from bulge and reside on the apex of the dermal papilla, providing melanin pigment to the growing hair shaft (Botchkareva et al., 2001; Slominski et al., 2004).

The dermal papilla is a specialised, mesenchymal-derived structure made up fibroblasts and can be considered as being the ‘control centre’ of the hair follicle. It is believed to be integral to instruct hair follicles to grow and form a particularly sized and pigmented hair shaft (Jahoda et al., 1984; Matsuzaki and Yoshizato, 1998; Van Neste and Tobin, 2004). Decade old studies indicated that dermal papilla cells are capable of inducing hair follicle development and the formation of the hair shaft when placed in non-hairy skin (Jahoda et al., 1984; Jahoda and Oliver, 1984; Jahoda and Reynolds, 1993; Jahoda et al., 1993). In human hair follicles the size of the dermal papilla correlates with the

number of matrix cells and the size of hair shaft produced (Elliott et al., 1999). In mice the hair shaft diameter also depends on the proliferative activity of the matrix keratinocytes (Sharov et al., 2006).

The importance of the dermal papilla was demonstrated in pioneering experiments in which transplanted micro-dissected dermal papillae induced hair follicle growth (Jahoda et al., 1984; Reynolds and Jahoda, 1992). Several studies have implied that the dermal papilla acts a niche for regulating stem cells. Panteleyev et al showed that mice with mutant Hr gene, dermal papilla cells fail to migrate upwards and break into clusters during the first catagen and subsequent hair cycles cease (Panteleyev et al., 1999).

The dermal papilla displays strong alkaline phosphatase activity during the hair growth cycle (Handjiski et al., 1994). The activity of alkaline phosphatase has been used as an indicator to detect the dermal papilla during the hair cycle. Alkaline phosphatase activity in the dermal papilla and connective tissue sheath (also known as dermal sheath) has been shown to reach its highest level in early anagen stage and its expression was seen to decrease after the mid-anagen of stage of the hair cycle. The changes in temporal and spatial alkaline phosphatase activity coincide with the hair-inductive property of the dermal papilla and dermal sheath (Iida et al., 2007; McElwee et al., 2003). Whereas, the role for alkaline phosphatase in the hair growth remains unclear, it has been shown that hair growth is reduced if alkaline phosphatase is inhibited (Iida et al., 2007).

1.3.7 Connective Tissue Sheath

The connective tissue sheath, also known as the dermal sheath, envelops the epithelial components of the hair follicle. It consists of an outer connective tissue sheath and inner basement membrane called the hyaline or glassy membrane, which is continuous with the interfollicular basement membrane (Cotsarelis and Botchkarev 2012). The connective tissue sheath runs adjacently to the full length of the follicle on either side of the basement membrane. Around the upper follicle there is a thin connective tissue sheath continuous with the papillary dermis and around the lower follicle the connective tissue sheath is more prominent (Jahoda and Reynolds 2001; Cotsarelis and Botchkarev 2012). When transplanted under the skin, the connective tissue sheath has the ability to form a new dermal papilla and induce new follicle formation, suggesting cells of the connective sheath can induce dermal papilla cells in initiating hair growth (Reynolds et al., 1999). It was shown that when the base of the hair follicle was amputated, it would regenerate with the dermal papilla reforming from adjacent connective tissue sheath cells, demonstrating that within the dermis they acted as progenitor cells (Inamatsu et al., 2006).

1.4 Hair Follicle Morphogenesis

Hair follicle morphogenesis is governed by unique expression of regulators which can either promote induction of follicles and subsequently hair follicle development, or are inhibitors of this process. These regulators encompass growth factors and their receptors, growth factor antagonists, adhesion molecules and intracellular signal transduction, producing the correct balance of

signals to regulate hair growth (Botchkarev and Paus, 2003; Stenn and Paus, 2001).

The formation of mammalian hair follicles occurs during embryogenesis through a series of reciprocal interactions between skin epithelial cells and underlying dermal cells (Hardy, 1992). In human skin, hair follicles begin to develop at approximately 9 weeks gestation, on the chin, upper lip and eyebrow regions of the embryo (Cotsarelis and Botchkarev 2012). It is morphologically divided by eight consecutive stages (Stages 0-8), characterised by the downgrowth of the developing follicle, the positioning of the dermal papilla, as well as development of the inner root sheath and harbouring melanocytes **(Figure 1.4)** (Paus and Cotsarelis, 1999).

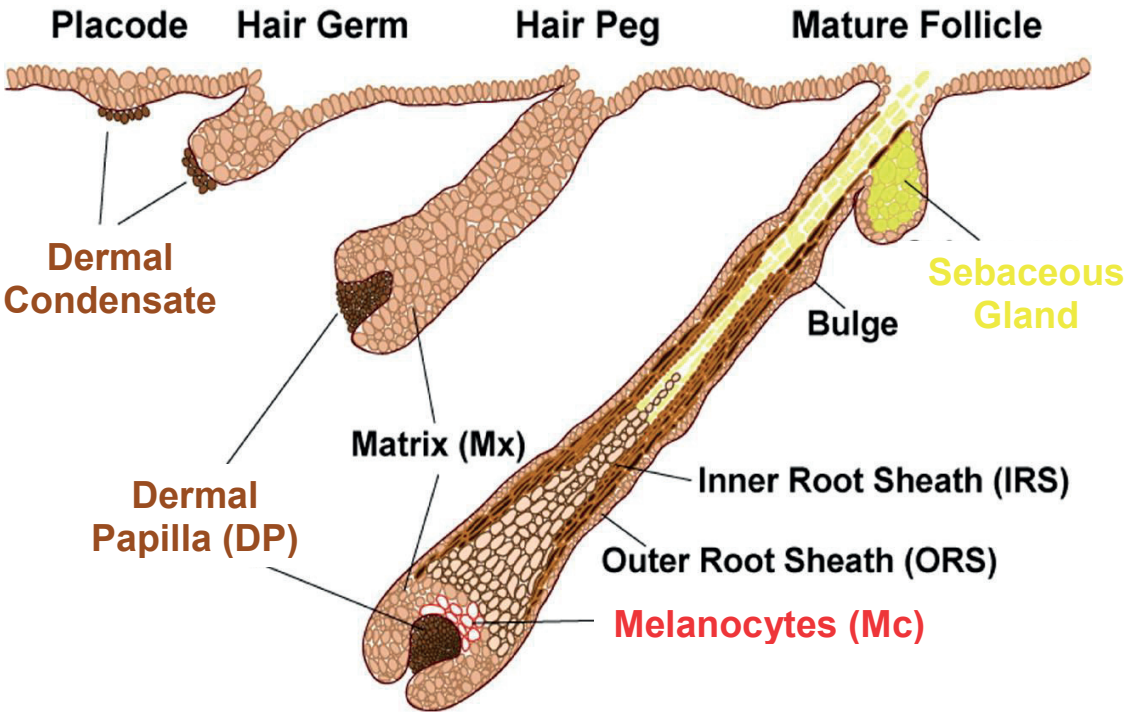

Figure 1.4. Embryonic stages of hair follicle morphogenesis. The process of hair follicle morphogenesis occurs relatively late in embryonic development which begins with the formation a hair follicle placode. A dermal condensate forms underneath the epithelial cells of the placode forming a hair germ. Further

downgrowth results in the formation a hair follicle peg. Continuing proliferation and differentiation eventually leads to the formation of a mature hair follicle. Adapted from Fuchs 2008

It is believed that the first signal to induce hair follicle formation originates from the dermis. This theory was derived from the fact that when dermis from mouse vibrissae is grafted below the epidermis of dorsal skin, whiskers develop on the back (Horne et al., 1986; Jahoda et al., 1984; Oliver and Jahoda, 1988). Also, when dermis from hair-bearing skin is transplanted onto non-hairy regions such as palmoplantar skin, hair follicles begin to develop, or when the opposite is done and dermis from hairless region was combined with epidermis of a hairy region, no hair follicles developed (Hardy, 1992; Jahoda et al., 1984; Kollar, 1970). This leads to the conclusion that the inductive properties lie within the dermis, since the origin of dermis dictates whether follicles developed.

The initial stage of hair morphogenesis (stage 0) begins with a single epithelial layer of basal keratinocytes. The epithelial cells that receive this first dermal signal form a thickening of columnar cells known as a placode (stage 1) **(Figure 1.4, 1.5)**. Subsequently, a signal from the placode leads to the formation of a mesenchymal (dermal) condensate just beneath the placode. Further interactions between the epithelial placode and mesenchymal condensate induce the proliferation in both these structures, leading to further downgrowth (Millar, 2002; Schmidt-Ullrich and Paus, 2005). The elongated placode eventually surrounds the dermal condensate, which becomes the dermal papilla. Rapid keratinocyte proliferation leads to the formation of the hair peg (stage 2). Further downgrowth of the hair germ leads to the formation of the hair 'peg' (stage 3-4), where the proximal keratinocytes begin to enclose the dermal

papilla, followed by the bulbous peg stage (stage 5-8). During stage 5, hair follicle keratinocytes begin to terminally differentiate forming the inner root sheath. The centre of the inner root sheath consists of terminally differentiated trichocytes, which go on to form the hair shaft (Schmidt-Ullrich and Paus, 2005). At stage 5, sebocytes become visible in the distal region of the developing hair follicle, while melanin granules and the hair shaft can be seen above the dermal papilla (Paus et al., 1999) Stages 6-7 are characterised by the visibility of the hair canal, the complete of enclosure of the dermal papilla and the tip of the hair shaft leaves the inner root sheath and enter the hair canal. At the final stage 8, the hair follicle reaches its maximal length and extends up the panniculus carnosus (in mice) and the hair haft emerges through the epidermis **(Figure 1.5)** (Paus et al., 1999).

In murine dorsal skin, hair follicles begin to develop at embryonic day 14.5 (E14.5), initially appearing as small epithelial placodes. The dorsal skin of mice is known to produce four distinct follicle types that vary in length, thickness and shape of hair shaft. These distinct follicle types are the guard, awl, auchene and zigzag hairs, distinguished by their length and number of bends (Schlake, 2007; Schneider et al., 2009). The most abundant follicle type is the zigzag which contains two bends in the shaft; the shafts of guard and awl contain no bends and auchene shafts consist of one bend. The first epithelial placodes that appear at E14.5 eventually develop into the primary guard follicles. These constitute approximately 1-5% of adult mouse coat and are characterised by their large follicle size and longer hair shaft length. Awl and auchene follicles are induced in the second wave from E16.5 to postnatal day 0.5 and zigzag hairs form beginning at E18.5 (Schlake, 2007; Schmidt-Ullrich and Paus, 2005).

1.5 Key signalling pathways involved in hair follicle development

1.5.1 Induction of hair follicle growth

The induction of hair follicle formation is a controlled process involving spatial and temporal regulation of inductive and inhibitory signals that together lead to formation of mature hair follicles. The initial stages of hair follicle morphogenesis are believed to be regulated in a sequential process of signals that alternate from the epidermis and dermis (Botchkarev and Paus, 2003; Millar, 2002). Although the induction of follicular growth was shown to originate from the dermis, the underlying mechanisms remain to be unravelled.

One of the major signalling pathways involved in hair follicle induction is Wnt/β-catenin signalling. The targeted deletion of β-catenin via K14 promoter prevents the formation of hair placodes (Huelsken et al., 2001). Ectopic expression of the secreted Wnt inhibitor Dickkopf1 (Dkk1) in mouse epidermis results in a complete failure of placode formation and blocks patterned expression of placode markers (Andl et al., 2002). In contrast, over-expression of Wnt/β-catenin signalling in the epidermis has been shown to induce extra hairs and hair-derived tumours (Gat et al., 1998; Millar, 2002). These data strongly suggest that Wnt signalling is crucial for initiating hair follicle development and Wnt signalling is believed to be essential for initiating the first dermal signal (Hardy, 1992), although it is still unclear which Wnt protein is crucial for inducing placode formation. After activation in the dermis, Wnt signalling also becomes active in the epidermis, where several Wnt proteins, including Wnt10a/b, and the secreted Wnt inhibitor Dkk4 are expressed (Bazzi et al., 2007; Zhang et al., 2009). Dkk4 is a direct target gene of Wnt/β-catenin signalling and is predominantly expressed in the hair follicle placode (Bazzi et al., 2007; Sick et

al., 2006). It has been reported that Dkk4 may play a role in inhibiting Wnt activity in the surrounding cells (Zhang et al., 2009). Over-expression of Dkk4 in the epidermis leads to retarded formation of secondary hair follicles but does not affect primary follicles (Cui et al., 2010). More recently Chen et al showed that forced activation of β-catenin in the dermis led to hyperproliferation of dermal fibroblasts producing a thicker dermis, enlarged epidermal placodes and dermal condensates that lead to prematurely differentiated hair follicles (Chen et al., 2012). Ablation of β-catenin in dermal fibroblasts prior to hair follicle induction prevents the expression of epidermal placode markers and the failure of primary hair follicle formation. This implies that widespread Wnt signalling in the dermis regulates the first signal/s to promote hair fate of epidermal cells (Chen et al., 2012)

Deletion of the transcription factor Lef-1, which is a transcriptional mediator of Wnt activity, resulted in an absence of most hair follicles in dorsal skin and lack of vibrissae follicles (van Genderen et al., 1994). In contrast, Lef-1 overexpression leads to increased number of hair follicles as well as ectopic hair growth in other epithelial tissue (Zhou et al., 1995). Lef-1 has been shown to negatively regulate the expression of E-cadherin in hair germ keratinocytes and promotes the loss of their adhesion to neighbouring epidermal keratinocytes, thereby stimulating hair follicle induction (Jamora et al., 2003). It has also been shown that Wnt/β-catenin signalling has a pivotal role in the formation of *de novo* hair follicles after wounding in murine skin. The selective ablation of Wnt signalling leads to abrogation of wound-induced folliculogenesis (Ito et al., 2007). A study by Enshell-Seijffers revealed a signalling loop that utilises Wnt/β-catenin signalling in epithelial progenitor cells and their mesenchymal niche regulates and coordinates the interaction between these

compartments to guide hair follicle morphogenesis (Enshell-Seijffers et al., 2010).

The tumour necrosis factor (TNF) pathway, which is mainly composed of Eda-A1 (ectodysplasin), Edar (ectodysplasin receptor) and Edardd (Ectodysplasin receptor death domain), has been shown to play a crucial role in the induction and development of the hair follicle. Eda is a ligand that that signals through downstream NFκB transcriptional activation after binding to Edar (Mikkola, 2011; Mikkola et al., 1999). Edar is a type I transmembrane protein and a member of the TNF receptor superfamily, with a cysteine-rich domain in the extracellular region as well as a potential death domain in its intracellular region (Headon and Overbeek, 1999). The deletion of both Eda and Edar in corresponding mouse mutants (Tabby and Downless) is accompanied by formation of a sparse coat and failure in induction of primary hair follicles (Headon and Overbeek, 1999). During embryogenesis Eda is detectable throughout the epidermis whilst Edar is expressed in early placodes. As embryogenesis progresses Eda becomes progressively restricted to the interfollicular epidermis (Laurikkala et al., 2002). Edardd associates with the Edar protein via its death domain, resulting in the downstream activation of NF-κB (Headon et al., 2001). Collectively, Eda-A1, Edar and Edardd function in a signalling pathway essential for morphogenesis of the primary hair follicles. Importantly, it has recently been shown that Edar is a Wnt-target gene whose expression is upregulated by Wnt signalling. Inhibition of Wnt prevents expression of Edar and activation of NF-κB. In addition both Wnt10b and Dkk4 have been shown to be target genes of NF- κB (Zhang et al., 2009). Therefore, Wnt/β-catenin signalling functions both as upstream and downstream of Eda-A1/Edar/Edardd/NF-κB signalling. Furthermore, Eda-A1/Edar mediated NF-κB

activation has been demonstrated to induce Shh expression, which promotes follicular growth (Schmidt-Ullrich et al., 2006). In view of the fact that both Eda and Edar are only expressed in the epidermis, studies have suggested that the Eda signalling pathway is important for placode patterning, affecting the induction of primary and zigzag hair follicles, but not necessary for initial placode formation (Botchkarev and Fessing, 2005; Schmidt-Ullrich et al., 2006; Zhang et al., 2009).

In addition to activators of hair follicle induction, the skin also contains a number of inhibitors of hair follicle induction. During hair follicle induction in mice, both BMP-2 and BMPRIa are expressed in the hair placode, while BMP-4 and noggin expression is seen in cells of mesenchymal condensation beneath the placode (Botchkarev et al., 1999a). It was shown that neutralisation of BMP-2 and BMP-4 inhibitory activity by noggin stimulates the initiation phase in hair follicle development. The deletion of noggin reduced placode density with the exception of guard hairs (Botchkarev et al., 1999a). As invagination of the epithelium begins there is a marked reduction in expression of E-cadherin, while P-cadherin is simultaneously up-regulated and prominent expression of P-cadherin persists in the proximal region of the hair follicle (Hirai et al., 1989). It has been shown that two distinct signalling pathways contribute to the down-regulation of E-cadherin; Wnt signalling, which results in the stabilisation of β-catenin and inhibition of BMP signalling by noggin to produce Lef-1 (Jamora et al., 2003). Active BMP signalling is known to inhibit the transcription of Lef-1 and contribute to maintenance of epidermal fate. However, noggin which is secreted from the dermal condensate of the secondary hair follicle interacts with BMP proteins and prevents receptor binding, leading to upregulation of Lef-1 expression at the placode (Botchkarev et al., 1999a; Botchkarev et al., 2002).

As a consequence, Wnt/β-catenin signalling is activated and E-cadherin expression is downregulated in the placode of the secondary hair follicle (Jamora et al., 2003). In addition, it has also been demonstrated that transgenic mice overexpressing E-cadherin in the epidermis results in a lack of hair follicles, providing further evidence that the cadherin switch plays a crucial role in changing cell-to-cell contacts in the hair follicle placode and promoting downgrowth (Jamora et al., 2003).

At the earliest stages of hair follicle induction, the molecular factors involved in determining epithelial cell fate for placodes versus interfollicular epidermis have been investigated (Nowak et al., 2008; Rhee et al., 2006). Two essential pathways which play a vital role in these cell fate decisions are EGF and KGF (also named FGF7). In a mouse model where FGFR2 receptor is knocked out, there is reduced follicular density and development of hair follicles is retarded (Petiot et al., 2003). Transgenic mice over-expressing FGF2 and FGF7 via K14 promoter have a reduced number of hair follicles and display epidermal hyper-proliferation, suggesting that FGF signalling may promote an epidermal fate rather than hair follicle cell fate (du Cros, 1993; Guo et al., 1993)

Collectively, arrays of epithelial-mesenchymal interactions acting via at least four distinct signalling pathways (Wnt, Edar, BMP and Shh) are interconnected in a signalling cascade that contributes to primary hair follicle development.

1.5.2 Hair follicle growth and differentiation

Following induction of hair follicles, the epithelial cells of the placodes begin to proliferate and produce downgrowths which eventually leads to the development of the mature hair follicle. Two signalling pathways essential for this downgrowth are Shh and PDGF (Platelet-derived growth factor).

Expression of Shh is seen in the developing placode and in the growing bulb of hair follicles (Bitgood and McMahon, 1995; Iseki et al., 1996). Patched (Ptc), a receptor for Shh, is expressed in both epidermal and dermal compartments from an early stage (Karlsson et al., 1999). In Shh knockout mice, there is an initial epithelium invagination and mesenchymal condensation at E15.5; however hair follicles become developmentally arrested at this point and by E18.5, hair follicle development is significantly retarded (Chiang et al., 1999; St-Jacques et al., 1998; Wang et al., 2000). The epithelium invagination and

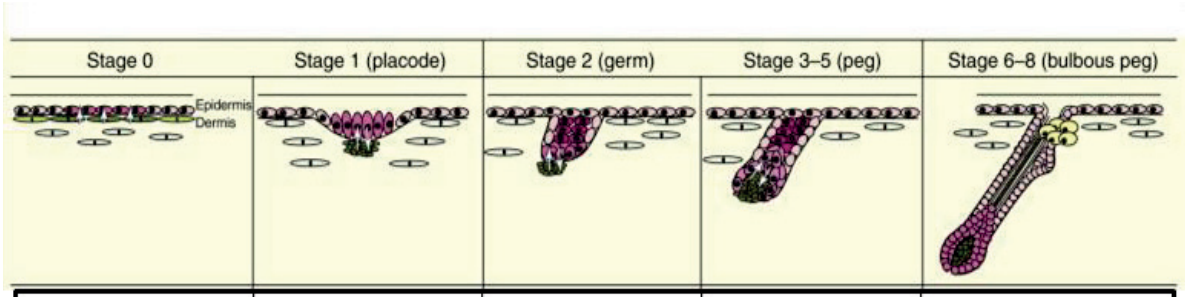

Interacting gradients of activators and inhibitors creating an inductive field in the epidermis (pre-germ). Specialised dermal fibroblasts gather underneath pre-germ	Visible hair placode. Promotion of placode growth: Wnt/β-Catenin, EdaA1/EDAR/NFκB, Noggin/Lef-1, P-Cadherin Inhibtion of placode fate in surrounding cells and placode growth: Dkk1, 2 & 4, BMP2, 4 & 7, p75NTR	Formation of hair peg: Shh, neurotrophins, Wnt10a, 10b, TGFβ2 Formation of dermal papilla: Shh, PDGF-A	Hair follicle polarity and shaft formation: Shh, Wnt/β-Catenin, Lef-1 Differentiating IRS: K1, K10, Cutl1, GATA-3 Differentiating ORS: K5, K15 Differentiation of hair shaft: Hair keratins, Lef-1, Msx-2, BMP2, BMP4, BMPRIa, Notch1 Dermal Papilla: BMP2, BMP4, Noggin. FGF7, HGF	Bulge: K15, K19 Sebaceous gland: Tcf-3, BMPRIa

Figure 1.5. Hair Follicle Morphogenesis and Key Signalling Molecules Involved. At Stage 0, interaction between the epidermis and underlying dermis involves local hair follicle growth activators such as Wnt/β-catenin signalling overriding hair follicle growth inhibitors, creating an inductive field. In the following Stages 1-2 the hair placode becomes visible and downward growth is initiated. The dermal condensate and dermal papilla begin to form and within the developing placode, BMP signalling is down-regulated by specific BMP antagonists in order for hair placode growth to occur. In stages 3-8 various

molecules are involved in the formation of the different lineages of the developing hair follicle. Adapted from Schneider et al 2009; Schmidt-Ulrich and Paus; Botchkarev and Paus 2003.

formation of mesenchymal condensates indicates that Shh is dispensable for hair follicle induction. The components of Shh, such as Ptch1, Smo, Gli1 and Gli2, are detected at lower levels, however levels of Wnt10b, Lef-1 and BMP2/4 are not affected in arrested follicles, indicating that hair follicle induction is independent of Shh, but Shh is necessary for hair follicle growth, and Shh signalling is either independent or operate as downstream of these inductive factors (Chiang et al., 1999; St-Jacques et al., 1998).

More recently, Woo et al showed when Smo, a mediator of Shh signalling is knocked out in early embryonic dermis there is a loss of dermal papilla precursor, the dermal condensate and the phenotype is similar to that of Shh deletion, demonstrating that Shh signalling within dermal condensates is essential for the development of the dermal papilla and subsequently hair follicle maturation (Woo et al., 2012).

The importance of PDGF in hair follicle morphogenesis was recognised due to the formation of sparse coats in PDGFa knockout mice, which eventually degenerate as the mice age (Karlsson et al., 1999). This study demonstrated the importance of epithelial-mesenchymal interaction as the PDGFa ligand is secreted exclusively by the epidermis and the PDGFRa receptor is exclusively expressed in the dermis (Karlsson et al., 1999). The majority of PDGFa mutant mice die during embryogenesis, with surviving mice displaying a sparse hair coat and thinner skin. The follicles that form appear to be normal indicating that PDGF signalling is not essential for hair follicle induction (Karlsson et al., 1999).

The TGFβ superfamily is also involved in regulating hair follicle development (Foitzik et al., 1999; Paus et al., 1997). In TGFβ-2 knockout mice there is delayed follicular growth at E18.5, reduced number of hair follicles, whereas embryonic skin explants with exogenous TGFβ-2 stimulated hair follicle induction (Foitzik et al., 1999).

BMP signalling is also required for differentiation of hair follicles. Mutation of BMPR1a gene leads to a reduction in levels of p-Smad 1/5/8 via which BMP signalling takes place, causing abnormal hair follicle formation (Andl et al., 2004). Andl et al demonstrated that CRE-mediated mutation of the gene encoding BMPR1a in the surface epithelium of mice, prevented external hairs from forming. The hair shaft and inner root sheath failed to differentiate and expression of known transcriptional regulators of follicular differentiation such as Foxn1 and Gata3 were markedly downregulated or absent in hair follicles of mutant mice (Andl et al., 2004). Lef-1 expression was maintained, but nuclear β-catenin was found to absent from the epithelium of severely affected mutant follicles, indicating that activation of the WNT pathway lies downstream of BMPR1a signalling in postnatal hair follicles. Mutant hair follicles failed to undergo catagen and instead continued to proliferate leading to the formation of follicular cysts and matricomas (Andl et al., 2004).

Notch signalling is another pathway involved in the growth and differentiation of hair follicles. During embryogenesis, Notch1 expression is seen in the epidermal part of the hair placode, but not in the underlying mesenchymal part (Kopan and Weintraub, 1993; Powell et al., 1998). Notch1 and its ligands Jagged1/2 are expressed in the precortex, differentiating cells of the inner root sheath and the hair shaft. Overexpression of Notch1 Intracellular Domain

(NICD) in the cells of the precortex leads to aberrant differentiation and hair loss by the end of the first hair cycle (Lin et al., 2000). Although Notch is not necessary for induction of hair follicles, it plays a key role in cell differentiation within hair follicles during late embryogenesis and adult life (Aubin-Houzelstein, 2012).

1.6 The Hair Cycle

The hair cycle encompasses the dynamic, rhythmic morphological changes orchestrated via a series of epithelial-mesenchymal interactions. The hair cycle consists of a growth phase (anagen), regressive phase (catagen) and a phase of relative quiescence (telogen). Thus an obvious question is why do hair follicles cycle? The reasons as to why the hair cycle occurs from an evolutionary perspective in mammalian animals, is to encompass several functions, which includes the ability to renew the protective function of hair (thermoregulation, camouflage) and adaptation to seasonal changes (shedding, social and sexual communication) (Stenn and Paus, 2001; Wu et al., 2008).

The purpose of hair cycling in humans from an evolutionary viewpoint is not as obvious, as these functional traits are not essential for human survival. However, possible reasons could be the cleansing of skin surface of debris and excretion of hazardous chemicals by encapsulation within trichocytes (Krause and Foitzik, 2006). Nonetheless, the hair cycle dictates the different characteristics of hair found across the body. The human body produces variations of hair depending on the location of the body. On areas such as the scalp and eyebrows, follicles consist of long, thick, terminal hairs, whereas areas such as the body and forehead are covered with short, thin and often unpigmented vellus hairs (Randall, 2008; Schneider et al., 2009).

The length of different hairs produced depends on the duration of the growth phase anagen, which can last from 2 to 6 years. Approximately 85% to 90% of all scalp hairs are within anagen follicles. The regressive phase catagen lasts only for a few weeks, followed by the relatively quiescent telogen phase, which lasts 2 to 4 months (Krause and Foitzik, 2006; Tobin, 2006). Several disorders of hair growth occur due to abnormalities in hair follicle cycling. Androgenetic alopecia, also known as male pattern baldness occurs due to shortening of the anagen phase, leading to hair loss due to the transformation of terminal hair follicles to vellus hair follicles. Hirsutism, a disorder in which excess hair growth occurs is due to a prolonged anagen phase and the conversion of vellus hair follicles to terminal hair follicles (Krause and Foitzik, 2006; Otberg et al., 2007). Therefore, understanding the underlying mechanisms that control this cycle and how the 'hair cycle clock' is regulated, will allow for clinical and pharmacological manipulations that will help to combat disorders of the hair.

The hair cycle in the back skin of mice is initially highly synchronised. Plikus et al showed that as mice age, hair follicle cycling slows down and patches of coordinated hair cycling eventually form distinct hair cycle domains, which become increasingly scattered as mice age (Plikus et al., 2008). The cycle in human hair follicles however, occurs in an autonomous pattern and can take up to 6 years (Krause and Foitzik, 2006). During the hair cycle, the lower inferior part of the hair follicle segment undergoes dynamic changes in morphology, whereas the upper 'permanent' region of the hair follicle maintains its structure throughout the cycle.

1.6.1 Telogen

Telogen is a phase of relative quiescence with regards to proliferative activity. The epithelial cells of the lower telogen follicle do not show significant DNA or RNA synthesis (Vogt et al., 2008). Telogen follicles are reduced to approximately about half the size of anagen follicles and do not extend beyond the upper dermis. They are characterised by their short length and lack of pigmentation due to the destruction of melanocytes and the absence of the inner root sheath. The compact round dermal papilla is closely attached to the secondary hair follicle germ containing hair follicle stem cells (Stenn and Paus, 2001; Vogt et al., 2008).

The hair follicle transition and transformation from telogen to anagen stages of the hair cycle are unique process of programmed organ regeneration characterised by activation of cell proliferation in the follicular germinative compartment located in the most proximal part of the telogen hair follicles close to dermal papilla (Stenn and Paus, 2001). The first telogen in mice lasts several days, whereas the second telogen lasts up to 3 weeks and the third is even longer. After each cycle the duration of telogen increases and follicular cycling slows down resulting in progressive asynchrony in pelage follicles and the formation of distinct hair cycle domains (Muller-Rover et al., 2001; Plikus et al., 2008). The research by Plikus et al led to redefinition of the hair cycle, with telogen divided into two phases, refractory telogen and competent telogen (Plikus et al., 2008). The refractory phase named so as it is refractory to follicle growth stimuli, characterised by the upregulation of BMP2/4. The competent phase characterised by the high sensitivity of bulge stem cells to anagen inducing factors (Plikus et al., 2008).

Although generally described as the resting phase, the components of telogen follicles (bulge, secondary hair germ and dermal papilla) are in fact engaged in cellular communication and in reality telogen follicles are far from being 'quiescent' (Botchkarev and Paus, 2003). Critical for initiation of the telogen-anagen transition seems to be a balance of local growth stimulators and inhibitors in the proximal region of the telogen hair follicle (Botchkarev and Paus, 2003). In telogen follicles, the bulge comes to rest above the secondary hair germ, which is in contact with the underlying dermal papilla, allowing for direct interaction between bulge stem cells and the dermal papilla. The dermal papilla is vital for stem cell activation and initiation of a new hair cycle. Once a critical level of stem cell activators is reached, anagen is induced (Krause and Foitzik, 2006). Activation of the Shh pathway in particular induces hair follicle transition from telogen to anagen (Sato et al., 1999). Confirmation of the high sensitivity of telogen follicles to Shh pathways was shown by the initiation of anagen through a single topical application of synthetic, nonpeptidyl small molecule agonists of the Hh pathway (Paladini et al., 2005). Conversely, telogen skin contains inhibitors of hair growth such as BMP2/4. It has been demonstrated that the initiation of anagen requires inhibition of BMP4/BMPRIa signalling by noggin. In the telogen hair follicles, BMP4 is produced by dermal papilla fibroblasts and keratinocytes of the matrix, interacting with BMPRIa, which is selectively expressed in the secondary hair germ and therefore inhibiting the early onset of anagen development (Botchkarev et al., 2001a).

Alterations to the growth modulators in the telogen stage may lead to the initiation or prevention of anagen. Therefore local balance of growth and stimulators and inhibitors in the proximal part of the follicles appears to be critical for new growth wave initiation (Botchkarev and Paus, 2003). Greco et al

found that in telogen follicles, Fgf7 and Fgf10 are expressed in the dermal papilla and act as activators of hair regeneration by stimulating the proliferation of hair germ cells and not the bulge during the telogen-anagen transition (Greco et al., 2009).

Kimuara-Ueki M et al showed that Fgf18 is expressed in the stem cell niche throughout telogen, and that it regulates the hair cycle through the non-growth phases (Kimura-Ueki et al., 2012). When the Fgf18 gene is conditionally knocked out in K5 expressing epithelial cells in mice, telogen becomes very short, giving rise to a rapid succession of hair cycles. In WT mice, hair follicle growth during anagen is strongly suppressed by local delivery of FGF18 protein. Their study demonstrated that epithelial FGF18 signalling and its reduction in the milieu of hair follicle stem cells are crucial for the maintenance of resting and growth phase, respectively (Kimura-Ueki et al., 2012).

At the end of telogen, the hair germ stabilises β-catenin (Greco et al., 2009). Choi et al showed that β-catenin is required within bulge and secondary hair germ cells for anagen initiation, with the deletion of β-catenin in K15 promoter-active bulge and secondary hair germ cells preventing follicles from progressing through anagen (Choi et al., 2013). Recently, Xing et al demonstrated that Wnt5a may inhibit the telogen-anagen transition to maintain a quiescent state of hair follicle stem cells (Xing et al., 2013). They showed that Wnt5a is expressed in cells of the bulge and secondary hair germ of telogen follicles. Overexpression of Wnt5a in the dorsal skin of mice led to a prolonged telogen stage and inhibition of anagen induction. However, after an extended period of time, four pelage hair types grew from hairless skin that was induced by Wnt5a, producing hair shafts with a normal phenotype. They showed that the

expression of β-catenin and some target genes of canonical Wnt signalling decreased after Wnt5a treatment (Xing et al., 2013).

Many signalling pathways work in tandem to regulate stem cell activity and are vital in the transition from telogen-to-anagen. The activation of stem cells from a quiescent state leading to proliferation and differentiation is a complex process, with the factors involved still being elucidated. Pathways which have been shown to be critical to these processes are the Wnt and BMP pathways. Although the cells of the telogen bulge exist in a Wnt restricted environment (DasGupta and Fuchs, 1999), they do however express transcriptional partners of β-catenin allowing them to process Wnt signals. In the quiescent bulge, Tcf3, a transcriptional cofactor of β-catenin, promotes stem cell quiescence and prevents differentiation in the absence of Wnt ligand (Nguyen et al., 2006). Also, Tcf4 along with Tcf3 promote self-renewal of stem cells of hair follicles and the epidermis during wounding (Nguyen et al., 2009). In the telogen-anagen transition in adult hair follicles, when β-catenin is continually expressed in resting stem cells, hair follicles precociously enter the anagen phase, implicating its role in activating bulge stem cells (Lo Celso et al., 2004; Lowry et al., 2005; Van Mater et al., 2003).

BMP signalling has also been shown to be important in the regulation of bulge stem cells. BMP signalling represses bulge cell proliferation and the loss of BMP signalling results in premature bulge cell activation (Blanpain et al., 2004; Kobielak et al., 2007). Plikus et al showed that cyclic dermal BMP signalling regulates stem cell activation during hair regeneration (Plikus et al., 2008). They showed that the wave of BMP2 expression is out of phase with Wnt/β-catenin signalling, which promotes the activation of stem cells, indicating the balance

between Wnt/β-catenin and BMP signalling is important in regulating the transition from quiescence to activation (Plikus et al., 2008).

A recent study by Nakajima et al showed the MED1 (mediator complex subunit 1) facilitates the maintenance of stem cell quiescence in the epidermis and hair follicle (Nakajima et al., 2013). Mice engineered with keratinocyte specific ablation of MED1, developed a normal epidermis and appendages and were macroscopically and microscopically normal until the second catagen phase of the hair cycle. The hair cycle in MED1 null mice was spontaneously repeated after the second telogen, which does not occur in WT mice (Nakajima et al., 2013). In normal mice telogen can last from thirty to sixty days (Muller-Rover et al 1999), however in MED1 null mice hair follicles entered the third anagen synchronously after only a week after the second telogen. After six months of age, MED1 null mice could not enter anagen, leading to sparse hair formation (Nakajima et al., 2013). FACS analysis using the bulge stem cell markers CD34 and integrin α6 found the number of stem cells was similar in 3 week old MED1 null and wild type mice, but the number of stem cells were reduced in MED1 -/- mice at 2 months of age (Nakajima et al., 2013).

1.6.2 Anagen

Anagen is the growth phase of the hair cycle and can be divided into 6 stages defined by specific morphological criteria (Muller-Rover et al., 2001). Anagen I is characterised by the growth of the dermal papilla and onset of mitotic activity in the overlying epithelium. During anagen II bulb matrix cells envelop the dermal papilla and begin differentiation. At anagen III the bulb matrix cells show differentiation into all follicular components. Anagen IV marks the reactivation of melanocytes. The hair shaft emerges at anagen V and dislodges telogen hair.

The new hair shaft emerges from the skin at anagen VI (Muller-Rover et al., 2001). It is characterised by rapid proliferation of keratinocytes that ultimately leads to the generation of a new hair shaft. During the anagen stage, the differentiation of epithelial stem cells leads to at least 8 different cell lines. This includes the formation of the outer root sheath, companion layer, Henle's and Huxley's layers, cuticle of the outer root sheath, cuticle of the hair shaft, shaft cortex and shaft medulla (Krause and Foitzik, 2006). The pigmentation and synthesis of the hair shaft occurs only during the anagen phase. In humans, during the first ten hair cycles in scalp follicles this works optimally, meaning until approximately 40 years of age. Subsequently there seems to be a genetically regulated exhaustion of the pigmentary potential of each follicle leading to greying of hair (Van Neste and Tobin, 2004). In mice the pigmentation of skin is coupled to the each stage of the hair cycle (Muller-Rover et al., 2001)

The onset of anagen requires a new lower follicle to be formed, which is produced by proliferation of the secondary hair germ. The dermal papilla and the overlying follicular epithelium are vital for this process as they activate these stem cells from the bulge region during the telogen phase of the hair cycle leading to the formation of highly proliferative keratinocytes which generate the anagen bulb (Cotsarelis et al., 1990; Paus and Cotsarelis, 1999). During anagen, relatively undifferentiated bulge cell progeny migrate down toward the dermal papilla and rapidly proliferate. This leads to the generation of transiently amplifying matrix cells, which begin to terminally differentiate causing the hair follicle to move deeper into the dermis and this movement down leads to the formation of the inner root sheath and hair shaft (Cotsarelis et al., 1990). At late anagen, the bulb is fully developed and envelops the dermal papilla which is

located deep in the subcutis and the hair shaft emerges from the skin (Muller-Rover et al., 2001).

Several key pathways are involved in the anagen phase which includes Wnt/β-catenin, Shh and BMP signalling (Botchkareva et al., 1999; Foitzik et al., 1999; Schmidt-Ullrich and Paus, 2005). The ablation of β-catenin not only prevents hair follicle morphogenesis but also impairs postnatal hair cycling (Huelsken et al., 2001). When β-catenin was ablated after follicles were formed, hairs were completely lost after the first cycle (Huelsken et al., 2001). It was shown that Wnt10a and b are expressed in postnatal follicles at anagen onset, but are absent from follicles in telogen (Reddy et al., 2001). Wnt/β-catenin signalling is also required for the differentiation of matrix keratinocytes in generating the hair shaft (DasGupta and Fuchs, 1999; Merrill et al., 2001).

Recently Myung et al showed that Wnt ligands secreted by the hair follicle epithelium are required for anagen induction and subsequently adult hair follicle regeneration (Myung et al., 2013). The loss of Wls (Wingless) in the follicular epithelium resulted in hair cycle arrest. Both the follicular epithelium and dermal papilla showed markedly decreased Wnt/β-catenin signalling during anagen induction compared with control hair follicles. Surprisingly, hair follicle stem cells that are responsible for follicle regeneration maintained expression of stem cell markers but exhibited significantly reduced proliferation (Myung et al., 2013). An elegant study by Choi et al showed that Wnt/β-catenin signalling is vital for hair follicle stem cell proliferation (Choi et al., 2013). Choi et al approached through three different methods; the first was through the inducible deletion of β-catenin globally in skin epithelia, the second was the deletion of β-catenin only in hair follicle stem cells and third only in the interfollicular epidermis and comparing

the phenotypes with those caused by the ectopic expression of Dkk1 (Choi et al., 2013). The deletion of β-catenin or ectopic Dkk1 expression blocked both plucking-induced and spontaneous anagen onset in adult mice. Interestingly they found that β-catenin was not required for hair follicle stem cell maintenance and follicles resumed proliferating after ectopic Dkk1 was removed, which supports findings of the study by Myung et al (Choi et al., 2013; Myung et al., 2013).

Although Shh is dispensable for hair follicle induction, it is required for the induction of anagen postnatally. Shh is expressed in a polarised manner on one side of the matrix named the lateral disk, which gives rise preferentially to the inner root sheath (Panteleyev et al., 2001). In mice over-expressing β-catenin, irregular patterns of Shh expression was seen on both sides of the hair follicle matrix, suggesting that Shh asymmetric expression in the matrix is vital for hair follicle polarity (Gat et al., 1998). Sato et al demonstrated that transient, localised overexpression of Shh in postnatal skin initiates the onset of the anagen growth phase of hair follicles (Sato et al., 1999). The overexpression of Shh led to increased follicle size, increased dermal and epidermal depth, increased melanogenesis and increased hair growth. These are all consistent with changes that occur as mouse skin enters anagen (Sato et al., 1999). When Shh is blocked through the administration of a Shh inhibitor, anagen progression is blocked (Wang et al., 2000). These studies collectively indicate that Shh plays a role in mediating the anagen phase.

The vitamin D receptor (VDR) has also been shown to be vital for anagen induction. VDR null mice undergo normal hair follicle morphogenesis but hairs fail to cycle (Sakai and Demay, 2000). Restoration of VDR in the keratinocytes

of VDR null mice restores the hair cycle defect which leads to the development of alopecia (Chen et al., 2001).

Insulin-like growth factor 1 (Igf-1) has also been identified in regulating hair follicle growth. Transgenic overexpression of Igf-1 in murine skin led to some hair follicles becoming elongated and guard hair shafts were longer than wild-type littermates (Weger and Schlake, 2005). Re-initiation of hair growth during the hair cycle was significantly retarded leading to a perturbed hair coat phenotype in Igf-1 transgenic mice. The study also revealed that this effect was due to the absence of zigzag hairs which adopted an alternative structure. Abnormal hair shaft differentiation was seen in Igf-1 transgenic mice and Pdgfra was identified as a molecular target of transgene expression. Therefore, Igf-1 has a mitogenic and morphogenetic function in pelage hair follicle (Weger and Schlake, 2005).

Hair follicle regeneration also requires BMP antagonism, as BMP signalling antagonises Wnt and Shh signalling. Recently Oshimori and Fuchs discovered that TGF-β2 counterbalances BMP mediated repression in hair follicle stem cell activation (Oshimori and Fuchs, 2012). Hair follicle stem cells that could not detect TGF-β2 exhibited significant delays in hair follicle regeneration. They showed that Tmeff1 was a target gene of the TGF-β2/Smad2/3 pathway which restricts and lowers BMP thresholds in hair follicle stem cells (Oshimori and Fuchs, 2012).

A study by Yuhki et al also confirmed the findings of Andl et al (Andl et al,. 2004), and also showed that BMPR1a is not only vital for hair follicle growth during development, but also vital for hair follicle cycling and hair shaft differentiation during the hair cycle (Yuhki et al., 2004). Using hair specific

Bmpr1a knockout mice (Hair-*Bmpr1a* KO mice), they found abnormal hair follicle differentiation and reduced cell growth of interfollicular epidermal cells in the foetal skin of these mutant mice (Yuhki et al., 2004). During postnatal development, Hair-*Bmpr1a* KO mice displayed a reduction in the number of hair follicles at 2 weeks of age and 10 month old mutant mice were hairless in affected regions (Yuhki et al., 2004). They also found that the hair shaft and inner root sheath development was severely impaired, with cysts forming at the hair canal of mutant hair follicles (Yuhki et al., 2004). In Hair-*Bmpr1a* KO mice, the translocation of β-catenin into the nucleus was significantly reduced in anagen follicles during the hair cycle. During the second anagen phase, they found abnormality of hair follicles, impaired cell cycling of matrix cells and complete hair loss in mutant mice (Yuhki et al., 2004).

1.6.3 Catagen

Catagen is the dynamic transition between anagen and telogen consisting of 8 different stages. The catagen phase encompasses highly controlled involution of the hair follicle via apoptosis and terminal differentiation (Muller-Rover et al., 2001).

During catagen the lower ‘cycling’ region of each hair follicle regresses entirely in a process that includes apoptosis of epithelial cells in the bulb and outer root sheath, the outermost epithelial layer (Lindner et al., 1997). This regression of the hair follicle in catagen is characterised by a cessation of proliferation and differentiation of hair matrix keratinocytes, termination of melanogenesis and activation of massive apoptosis in the hair matrix (Botchkareva et al., 2006; Krause and Foitzik, 2006; Lindner et al., 1997; Mecklenburg et al., 2000). In contrast to the outer root sheath and hair matrix there is no programmed cell

death in the dermal papilla, at least in part due to the expression of the apoptosis suppressor Bcl-2 (Lindner et al., 1997; Muller-Rover et al., 1999). Catagen is also characterised by the formation of a club hair that connects the proximal part of the hair shaft with the surrounding hair follicle epithelium and anchors hair in the telogen hair follicle. During catagen, the dermal papilla is transformed into a cluster of quiescent cells in close contact with the regressing epithelium, which moves from the subcutis to the dermis/subcutis border to contact the distal portion of the follicular epithelium, including the secondary hair germ and the bulge (Botchkareva et al., 2006; Muller-Rover et al., 2001).

One of the important catagen inducers is Fgf5 (Hebert et al., 1994). The expression of Fgf5 is seen in the outer root sheath at anagen VI and is downregulated just before catagen onset (Hebert et al., 1994; Rosenquist and Martin, 1996). Fgf5 null mice have a prolonged anagen phase causing an angora phenotype with hair twice as long as normal (Sundberg et al., 1997). In addition to Fgf5 other factors known to promote the transition from anagen to catagen include epidermal growth factor (EGF), neurotrophins such as brain-derived neurotrophic factor (BDNF), NT-3, NT-4 as well as TGFβ-family members (Alonso and Fuchs, 2006)

In mice with a targeted disruption of EGFR (epidermal growth factor receptor), follicles have an extended anagen phase (Hansen et al., 1997). Members of the neurotrophin family which includes BDNF, NT-3 and 4 and their high affinity receptor TrκB were also shown to be regulators of catagen (Botchkarev et al., 2000; Botchkarev et al., 1999b; Botchkarev et al., 2003). BDNF and NT-4 were expressed in the regressing hair follicle compartments, whereas TrkB was seen in the dermal papilla, epithelial strand, and hair germ. BDNF or NT-4 knockout

mice showed significant catagen retardation, whereas BDNF-overexpressing mice displayed acceleration of catagen and significant shortening of hair length (Botchkarev et al., 1999b). Neurotrophins accelerate catagen most likely by stimulating the p75 neurotrophin receptor (p75NTR), which is expressed in the regressing outer root sheath and is known to mediate apoptosis when activated alone (Botchkarev et al., 2000; Botchkarev et al., 2003). Spontaneous catagen development was compared *in vivo* between p75NTR KO and WT mice. There was significant catagen retardation in p75NTR KO mice compared to WT (Botchkarev et al., 2000).

The transcription factor p53 mediates a variety of biological responses including apoptotic cell death. p53 is strongly expressed and co-localised with apoptotic markers in the regressing hair follicle compartments during catagen (Botchkarev et al., 2001b). In p53 KO mice there is a significant retardation of catagen compared to WT mice, accompanied by significant decrease in the number of apoptotic cells in the matrix (Botchkarev et al., 2001b).

TGFβ-1 is also involved in regulating catagen. In TGFβ-1 null mice, hair follicles were found to be still in early catagen at postnatal day 18, whereas WT mice had entered telogen (Foitzik et al., 2000) . In addition, TGFβ-1 null mice displayed a higher number of Ki67 positive cells and fewer apoptotic cells, compared to WT. Inversely, when TGFβ-1 was injected into the back skin of mice, it induced premature catagen development, coupled with a decrease in proliferating follicular keratinocytes cells and an increase in TUNEL positive cells (Foitzik et al., 2000). In CRE-mediated mutation of the gene encoding BMPRIa hair follicle matrix cells failed to differentiate towards hair shaft or inner root sheath and expression of several known transcriptional regulators of hair

shaft and inner root sheath differentiation was decreased or absent. Mutant follicles failed to undergo catagen, instead continuing to proliferate to produce matricomas and follicular cysts (Andl et al., 2004).

An additional controller of the catagen phase was identified as the hr (hairless) gene. The hr gene is responsible for the strong connection between the condensing DP and the diminishing hair follicle epithelium in catagen and telogen follicles (Panteleyev et al., 2000). The hr transcription factor has been shown to be an important regulator of apoptosis in the hair follicle. Apoptosis is strongly increased in the hair matrix keratinocytes of hr mutant mice, resulting in premature entry of follicles to catagen. This subsequently leads to disintegration of the dermal papilla from the follicular epithelium and permanent hair loss (Panteleyev et al., 2000). Vitamin D receptor (VDR) gene ablation in mice leads to hair loss and the phenotype resembled hair loss caused by mutations in the hr gene (Miller et al., 2001), thereby suggesting a common signalling pathway for both hr and VDR. Subsequently it was shown that hr protein serves as a transcription co-repressor for the VDR. This suggests that interactions between hr protein and VDR may contribute to apoptosis in hair follicle matrix keratinocytes (Hsieh et al., 2003; Potter et al., 2001)

Wnt signalling has also been implicated in regulating the catagen phase. Recently, using recombinant human Dkk-1, Kwack et al showed that Dkk-1 promotes catagen progression (Kwack et al., 2012). When Dkk-1 was neutralised using an anti-Dkk-1 antibody, catagen progression was delayed thus prolonging anagen. This correlated with a decrease in hair follicle length, whereas anti-Dkk-1 antibody led to an increase in hair follicle length (Kwack et al., 2012).

1.6.4 Exogen

Considered to be independent from the rest of the hair cycle, the process of shedding hair is now recognised as a phase termed exogen. The exogen phase centres on the release of club fibre and any signalling or structural changes that may control the process of the club fibre being released (Higgins et al., 2009; Stenn, 2005). It is the least understood phase and there are currently two hypotheses regarding the process of shedding the club fibre. The first is that it is a passive process and that the shedding of club fibre is by caused by mechanical force by the new emerging hair shaft which pushes out the club fibre. The second is that it is an active process which is regulated through signalling which controls the breakdown of club fibre and its surrounding epithelial sac, leading to the club fibre being released (Higgins et al., 2009). A study by Milner et al suggests that the theory of club fibre being physically pushed out by a new growing hair fibre is unlikely (Milner et al., 2002). Using microscopy, examination of hair shafts shed and plucked telogen hair shafts reveal distinct morphological differences in the bases. In shed hairs the base of the hair fibres have sculpted edges and are bordered by cell membranes with deteriorating nuclei, whereas plucked telogen hairs have a smooth edged border and are rich in cells with intact nuclei and with separation fractures within basal cell cytoplasm (Milner et al., 2002). The morphology of the base of the hair suggests that exogen involves a proteolytic event occurs in the cells of the telogen shaft. Studies in desmoglein-3 knockout mice showed that these mice retain hair shafts for longer, reiterating the importance of adhesion molecules and programmed cell death in the retention and release of club fibres (Koch et al., 1998)

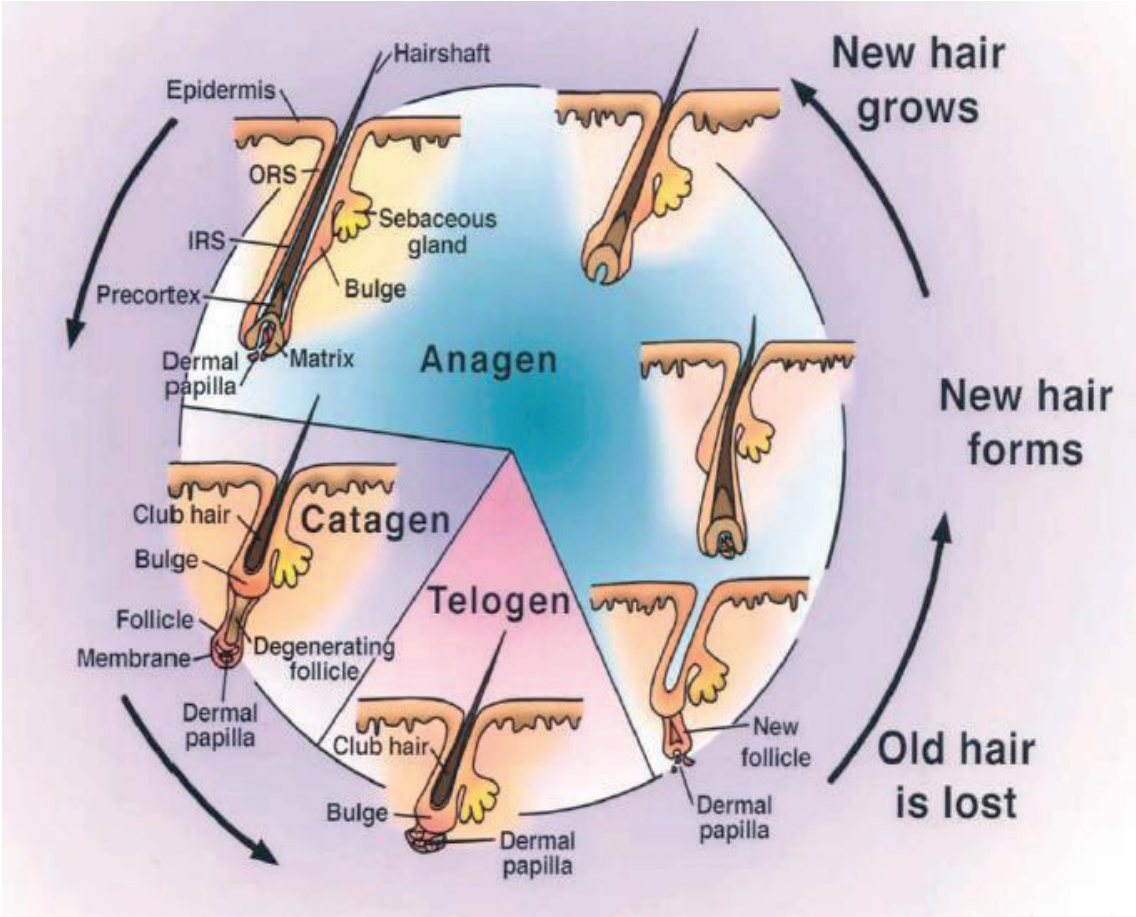

Figure 1.6. The Hair Cycle. The hair cycle consists of three different phases: anagen (growth phase), catagen (regression phase) and telogen (quiescent phase). In order to continuously renew hair follicle growth to replace the hair that degenerated and was released, it requires a limitless supply of stem cells, which are located in the bulge. Periodically, upon initiation of a new anagen, division of stem cells provides proliferative progeny that are directed by the dermal papilla to differentiate and form a new hair shaft. IRS, inner root sheath (blue); ORS outer root sheath. Adapted from Fuchs 2001.

1.7 Hair Follicle Stem Cells

Adult stem cells have the unique trait of generating differentiated cell types within the tissue in which they exist and are considered to have the ability to indefinitely self-renew in order to maintain the stem cell pool. These properties of stem cells allows them to maintain tissue homeostasis as well contribute to regeneration after injury (Blanpain and Fuchs, 2009; Cotsarelis et al., 1990). The hair follicle shows dynamic, morphological changes throughout adult life, regenerating in continuous cycling bouts. As a result of these changes, it has long been hypothesised that the hair follicle should possess a niche of stem cells that are relatively quiescent and function as a reservoir of stem cells for the hair cycle. In fact this cyclical process of growth and regression which occurs throughout a lifetime is largely governed by the presence of multipotent epithelial stem cells which reside in a specific niche referred to as the 'bulge,' a name first coined over a century ago (Stohr 1903). This niche provides the ideal microenvironment, including neighbouring cells and molecular signals, from where these hair follicle stem cells regulate not only hair growth, but also tissue homeostasis and wound repair (Fuchs, 2008). The accessibility of hair follicles makes their stem cell population, located in this specific niche, an attractive model for studying adult stem cells. These adult stem cells are characterised by their slow-cycling nature, thought to help maintain their stemness and more specifically their ability to self-renew and remain undifferentiated throughout a lifetime. In maintaining normal homeostasis, stem cells often exit their niche and progress to become transit-amplifying cells, undergoing rapid divisions before committing to terminal differentiation (Fuchs, 2008; Myung and Ito, 2012).

In 1990, a breakthrough study by Cotsarelis et al, determined that slow-cycling, label retaining cells (LRCs) in murine hair follicles, were located at the bulge identifying that this was the niche in which epithelial stem cells reside (Cotsarelis et al., 1990). By utilising 3H-thymidine 'pulse', which labels newly synthesised DNA, the labelled DNA becomes diluted as TA cells rapidly divide, leaving stem cells which rarely divide with traceable levels of the label. An elegant study by Tumbar et al using tetracycline regulated histone H2B linked to GFP (green fluorescent protein) also demonstrated the location of LRCs. After mice were continuously fed Tetracycline to suppress expression H2B-GFP, only slow cycling bulge were detected as H2B-GFP LRCs (Tumbar et al., 2004). They also showed that during anagen, newly formed GFP-positive stem cells originating from the bulge, form the outer root sheath, the cells of the hair matrix and inner root sheath, indicating their origins in the bulge of the outer root sheath. When skin was wounded, these GFP-labelled stem cells exited the bulge, migrated, and proliferated to repopulate the infundibulum and epidermis (Tumbar et al., 2004). Another study by Oshima et al showed that in bulge cells traced with a lacZ reporter gene in mice, bulge-derived cells migrate to the matrix of the follicle during anagen and contribute to all cell layers of the hair follicle (Oshima et al., 2001). Clonogenic assays carried out in dissected bulge from rat whiskers showed the highest colony-forming efficiency in comparison to keratinocytes of the matrix (Kobayashi et al., 1993). Although bulge stem cells are multipotent and can differentiate into all epidermal lineages as demonstrated by implantation into immunodeficient mice and are involved in the homeostasis of hair follicles cells below the sebaceous gland, they do not contribute to the formation of the sebaceous gland and interfollicular epidermis under normal physiological conditions (Levy et al., 2005; Morris et al., 2004).

However, under conditions such as wounding, bulge stem cells contribute to the reepithelialisation of the interfollicular epidermis (Cotsarelis et al., 1990; Jaks et al., 2008; Nowak et al., 2008; Tumbar et al., 2004).

Identifying molecular markers that are bulge-specific has provided a more in depth characterisation of bulge stem cells. These markers encompass cell surface markers, integrins, keratins and transcription factors. Hair follicle stem cells express the integrins α6β4 and α3β1, K5, K14 and K15, CD34 and Lgr5. (Blanpain et al., 2004; Morris et al., 2004; Tumbar et al., 2004). The identification of CD34 as a bulge stem cell marker allowed bulge cells to be characterised in cell culture, where CD34 positive cells showed enhanced colony forming ability as well as the reconstitution of hair follicle and interfollicular epidermis (Blanpain et al., 2004; Trempus et al., 2003; Trempus et al., 2007). K15 was initially shown to be expressed in the bulge in human follicles (Lyle et al., 1998). It was identified as a marker after *in vivo* lineage tracing experiments showed that the progeny of K15 positive stem cells contributed to all epithelial lineages of the hair follicle (Morris et al., 2004).

Lhx2, a downstream target of Shh, was one of the first stem cell markers found to be expressed specifically in embryonic placodes in addition to stem cells of the bulge in postnatal hair follicles. Lhx2 has been shown to have a key role in hair follicle stem cell maintenance and activation. Loss-of-function mutations of Lhx2 has shown to lead to formation of fewer number of hair follicles, but with the presence of more active stem cells, which are unable to maintain stem-cell characteristics in mouse skin (Fuchs, 2007; Rhee et al., 2006). Recently Folgueras et al demonstrated that Lhx2 regulates a significant number of hair follicle stem cell signature genes and cytoskeletal and adhesion molecules

within the hair follicle stem cell niche (Folgueras et al., 2013). Surprisingly, the reason they found as to why Lhx2 loss leads to baldness was not due to exhaustion of hair follicle stem cell proliferative activity or blocking Wnt signalling at the niche base, but that the loss perturbs hair follicle stem cell polarisation and niche architecture. Without Lhx2, the niche can no longer anchor its hair and maintain the proper behaviour of its stem cells (Folgueras et al., 2013).

When the transcription factor Sox9 (sex determining region Y)-box 9 is conditionally ablated postnatally in the skin, the expression of the bulge stem cells marker CD34 is lost and hair follicles fail to cycle (Vidal et al., 2005). When Sox9, which is originally expressed in suprabasal cells of the hair follicle placode and later in the bulge, is ablated in the embryo, hair morphogenesis ceases, sebaceous glands fail to form and bulge cells fail to form (Nowak et al., 2008). In addition to these markers, hair follicle stem cells can also be identified by other markers which include Nestin (Li et al., 2003), Tcf3 (Nguyen et al., 2006), Nfatc1 (Horsley et al., 2008), Lgr6 (Snippert et al., 2010) and Gli1 (Brownell et al., 2011).

Although a definite hair follicle stem cell marker in the mouse has not been determined, in the human hair follicles several bulge stem cell markers have been identified, in particular CD200 positive cells show a high-colony forming ability (Ohyama et al., 2006). In addition, K15 was found to be preferentially expressed in the bulge of human hair follicles (Cotsarelis, 2006). Overall, bulge stem cells can be dependably identified and thus studied via their slow-cycling feature, their location and the existence of a wide variety of molecular markers.

Until recently, the bulge was considered the most vital epithelial stem cell pool required for follicular regeneration. However, the distinct structure which sits above the dermal papilla in the telogen follicle referred to as the secondary hair germ is now recognised as a distinct niche itself. Ito et al examined morphogenesis of the telogen bulge and secondary hair germ during catagen after inducing anagen via depilation. Using BrdU pulse-chase they determined almost all label uptake occurred by hair follicle epithelial cells during early anagen. As anagen progresses the label was confined to the upper outer root sheath corresponding to the bulge area, but the label became undetectable in the proliferating lower matrix cells (Ito et al., 2004). In the telogen phase, the bulge of the telogen follicle and the secondary hair follicle consisted mainly of label retaining cells, demonstrating that the bulge of telogen follicle and the secondary hair germ are regenerated by label retaining cells of anagen follicles (Ito et al., 2004). Greco et al also showed this in the spontaneous hair cycle (Greco et al., 2009). They demonstrated using BrdU pulse-chase, that during early hair follicle regeneration the first cells to incorporate BrdU are cells of the secondary hair germ, followed by bulge stem cells, suggesting a two-step mechanism of hair follicle regeneration (Greco et al., 2009).

In contrast to the bulge, the cells of the secondary hair germ do not express CD34 or Nfatc1 but are rich in P-cadherin positive cells (Greco et al., 2009). The G-protein coupled receptor Lgr5 is expressed on keratinocytes of the secondary hair germ, in the telogen bulge and the lower outer root sheath of anagen follicles (Jaks et al., 2008). The expression of Lgr5 overlaps with CD34 and K15 in the telogen follicle, from the lower bulge to the secondary hair germ. Although Lgr5 positive cells seldom include LRCs and actively proliferate at anagen onset, they behave as fully functional stem cells *in vitro* and *in vivo* thus

supporting the coexistence of quiescent and active stem cells (Jaks et al., 2008; Li and Clevers, 2010).

The bulge also acts a source of stem cells for the sebaceous gland. The sebaceous gland is a terminally differentiated structure that is a part of the pilosebaceous unit. It buds from the upper outer root sheath, residing above the bulge. Differentiated sebocytes produce and secrete lipid-rich sebum into the hair canal that is excreted onto the skin surface (Alonso and Rosenfield, 2003). In mice, the stem cells that give rise to the sebaceous gland are located in the central isthmus, directly above the bulge and are marked by the presence of Lgr6 positive cells (Snippert et al., 2010). Lineage tracing revealed that this population of Lgr6 positive cells are multipotent and can also produce the hair follicle and the interfollicular epidermis (Snippert et al., 2010). Horsley et al discovered a population of cells within the sebaceous gland that expressed Blimp1 (B lymphocyte-induced maturation protein 1) (Horsley et al., 2006). They showed that when Blimp1 expression is suppressed, abnormally large sebaceous glands form, with enhanced pools of slow-cycling progenitors and proliferative cells, in addition to increased c-Myc expression (Horsley et al., 2006).

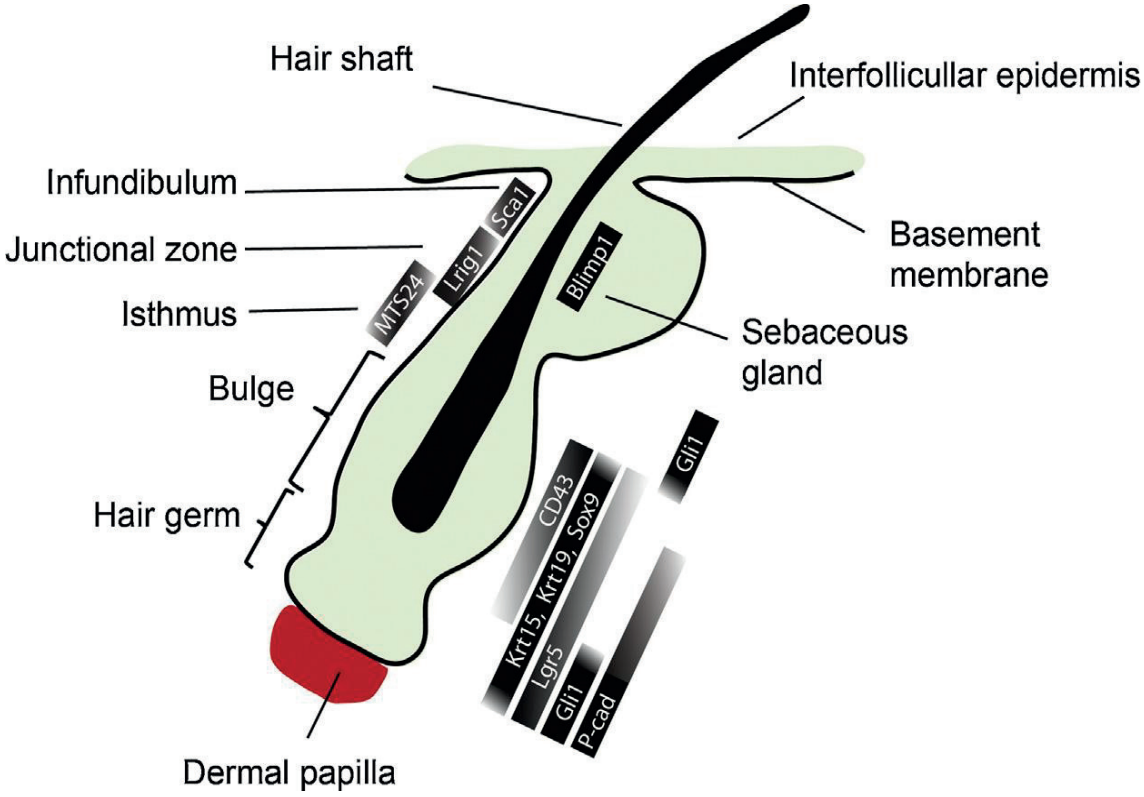

Figure 1.7. Stem cell populations of the hair follicle. Hair follicle stem cells reside in the bulge, while a pool of progenitor cells, which forms the secondary hair germ, is situated directly below the bulge and in contact with the mesenchymal dermal papilla. Other epithelial cell populations exist in defined anatomical tissue compartments located above the bulge. The hair follicle niche displays a pronounced molecular heterogeneity, which is evident by the distribution and level of expression of various genes Adapted from Rompolas and Greco (2014).

1.8 MicroRNAs

MicroRNAs (miRNAs) are a class of small, approximately 22nt long, non-coding RNAs that control diverse biological functions by promoting degradation or inhibition of translation of target mRNAs (Ambros, 2004; Bartel, 2004). Since the initial discovery of the first miRNA lin-4 in *C.Elegans* in 1993 (Lee et al., 1993) thousands of miRNAs have been discovered in unicellular eukaryotes, plants and animals signifying the vital role that miRNAs play in gene regulation (Siomi and Siomi, 2010). The initial discovery of the first miRNA lin-4 in 1993 did not set a precedent for research into the world of miRNAs. It was several years later when research carried out by Craig Mello and Andrew Fire describing the phenomena of RNA interference (RNAi) (Fire et al., 1998), which led them to receiving the Nobel Prize in Physiology or Medicine in 2006. Using the *C. Elegans* model they found that a few molecules of dsRNA were sufficient to reduce the expression of a specific mRNA (Fire et al., 1998). A second miRNA, let-7, which controls the larval development of C.elegans was discovered by Reinhart el al several years later (Reinhart et al., 2000). These two small RNAs lin-4 and let-7 were initially named as small temporal RNAs (stRNAs) (Pasquinelli et al., 2000) due to their involvement in the control of development and were renamed as miRNAs in 2001 (Lagos-Quintana et al., 2001). Other types of small RNAs have also been found in plants and animals, which include endogenous small interfering RNAs (siRNAs) (Ambros et al., 2003; Reinhart and Bartel, 2002) and Piwi-interacting RNAs (piRNAs) (Aravin et al., 2007). Although miRNAs fall into the phenomenon of RNAi, they differ from other small RNAs in their biogenesis. miRNAs form distinct hairpin structures (Bartel, 2004), whereas other endogenous small RNAs are derived from much longer hairpins that produce a wider range of small RNAs (siRNAs), or from

precursors without any suspected double-stranded feature (piRNAs) (Bartel, 2009).

miRNAs are now recognised as fundamental players in biological processes from development, cell proliferation, differentiation, maintenance of stem cells to apoptosis (Abbott et al., 2005; Cheng et al., 2005; Yi et al., 2008). Approximately 800 miRNA genes have been identified in the human genome, which is ~3% of the number of protein-coding genes and it is estimated approximately 30% of genes may be regulated by miRNAs. Thus miRNAs constitute one of the most abundant classes of gene-regulatory molecules (Krol et al., 2010). It is widely acknowledged that miRNAs control the expression of genes through Watson-Crick base pairing to the 3'- untranslated region (3'-UTR) of target mRNAs and inhibiting protein synthesis by either translational repression or degradation (Krol et al., 2010; Siomi and Siomi, 2010).

1.8.1 MicroRNA Biogenesis

The biogenesis of miRNAs is evolutionary conserved and involves sequential endonucleolytic cleavages mediated by two RNase II enzymes Drosha and Dicer (Cullen, 2004). Transcription of microRNAs is one of the main regulatory steps in miRNA biogenesis. The first step in microRNA biogenesis begins with transcription by RNA polymerase II, however some miRNAs are transcribed by RNA polymerase III (Borchert et al., 2006). Mapping of the promoters of 175 human miRNA genes through nucleosome positioning and ChIP-on-chip analysis suggests that the characteristics of miRNA gene promoters such as frequencies of CpG islands, TATA box, initiator elements and histone

modifications are similar to those of protein coding genes (Corcoran et al., 2009; Ozsolak et al., 2008).

miRNAs are generally classified as “intergenic” or “intragenic” depending on their location in the genome. Intergenic miRNAs are known to be transcribed as independent transcription units, while intragenic miRNAs are believed to be processed from the introns of their hosting transcription units and hence share common regulatory mechanisms and expression patterns with its host gene (Ramalingam et al., 2014)

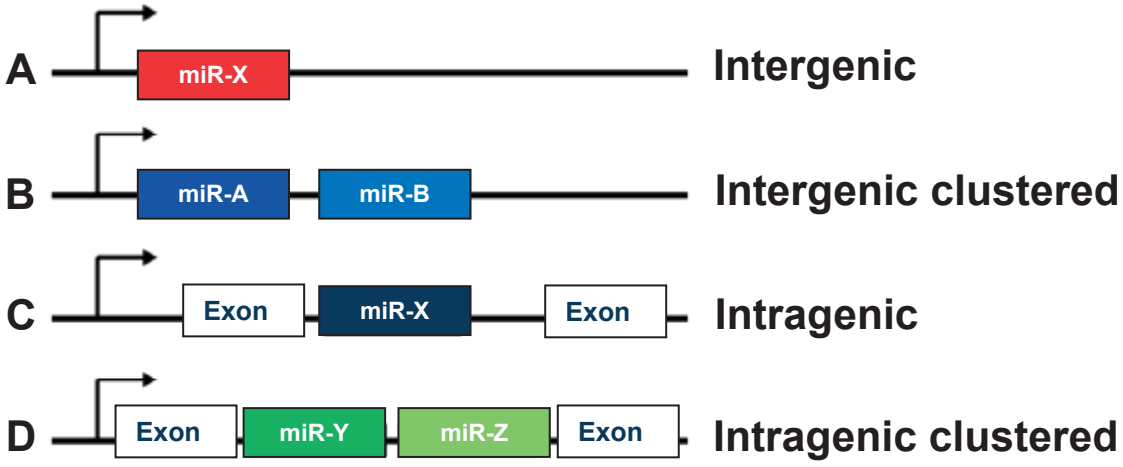

Figure 1.9. Genomic organisation of microRNAs. **A**) MicroRNAs can be transcribed from intergenic regions which are distinct from known transcript units. (**B**) They can be transcribed as a cluster of primary transcripts with a shared promoter. (**C**) Intragenic miRNAs are found in the introns of annotated genes, both coding and non-coding and are transcribed from the same promoter as their host genes. (**D**) Intragenic miRNAs can also be transcribed as a cluster of miRNAs.

Transcription by RNA pol II leads to the generation of primary microRNA (pri-miRNA), which are hairpin structures generally several thousand nucleotides

(Figure 1.10). The initial step of microRNA processing is catalysed in the nucleus by the RNase III enzyme, Drosha (Denli et al., 2004; Lee et al., 2003; Zeng et al., 2005). Drosha cleaves at the base of the stem loop structure of the pri-miRNA to generate a ~60-100 nt hairpin pre-miRNA structure, with a characteristic 2 nt overhang at the 3' end (Lee et al., 2003). Drosha forms a large complex known as the 'microprocessor complex' located in the nucleus and contains two RNase-III domains and an amino-terminal segment (Lee et al., 2003). This complex consists of Drosha and its cofactor DiGeorge Syndrome Critical Region 8 (DGCR8), a protein containing two dsRNA-binding domains, which cleave pri-miRNAs to form pre-miRNAs (Chen and Meister, 2005; Gregory et al., 2004; Han et al., 2004). DGCR8 functions at least in part by binding to the junction between the single-stranded RNA and double-stranded region of the pri-miRNA stem in order to direct Drosha cleavage ~11 bp away from the region **(Figure 1.10)** (Han et al., 2006).

Pre-miRNAs are approximately 70nt long with one to four nt 3' overhangs, 25-30 bp stems and relatively small loops. Drosha also generates either the 5' or 3' end of the mature miRNA, depending on which strand of the pre-miRNA is selected by RISC (Lee et al., 2003). After cleavage by Drosha, the pre-miRNA is transported out of the nucleus via interaction with Exportin-5 (Exp5) and Ran-GTP. Exp-5 interacts with dsRNA longer than 14 bp and has been shown to bind directly and specifically to correctly processed pre-miRNAs (Lund et al., 2004; Yi et al., 2003)

Once in the cytoplasm, the pre-miRNA undergoes further processing by Dicer, which cleaves the pre-miRNA to an approximately 22nt long miRNA duplex (dsRNA product). The two strands of the duplex are separated with one strand,

known as the guide strand goes on to produce the mature miRNA, whereas the other passenger strand (miRNA*) is degraded. The mature miRNA associates with an Argonaute protein within the large protein complex RISC (RNA-induced silencing complex) forming the miRNA-induced silencing complex (miRISC), where it acts as a guide to repress target mRNAs by binding to specific regions in the 3'-untranslated region (3'-UTR) **(Fig 1.10)** (Flynt and Lai, 2008; Schwarz et al., 2003). Although the exact mechanisms behind the targeting process of the miRISC complex are not fully understood, a key factor in targeting mRNAs is base pairing between nucleotides 2-7 of the miRNA transcript known as the 'seed region' and the 3 UTR' of target mRNA (Lewis et al., 2005).

Similarly to Drosha, Dicer also has a double stranded binding protein, known as TRBP (the human immunodeficiency virus transactivation response RNA-binding protein). Association of TRBP with Dicer enhances Dicer stability and processing activity (Haase et al., 2005). It was found that the Dicer-TRBP complex had a close association with the RISC complex. The knockdown of TRBP leads to Dicer destabilisation and subsequent loss of miRNA biogenesis (Chendrimada et al., 2005).

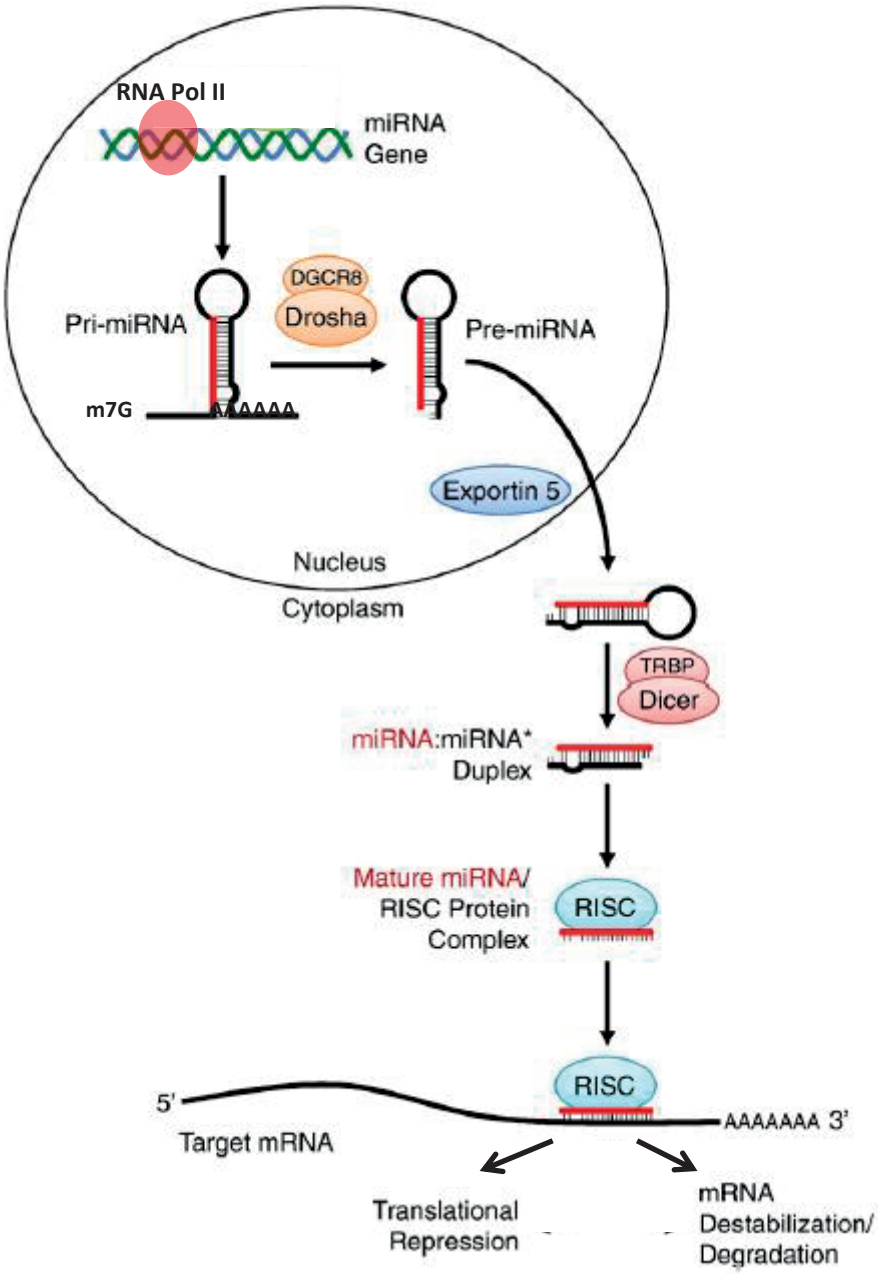

Figure.1.10 Biogenesis of MicroRNAs. miRNAs are initially transcribed in the nucleus by RNA polymerase II (RNA Pol II) as a long, capped and polyadenylated primary-microRNA (pri-miRNA). The Drosha complex, (consisting of Drosha and DGCR8) crops the pri-miRNA into a hairpin-shaped precursor-miRNA which is further processed by the Dicer complex (consisting of Dicer and TRBP). Following processing by the Dicer complex, the resulting miRNA:miRNA* is disassociated and the mature miRNA is incorporated into the RISC (forming the miRISC complex). Here it functions to mediate gene

silencing either by translational inhibition or by promoting the degradation of target mRNAs. Adapted from Gurtan and Sharp 2013.

1.8.2 RISC complex

The association of Dicer with several other proteins in a complex termed the RISC-loading complex (RLC) allows the tight coupling of Dicer cleavage to the incorporation of miRNA into the RISC (Chendrimada et al., 2005). After cleavage of the pre-miRNA by Dicer the outcome is the formation of an unstable dsRNA composed of the active guide strand (miRNA) and the passenger (miRNA*) strand. Selection of the miRNA strand which is incorporated into the RISC can be regulated in a cell-type and tissue-specific manner. An example of this is miR-30e-3p (termed 3p as it originates from the 3' arm of the pre-miRNA transcript) which is expressed in the stomach whereas miR-30e-5p (from the 5' arm) expression is expressed more specifically in the spleen (Ro et al., 2007).

The Argonaute family of proteins, consisting of Ago-1-4 are the primary components of the RISC complex and the effectors of miRNA mediated repression of target mRNAs (Hutvagner and Simard, 2008). Whilst all of the Ago proteins have the ability to interact with miRNAs and siRNAs, Ago2 is the only one with RNA cleavage activity and is thought to play a critical role in miRNA mediated mRNA silencing (Hutvagner and Simard, 2008). The total level of Ago proteins within cells also contributes to global miRNA biogenesis and regulation. When Ago proteins are ectopically expressed, it results in a significant increase in mature miRNAs (Diederichs and Haber, 2007).

1.8.3 Posttranscriptional Regulation of Gene Expression

Depending on the complementarity to which miRNA binds to target genes, there are two possible outcomes for the targeted mRNA. One is that the target mRNA is cleaved and degraded. The other is translational repression of the target mRNA. The outcome of degradation or translational repression depends on the complementarity to which miRNA binds to target genes. For example in plants, the majority of miRNAs bind with near perfect complementarity, leading to mRNA cleavage and degradation (Jones-Rhoades et al., 2006). In animals however, near perfect complementarity is rare, with the majority of miRNAs generally imperfectly pairing with target miRNAs, with the main characteristic being the pairing of the "seed" region with the 3 UTR' therefore translational repression rather than degradation is the outcome (Grimson et al., 2007). The majority of bioinformatic prediction programs use this principle for target prediction based on seed recognition (Sethupathy et al., 2006). This interaction allows a single miRNA to inhibit the expression of hundreds of different mRNAs (Lim et al., 2005; Selbach et al., 2008). This unique characteristic contributes to the fact that the biological effect of miRNAs relies more on the synergy of collective target inhibition. The means by which miRNAs generally function is a moderate inhibition of numerous mRNAs, with only unique targets when inhibited producing strong phenotypes (Flynt and Lai, 2008). This ability of miRNAs makes them a core component of an already complex gene regulatory network, ensuring correct levels of protein expression.

1.8.4 Regulation of miRNAs

The analysis of miRNA promoter regions indicates that miRNA transcription is complex as that of protein-coding genes and thus miRNA promoters are under the control of transcription factors, enhancers and epigenetic factors such as DNA methylation (Breving and Esquela-Kerscher, 2010). Several transcriptional factors such as p53, c-Myc and E2F have been identified as regulating the transcription of miRNAs. The tumour suppressor gene p53 was found to activate the transcription of the miR-34 family by binding to the promoter region for this family (Bommer et al., 2007; Chang et al., 2007; He et al., 2007). The oncogene c-Myc has been shown to up-regulate the expression of the miR-17-92 cluster, but also represses a number of miRNAs (Mendell, 2008). Transcription factors belonging to the E2F family have also been reported to increase expression of several miRNAs (Bueno et al., 2010). miRNAs, such as the ones encoded by the mir-106b-25 or mir-15b-16-2 clusters were found to be induced by E2F1 or E2F3 in mouse embryonic fibroblasts. Using siRNA for E2F1-knockout or E2F3-knockdown in cell culture these miRNAs were downregulated, suggesting the functional relevance of these transcription factors in the control of these small RNAs (Bueno et al., 2010).

Recent evidence has emerged that miRNAs themselves are regulated by other classes of RNA. Endogenous RNAs also referred to as competitive endogenous RNA (ceRNA), as they influence each other's levels by competing for the same pool of miRNA. ceRNA encompasses several types of RNA which includes pseudogenes, long noncoding RNA (lncRNA) and circular RNA (circRNA) (Bak and Mikkelsen, 2014). Work by Poliseno et al investigating the lncRNA tumour suppressor pseduogene PTENP1, brought into view that its biological function

maybe to act as a ‘decoy’ through sequestration of miRNAs to affect their regulation of expressed genes (Poliseno et al., 2010) . The 3’ UTR of PTENP1 mRNA has 95% identity with the 3’ UTR of PTEN and contains sites for five miRNAs: miR-19, 21, 17-5p/20, 26 and miR-214 which carry conserved binding sites in the 3’ UTR of PTEN. The ability to bind to the same regulatory miRNA sequences that normally target the mRNA of the PTEN tumour suppressor gene prevents the down-regulation of PTEN mRNA and allowing its translation to protein (Poliseno et al., 2010).

More recently, circular RNAs (circRNA) were discovered to act as natural ‘miRNA sponges’ (Hansen et al., 2013). Hansen et al showed that a circRNA acts as a sponge for miR-7, thus named it as circular transcript for miR-7 (ciRS-7). They observed 73 conserved binding sites for miR-7 in this circRNA and found it strongly represses miR-7 activity resulting in the upregulation of miR-7 targets (Hansen et al., 2013)

1.9 microRNAs in the Skin and Hair Follicle

microRNA mediated regulation adds another dimension of gene regulation in controlling protein output. The significance of this additional level of regulation in skin development and homeostasis is unravelling, and began with several studies that targeted key components of miRNA biogenesis.

Dicer is one of the key enzymes in processing miRNA to produce functional mature miRNA. Dicer knockout in mice leads to the arrest of mechanisms triggered by mature miRNA, consequently leading to developmental abnormalities in many organs causing embryonic lethality, with the embryo being aborted at E7.5 before skin development begins (Bernstein et al., 2003). Mice lacking DGCR8, which is required by the Drosha enzyme for processing

miRNAs, also led to the death of mice during early embryogenesis (Wang et al., 2007)

Pioneering studies to uncover a role of miRNAs in the skin showed that epidermal-specific deletion of Dicer using CRE-recombinase under the control of K14 promoter, eliminated production of all miRNAs, leading to severe defects in skin and hair follicle morphogenesis (Andl et al., 2006; Yi et al., 2006). These studies also revealed the differences between miRNA-dependent regulatory mechanisms required for formation of the epidermis and hair follicle. Dicer is present in developing hair placodes, the epidermis and outer root sheath of hair follicles (Andl et al., 2006). Hair follicles of newborn Dicer-deficient mice were initially underdeveloped and failed to invaginate into the dermis, but rather evaginated upward into the epidermis leading to formation of hair cysts (Andl et al., 2006; Yi et al., 2006). The failure to form and maintain hair follicles seems to be related to the early loss of stem cells, shown by a lack of bulge stem cell markers such as K15 and CD34 (Andl et al., 2006). The depletion of Dicer also led to the loss of expression of key signalling molecules, for instance Shh and Notch1 by postnatal day 7 (Andl et al., 2006). The loss of Notch1 may be responsible for the hyperproliferative epidermal phenotype (Proweller et al., 2006) in Dicer-depleted epidermis. In contrast to the defective hair follicle morphogenesis, the interfollicular epidermis remained on the whole unaffected and maintained its normal differentiation (Andl et al., 2006; Yi et al., 2006). These studies demonstrated the remarkable differences in the formation of the epidermis in comparison to the hair follicle and imply that certain miRNA or their target genes are specific for follicular stem cells but not for that of the interfollicular epidermis.

In addition to playing a role in miRNA biogenesis, Dicer is known to process other classes of small RNAs. In contrast, its cofactor DGCR8 is considered essential for miRNA biogenesis. Following studies of Dicer knockout mice, Yi et al utilised mice harbouring a conditional null Dgcr8 allele and crossed them with mice expressing K14-Cre (Yi et al., 2009). Mice that were Dicer or DGCR8 deficient showed indistinguishable phenotypes including evaginated follicles and severe defects in epidermal differentiation and barrier formation leading to dehydration and neonatal death (Yi et al., 2009). These studies hence establish that in skin, the primary function of both proteins is the biogenesis of miRNAs that are essential in the development of skin and hair follicles. They demonstrate that the loss of miRNA gene expression might differentially impact the execution of gene expression programs in distinct keratinocyte populations and that miRNAs exhibit a different effect on the follicular epithelium and the interfollicular epidermis.

More recently, an elegant study by Teta et al demonstrated that miRNAs are essential for postnatal hair growth (Teta et al., 2012). A knockout of the Drosha and Dicer enzymes during the anagen phase prevented hair follicles from entering a normal catagen phase, with eventual follicular degradation and stem cell loss (Teta et al., 2012). When Drosha and Dicer were deleted in the resting telogen phase hair follicles, follicular structure or epithelial stem cell maintenance was not affected and anagen induction through plucking of hair shafts led to proliferation and formation of a primitive transit amplifying matrix population. However, mutant matrix cells exhibited apoptosis and DNA damage leading to follicular degradation (Teta et al., 2012). This study revealed multiple functions of Drosha and Dicer in suppressing DNA damage in proliferating

matrix cells, facilitating the catagen phase of the hair cycle and maintaining follicular structure and their associated stem cells.

Ago proteins, which are vital components of the RISC complex, have also been shown to be vital for proper gene regulation. Recently Wang et al found that when both Ago1 and Ago2 are ablated together in the skin, the global expression of miRNAs is severely compromised causing severe defects in skin morphogenesis (Wang et al., 2012a). While these studies reveal that miRNAs in general are vital for formation and maintenance of skin and hair follicles, these knockout studies represent the loss of large sets of miRNAs and thus do not elucidate the significance of individual miRNA deletion in the skin.

The profiling of miRNA in the cells of epidermal and hair follicle lineages revealed their distinct expression patterns in the epidermis and hair follicle. Five microRNAs, miR-199a, miR-214, miR-126, miR-143 and miR-152 were identified by Yi et al as being widespread in the hair follicle in comparison to their presence in the epidermis alone (Yi et al., 2006). The contrast in expression of miRNAs reveals the specific spatio-temporal patterns of gene silencing during skin development which contributes to the commitment of cells to either epidermal or hair follicle cell fate.

1.9.1 microRNAs in the Skin and Hair Follicle Development

Several miRNAs have been identified as exerting specific functions in the skin (Aberdam et al., 2008; Wang et al., 2013a; Yi and Fuchs, 2010). One particular miRNA, miR-205, is involved in regulating epidermal homeostasis and regeneration. Recently Wang et al demonstrated one of the first examples of the deletion of single miRNA that causes severe developmental defects and compromises the function of skin and hair follicle stem cells (Wang et al.,

2013a). They showed that miR-205 controls neonatal expansion of skin stem cells resulting in neonatal lethality with severe defects in epidermal and hair follicle growth (Wang et al., 2013a). The ablation of miR-205 impairs the proliferation of interfollicular progenitors, with miR-205 KO progenitors displaying significantly reduced proliferation in comparison to wild type, most likely contributing to the thinner epidermis in miR-205 KO mice (Wang et al., 2013a). The proliferation of progenitors and stem cells in hair follicles was also compromised. In the hair follicle, BrdU analysis revealed that the hair follicle stem cells and outer root sheath progenitors were less proliferative in skin of KO mice. In contrast, the transit-amplifying matrix cells were equally proliferative between WT and KO mice (Wang et al., 2013a). The high enrichment of miR-205 in the hair follicle stem cells and outer root sheath but not in matrix cells indicates that the miR-205 specifically compromises the proliferation of progenitors and hair follicle stem cells (Wang et al., 2013a). A study by Yu et al showed that miR-205 is expressed in the epidermis and protects keratinocytes from apoptosis by targeting SHIP2 (SH2-containing phospoinositide), enhancing the Akt-signalling pathway (Yu et al., 2008). When miR-205 is suppressed in keratinocytes, migration is impaired due to cytoskeletal reorganisation, reduction in filamentous actin levels and an increase in focal contacts (Yu et al., 2010).

Yi et al also showed that one particular miRNA, miR-203, is scarcely detectable in mouse epidermis at E13.5 skin (when the skin is still a single layered epithelium), but was discovered as one of the most abundant miRNAs after embryonic day 15, when stratification begins, suggesting that its expression is induced during differentiation and stratification (Yi et al., 2008). In-situ hybridisation of mature skin revealed that miR-203 is expressed at high levels in

differentiated cells for instance the suprabasal epidermis and the inner root sheath of the hair follicle, but not expressed in areas of progenitor or stem cells such as the basal layer of the epidermis, in the hair follicle bulge or matrix (Yi et al., 2008). Transgenic mice over-expressing miR-203 in the epidermal basal layer frequently died shortly after birth and were characterised by a thinner epidermis and depletion of K5 positive basal layer cells (Yi et al., 2008). miR-203 has only limited potential to induce terminal keratinocyte differentiation (Lena et al., 2008), signifying that the main function of this miRNA is to restrict the epidermal proliferation and induce epidermal differentiation. Thus miR-203 defines a molecular boundary between proliferation and differentiation in suprabasal cells.

The transcription factor p63 was identified as an important target of miR-203 in epidermal keratinocytes (Lena et al., 2008; Yi et al., 2008). During embryogenesis p63 initiates epithelial stratification and maintains the proliferative potential of keratinocytes in the basal layers of mature epidermis (Koster and Roop, 2004). p63 belongs to the p53 family and the p63 gene expresses two proteins, one with an amino-terminal transactivation domain (TAp63) and one without (ΔNp63). Each isoform performs a distinct function in controlling keratinocyte proliferation and differentiation (Candi et al., 2006). miR-203 targets the ΔNp63, which is strongly expressed in the basal layer and is an essential regulator of stem cell maintenance in stratified epithelial tissues. Deletion of p63 in mice results in loss of all stratified epithelium (Senoo et al., 2007). When stem cells begin to differentiate into stratified epithelium in producing the epidermal barrier, miR-203 expression increases to suppress the activity of p63. The translational repression of p63 by miR-203 results in the inhibition of the proliferative potential of epidermal stem cells. Consequently, the

down regulation of p63 allows terminal differentiation to take place (Yi et al., 2008). This study provides an example of how miRNAs act as mediators, with miR-203 ensuring the transition of keratinocytes from proliferative, undifferentiated cells to terminally differentiated squamous epithelium. By mediating this process of differentiation, miR-203 helps form the vital skin barrier required to prevent dehydration and protect underlying organs from external threats.

Recent studies by Amelio et al have shown the importance of another miRNA, miR-24, in regulating epidermal differentiation by controlling actin adhesion and cell migration, and hair follicle morphogenesis by targeting Tcf-3 (Amelio et al., 2013; Amelio et al., 2012) . Using human keratinocytes and mouse epidermis, they demonstrated that miR-24 directly controls actin cable formation and cell mobility. Over-expression of miR-24 in proliferating cells was sufficient to trigger keratinocyte differentiation both in vitro and in vivo and directly targeted several cytoskeletal modulators (PAK4, Tks5 and ArhGAP19) (Amelio et al., 2012). When these targets were silenced the effects were the similar as produced by miR-24 over-expression. Restoration of these three targets blocked the effects of miR-24 over-expression (Amelio et al., 2012). Transgenic mice over-expressing miR-24 via K5 promoter resulted in defected hair follicle morphogenesis, with thinning of the hair coat and altered hair follicle structure (Amelio et al., 2013). They found altered expression of differentiation markers and that miR-24 directly represses the hair keratinocyte stemness regulator Tcf-3 (Amelio et al., 2013).

1.9.2 MicroRNAs and the Hair Follicle Cycle

Global miRNA profiling in the skin during the distinct stages of the hair cycle revealed diverse changes in expression of over 200 miRNAs (Mardaryev et al 2010). Although the bulk of these miRNAs were associated with the telogen phase of the hair cycle (Mardaryev et al., 2010), several have been shown to be vital for hair follicle growth. While the phenotypes observed in conditional knockout mice indicate that miRNAs overall are vital for normal hair growth, Mardaryev et al demonstrated the significance of an individual miRNA in the hair growth cycle (Mardaryev et al., 2010). It was shown that miR-31 is involved in regulating the anagen phase in the hair cycle through negative regulation of Fgf10, the components of BMP and Wnt signalling sclerostin and BAMBI, Dlx3 transcription factor, in addition to keratin genes. MiR-31 directly targets K16, K17, Dlx3 and Fgf10 (Mardaryev et al., 2010). Inhibition of miR-31 in the early and mid anagen phase resulted in accelerated anagen phase and altered differentiation of hair matrix keratinocytes (Mardaryev et al., 2010).

A study by Zhang et al. demonstrated that a subset of miRNAs was preferentially expressed in the bulge (Zhang et al., 2011), which is a reservoir of multipotent stem cells that give rise to several cell lineages, including keratinocytes, sebocytes and the melanocytes (Botchkareva et al., 2001; Cotsarelis, 2006; Snippert et al., 2010). Specifically miR-125b is strongly expressed in stem cells and dramatically decreased in stem cell progeny and was functionally relevant to tissue homeostasis (Zhang et al., 2011). The functions of miR-125b were identified by sustaining its expression in K14 expressing cells where it is normally expressed at low levels, such as the outer root sheath and the matrix. Overexpression of miR-125b in skin stem cells and

their progeny in transgenic mice resulted in hyperthickened epidermis, enlarged sebaceous glands and the development of alopecia. All these effects were fully reversible upon restoring normal miR-125b expression (Zhang et al., 2011). Two key transcription factors, Blimp1 and Vdr, were identified as are direct targets of miR-125b, which function as mediators of the phenotypic properties produced in miR-125b transgenic mice (Zhang et al., 2011). Vdr is required for hair follicle differentiation (Palmer et al., 2008), whilst Blimp1 is a critical regulator of sebaceous gland development (Horsley et al., 2006). Thus it has been speculated that by co-ordinately fine-tuning a large number of proteins, miR-125b acts as a rheostat to regulate the control of stem cell proliferation, differentiation and cell fate (Yi and Fuchs, 2011; Zhang et al., 2011).

1.9.3 MicroRNAs and the Hair Follicle Pigmentation

The pigmentation of hair follicles occurs through interactions between matrix keratinocytes, melanocytes, and fibroblasts of the dermal papilla. These three components make up the follicular melanin unit (Slominski et al., 2005). The process of melanogenesis is a multistep process controlled by several key enzymes which includes tyrosinase (Tyr), tyrosinase-related protein 1 (Trp1), tyrosinase-related protein 2 (Trp2) (Yamaguchi and Hearing, 2009). The microphthalmia associated transcription factor (MITF) is the most vital transcription factor involved in regulating melanocyte functions (Lin and Fisher, 2007; Yamaguchi and Hearing, 2009). Levy et al showed that MITF directly regulates expression of Dicer, which expression is upregulated during melanocyte differentiation (Levy et al., 2010). They showed increased levels of Dicer and Mitf in the differentiated melanocytes located in the bulb of anagen hair follicles, in comparison to bulge where the melanocyte stem cells reside

(Levy et al., 2010). The correlation of Dicer and MITF mRNA expression was also investigated via qRT-PCR in primary human melanocytes and expression patterns were found to highly parallel. A knockout model was developed using mice harbouring the floxed Dicer allele, bred with mice expressing CRE-recombinase driven by the tyrosinase promoter. The targeted deletion of Dicer in the melanocyte lineage led to loss of epidermal and follicular melanocytes and mice subsequently developed a white coat (Levy et al., 2010).The effects of Dicer on melanocyte survival were mediated by miR-17, because the upregulation of miR-17 correlated with a decrease in expression of the pro-apoptotic gene BIM. In addition, partial rescue of melanocytes from apoptosis caused by loss of Dicer was achieved by BIM knockdown using (Levy et al., 2010)

1.9.4 MicroRNAs as Downstream Effectors

The downstream regulation of miRNAs is also involved in controlling the characteristics of skin keratinocytes. A study by Antonini et al showed that p63 maintains cell cycle progression by directly repressing members of the miR-34 family (Antonini et al., 2010). When p63 expression was reduced in primary mouse keratinocytes using siRNA, increased levels of miR-34a and miR-34c was observed, with concomitant cell cycle arrest and inhibition of the cell cycle regulators cyclin D1 and Cdk4. Down-regulation of miR-34a and miR-34c substantially restored cell cycle progression and expression of cyclin D1 and Cdk4, indicating that these specific miR-34 family members have a significant role downstream of p63 in controlling epidermal cell proliferation (Antonini et al., 2010).

A study by Ahmed et al identified that BMP4 negatively regulates the expression of miR-21 in epidermal keratinocytes and the anti-tumour activity of BMPs in the skin is mediated, at least in part via miR-21 target genes, such as Pdcd4, Timp1, Pten and Tpm1 (Ahmed et al., 2011). In primary mouse keratinocytes transfected with BMP4 the expression of miR-21 was significantly reduced in the keratinocytes. Consistent with this finding was the significantly increased levels of miR-21 in transgenic mice overexpressing the BMP antagonist noggin under control of the K14 promoter. Transfection of primary mouse keratinocytes with a miR-21 mimic, led to the identification of the existence of two groups of BMP target genes, which are differentially regulated by miR-21 (Ahmed et al., 2011). These included selected BMP-dependent tumour-suppressor genes (Pten, Pdcd4, Timp3 and Tpm1) negatively regulated by miR-21, as well as miR-21-independent Id1, Id2, Id3 and Msx2 that predominantly mediate the effects of BMPs on cell differentiation. In primary mouse keratinocytes and HaCaT cells transfected with miR-21 mimic, miR-21 prevented the inhibitory effects of BMP4 on cell proliferation and migration (Ahmed et al., 2011)

Taken together, these studies reiterate the concept that microRNAs play an important role in skin and hair follicle biology. The balance of gene expression is regulated through the targeting of several signalling pathways by miRNA, in distinct skin cell populations, essential for execution differentiated-associated gene expression programs and cell communication during development and homeostasis. However, more research is required to elucidate the role of additional individual miRNAs in controlling gene regulation during hair development and cycling, wound response, and skin aging.

Research Aims

Hair follicle development and growth encompass numerous biological processes that occur in the human body such as cell proliferation, differentiation, migration and apoptosis. Therefore the hair follicle serves as a crucial and viable model which transcends hair biology. miRNAs have emerged as crucial layer of gene regulation that control various biological functions. In recent years, considerable progress has been made in in identifying the molecular mechanisms underlying the regulatory functions of miRNAs in skin and hair follicle development and growth (Aberdam et al., 2008; Andl et al., 2006; Yi et al., 2006; Yi et al., 2009). However, the regulatory role of many miRNAs in skin and hair follicle homeostasis remains to be elucidated, which could provide a greater insight into how biological processes function normally and in disorders which arise in the skin and hair follicle.

This project investigates the role for microRNA-214 in hair follicle development and cycling. It will be addressed via the following aims:

(i) To investigate the spatio-temporal expression of miR-214 during hair morphogenesis and hair cycling by utilising quantitative PCR analysis and *in-situ* hybridisation

(ii) To determine the regulatory role of miR-214 on hair follicle development and cycling by exploring a phenotype of doxycycline-inducible miR-214 (K14-rtTA/TRE-miR-214) transgenic mice. How modulation of miR-214 levels affects proliferation and differentiation will be defined.

(iii) To determine genome-wide changes in the keratinocyte gene expression programme induced by miR-214: microarray analysis, qRT-PCR validation

and immunofluorescence analysis will be utilised to compare changes in gene expression in the skin and hair follicles of K14-rtTA/TRE-miR-214 and wild-type mice.

(iv) To identify miR-214 target genes in the keratinocytes by employing the bioinformatic analysis and luciferase reporter assays.

2.0 Material and Methods

2.1 Animals

Animal studies were performed under protocols approved by Home Office Project Licence (UK) and Boston University (USA). K14-rtTA/TRE-miR-214 mice were generated on FVB background. Mice had free access to food (standard rodent diet) and water. Animal housing was maintained under continuous 12-hour light and dark cycles with temperature and humidity at 21±1°C and 40-60%, respectively. All animal handling and experimentation was undertaken by Dr A Mardaryev at the University of Bradford and Dr A Sharov at Boston University.

TRE-miR-214 construct was generated by Dr M Ahmed (University of Bradford). To generate TRE-miR-214 construct, DNA fragment, containing the primary-mmu-miR-214 coding sequence was isolated from pCMV-miR-214 plasmid DNA (Origene, USA) followed by blunt-end ligation into the pSTblue-1 vector (Millipore, UK). This fragment was then excised and ligated into BamHI-SalI sites of the pTRE2-Dual 2 plasmid (Clontech, UK), which contains a pTight promoter consisting of a modified minimal CMV promoter, and seven direct repeats of a 36 bp regulatory sequence that contains the 19 bp tet-operator sequence, mCherry, and an internal ribosome entry site (IRES2) (**Figure 2.1**). All cloning was verified by sequencing. A PspxI fragment from TRE-miR-214 construct was purified and pronuclear injections were performed in the Transgenic Core at the Boston University School of Medicine using FVB/NJ mice as a genetic background.

Founders were identified by PCR using transgene promoter specific DNA primers: forward; 5-GTTCATGTACGGCTCCAAG-3 and Reverse; 5-CGCAGCTTCACCTTGTAG-3. To generate double-transgenic K14-rtTA/TRE-

miR-214 mice, TRE-miR-214 mice were crossed with K14-rtTA according to standard protocols. To activate expression of tet/doxycycline-responsive transgenes, mice were fed chow containing 625mg Doxycycline (Dox)/kg chow (Bio-Serv).

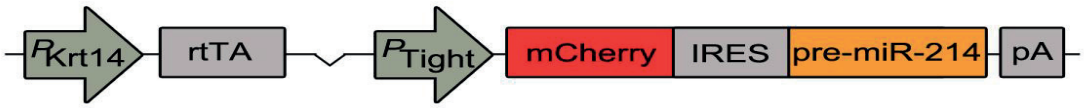

Figure 2.1. Inducible miR-214 transgene construct under control of tetracycline-response element

2.1.2 Genotyping

Genotyping was carried out using conventional PCR. Approximately 80 cryosections of tissue samples, cut 10µm thick in sterile conditions were added to a 1.6ml eppendorf tube kept on dry ice. Samples were briefly spun down before the addition of 50 mM NaOH (600µl per tube). Samples were placed in a water-bath at 90°C for at least 30 minutes to favour tissue degradation and DNA extraction. The reaction was inactivated by adding 50µl of 1M TrisHCl (ph 7.6) to each tube. Following this samples were mixed using a vortex and spun down at 14,000g for 5 minutes at 4°C. 2µl of supernatant containing DNA was then used for the PCR reaction. The following amounts were used for each PCR reaction: DNA 2µl, Primer Forward (1x) 0.1µl Primer Reverse (1x) 0.1µl dNTPs (0.2mM) 0.4µl Taq Polymerase 0.1µl Buffer (5X) 4µl H_2O 13.3µl. Following PCR, amplified products were detected using gel electrophoresis. Samples were subjected to electrophoresis at 100V on 1% agarose gel stained in ethidium

bromide. A 1kb molecular weight ladder was used in addition to positive and negative controls.

For K14-rtTA mouse genotyping, primer sequences were used provided by the Jackson Laboratory, including forward primer: oIMR7862 - 5′-CACGATACACCTGACTAGCTGGGTG-3′ and reverse primer oIMR7863: 5′-CATCACCCACAGGCTAGCGCCAACT-3.′ For TRE-miR-214 mice, the forward primer 5'-AGAACGTATGTCGAGGTAG-3' and reverse primer 5' – TTGGAGCCGTACATGAAC-3' were used.

PCR was performed under the following cycling conditions: 94°C for 3 minutes, [94°C for 30 seconds, 67°C for 60 seconds, 72°C for 60 seconds] for 35 cycles, 72°C for 2 minutes)

2.2 Tissue collection

Tissue samples were collected at several developmental time-points using established procedures (Paus et al., 1999). Embryonic and postnatal samples were collected after pregnant mice were fed doxycycline at embryonic day 10 in order to activate expression of tet/doxycycline-responsive transgenes. Tissue samples were collected at embryonic day 15, 17 and 19 (E15, E17, E19). For postnatal samples tissue was collected at postnatal days 1 and 8.

The hair cycle was induced in the back skin of 9-week-old mice by depilation using a wax/rosin mixture. At this point follicles are in telogen and the depilation of mice induces a new anagen phase across the depilated area (Muller-Rover et al., 2001). Before depilation, mice were fed doxycycline continuously for 1 week and tissue samples were collected at 3, 5, 8 and 12 days post depilation.

Harvested skin was embedded in OCT mounting media (Tissue tek, CA, USA) and frozen in liquid nitrogen (Paus et al., 1999).

2.2.1 Isolation and culture of primary mouse epidermal keratinocytes

Primary mouse epidermal keratinocytes (PMEKs) were prepared from newborn mice at postnatal days 2-3. PMEKs were isolated and cultured as described previously (Lichti et al., 2008). Mice were euthanized following Home Office guidelines, by Dr A Mardaryev. Mouse pups were rinsed in deionised water and washed in 70% ethanol twice for 2 minutes. The following procedures were carried out in a laminar-flow cell culture hood with sterilised tools. The limbs of the mice were removed at the joints to allow easier removal of skin. The tail and genitalia were removed and an incision was made along the dorsal midline and the skin was dissected from the body of the mice using forceps. The skin was floated dermis side-down in 0.25% trypsin without EDTA overnight at 4°C. Following overnight incubation with trypsin, the epidermis was separated from the dermis. The epidermis was transferred to a 50ml falcon tube containing Eagle's minimal essential medium (EMEM) (Lonza, Slough, UK) supplemented with 4% chelated foetal bovine serum (FBS) (Gibco, UK), 100 units/ml pencillin & 100 µg/ml streptomycin, 0.05mM calcium chloride (Sigma- Aldrich), $2x10^{-9}$M 3,3' 5-triiodo-L-thyronine (T3) (Sigma-Aldrich), 2mM L-glutamine (Gibco, UK), 0.4µg.ml hydrocortisone, 5µg/ml bovine serum, 10^{-10} M cholera toxin (Sigma-Aldrich) and 10ng/ml epidermal growth factor (EGF) (Invitrogen, UK). The epidermis was minced using sterile scissors and a 10ml pipette to release the keratinocytes. This was followed by filtration using a sterile 70µm nylon filter (BD Biosciences) into a fresh falcon tube to remove cornified sheets. Cell culture plates were coated with type I collagen, prepared by coating the base

with a solution consisting of Hank's balances salt solution (HBSS) (Gibco, UK), 100mg/ml bovine serum albumin (BSA) (Sigma-Aldrich), 1M HEPES pH 6.5 (Gibco, UK) and 3mg/ml collagen (Invitrogen). The excess collagen solution was aspirated and the plates were allowed to dry before plating the PMKs into at required density into media. PMEKs were grown in EMEM calcium-free medium (Lonza, Slough, UK) supplemented with 0.05 mM calcium, at 33°C, 8% CO_2 (Scientific Laboratory Suppliers, Hessle, UK) until 60–70% confluent.

2.2.2 Cell transfection

PMEKs were transfected with 200 nM synthetic miR-214 inhibitor (anti-miR-214), miR-214 mimic (pro-miR-214) or miRNA negative controls (Dharmacon), using Lipofectamine RNAiMax (Invitrogen, Paisley, UK). Lipofectamine RNAiMax and synthetic miRNA mixture was incubated for 20 minutes at room temperature in a ratio of 2:1 and subsequently added to PMEKs in antibiotic free media and incubated for 4 hours at 33°C, 8% CO_2. After 4 hours, media was aspirated and complete media was added to the plates. Cells were harvested 24 hours after transfection and used for further analysis.

2.2.3 Luciferase reporter assay. HaCaT cells were grown in Dulbecco's modified Eagle's medium (Invitrogen, UK) supplemented with heat-inactivated 10% FBS in an atmosphere of 5% CO2 at 37°C, until 60–70% confluent. 3′UTR fragments of *β-catenin* and *Shh* containing miR-214 putative target sites were amplified from mouse genomic DNA using forward and reverse primers containing XhoI and NotI restriction sequences, respectively. For 3′UTR of *β-catenin* fragment 5-CGAGGAGTAACAATACAAATGG-3 and 5-CAGGTTCACTAGAACATAACAC-3 forward and reverse primers, respectively, were used. To amplify a fragment of 3'UTR of *Shh* 5-

ATGAACGGACCTTCAAGAGC -3 and 5-GCATAGCAGGAGAGGAATGC -3 primers were used. The amplified fragments were cloned at XhoI and NotI sites downstream of CV40 promoter-driven Renilla luciferase cassette in pCHECK2 (Promega, UK). Site directed mutagenesis was performed using QuikChange II XL Site-Directed Mutagenesis Kit (Agilent Technologies, UK) to mutate β-catenin binding site following manufacturer's instructions. For dual luciferase assay, these constructs (200 ng) were co-transfected with 200 nM miR-214 mimic or negative control mimic (Dharmacon) into HaCaT cells using 0.5 µl Lipofectamine 2000 (Invitrogen, UK) in 96-well plates. At 24 h after transfection, the relative luciferase activities were determined using Dual-Glo Luciferase Assay System (Promega, UK). Assay was performed in triplicate for three independent trials.

2.2.4 TOPFlash and FOPFlash Wnt reporter assays. HaCaT cells were seeded onto 12-well dishes 24 hours before transfection. At 80% confluency, a TOPFlash Wnt reporter plasmid (Addgene plasmid 12456) was transfected into each well in combination with i) control oligonucleotide (200 nM), ii) 10µM of BIO (R&D Systems, UK), iii) pro-miR-214 (200 nM), and iv) pro-miR-214 (200 nM) and 10µM BIO. BIO (6-bromoindirubin-3'-oxime) induces Wnt signalling by targeting Glycogen Synthase Kinase 3 (GSK3), a component of the β-catenin degradation complex (Sato et al., 2004). Transfection was performed using Lipofectamine 2000 (Invitrogen). FOPFlash (TOPFlash mutant) reporter plasmid (Addgene plasmid 12457) was used as a control. Lipofectamine 2000 and plasmid mixture was incubated for 20 minutes at room temperature in a ratio of 2:1 and subsequently added to HaCats in antibiotic free media and incubated for 4 hours at 33°C, 8% CO_2. The cells were cultured for 24 hours and relative luciferase activities were determined using Dual-Glo-luciferase assay system

(Promega, UK) on the Infinite 2000 micro-plate reader. All assays were performed in triplicate for three independent trials.

2.3 RNA Isolation

2.3.1 Isolation from the skin:

Total RNA was isolated from snap frozen experimental samples by using TRIzol (Qiagen, Crawley, UK). Approximately 100 cryosections of tissue samples cut 10µm thick in sterile conditions were added to a 1.6ml eppendorf tube kept on dry ice. One ml of TRIzol RNA isolation reagent was added to the tissue sections and homogenised via vortexing prior to storage at -80°C. RNA was isolated following manufacturer's instructions. RNA samples were thawed out for approximately 5 minutes and vortexed to ensure complete homogenisation. Following this 100µl BCP (1-Bromo-3-chloropropane) was added and thoroughly mixed and incubated at room temperature for 15 minutes. Samples were centrifuged at 12,000xG for 15 minutes at 4°C and the aqueous phase was transferred to a new eppendorf tube. 500µl of isopropanol was added and incubated at room temperature for 15 minutes. Samples were again centrifuged for 8 minutes in order to for the RNA to form a pellet. 75% ethanol was added to samples followed by centrifugation at 7500xG for 5 minutes. The supernatant was removed and the RNA pellet was dissolved in sterile Tris-EDTA buffer.

2.3.2 Isolation from cells

Total RNA was isolated from cultured keratinocytes after transfection using TRIzol. 1ml was added to each well of a 6 well plate and a sterile cell scraper was used to detach cells before being added to a 1.6ml eppendorf and stored at -80°C. RNA was isolated as described in 2.3.1.

2.3.3 DNase treatment

In order to reduce genomic DNA contamination, RNA samples were treated using Turbo DNase kit (Ambion). 0.1 volume 10X TURBO DNase buffer and 1µl TURBO DNase was added to the RNA and mixed gently. Samples were then incubated at 37°C for 20-30 minutes. Re-suspended DNase Inactivation Reagent was added to the sample (0.1 volume) and mixed well followed by incubation for 2 minutes at room temperature, mixing occasionally. Samples were centrifuged 10,000xG for 1.5 minutes and RNA was transferred to a fresh eppendorf tube.

2.4. Real Time PCR for detection of miR-214 using TaQman method

2.4.1 Principle:

cDNA synthesis of miRNA requires a specialised novel stem loop Reverse Transcription (RT) primer during reverse transcriptase reaction. This stem loop RT primer overcomes the fundamental problem of miRNA being very short (approx. 22nt long). The TaqMan® Assay kit (Applied Biosystems, USA) overcomes this problem by extending the 3' end of the mature miRNA, via binding of RT primer, therefore providing a longer reverse transcription product suitable for real time PCR (Chen et al., 2005; Schmittgen et al., 2008).

2.4.2 TaqMan complementary DNA (cDNA) Synthesis:

RNA was isolated from cells or tissue samples using TRIzol reagent (Qiagen, Crawley, UK) as described in 2.3.1 followed by Turbo DNase treatment, as described in 2.3.3. cDNA was synthesised using TaqMan® Assay Kit (Applied Biosystems, USA) following manufacturer's instructions. The following reagents were used for each reverse transcription: 0.15 µl of 100mM dNTPs, 1µl of

multiscribe reverse transcriptase, 1.5µl 10X reverse transcriptase buffer, 0.19µl RNase inhibitor (20units/µl) and 4.6µl water. 7µl of this master mix was combined with 5ng of total RNA. This was mixed gently and 3µl of RT primer (Applied Biosystems, USA) assay was added to reaction mix followed by brief centrifugation. cDNA was synthesised using a Master Cycler gradient machine (Eppendorph, Cambridge, UK) under the following cycling conditions: 16°C for 30 minutes, followed by 42°C for 30 minutes and 85°C for 5 minutes.

2.4.3 Taqman real-time PCR procedure for miRNA expression

Expression of miR-214 was determined using TaqMan real-time PCR Assay (Applied Biosystems, USA) under the following cycling conditions: 95°C for 10 min, followed by 40 cycles of: 95°C for 15 s, and 60°C for 60 s. Differences between samples and controls were calculated based on the Ct ($^{\Delta\Delta}$Ct) method and normalised to the small nucleolar RNA 202 values (SnoRNA) using Genex database software (Bio-Rad, UK). SnoRNAs are constitutively expressed across all tissues; the use of same assay chemistry and RNA isolation protocols makes snoRNAs ideal candidates for normalisation of miRNA expression (Chen et al., 2005). Data were pooled, the means ± SD. were calculated, and statistical analysis was performed using an unpaired Student's t-test.

2.4.4 First-strand cDNA qRT-PCR:

RNA was isolated from the cells or tissue as in 2.3.1. For qRT-PCR, 1µg of each RNA sample was used as a template for cDNA synthesis using Reverse Transcription synthesis system (Promega, UK). 1µg of RNA was incubated at 70°C for 10 minutes. The following mixture was prepared on ice: 4µl 20µM $MgCl_2$, 2µl of Reverse Transcription buffer 10X, 2µl dNTP mix 10mM, 0.5 µl RNase inhibitor, 0.6µl AMV Reverse Transcriptase, 0.5µg of random primers.

Final volume was made up 20µl. The mixture was added to the RNA and incubated in a thermal cycler with the following conditions: 23°C for 10 minutes, 42°C for 15 minutes, 95°C for 5 minutes and 4°C for 5 minutes.

2.4.5 Real-Time PCR procedure:

qRT-PCR was performed with using Applied Biosystems Fast PCR mix, using 10ng cDNA and 1µM primers. PCR primers were designed with Beacon Designer software (Premier Biosoft International; **Table 1**). Optimum annealing temperature was determined for primers by performing qRT-PCR at five different temperatures using mouse reference cDNA: 55°C, 57°C, 59°C and 61°C and 63°C. Analysis of melting curves was used to determine optimum annealing temperature. Amplification was performed using the following conditions using StepOnePlus™ System PCR system (Applied Biosystems): 95°C for 5 minutes, followed by 40 cycles of denaturation (95°C for 15 seconds), annealing (30 seconds at temperature experimentally determined for each primer pairs) and elongation (72°C for 15 seconds). For each gene of interest, qRT-PCR was performed in triplicates. Differences between samples and controls were calculated using Ct ($^{\Delta\Delta}$Ct) equitation method and normalised to the beta-actin. Beta-actin (β-actin) is frequently and constitutively expressed in most tissues and cells, thus referred to as a housekeeping gene.

Table 1: List of primer sequences for qRT-PCR

Gene	Accession number	Sense Sequence	Anti-sense Sequence
β-actin (ACTB)	NM_007393	TTCCAGCCTTCCTTCTTG	GGAGCCAGAGCAGTAATC
β-catenin (Ctnnb1)	NM_001165902	GCCACCAAACAGATACATAC	CCTCTCAGCAACTCTACAG
Cyclin dependent kinase inhibitor 2a	NM_009877	GCTCTTTGTGTTCCGCTG	CTCTGCTCTTGGGATTGG

(Cdkn2a/p16)			
Cyclin dependent kinase inhibitor 2d (Cdkn2d/p19)	NM_009878	GGCTCCTACAGGCAACAG	TAGATGGCTCACACTTCAGG
Cyclin D1 (Ccnd1)	NM_007631	GAGACCATTCCCTTGACTGC	GAAATGAACTTCACATCTGTGGC
Cyclin D2 (Ccnd2)	NM_009829	GGATGCTAGAGGTCTGTGAGG	CCAACACTACCAGTTCCCAC
Cyclin B1 (Ccnb1)	NM_172301	ATAATCCCTCTCCAAGCCCG	CTGCTCTTCCTCCAGTTGTC
Cyclin Dependent Kinase 1 (CDK1)	NM_007659	ATCAGACTTGAAAGCGAGGA	GGTGTAAGTAACTCTTAACGAGTG
Ectodysplasin receptor (Edar)	NM_010100	GCCCCACCGAGTTGCCGTTT	CCAGCCGCTCGATCTGCACC
Lymphoid enhancer binding factor1 (Lef-1)	NM_001276402	ACTCCAAGCAAGGCATGTC	GGGTGATCTGTCCAACGC
Patched 2 (Ptch2)	NM_008958	TCCGCACCTCATATCCTAGC	CTGTCTCAATTACAGCCACTCG
Smoothened (Smo)	NM_176996	GCTGGAGTAGTCTGGTTCGT	GAGTCTCCATCTACCTGAGCC
Sclerostin domain containing 1 (Sostdc1)	NM_025312	CTTCCTCCTGCCATTCATCTC	GAACTCGACTGTTTCGATCCAG
Sonic Hedgehog (Shh)	NM_009170	GTTTATTCCCAACGTAGCCGA	CTTGTCTTTGCACCTCTGAGTC

2.5 Microarray

Newborn K14-rtTA/TRE-miR-214 and WT mice were treated with doxycycline for 48 hr to induce miR-214 expression. Back skins were harvested and treated with dispase at 37°C for 30 min to obtain epidermis and hair follicle epithelium. Total RNA was isolated by TRIzol (Sigma) and processed for microarray analysis by using 41K Whole Mouse Genome 60-mer oligo-microarray (Agilent Technologies, Mogen, St. Louis, MO). Microarray data was validated using qRT-PCR from RNA samples of K14-rtTA/TRE-miR-214 and WT mice. Microarray gene expression data from K14-rtTA/TRE-miR-214 mice was

normalised to corresponding data from WT mice and functionally annotated by Dr K Poterlowicz at University of Bradford. Fold changes in gene expression were determined as a ratio of normalised expression values.

2.6 In situ hybridization

For miRNA detection, skin cryosections (10 μm) were fixed in 4% paraformaldehyde for 10 minutes at room temperature. After acetylation in triethanolamine buffer (4.5 mM triethanolamine, 6M HCl and 3 mM acetic acid anhydride) for 10 minutes and premobilisation (1% Triton X-100/1xDEPC treated phosphate buffer-saline) for 30 minutes, slides were hybridised with 2.5 pmol DIG-labelled miR-214 probe (Exiqon, Copenhagen, Denmark) diluted in hybridization buffer (50% formamide DI, 2× SCC, 1% dextran sulfate, and 0.4 mg/ml t-RNA) for 16-18 h at 55°C overnight. Slides were subsequently washed in 2x SCC (4 times, 10 minutes each at 67°C), 0.1x SCC (60 minutes at 67°C), 0.2x SCC (10 minutes at Room Temperature). Immunodetection of miR-214 was performed with sheep alkaline phosphatase conjugated anti-DIG antibody (1:5000; Roche, Germany) for 3 hours at room temperature, followed by a staining reaction with nitro-blue tetrazolium (NBT) and 5-bromo-4-chloro-3'-indolyphosphate (BCIP) solution (Roche, Germany) for 16-18 hours at room temperature. Slides were washed twice using PBS, 5 minutes for each wash, before being mounted with mounting media.

2.7 Immunohistochemistry

For immunohistochemistry, tissue sections were fixed in either 4% PFA for 10 minutes at room temperature or acetone for 10 minutes at -20°C. Tissue sections stained with phospo-H3 were additionally permeabilised with 100% methanol at -20°C for 10 minutes, followed by blocking in 10% donkey serum

for 1 hour. Primary antibodies used in this study are listed in **Table 2**. Cryosections were incubated with primary antisera overnight at 4°C, followed by application of corresponding Alexa-555-labelled or Alexa-488-antibodies (Invitrogen; diluted 1:200) for 1 hour at 37°C. Only primary antibody was used for a negative control. Incubation steps were interspersed by four washes with phosphate buffer-saline (PBS), 5 minutes each wash. Sections were counter stained with DAPI (4', 6-diamidino-2-phenylindole) in mounting media (Vector Labs). Image preparation and analysis were performed using a fluorescent microscope in combination with DS-C1 digital camera and ACT-2U image analysis software (Nikon, Tokyo, Japan). Confocal images were captured using the Zeiss LSM 510 Meta Confocal Microscope.

Table 2: Primary Antibodies

Antigen	Host	Dilution	Source
β-Catenin	Rabbit	1:2000	Abcam, UK
CD34	Goat	1:200	BD Pharmingen, UK
Cytokeratin 10	Rabbit	1:500	Abcam, UK
Cytokeratin 14	Guinea Pig	1:500	Acis, USA
Dlx3	Goat	1:500	Santa Cruz, USA
Edar	Goat	1:500	R&D Sytems
Ki67	Rabbit	1:100	Abcam, UK
Lef-1	Rabbit	1:100	Cell signalling, UK
Lhx2	Goat	1:200	Santa Cruz, USA
Loricin	Rabbit	1:100	Abcam, UK
Phospho-histone H3 (Ser28)	Rabbit	1:100	Cell Signalling, UK
Phospho-Smad 1/5/8	Rabbit	1:500	Abcam, UK
Sox9	Rabbit	1:250	Santa Cruz, USA
Shh	Rabbit	1:100	Santa Cruz, USA

2.8 Alkaline phosphatase staining

For morphological assessment of skin sections, alkaline phosphatase (AP) staining was performed. In the skin, alkaline phosphatase is strongly expressed by fibroblasts within the dermal papilla; hence it is a useful tool to identify stages of follicular development and cycling (Handjiski et al., 1994). For alkaline phosphatase staining cryosections (10μm) were fixed in 4% PFA for 10 minutes at room temperature and then washed twice in PBS, 5 minutes for each wash. Slides were then incubated in developing solution (100 mM NaCl pH 8.3, 100 mM Tris, pH 9.5 and 20 mM HCL, 0.05% Naphtol ASBI phosphate, 0.5% DMF, 25 mM Sodium Nitrite and 5% new fuchsin) for 15 minutes at room temperature, followed by counterstaining with haematoxylin for 1 minute at room temperature. Slides were washed in running water and mounted.

2.9 Histomorphometry and statistical analysis.

Histomorphometry analysis of hair follicles was performed using every tenth cryosection of dorsal skin of K14-rtTA/TRE-miR-214 and wild-type mice in order to exclude the repetitive evaluation of the same hair follicle. The number of hair follicles per mm of epidermal length was calculated using sections from dorsal skin of K14-rtTA/TRE-miR-214 and WT samples at the different developmental points, including E17.5, P0.5, and P8.5 days (n=3 per each experimental group).

Proliferation in the epidermis was assessed by the calculation of the number of Ki67+ cells to the DAPI+ cells in 50-60 microscopic fields. Proliferation in the hair follicle was assessed by calculating the ratio of pH3(Ser28)+ to DAPI+ cells per hair bulb in 50 to 60 hair follicles of either K14-rtTA/TRE-miR-214 or WT mice. Hair bulb diameter was measured across the widest part of the bulb

(critical line of Auber) derived from three animals per experimental and control group. Altogether, 200–350 follicles in 50–60 microscopic fields, derived from three K14-rtTA/TRE-miR-214 animals from distinct time points were analyzed and compared to a corresponding number of hair follicles from the appropriate, age-matched wild-type mice.

For the assessment of the hair shaft length and width, hair were plucked from the back skin of K14-rtTA/TRE-miR-214 (*n*=4) and wild-type mice (*n*=4) at P22, i.e., in the telogen phase of the hair cycle. Quantitative analysis of the different types of the hair shafts produced in dorsal skin (guard, awl, auchene and zigzag) was done by the analysis of approximately 250 plucked hair shafts using morphological criteria as described previously (Sharov et al., 2006)

The percentage of hair follicles in different stages of hair cycle was assessed and calculated in K14-rtTA/TRE-miR-214 at day 3 and 5 post depilation-induced hair cycle, respectively, as well as in their corresponding wild-type littermates. All evaluations were performed on the basis of accepted, well-defined morphologic criteria of hair follicle classification (Muller-Rover et al., 2001).

Comparative analysis of Sox9+ cells was done by evaluating the ratio of the number Sox9+ to DAPI+ cells in the outer root sheath (from the distal end of the bulb to the sebaceous duct). In total, 50 to 60 follicles of either WT or K14-rtTA/TRE-miR-214 mice were included in the analysis. Data were pooled, the means ± SD. were calculated, and statistical analysis was performed using an unpaired Student's t-test.

3.0 Results

3.1 miR-214 exhibits discrete expression patterns in the epidermis and hair follicles in developing and postnatal skin

To understand a role of miR-214 in the control of skin morphogenesis and hair follicle cycling, miR-214 expression was initially examined in mouse dorsal skin at different developmental stages. qRT-PCR analysis revealed low levels of miR-214 expression in embryonic skin at day 14.5 (E14.5) during onset of the hair follicle development, whilst its expression was dramatically elevated in the skin of newborn mice **(Fig. 3.1 a)**. High miR-214 expression levels were maintained in the skin until postnatal day 12 (P12), whilst during transition to catagen (P16-17), its expression decreased and remained low during subsequent telogen phase (P20-22) **(Fig. 3.1 b)**.

In situ hybridisation analysis showed that in E14.5 skin, miR-214 expression was first seen in the supra-basal epiermal layers followed by more homogenous distribution among the distinct epidermal layers at E17.5 (**Fig. 3.1 c**). Hair follicle placodes also showed miR-214 expression during all stages of embryonic skin development (**Fig. 3.1 c**). During more advanced stages of hair follicle morphogenesis (P0.5-P3.5), miR-214 expression predominated in the supra-basal epidermal layers and throughout the epithelium of stage 3-6 hair follicles (**Fig. 3.1 e**), while in fully developed hair follicles, miR-214 expression significantly increased in the developing hair matrix and individual cells of the outer root sheath (**Fig. 3.1 f**).

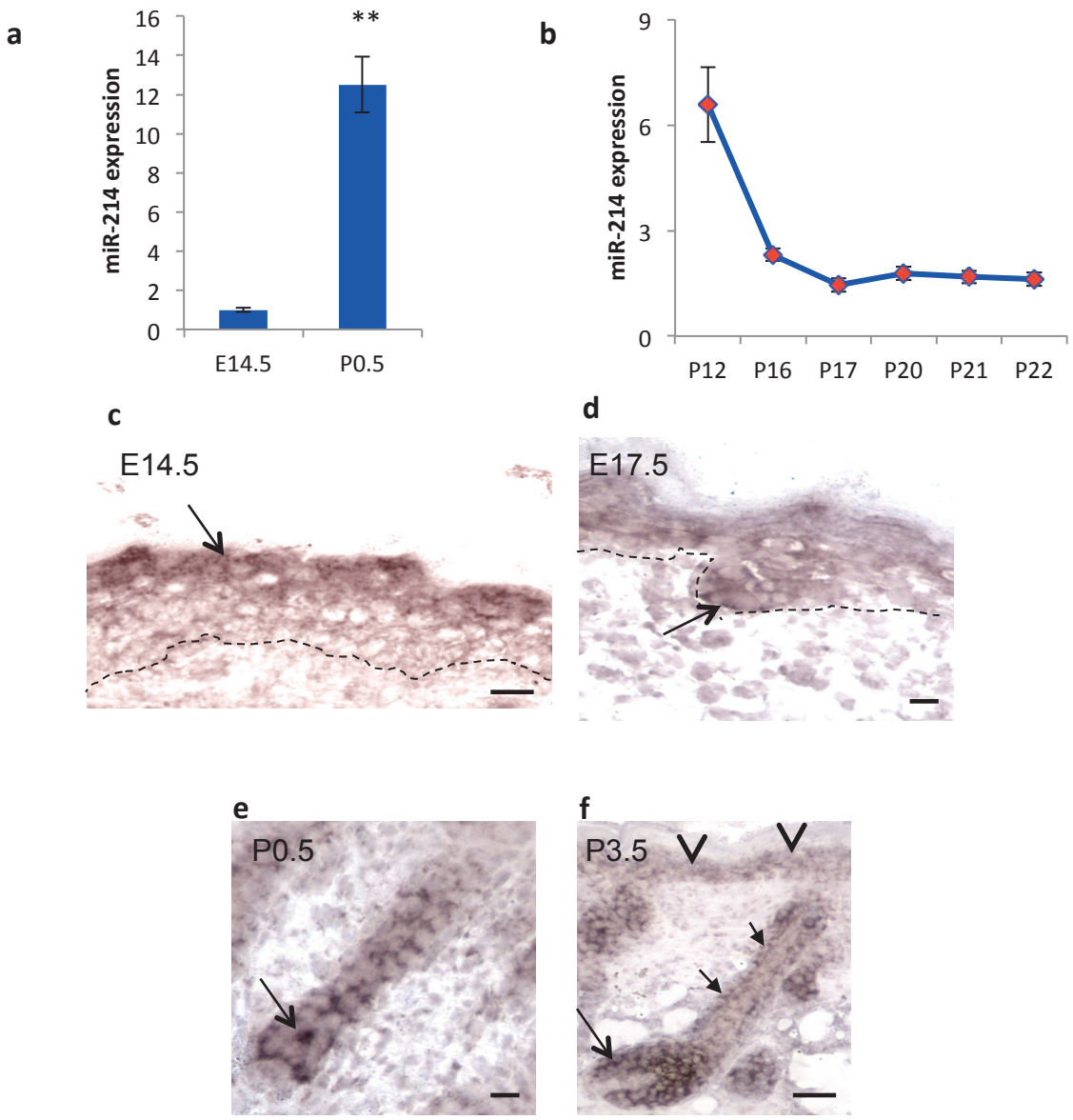

Figure 3.1. Relative and spatio-temporal expression of miR-214 during hair follicle morphogenesis. (a) TaqMan qRT-PCR of miR-214 expression: low levels of miR-214 in embryonic skin at day 14.5 (E14.5), significant increase of miR-214 in the skin of newborn mice at postnatal day 0.5 (P0.5); **(b)** high expression of miR-214 in the anagen-like stage (P12), expression decreases during catagen (P16-17) and low levels of expression in telogen skin (P20-P22); **(c-f)** In-situ hybridisation of miR-214 during hair follicle morphogenesis: **(c)** in E14.5 skin, miR-214 is detected in the supra-basal layers of the epidermis (arrow); **(d)** miR-214 is expressed in the developing hair placodes at E17; **(e)** during more advanced stages of morphogenesis (P0.5), miR-214 is throughout the epithelium of stage 3-6 hair follicles (arrow); **(f)** miR-214 expression in the epidermis (arrowheads), and in the developing hair matrix (arrows) and individual cells of the outer root sheath (small arrows) in fully developed hair follicles (stage 8, P3.5), **P value<0.02, Unpaired students t-test; n=3. Scale bar 50μm.

3.2 miR-214 shows discrete expression patterns in the epidermis and hair follicles during the hair cycle

In order to produce a synchronised hair follicle cycle, the established method of depilating hair follicles from the dorsal skin of 7 week-old mice, when all hair follicles are in telogen, was utilised (Muller-Rover et al., 2001). Removing hair shafts immediately induces homogenous anagen development over the entire depilated region. Skin was initially harvested at the telogen stage (unmanipulated skin) followed by anagen II [3 days post depilation (dpd)], anagen IV (5 dpd), anagen VI (8-12 dpd) and catagen (17-19 dpd).

qRT-PCR analysis revealed similar fluctuations in miR-214 levels in adult skin during depilation-induced hair cycle: miR-214 expression progressively increased during hair follicle transition from telogen to anagen and was maximal during late anagen stage of the hair cycle (day 12 post depilation) followed by rapid decrease during catagen (**Fig. 3.2 a**).

In situ hybridisation showed that during the hair follicle cycle, miR-214 expression was restricted to the secondary hair germ of the telogen follicles **(Fig. 3.2 b)**, while during early anagen phase miR-214 expression appeared in the growing hair matrix, the outer root sheath and in the bulge area (**Fig. 3.2 c**). In fully developed anagen follicles, miR-214 was prominently expressed in the hair matrix, as well as in the distinct cells of the outer root sheath (**Fig. 3.2 d**). During catagen, miR-214 expression was seen in the regressing hair matrix, outer root sheath and in the epithelial strand of the mid-catagen hair follicle, whilst its expression disappeared from the epithelial strand at the advanced catagen stages (**Fig. 3.2 e**). These data suggest that miR-214 shows discrete expression patterns in the selected epithelial compartments of the skin.

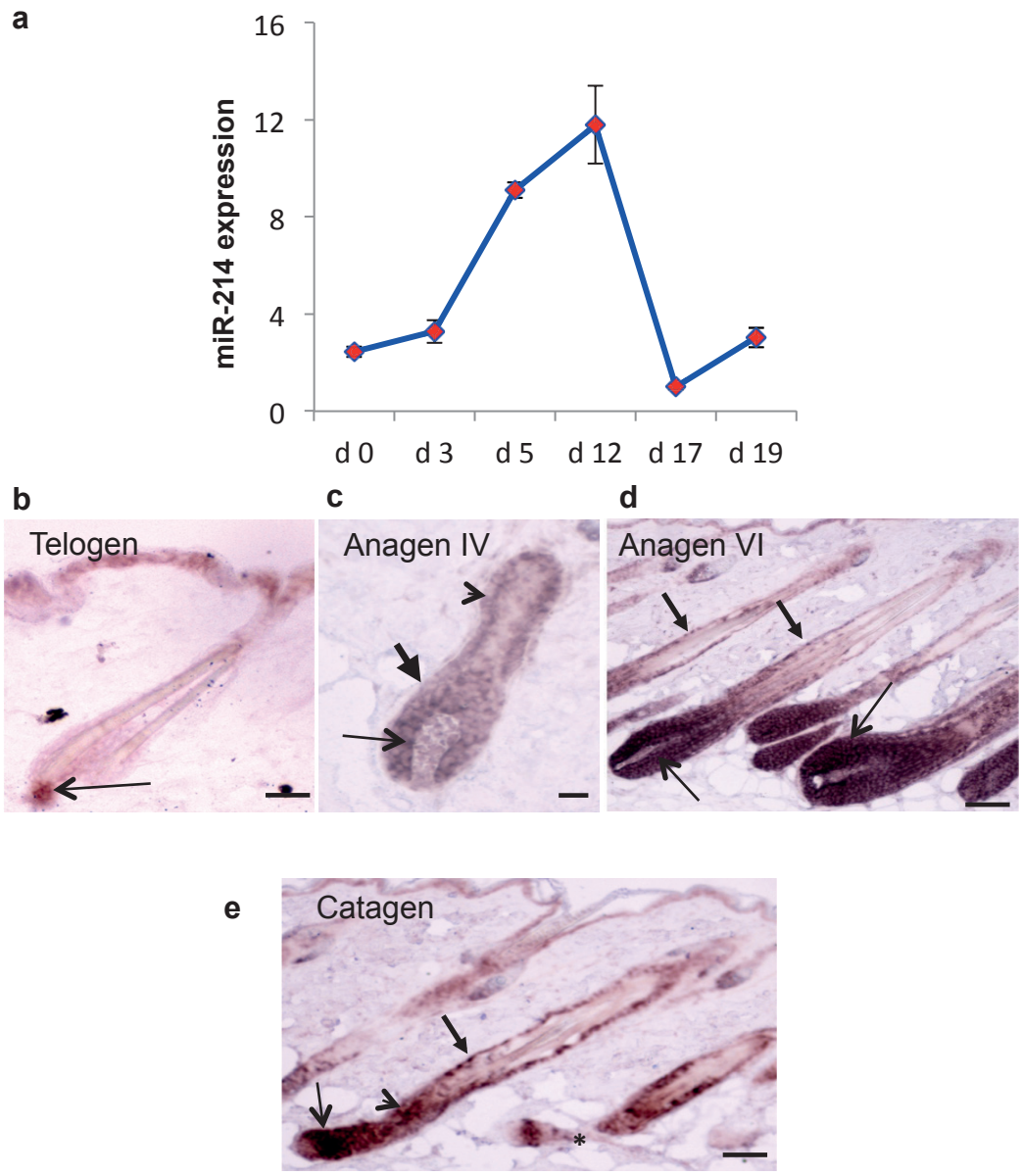

Figure 3.2. Relative and spatio-temporal expression of miR-214 during hair follicle cycling. (a) TaqMan qRT-PCR of miR-214 during depilation-induced hair cycle: expression of miR-214 increases during telogen-anagen transition and reaches maximal levels during late anagen (12 dpd), followed by a decrease during catagen (17 dpd); **(b-e)** In-situ hybridisation of miR-214 during depilation-induced hair cycle: **(b)** miR-214 was detected in the secondary hair germ of telogen follicle (arrow); **(c)** In mid-anagen hair follicles, miR-214 is expressed in the matrix (arrow), the outer root sheath (small arrow) and the bulge (arrowhead); **(d)** In late anagen, prominent expression of miR-214 was detected in the hair matrix (arrows), in the outer root sheath (small arrows); **(e)** In catagen, miR-214 is expressed in the regressing hair matrix (arrow), the outer root sheath (small arrow) and in the epithelial strand of the mid-catagen hair follicle (arrowhead); in advanced catagen hair follicles, miR-214 expression disappears from the epithelial strand (asterisk), scale bar 50μm. Abbreviations: dpd - days post-depilation

In the epidermis, it is predominantly localised in the supra-basal epidermal layers, while considerably weaker expression is detectable in the basal epidermal layer. In the hair follicle, it is prominently expressed in the stem cells (secondary hair germ) and their lineage committed progenies in the outer root sheath and hair matrix.

3.3 Generation of K14-rtTA/TRE-miR-214 transgenic mice

To further elucidate the role of miR-214 in skin and hair follicle development, Krt14-driven over-expression in mice was used as a model. In order to amplify the miR-214 effects on epithelial progenitor cell population (basal epidermal layer, hair follicle outer root sheath), where miR-214 was relatively under-expressed compared to more differentiated keratinocytes of suprabasal epidermal layer or hair follicle matrix (**Fig. 3.1 c, d; Fig. 3.2 b, c, d**), mice overexpressing miR-214 under the control of doxycyclin-inducible Krt14-promoter (K14-rtTA/miR-214-TRE or double transgenic, DTG) were generated.

Mice were genotyped using conventional PCR. The K14 and miR-214 primers were designed specifically for the promoter region that was integrated into the genome for transgenic mice. The primers were then used to characterise wild type and K14-rtTA/TRE-miR-214 transgenic mice. These primers only bind to specific regions used to generate transgenic mice; therefore samples that produced bands for both K14 and miR-214 indicated successful amplification of the miR-214 target sequence by the transgene promoter construct. Mice samples that produced no bands for both sequences were classed as wild type **(Figure 3.3 a).** To validate further, expression of transgene was determined by qRT-PCR and immunofluorescence. Induction of transgene by doxycycline (Dox) starting from day 10 of embryonic development (E10.5), which

corresponds to the onset of K14 expression in the developing epidermis (Byrne et al., 1994), caused a significant increase in the level of miR-214 in the skin of DTG mice, which was confirmed by qRT-PCR (**Fig. 3.3 b**). Transgene activation was also confirmed by the detection of a red fluorescent transgenic reporter mCherry, which was a part of the transgenic construct. mCherry fluorescence was seen in the basal epidermal layer of DTG mouse skin at E15.5, whilst it was undetectable in the epidermis of WT mice (**Fig. 3.3 c**).

3.4 K14-rtTA/TRE-miR-214 mice exhibited less visible hair shafts in comparison to WT littermates

WT and DTG littermates were given doxycycline from embryonic day 10 and photographed at postnatal day 15 (P15) **(Fig. 3.4 a).** DTG mice were viable, fertile and looked similar to their WT littermates at birth. However, as mice started to produce the visible hair shafts, DTG mice could be easily distinguished by the appearance of a “rough” fur coat, in contrast to WT mice producing a normal ‘smooth’ fur coat. (**Fig. 3.4 b**).

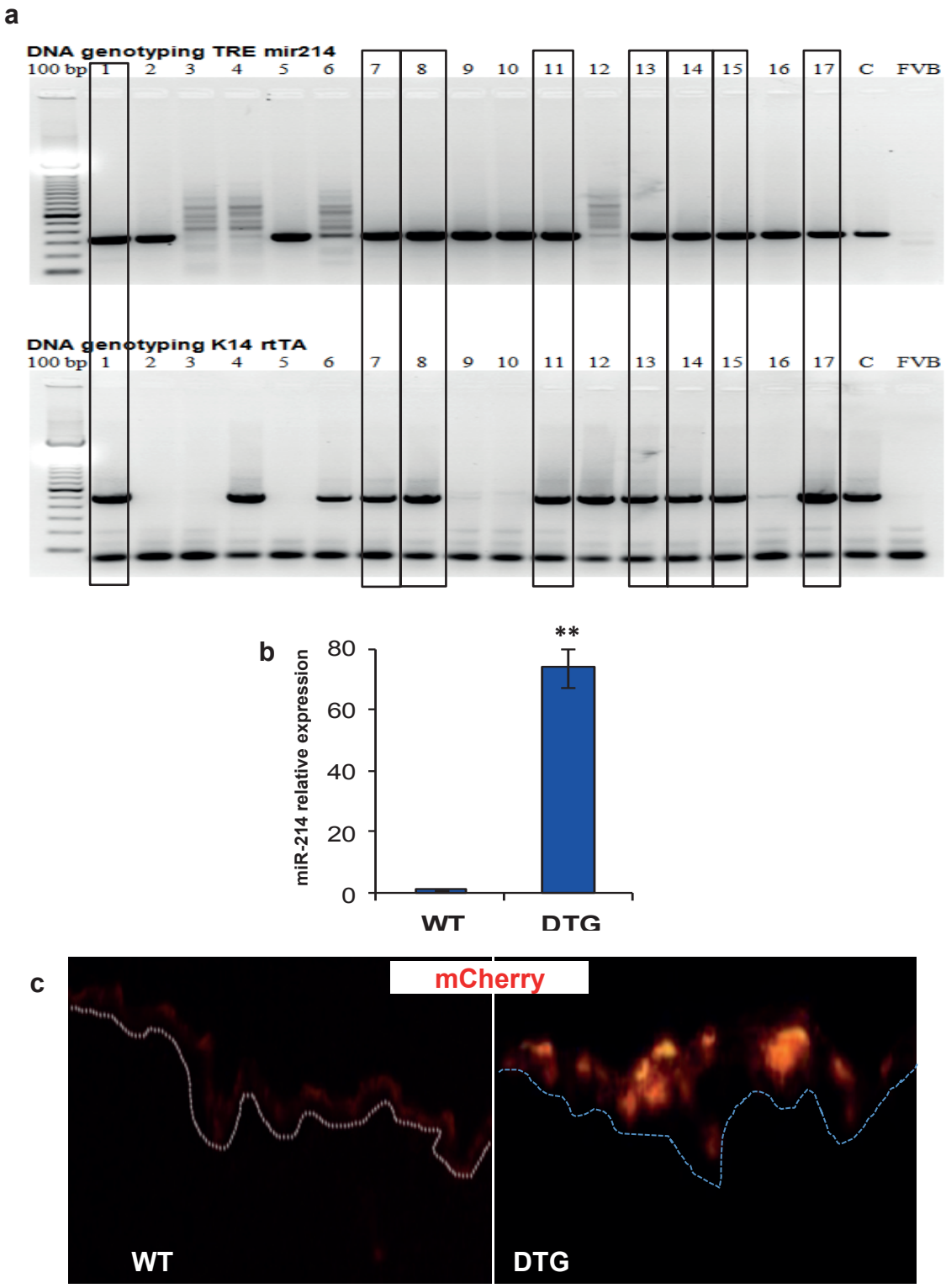

Figure 3.3 Genotyping of wild type and K14-rtTA/TRE-miR-214 transgenic mice. (a) Mice were genotyped using conventional PCR. Samples that produced bands for both K14 and miR-214 indicated successful amplification of the transgene promoter construct and were characterised as DTG. Samples that did not produce any bands were classed as WT. The gel also contains a negative control of FVB mice selected from a different litter of mice and a positive control from a previously identified K14-rtTA/TRE-miR-214 mouse. DTG mice samples are circled; **(b)** TaqMan qRT-PCR: significant increase of miR-214 levels in the skin of DTG mice (**P<0.02, unpaired students t-test; n=3); **(c)** mCherry fluorescence in the epithelium of DTG mice indicating activation of miR-214. Abbreviations: WT –wild type, DTG – double transgenic mice

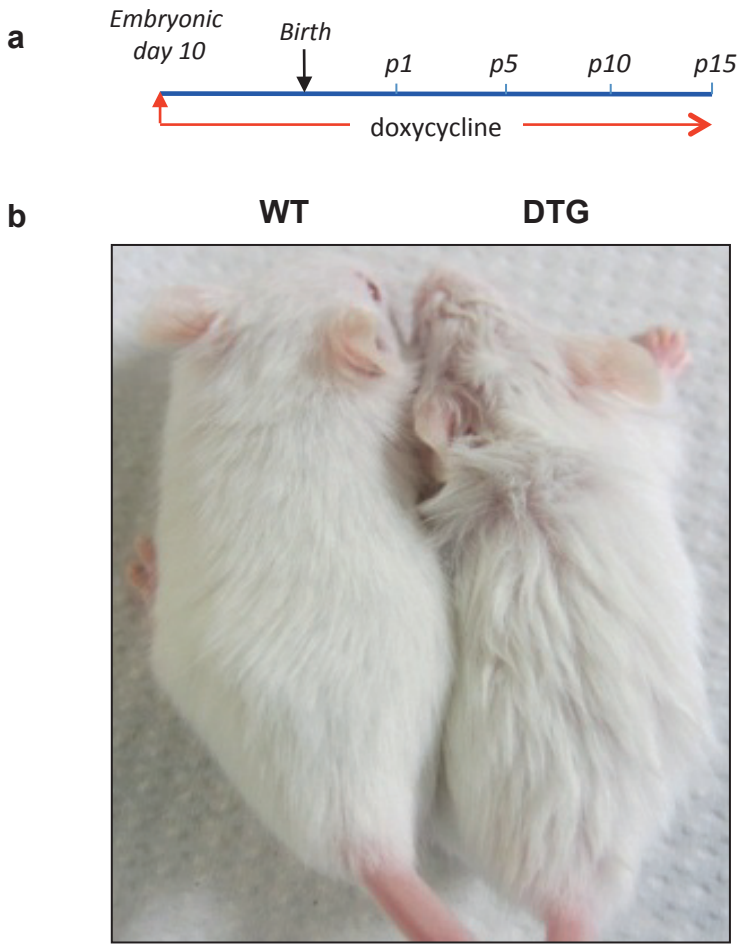

Figure 3.4. Photograph of wild-type and K14-rtTA/TRE-miR-214 mice at postnatal day 15. (a) Schematic illustration of the experimental design; **(b)** K14-rtTA/TRE-miR-214 (DTG) mice, exhibited a 'rough' fur coat, whereas wild-type mouse shows an appearance of a 'smooth' fur coat.

3.5 K14 driven overexpression of miR-214 results in a thinner epidermis and reduced epidermal proliferation in DTG mice compared to WT littermates

Histomorphological analysis of epidermal thickness during distinct developmental time points revealed that epidermis of DTG mice was significantly thinner during early stages of morphogenesis (E15.5 and P0.5) as well as upon a completion of hair follicle morphogenesis (P8) **(Fig. 3.5 a)**. To assess whether it was due to the differences in proliferation and/or differentiation, expression of a marker of proliferation Ki-67 and the markers of epidermal differentiation Keratin 14, Keratin 10 and Loricrin was analysed.

Ki-67 expression was visibly reduced in the epidermis of DTG mice **(Fig. 3.5 b)**. Quantitative analysis of the number of Ki67 positive cells in the epidermis suggested a significant reduction in the number of Ki67 positive cells in DTG mice compared to WT controls at early embryonic developmental stages (E15.5) as well as at the latest points of postnatal development (P8.5) (**Fig. 3.5 c**)

The expression of K14 in basal and K10 and Loricrin in supra-basal epidermal layers in DTG mice were quite similar to WT epidermis (**Fig. 3.5 d, e**), suggesting that miR-214 over-expression does not alter epidermal differentiation.

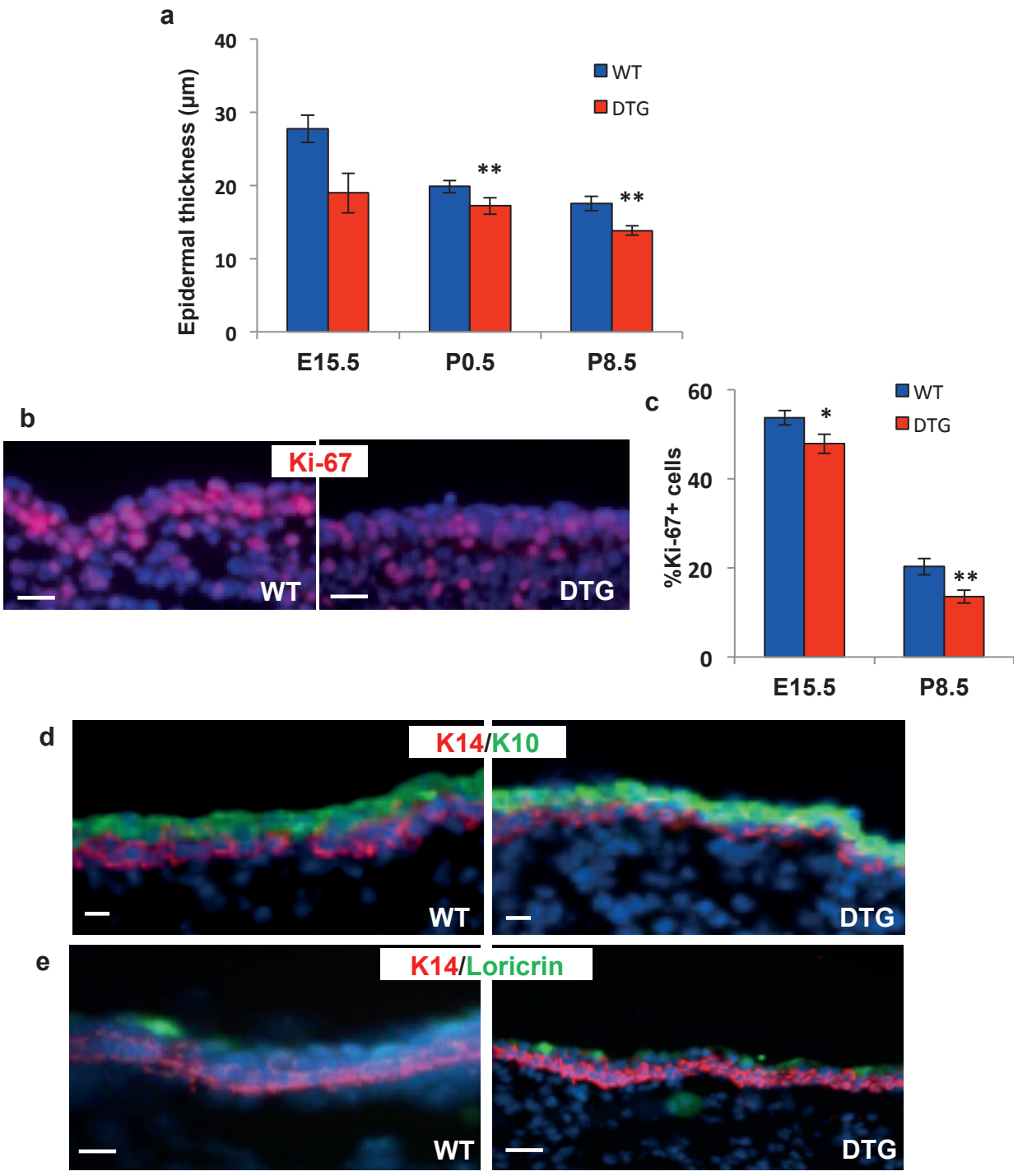

Figure 3.5. Analysis of epidermal development in wild-type and K14-rtTA/TRE-miR-214 mice. **(a)** Histomorphological analysis of epidermal thickness in WT and DTG mice; a significant reduction in thickness in DTG mice at E15.5, P0.5, P8.5; **(b)** Immunodetection of marker of proliferation Ki-67: visible decrease in the number of Ki-67+ cells in the epidermis of E14.5 skin; **(c)** Quantitative analysis of Ki-67+ cells in the epidermis of WT and DTG mice: significant reduction in Ki-67+ cells at E15.5 and P8.5 in the epidermis of DTG mice; **(d-e)** Immunodetection of markers of differentiation (K14, K10 and Loricrin) in E14.5 skin: no visible differences between expression of K14, K10 and Loricrin in WT and DTG mice at E15.5. (*P value<0.05, **P<0.02, unpaired students t-test; n=3). Scale bar 50µm.

3.6 Over-expression of miR-214 causes an inhibitory effect on hair follicle morphogenesis

Histomorphological analysis of dorsal skin of DTG mice revealed a visible reduction in the number and size of hair follicles during all developmental points **(Fig. 3.6 a)**. The overexpression of miR-214 caused a reduction of approximately 30% of hair follicle placodes in the back skin of DTG mice compared to WT littermates at embryonic day 15 (**Fig. 3.6 b**).The number of induced hair follicles was also significantly decreased in DTG mice at E17.5, P0.5 and P8 compared to WT controls (**Fig. 3.6 c**). This suggests that miR-214 over-expression alters the process of induction in both primary and secondary hair follicles

To analyse whether overexpression of miR-214 affected the rate of hair follicle development, stages of hair follicle morphogenesis were quantified according to established morphological criteria (Paus et al., 1999) **(Fig. 3.6 d).** Quantification of hair follicle stages at embryonic day 19.5 during hair morphogenesis revealed the majority of hair follicles were in stages 2-4 in both WT and DTG mice **(Fig. 3.6 d).** Therefore, overexpression of miR-214 does not affect the rate of hair morphogenesis in DTG mice compared to WT littermates.

At postnatal day 8 all hair follicles in DTG mice reached the first anagen-like phase similarly to WT controls (**Fig. 3.6 a**). In addition, a total skin thickness was significantly reduced in the skin of DTG mice to WT littermates (**Fig. 3.6 e**).

.

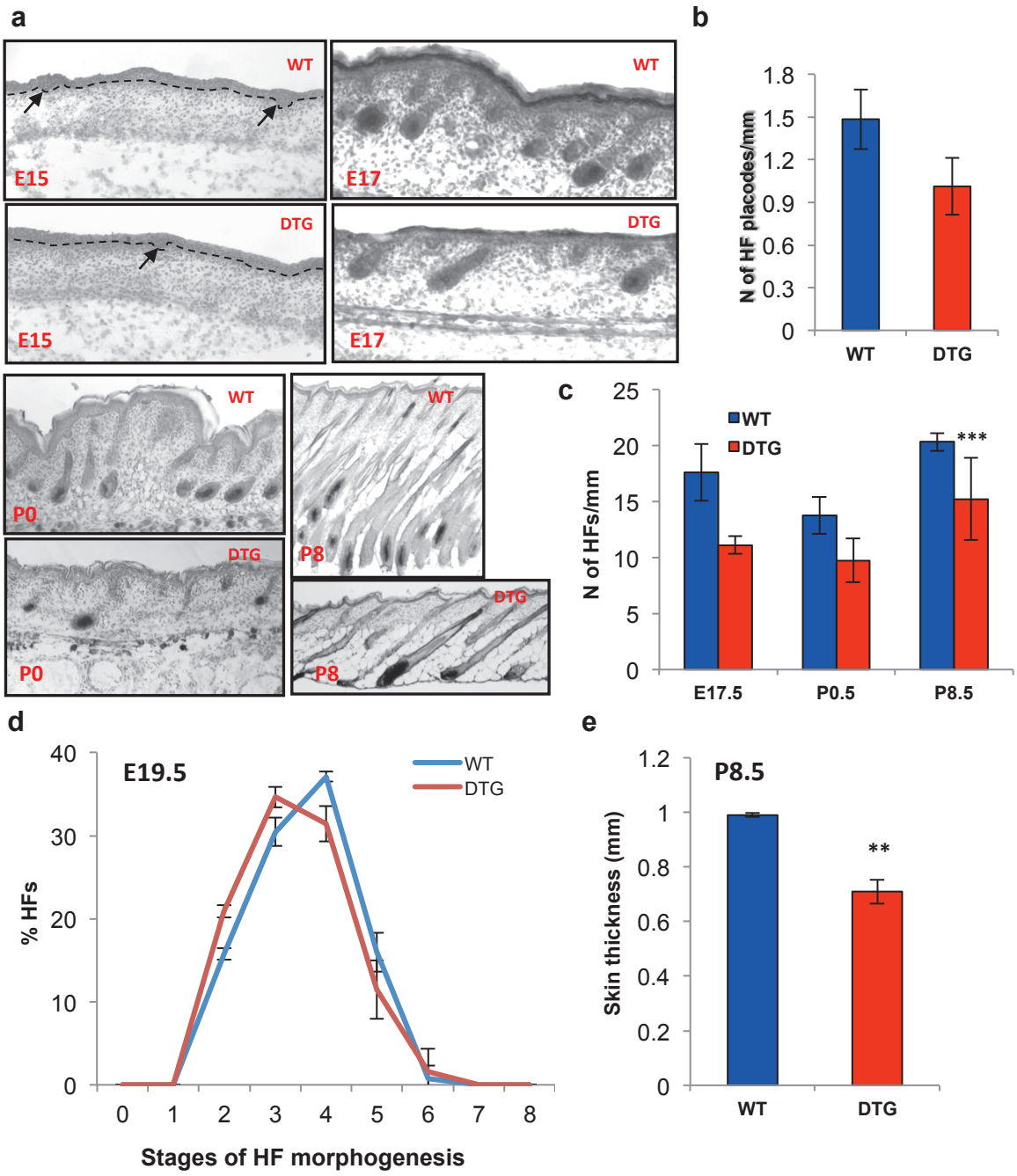

Figure 3.6. Overexpression of miR-214 exerts an inhibitory effect on hair follicle morphogenesis. (a) Microphotographs of histology of back skin; visible reduction in the number of hair placodes and hair follicles from embryonic day 15 to postnatal day 8; **(b)** quantitative analysis of the number of hair placodes at embryonic day 15 per mm of epidermal length; significant reduction in DTG mice compared to WT littermates; **(c)** quantitative analysis of the number of hair follicles per mm of skin from embryonic day 17.5 to postnatal day 8.5; significant reduction in the total number of hair follicles in DTG mice compared to WT littermates; **(d)** quantification of hair follicle at the different stages of morphogenesis at embryonic day 19.5 in WT and DTG mice using established morphological criteria (Paus et al. 1999); no significant difference between WT and DTG mice; **(e)** analysis of total skin thickness at postnatal day 8. (*P value<0.05,**P<0.02,***P<0.001, unpaired students t-test.)

In contrast to WT hair follicles, epithelial portion of the fully developed anagen-like hair follicle was significantly shorter in the skin of DTG mice at postnatal day 8 **(Fig. 3.7 a).**

To determine if reduced number of the hair follicles seen in the miR-214 overexpressing mice were due to the under developing of the specific hair follicle type, the proportion of guard, awl, auchene and zigzag follicles was evaluated in DTG and WT mice. Hair shafts were plucked from WT and DTG mice at postnatal day 20 for analysis **(Fig. 3.7 b)**. The plucked hair shafts were separated by different types and counted in order to determine the proportion of each hair type in WT and DTG mice. Analysis revealed the proportions of the guard, awl, auchene and zigzag hair shafts in DTG mice were similar to those in WT mice **(Fig. 3.7 c)**. However analysis of hair shaft thickness revealed a significant decrease in the thickness of guard, awl, auchene and zigzag hairs in DTG mice compared to WT littermates (**Fig. 3.7 d**), whereas no significant difference in the shaft length between WT and DTG mice was detected **(Fig. 3.7 e).**

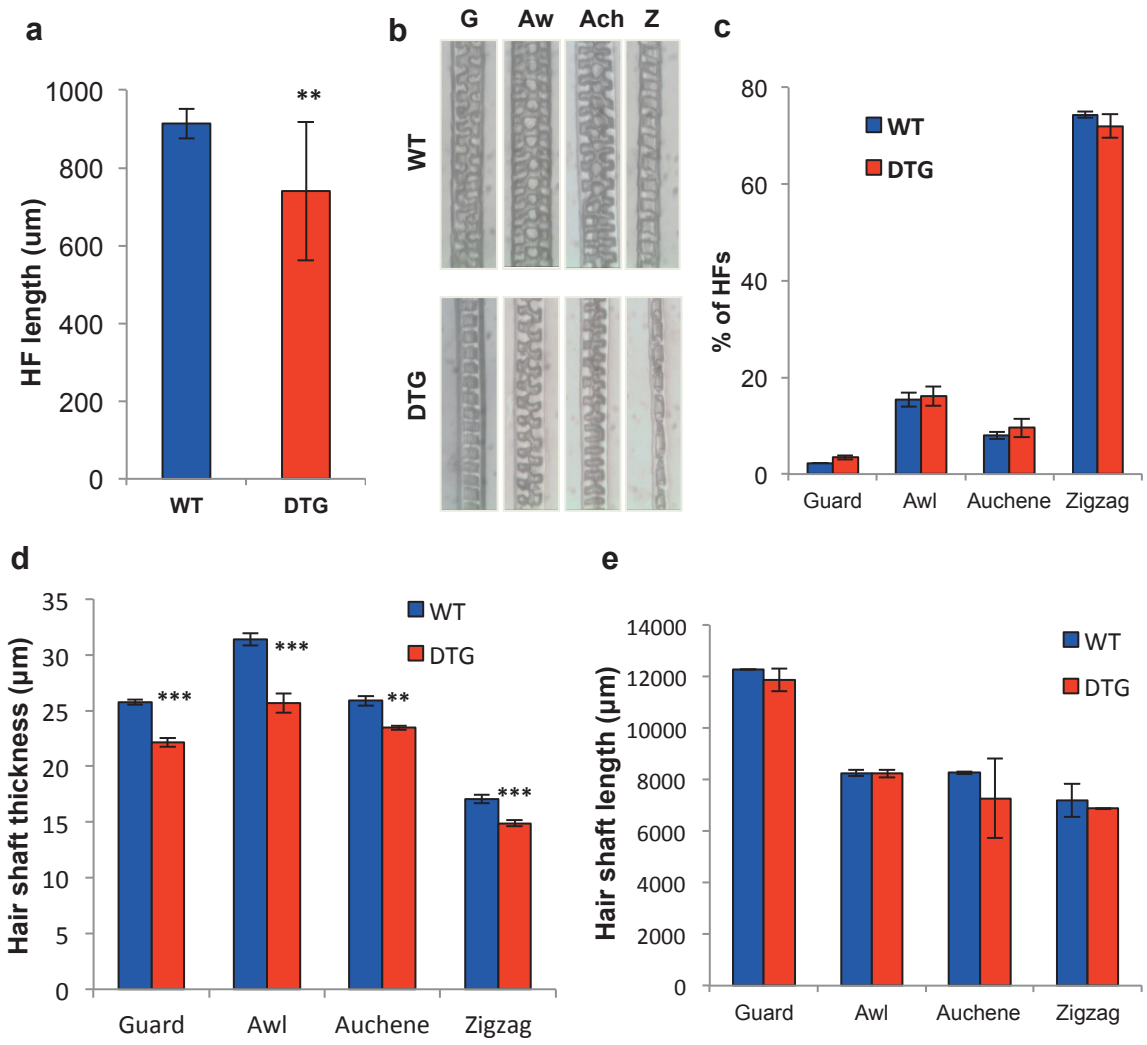

Figure 3.7 Analysis of different hair follicle types in wild-type and K14-rtTA/TRE-miR-214 mice. (a) Analysis of hair follicle length at postnatal day 8 in WT and DTG mice; significant reduction in the length of DTG hair follicles compared to WT; **(b)** microphotographs of hair shaft types (guard, awl, auchene and zigzag) plucked from mice at postnatal day 20; visible reduction of hair shaft thickness of all hair shaft types in DTG mice compared to WT; **(c)** quantification of hair shaft types in WT and DTG mice; no significant difference between WT and DTG mice; **(d)** morphometric analysis of hair shaft thickness plucked from mice at postnatal day 20; significant reduction of hair shaft thickness in all hair shaft types in DTG mice compared to WT; **(e)** morphometric analysis of hair shaft length at postnatal day 8; no significant difference between WT and DTG mice. (mean ± SD, **P value<0.02, ***P<0.001, unpaired Student's t-test); Abbreviations: G-guard, Aw-awl, Ach-auchene, Z-zigzag

3.7 Over-expression of miR-214 causes a reduction in the hair bulb size

To assess the effect of miR-214 overexpression on proliferation of hair bulb keratinocytes during hair follicle morphogenesis, immunofluorescence of pH3 (Ser28) was performed at postnatal day 8 **(Fig. 3.8 a, b)**. Quantification of pH3 (Ser28) positive cells revealed a significant reduction in proliferating cells in the hair bulbs of DTG mice compared to WT littermates **(Fig. 3.8 b)**.

To analyse effects of miR-214 overexpression on hair bulb size, the diameter of hair bulbs was measured across the widest area (critical line of Auber) in WT and DTG mice at postnatal day 8 **(Fig 3.8 d).** Analysis of hair bulb diameter revealed a significant reduction in the diameter of the hair bulbs of DTG mice compared to WT littermates **(Fig. 3.8 d).**

Analysis was also carried out to determine whether miR-214 overexpression affects the dermal papilla of hair follicles. Quantification of the number of dermal papilla cells was performed in WT and DTG mice at postnatal day 8 **(Fig. 3.8 e)**. Quantitative analysis revealed a significant reduction in the number of dermal papilla cells in the hair follicles of DTG mice compared to WT littermates **(Fig. 3.8 e).**

To further analyse possible causes of decreased proliferative activity due to miR-214 overexpression, qRT-PCR analysis of Cdkn2d and Igf-1 was performed in postnatal day 8 skin **(Fig 3.8 f, g)**. Cdkn2d (p19) is a cyclin-dependent kinase inhibitor, which inhibits the activity of cyclins preventing progress of the cell cycle (Hirai et al., 1995). Igf-1 is crucial for proper hair shaft differentiation and was shown to have a mitogenic and morphogenetic function in pelage hair follicle (Weger and Schlake, 2005). qRT-PCR analysis of Cdkn2d revealed a significant increase in DTG mice compared to WT littermates **(Fig**

3.8 f). qRT-PCR analysis of Igf-1 revealed a significant decrease in DTG mice compared to WT littermates **(Fig 3.8 g).**

To further investigate the possible effects of miR-214 overexpression on the dermal papilla, qRT-PCR analysis of Fgf7 and Fgf10 in skin of mice at postnatal day 8 was performed **(Fig. 3.8 h)**. Fgf7 and Fgf10 are expressed in the dermal papilla and can stimulate the proliferation of adjacent epithelial cells of the hair follicle and are also required for hair shaft differentiation (Greco et al., 2009; Schlake, 2005). qRT-PCR analysis revealed no significant difference in levels of transcripts of Fgf7 and Fgf10 in WT and DTG mice at postnatal day 8, suggesting that miR-214 overexpression does not alter the expression of these genes **(Fig. 3.8 h).**

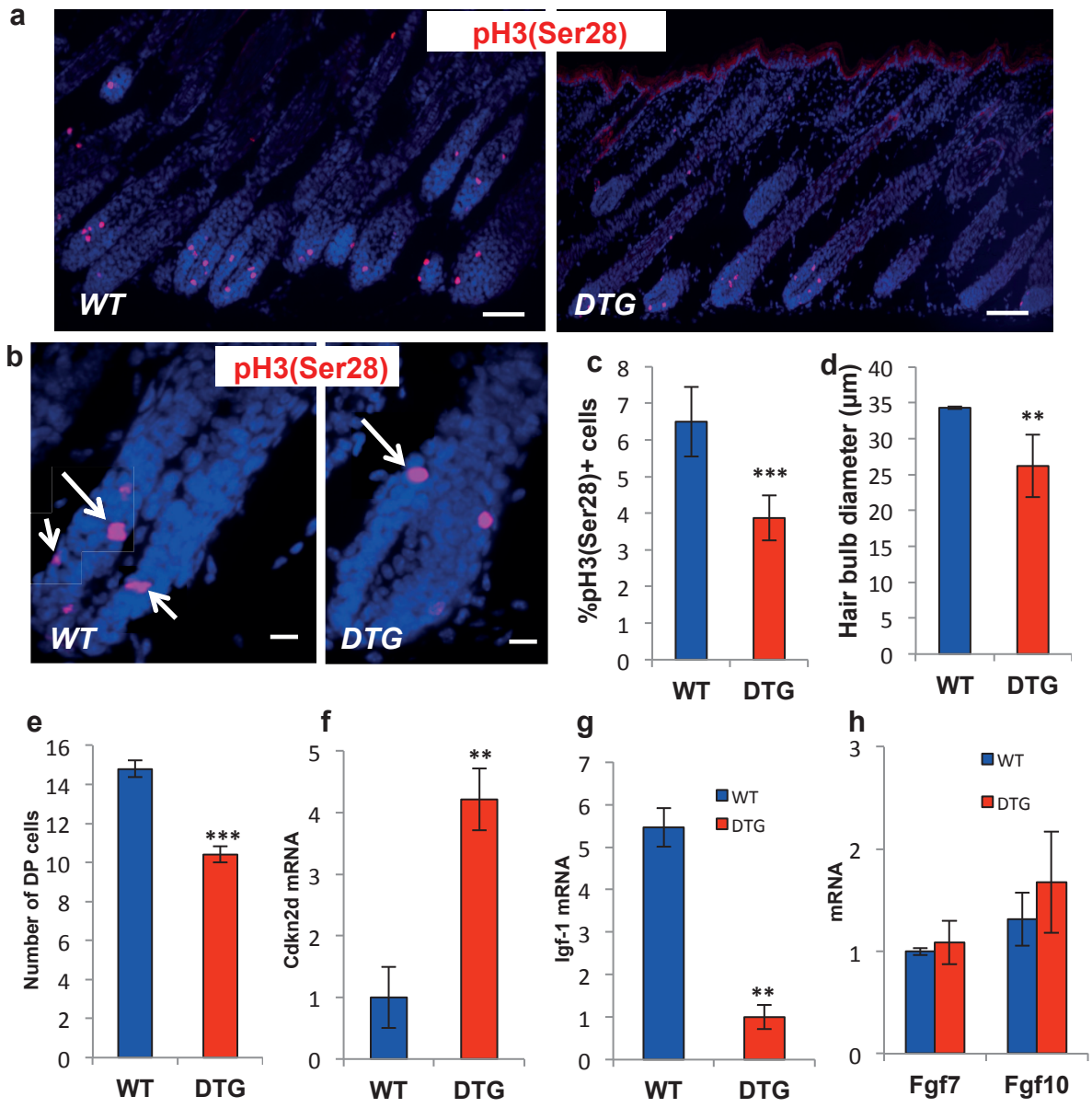

Figure 3.8. Analysis of hair follicle size in wild-type and K14-rtTA/TRE-miR-214 mice at postnatal day 8. **(a-b)** Immunofluorescence analysis of pH3 (Ser28) to mark proliferating cells in the hair bulbs; visible reduction in pH3 (Ser28)+ cells in the hair bulbs of DTG mice compared to WT littermates at 10X and 40X magnification (**a-b**), respectively; **(c)** quantitative analysis of pH3(Ser28)+ cells per hair follicle bulb: significant reduction in the number of pH3(Ser28)+ cells in DTG mice compared to WT; **(d)** measurement of hair bulb diameter: significant reduction in DTG mice compared to WT; **(e)** quantification of dermal papilla (DP) cells per hair bulb: significant reduction in the number of dermal papilla cells in the hair bulbs of DTG mice compared to WT; **(f)** qRT-PCR analysis of Cdkn2d: significant increase in Cdkn2d transcript levels in the skin of DTG mice compared to WT littermates; **(g)** qRT-PCR analysis of Igf-1: significant decrease in Igf-1 mRNA in the skin of DTG mice compared to WT littermates; **(h)** qRT-PCR analysis of Fgf7 and Fgf10; no significant difference in expression of Fgf7 and Fgf10 between WT and DTG mice (mean ± SD,***P value<0.001,**P<0.02 unpaired Student's t-test; n=3). Scale bar 50µm.

3.8 Overexpression of miR-214 causes a reduction in the stem cell marker Lhx2

To further elucidate the phenotypic properties of DTG mice, immunefluorescence analysis of the stem cell marker Lhx2 was performed at postnatal day 8 **(Fig. 3.9)**. Lhx2 immunoreactivity was noticeably reduced in DTG hair follicles compared to WT hair follicles **(Fig. 3.9).** Fewer Lhx2 positive cells were seen in the bulge and the outer root sheath in the follicles of miR-214 overexpressing mice compared to the WT littermates **(Fig. 3.9)**. These data indicate that overexpression of miR-214 may have a negative impact on stem cells and their activity.

Taken together, the changes in visual coat appearance in K14-rtTA/TRE-miR-214 DTG mice are the result of the reduced number of the hair follicles and the decreased hair shafts thickness, associated with the development of smaller follicles in size due to the inhibited proliferation and stem cell activity,

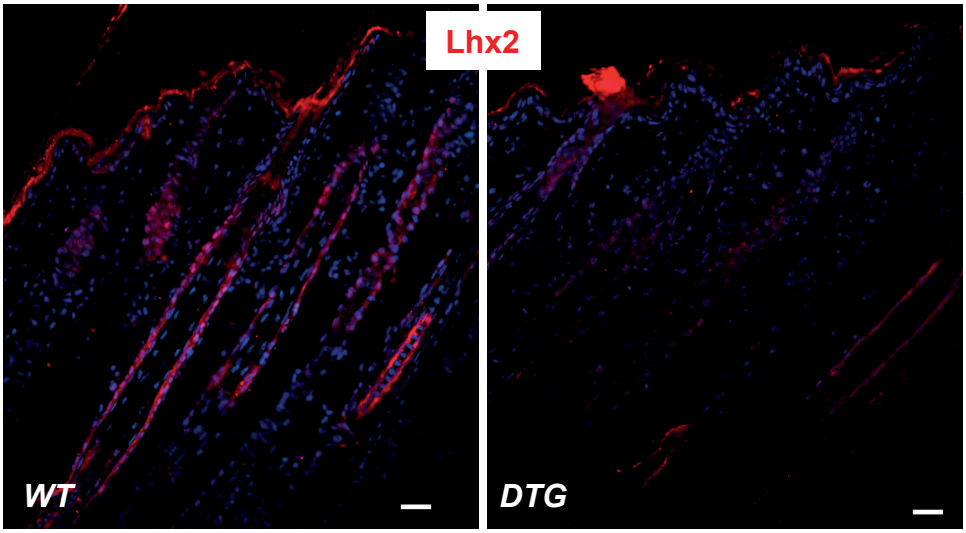

Figure 3.9. Analysis of the stem cell marker Lhx2 in the hair follicles at postnatal day 8. Immunofluorescence analysis of Lhx2 (red): visible reduction of Lhx2 in the outer root sheath and bulge of DTG hair follicles compared to WT.
Blue nuclear counterstaining with DAPI. Scale bar 50µm.

3.9 Gain of miR-214 activity in postnatal skin alters hair follicle cycling and hair follicle size

To explore the effects of miR-214 on hair follicle cycling, DTG mice were treated with Doxycyclin during telogen phase followed by the induction of a synchronised hair cycle by depilation (**Fig. 3.10 a**). In order to analyse effects on the hair cycle, microphotographs of the histology of back skin of WT and DTG mice at days 3 (anagen II), 5 (anagen IV), 8 (anagen VI) and 12 (anagen VI) of depilation-induced hair cycle were taken (**Fig. 3.10 b)**.

Hair follicles were quantified at different stages and sub-stages of the hair cycle according to established morphological criteria (Muller-Rover et al., 2001). Although telogen-anagen transition was initiated in both WT and DTG mice, DTG mice showed a significant delay in early anagen development; at day 3 of depilation-induced hair cycle DTG mice had a significantly higher number of follicles were in anagen I and significantly less hair follicles in anagen II in DTG mice compared to WT littermate (**Fig. 3.10 b, c**). At day 5 of depilation-induced hair cycle, a significantly higher number of hair follicles were in anagen I in DTG mice compared to WT and a significantly higher number of hair follicles in anagen IV in WT mice compared to DTG littermates (**Fig. 3.10 b, d**). This suggests that miR-214 overexpression affects the rate of hair follicle growth during the hair cycle.

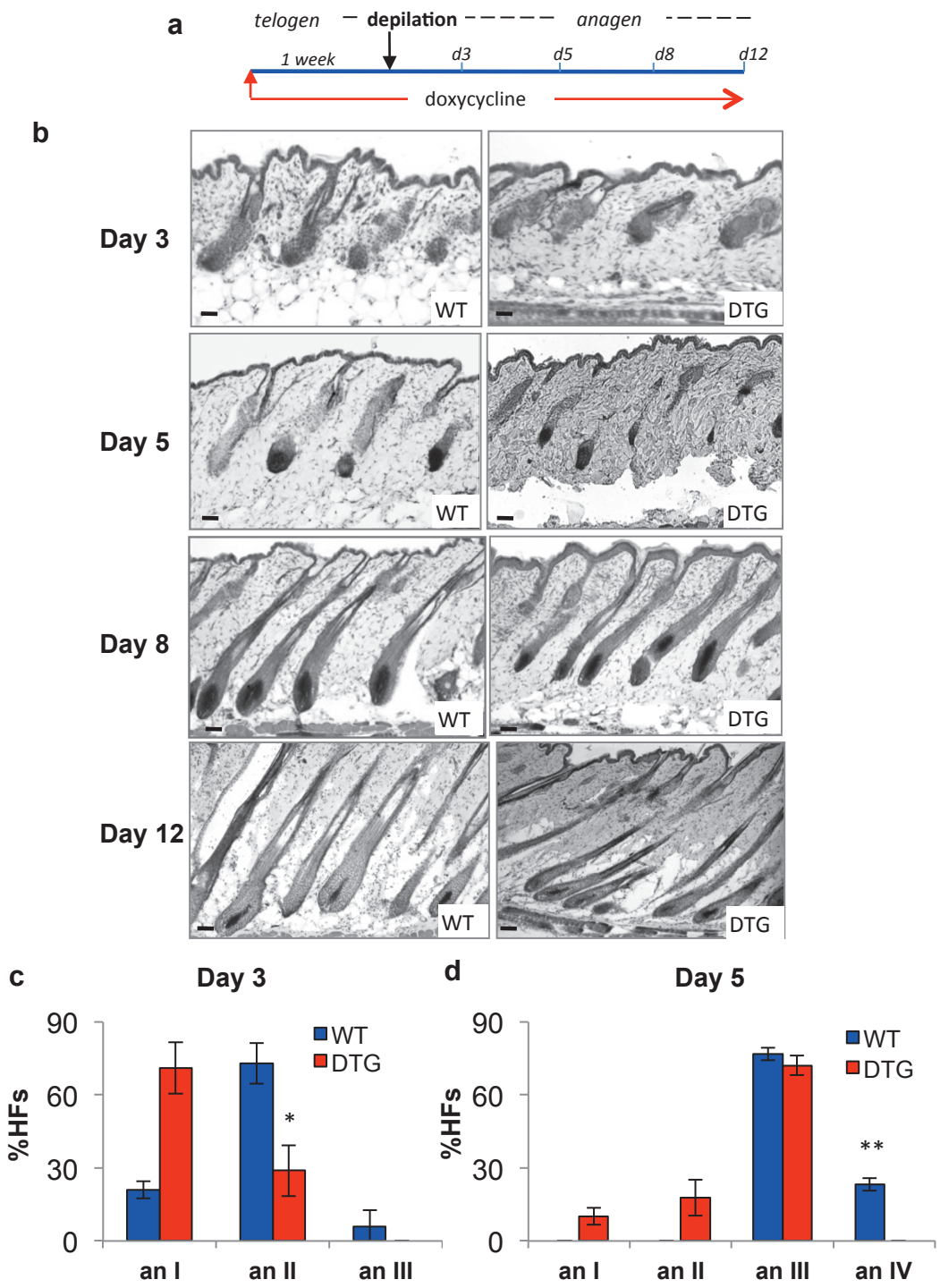

Figure 3.10. Overexpression of miR-214 inhibits hair cycle progression.
(a) Schematic illustration of the experimental design; **(b)** microphotographs of histology of back skin of WT and DTG mice at days 3 (anagen II), 5 (anagen IV), 8 (anagen VI) and 12 (anagen VI) after depilation; **(c)** quantitative histomorphometry of hair follicles at different anagen sub-stages at day 3 of depilation-induced hair cycle: significant increase in anagen I hair follicles and a significant decrease in anagen II hair follicles in DTG mice compared to WT littermates; **(d)** quantitative histomorphometry of hair follicles at different anagen sub-stages at day 5 of depilation-induced hair cycle: significantly higher number of anagen I hair follicles and significantly lower number of anagen IV hair follicles in DTG mice compared to WT littermates. (mean ± SD, *P value<0.05, **p<0.02 unpaired students t-test). Scale bar 50μm.

To further analyse the effects of miR-214 overexpression during the hair cycle, the diameter of hair bulbs and length of hair follicles were assessed. At both day 5 of depilation-induced hair cycle when hair follicles are in anagen IV and day 12 of depilation-induced hair cycle when hair follicles are in anagen VI, the diameter of hair bulbs in DTG mice were significantly reduced compared to the WT controls (**Fig. 3.11 a**). At day 5 of depilation-induced hair cycle when hair follicles are in anagen VI, hair follicles were significantly shorter in DTG mice compared to WT **(Fig 3.11 b)**. Similar to the data obtained on hair follicle morphogenesis in which anagen-like hair follicles in DTG mice were shorter, anagen VI hair follicles at day 12 of depilation-induced hair cycle were significantly shorter in DTG mice compared to WT littermates **(Fig.3.11 b)**.

To analyse the effects of miR-214 overexpression on hair shafts produced during depilation-induced hair cycle, hair shafts were plucked at day 26 after depilation. Hair shaft thickness was significantly reduced in DTG mice compared to the control **(Fig. 3.11 c)**. However, no significant difference in hair shaft length was detected between WT and DTG **(3.11 d).** These findings are similar to the observations made for the hair shaft changes seen in miR-214 overexpressing mice during hair follicle morphogenesis.

To determine the possible causes of reduction in hair bulb size and hair follicle length, analysis of proliferation, differentiation and apoptosis was performed.

Quantitative analysis of the number of pH3 (Ser28) positive cells revealed a significant reduction in proliferation in the hair follicles of DTG mice at days 3 (anagen II), 5 (anagen IV) and 12 (anagen VI) of depilation-induced hair cycle, compared to WT littermates **(Fig. 3.12 a-e).**

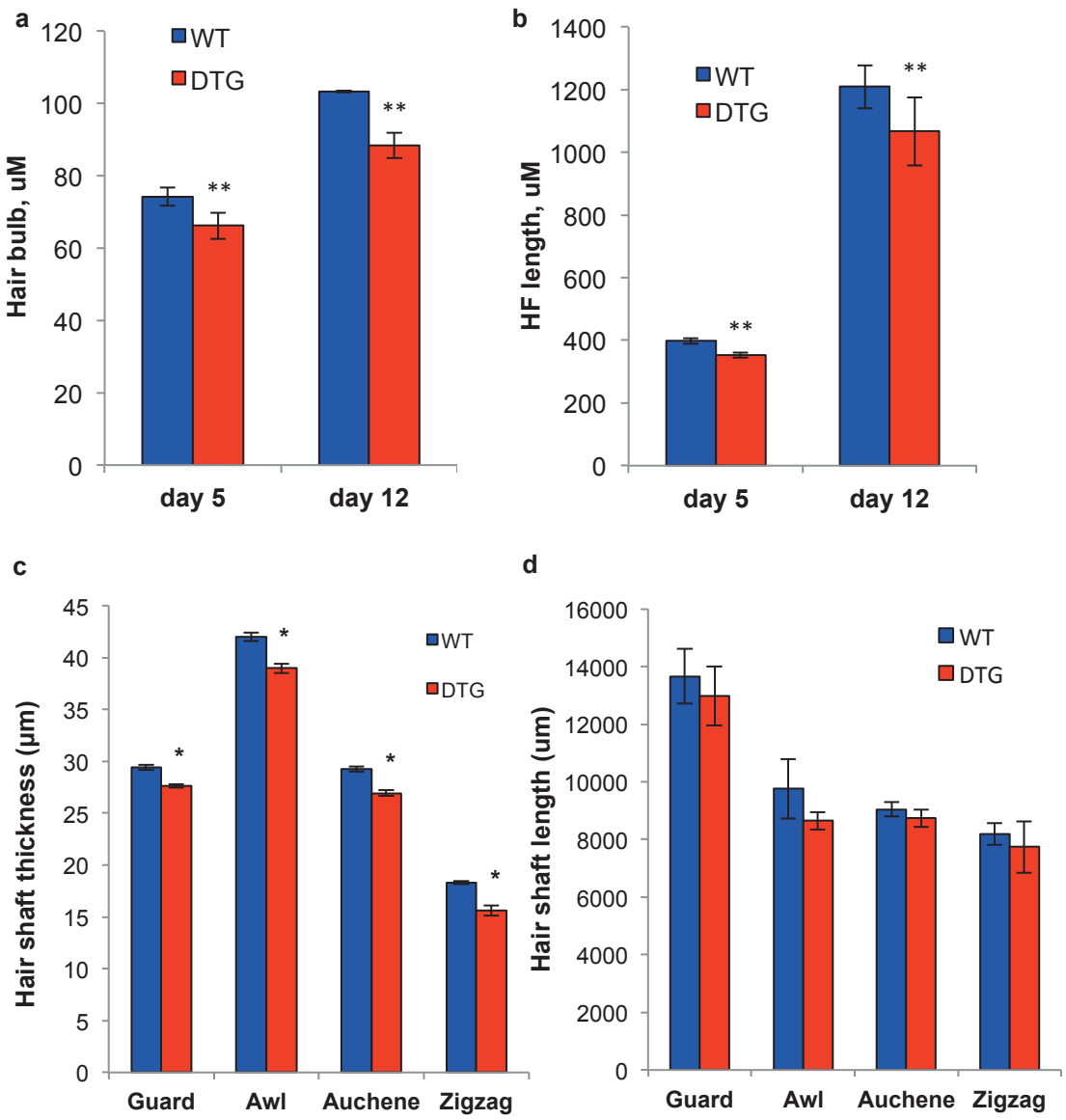

Figure 3.11. Morphometric analysis of hair follicles and shafts after depilation-induced hair cycle (a) Morphometric analysis of hair bulb diameter measured across the widest part (line of Auber) at days 5 (anagen IV) and 12 (anagen VI) after depilation: significant reduction of hair bulb diameter in DTG mice compared to WT littermates; **(b)** analysis of hair follicle length at days 5 and 12 after depilation: significant reduction in the length of hair follicles in DTG mice compared to WT littermates; **(c)** analysis of hair shaft thickness: significant reduction of all hair shaft types (guard, awl, auchene and zigzag) in DTG mice compared to WT littermates; **(d)** analysis of hair shaft length: no significant difference in all hair shaft types (guard, awl, auchene and zigzag) between WT and DTG mice. (mean ± SD, *P value<0.05, **P value<0.02, unpaired Student's t-test).

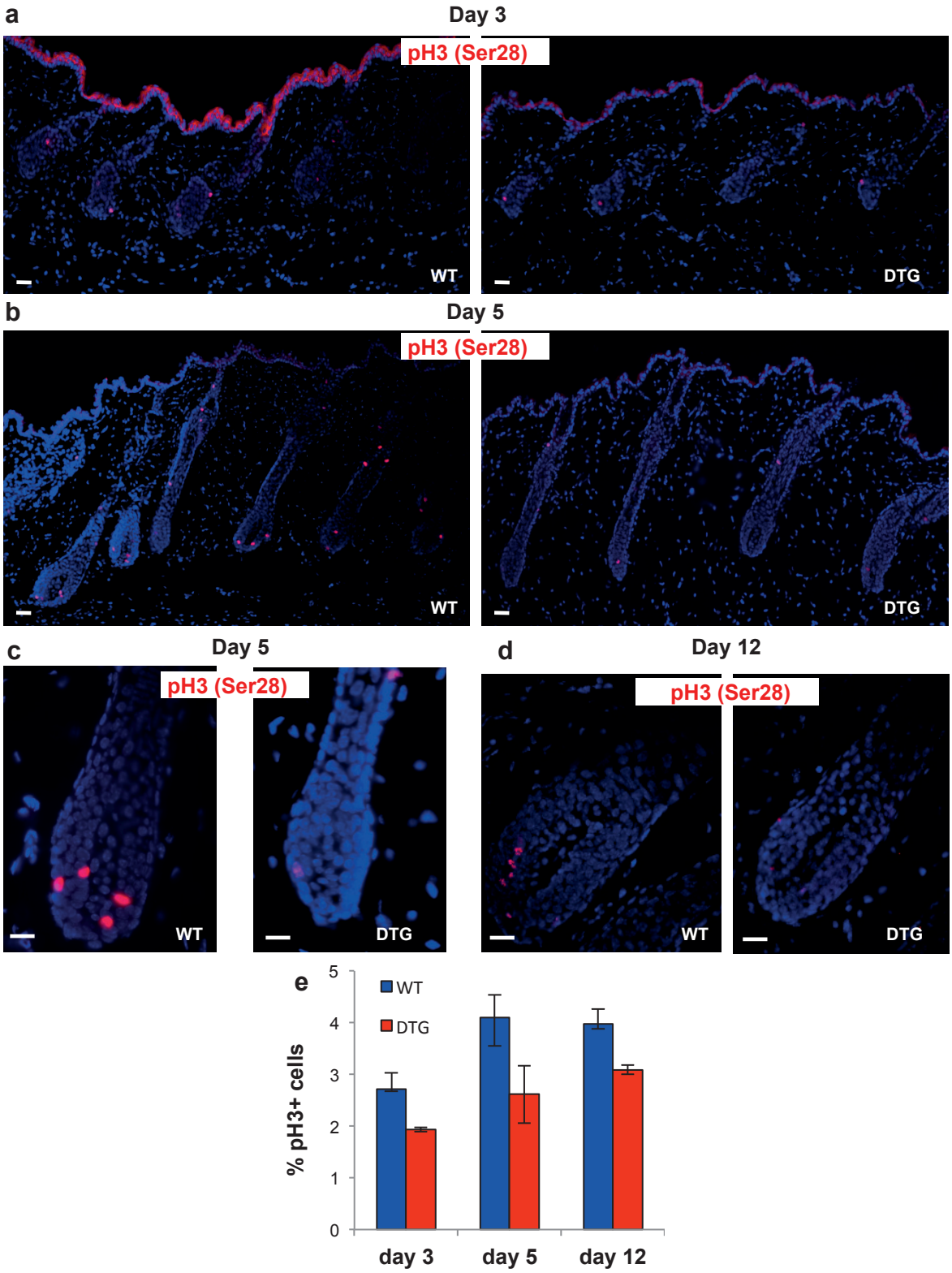

Figure 3.12. Analysis of proliferation in the hair follicle during depilation-induced hair cycle. (a) Immunofluorescence of pH3(Ser28) to mark proliferating cells at day 3 (anagen II) after depilation; **(b-c)** immunofluorescence of pH3(Ser28) at day 5 of depilation-induced hair cycle (anagen IV), 10x and 40x magnification, respectively: visible reduction in the number of pH3(Ser28) positive cells in the hair bulb of DTG mice compared to WT; **(d)** immunofluorescence of pH3(Ser28) at day 12 of depilation-induced hair cycle (anagen VI): a visible reduction in the number of pH3(Ser28) positive cells in the hair bulbs of DTG mice compared to WT; **(e)** quantification of pH3(Ser28) positive cells at days 3, 5 and 12 of depilation-induced hair cycle: significant reduction of pH3(Ser28)+ cells in the follicles of DTG compared to WT mice. (mean ± SD, *P value<0.05, ***P<0.002 unpaired Student's t-test). Scale bar 50µm.

Expression of Dlx3, a transcription factor involved in the control of hair follicle keratinocyte differentiation (Hwang et al., 2008), was less pronounced in the inner root sheath of the transgenic anagen VI hair follicles versus the controls in hair follicles (**Fig. 3.13 a**).

To explore the changes in apoptosis active form of Caspase-3 was used as it plays key effector roles in apoptosis (Riedl and Shi, 2004; Walsh et al., 2008). No visible difference in the number of active Caspase-3 positive cells in the anagen VI hair follicles was seen between WT and DTG mice **(Fig. 3.13 b).**

This data suggest that reduction in hair bulb size and follicle length seen in miR-214 overexpressing mice is associated with the significantly decreased cell proliferation in the hair matrix, but not a cell death. In addition, miR-214 negatively affects hair follicle differentiation during the hair cycle.

Next, the changes in the morphology and activity of the dermal papilla in miR-214 overexpressing mice were analysed. Sox2 immunofluorescence was performed in anagen VI hair follicles at day 12 of depilation-induced hair cycle as a marker of dermal papilla fibroblasts (Driskell et al., 2009; Rendl et al., 2005) (**Fig. 3. 14 a**). Quantitative analysis revealed a significant reduction in the number of dermal papilla cells in transgenic hair follicles compared to WT littermates (**Fig. 3.14 b**).

qRT-PCR analysis of Fgf7 and Fgf10, which are known to be expressed in the dermal papilla and stimulate adjacent epithelial cells, did not show significant difference in the levels of their transcripts in the anagen VI follicles between transgenic and WT mice **(Fig. 3.14 c),** which was consistent with observations during hair follicle morphogenesis.

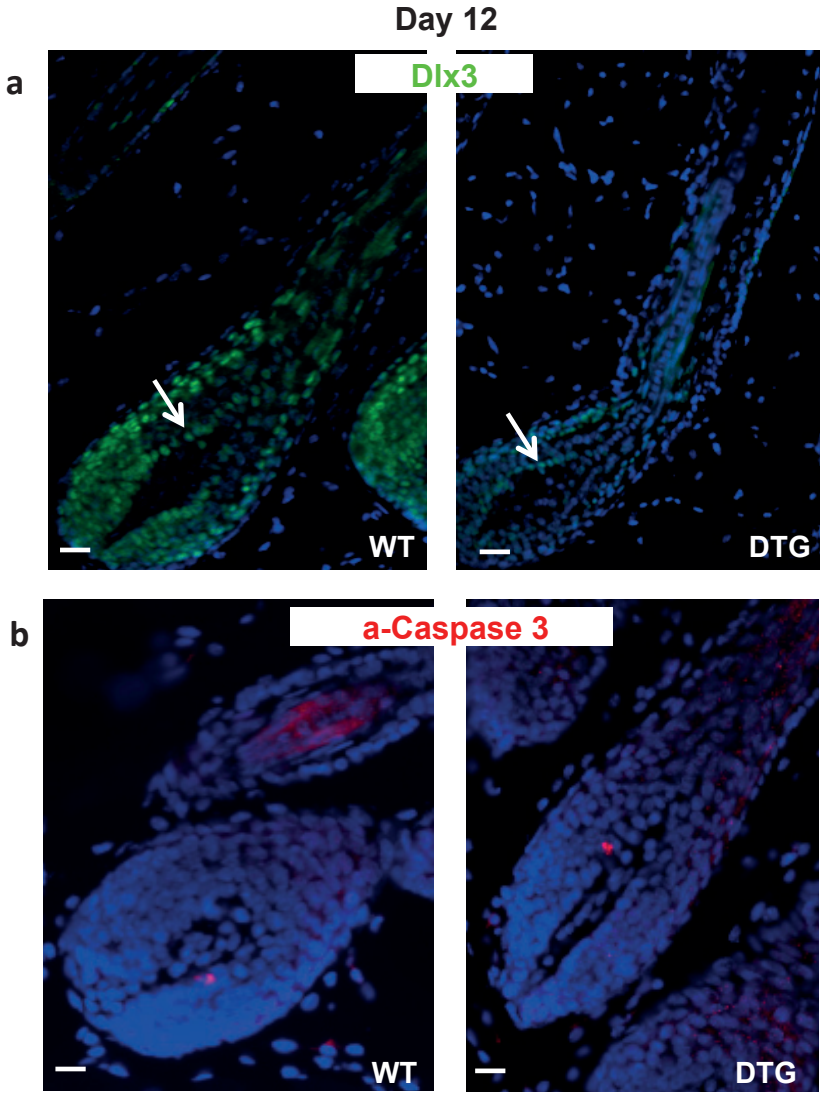

Figure 3.13 Analysis of differentiation and apoptosis in the hair follicles in anagen VI. (a) Immunofluorescence analysis of Dlx3 (green) in anagen VI follicles at day 12 of depilation-induced hair cycle: visible reduction in the expression of Dlx3 in the inner root sheath of DTG hair follicles compared to WT littermates; **(b)** immunofluorescence analysis of active Caspase 3 (red) in hair bulbs in anagen VI hair follicles at day 12 of depilation-induced hair cycle: no visible difference in expression of active Caspase 3 between WT and DTG mice.
Blue nuclear counterstain with DAPI.

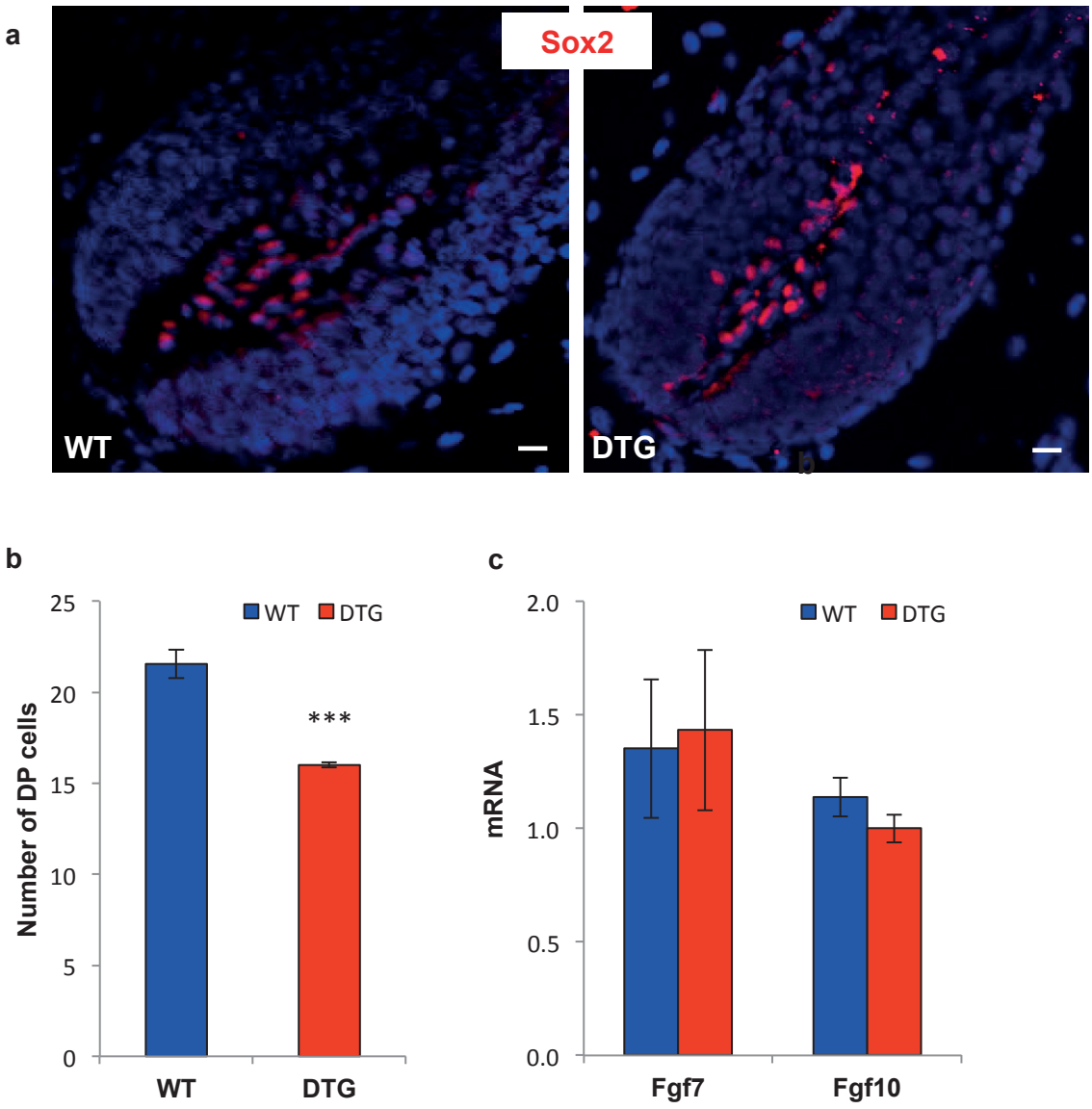

Figure. 3.15. Analysis of the dermal papilla of anagen IV hair follicles. **(a)** Immunofluorescence analysis of Sox2 in hair follicles at day 12 of depilation-induced hair cycle: no noticeable difference in expression of Sox2 in the dermal papillae of WT and DTG mice; **(b)** quantification of dermal papilla cells in anagen VI hair follicles at day 12 of depilation-induced hair cycle: significant reduction in the number of dermal papilla cells in the hair follicles of DTG mice compared to WT; **(c)** qRT-PCR analysis of Fgf7 and Fgf10 expression in skin at day 12 of depilation-induced hair cycle: no significant differences in the transcript levels of Fgf7 and Fgf10 between WT and DTG mice (mean ± SD, ***P value<0.001, unpaired Student's t-test), scale bar 50μm.

3.10 miR-214 overexpression induces complex changes in gene expression programs in keratinocytes

To explore molecular mechanisms underlying the phenotype in miR-214 transgenic mice and identify potential targets of miR-214 in the keratinocytes, global mRNA expression profiling was performed in the back skin epithelium of neonatal DTG mice (P2.5) which received doxycycline for 48 hours prior to skin collection (**Fig. 3.15 a**). The raw microarray expression profiles were background corrected and normalized with Bioconductor package limma (Smyth et al., 2005) and genes with more than two fold expression change in the epithelium of DTG mice compared to WT controls were identified as differentially expressed (**Fig. 3.15 b**). The in-house functional ontology database was used to categorise differentially expressed genes to the set of 12 distinct functional categories (Lewis et al., 2014). Bioinformatic analysis of the microarray data revealed 2-fold and higher changes in expression of 1026 genes in keratinocytes of DTG mice compared to WT controls (**Fig. 3.15 b**, **Supplementary Table 1**). Differentially expressed genes which belong to “Cell Cycle” and “Signalling” categories were further validated by qRT-PCR.

Microarray analysis revealed substantial decrease in the expression of cyclins and cyclin-dependent kinases in the epithelium of miR-214 overexpressing mice (**Appen**). By qRT-PCR it was confirmed that the transcript levels of *Ccnb1, Ccnd1, Ccnd2 and Cdk1* (cyclin B1, cyclin D1, cyclin D2 and cyclin-dependent kinase 1) were significantly lower in DTG mice compared to the WT littermates (**Fig. 3.16 a**). These data suggest that miR-214 exerts inhibitory effects on cell proliferation, which were consistent with the epidermal and hair follicle phenotypes seen in DTG mice (**Fig. 3.6**).

Interestingly, microarray analysis detected changes in the expression of the genes encoding the components of several signalling pathways which are crucial for hair follicle development and cycling, such as Wnt, Shh, Edar, and BMP (Blanpain and Fuchs, 2009; Botchkarev and Paus, 2003; Schmidt-Ullrich et al., 2006). qRT-PCR validation of the microarray results showed significant downregulation of β-catenin (*Ctnnb1)* **(Fig. 3.16 b)** and Lef-1 **(Fig. 3. 16 c)** expression in the epithelium of DTG mice, suggesting a modulation of the activity of Wnt signalling pathway induced by miR-214. Overexpression of miR-214 led to a significant decrease in the expression of Wnt inhibitor Sostdc1 in **(Fig. 3.16 c)** and Edar (**Fig. 3.16 d)** in DTG epithelium compared to WT. Also, expressions of several genes that belong to Hedgehog signalling such as Shh and its receptors Smo and Ptch2 were dramatically decreased in the epithelium of DTG versus wild type mice (**Fig. 3.16 e)**.

These data provide the evidence that the effects of miR-214 on hair follicle development and cycling are mediated, at least in part, by the genes that control keratinocyte proliferation and modulate the activities of key signalling pathways (Wnt, Hedgehog, Bmp, Edar) that regulate skin development and hair growth.

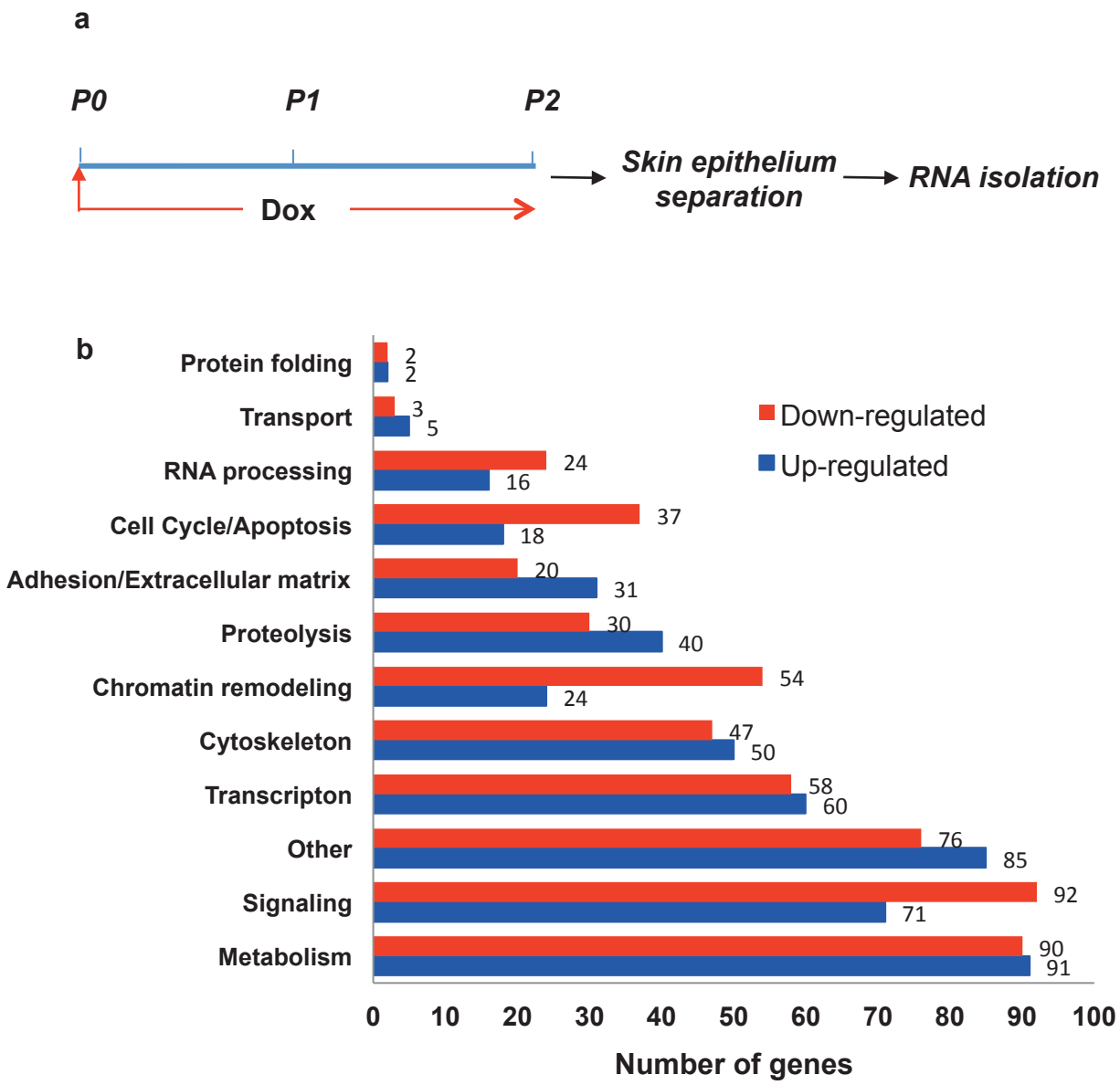

Figure 3.15. Global gene expression profiling of the back skin epithelium of WT and K14-rtTA/TRE-miR-214 mice. (a) Schematic illustration of the experimental design; **(b)** microarray analysis of the global gene expression in the back skin epithelium of DTG versus WT: functional assignments of the gene with altered expression.

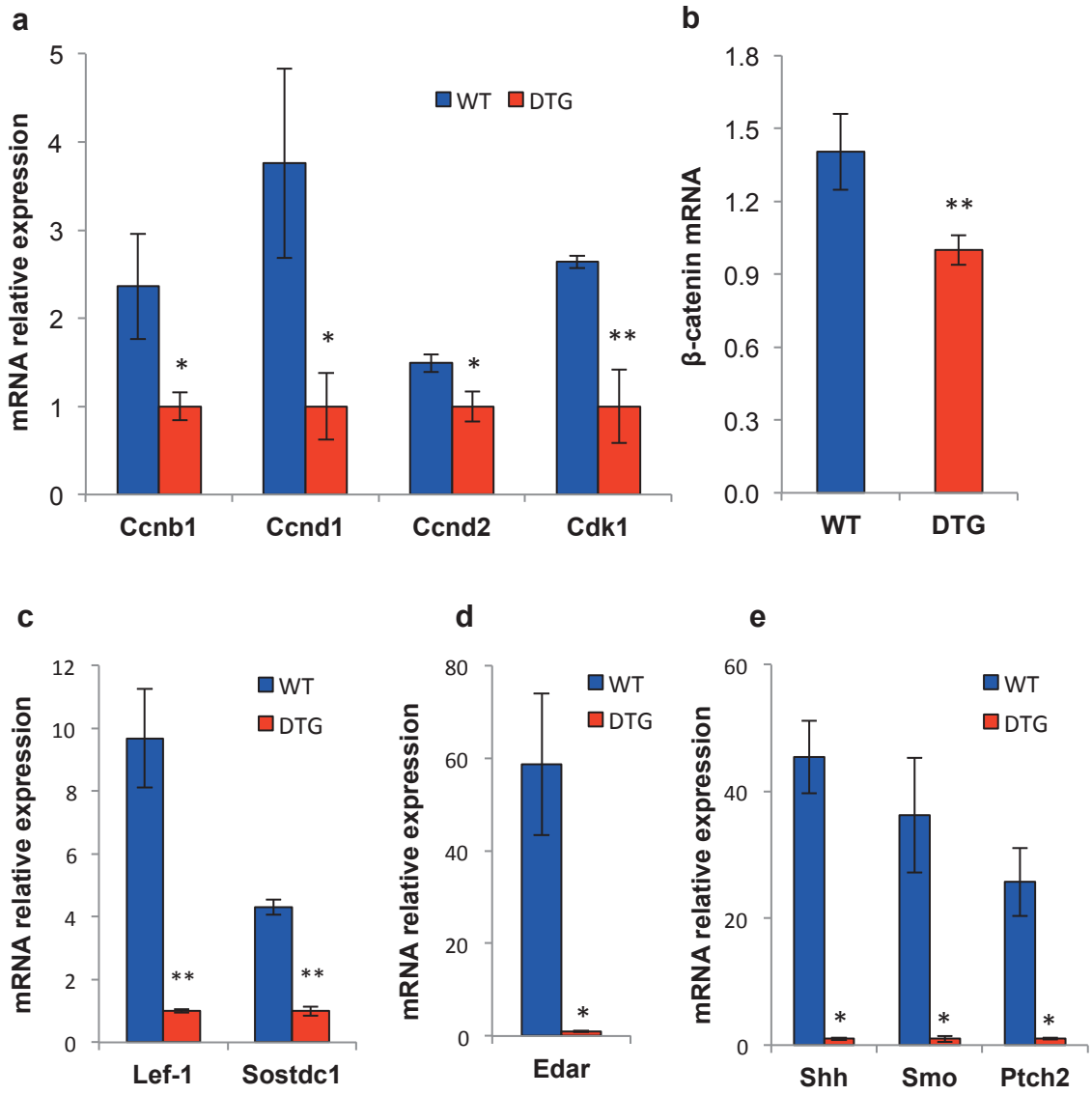

Figure. 3.16. Validation of microarray analysis by qRT-PCR;
(a-e) qRT-PCR analysis of the selected genes involved in the cell cycle control and members of the Wnt, Hh and Eda signalling pathways in the epithelium of mice at postnatal day 2; **(a)** a significant reduction in the expression of Ccnb1, Ccnd1, Ccnd2 and Cdk1 in DTG mice compared to WT; **(b)** a significant reduction in the expression of β-catenin in DTG mice compared to WT; **(c)** significant reduction in the expression of Lef-1 and Sostdc1 in DTG mice compared to WT; **(d)** significant reduction in the expression of Shh, Smo and Ptch2 in DTG mice compared to WT; **(e)** significant reduction in the expression of Edar in DTG mice compared to WT (mean ± SD, *P value<0.05, **P<0.02, unpaired student's t-test).

3.11 miR-214 overexpression in epithelial progenitor cells alters expression of key regulators of the hair follicle development and cycling

To further investigate the effects of gain of miR-214 functions on the activity of selected signalling pathways in skin, the pattern of expression of their different components in embryonic and postnatal skin of DTG and age-matched WT mice was determined via immunofluorescence analysis.

Immunofluorescence of β-Catenin, a key mediator of the Wnt pathway activity, showed decreased expression in the hair follicle placodes (stage 2 of hair morphogenesis) in skin of DTG mice in comparison to the WT littermates **(Fig. 3.17 a)**. The expression of β-catenin was also reduced in the epithelium of DTG hair follicles at stage 4 of morphogenesis compared to WT littermates **(Fig. 3.17 b)**. The expression of β-Catenin was also reduced in the hair matrix of fully developed anagen-like hair follicles in DTG mice compared to WT littermates at postnatal day 8 **(Fig. 3.17 c).**

Immunofluorescence analysis of Lef-1, the transcriptional cofactor of β-catenin, also showed reduced expression in the epithelium and mesenchyme in hair follicle placodes (stage 2 of hair morphogenesis) of DTG mice compared to WT **(Fig. 3.18 a).** There was also a prominent reduction in Lef-1 immunoreactivity in the epithelium and dermal papilla in DTG hair follicles at stage 3 of hair morphogenesis compared to WT **(Fig. 3.18 b).** Expression of Lef-1 was also reduced in the hair matrix of DTG mice compared to WT littermates at postnatal day 8 **(Fig. 3.18 c).**

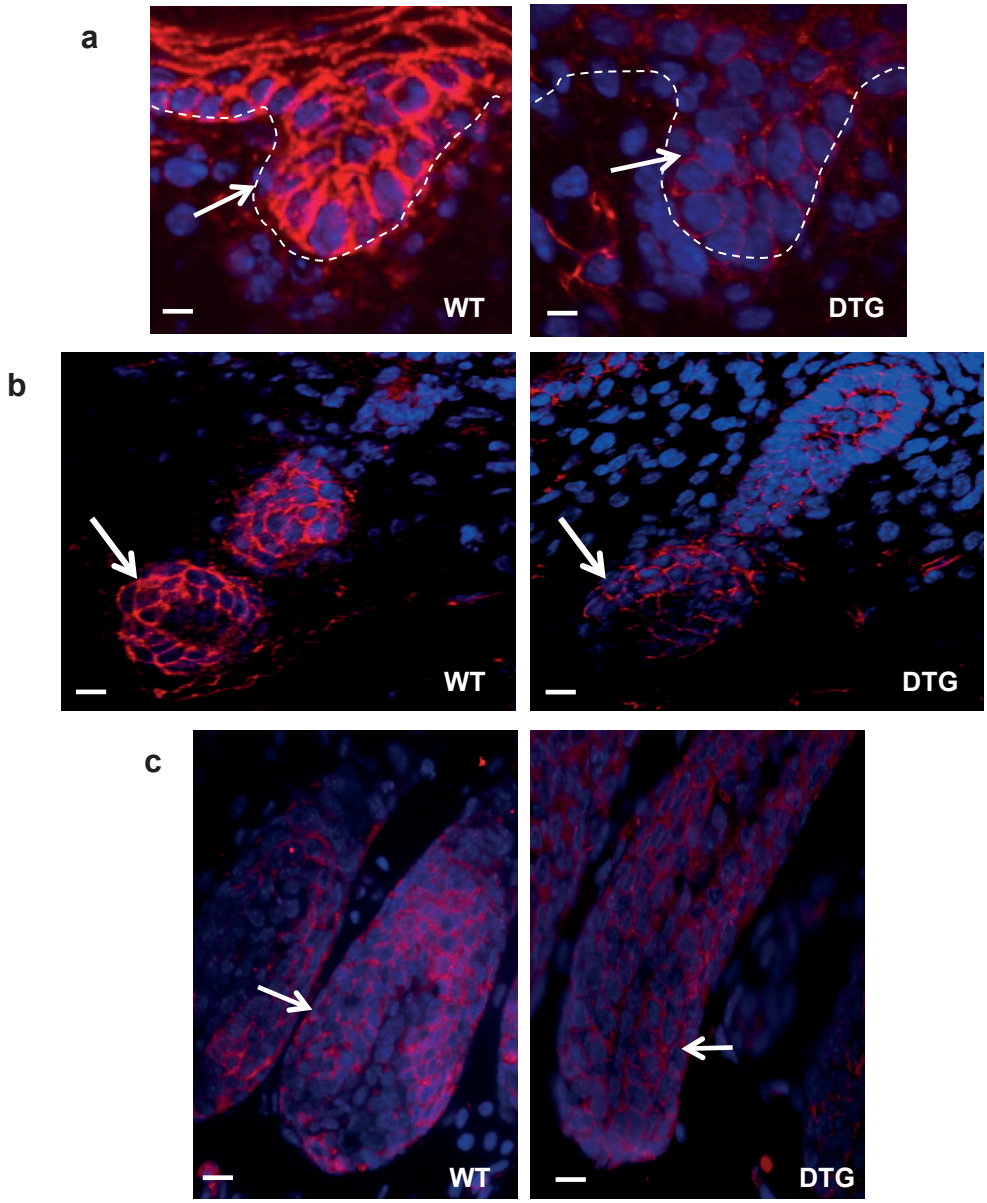

Figure 3.17. Analysis of β-catenin expression during hair follicle morphogenesis by immunofluorescence (red). (a) decreased expression of β-catenin in the hair follicle placode (morphogenesis stage 2) in skin of DTG mice compared to WT littermates (arrows); **(b)** reduction in the expression of β-catenin (arrow) in the hair matrix of DTG follicles in stage 4 of morphogenesis; **(c)** reduction in expression β-catenin in the hair matrix of fully developed anagen-like hair follicles of DTG mice compared to WT (arrows). Scale bar 50μm.
Blue nuclear counterstaining with DAPI.

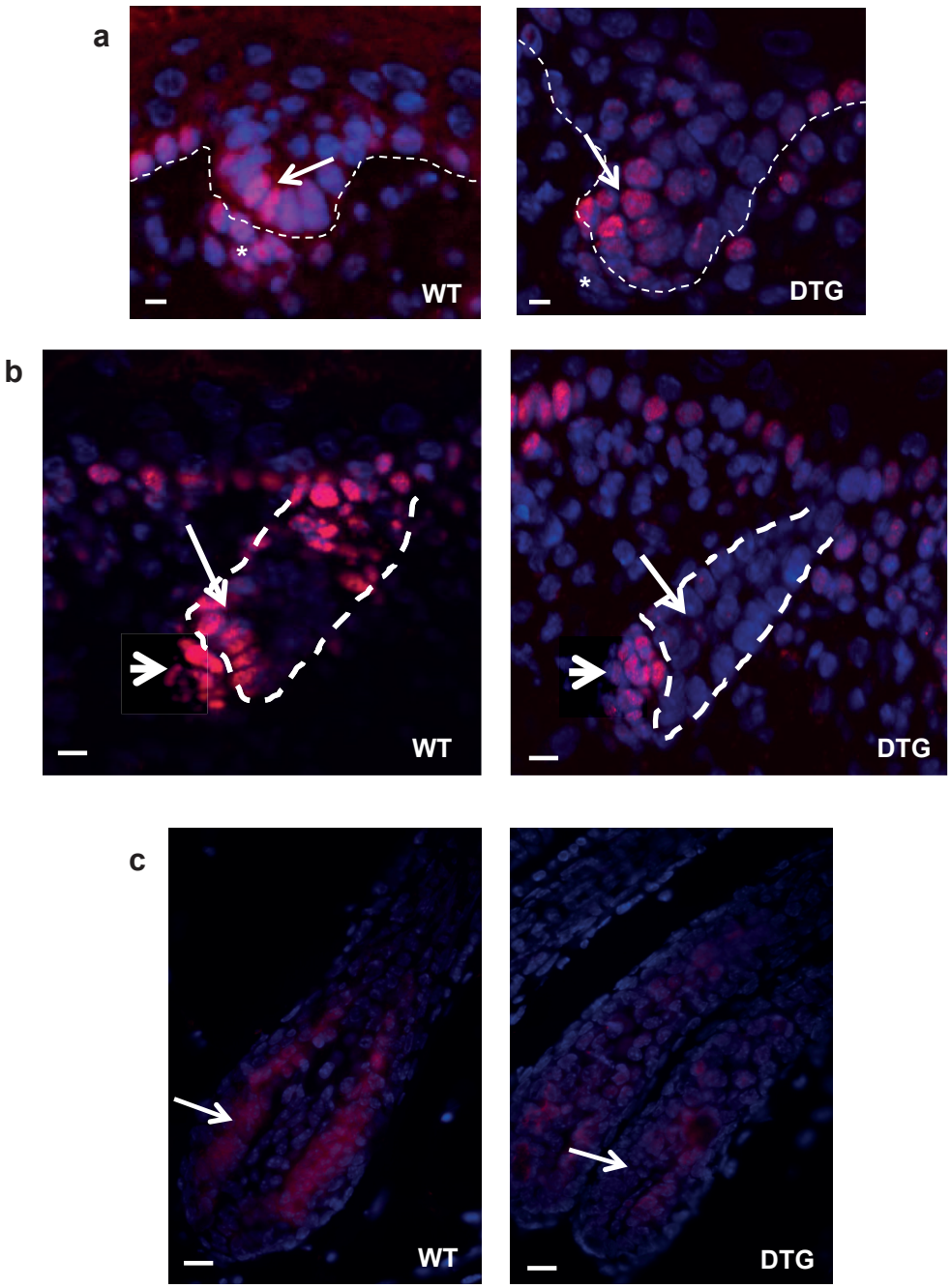

Figure 3.18. Analysis of Lef-1 expression during hair follicle morphogenesis by immunofluorescence (red colour)
(a) visible reduction in Lef-1 expression in the epithelium (arrow) and mesenchyme (asterisk) of hair placodes of DTG mice compared to WT littermates at embryonic day 17; **(b)** dramatic decrease in Lef-1 immunofluorescence in the epithelium (arrows) and noticeable Lef-1 reduction in the dermal papilla (arrowheads) in DTG hair follicles at stage 3 of morphogenesis versus WT; **(c)** reduction in expression of Lef-1 in the hair matrix of DTG mice compared to WT littermates (arrows). Scale bar 50μm.

The downregulation of β-catenin and Lef-1, which are key mediators of the Wnt signalling pathway, indicates that miR-214 overexpression targets this pathway that contributes to the underlying phenotype in DTG mice seen during hair follicle morphogenesis.

Analysis of Shh pathway, another key regulator of hair follicle growth, was also performed during hair follicle morphogenesis **(Fig. 3.19)**. A reduction in expression of Shh was seen in hair follicle placodes (stage 2 of hair morphogenesis) in DTG mice compared to WT **(Fig 3.19 a)**. In fully developed hair follicles (P8), expression of a transcription factor Gli-1, which mediates the activity of Shh, was also significantly decreased in DTG versus WT mice **(Fig. 3.19 c).**

Consistent with the microarray data, expression of Edar appeared to be reduced in the epithelium of developing hair placodes (stage 2 of hair follicle morphogenesis) and in the matrix of more developed hair follicles in DTG mice compared to the corresponding control **(Fig. 3.20 a, b)**.

In contrast, immunofluorescence analysis of pSmad 1/5/8, as an indicator of Bmp signalling activity, revealed more prominent expression of pSmad1/5/8 in the epithelium of hair follicle placodes (stage 2 of hair morphogenesis) in DTG mice compared to WT **(Fig. 3.21 a).** Also, more prominent pSmad 1/5/8 expression was seen in the inner root sheath and hair shaft of DTG hair follicles compared to WT at postnatal day 8 **(Fig. 3.21 b).**

These findings suggest that inhibitory effects of miR-214 on hair follicle morphogenesis were associated with decreased activity of the Wnt, Shh and Edar signalling pathways and activation of BMP signalling, which all contribute to the phenotype seen in DTG mice during hair follicle morphogenesis.

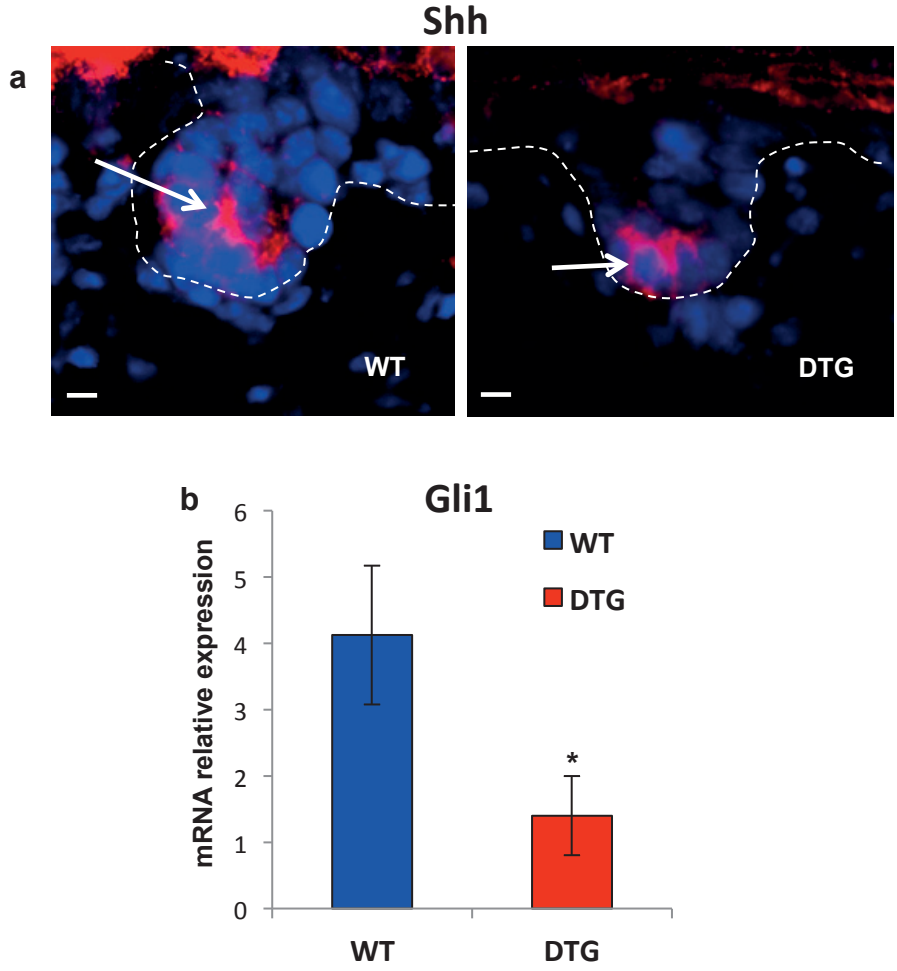

Figure 3.19. Analysis of Shh pathway during hair follicle morphogenesis. (a) Immunofluorescence analysis of Shh in hair follicle placodes in stage 2 of morphogenesis at embryonic day 17; reduction of Shh expression in hair follicle placodes of DTG mice compared to WT littermates; **(b)** qRT-PCR analysis of Gli-1 expression in skin at postnatal day 8: significant reduction in the level of Gli-1 transcripts in DTG mice compared to WT littermates (mean ± SD *P value<0.05, unpaired Student's t-test). Scale bar 50μm.

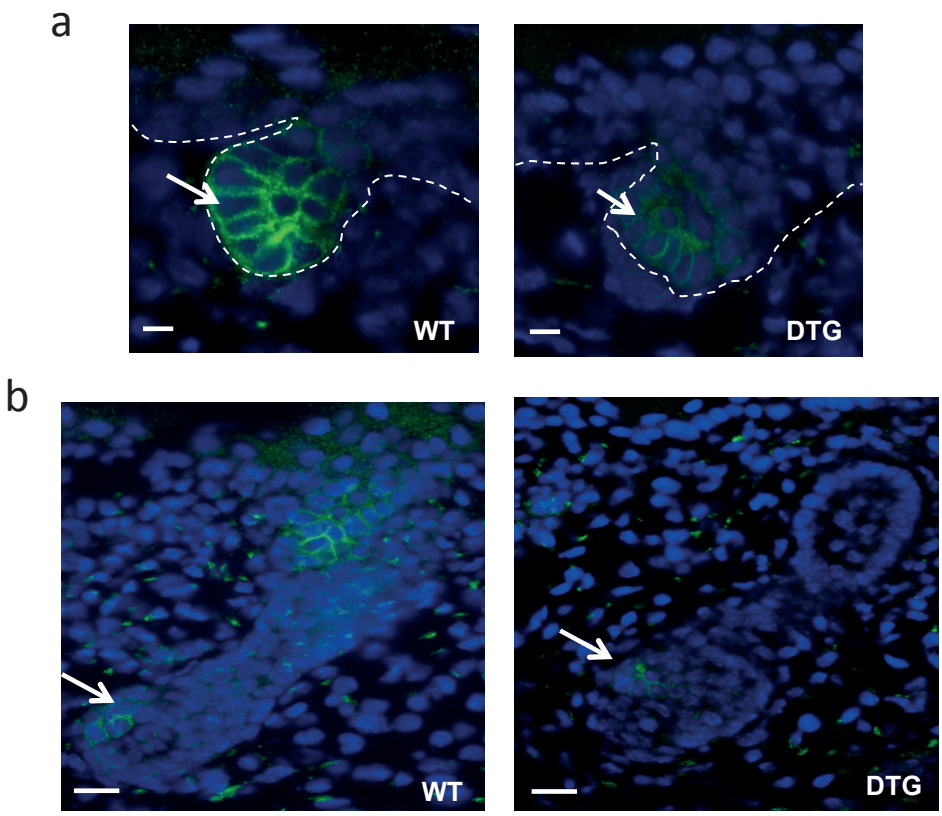

Figure 3.20. Analysis of Edar expression during hair follicle morphogenesis by immunofluorescence (green colour).
(a) Decreased expression of Edar in the epithelium of hair follicle placodes of DTG mice compared to WT (stage 2 of morphogenesis, embryonic day 17, arrows); **(b)** reduced immunofluorescence of Edar in the hair matrix of DTG follicles in stage 4 of morphogenesis. Scale bar 50µm.
Blue nuclear counterstaining with DAPI

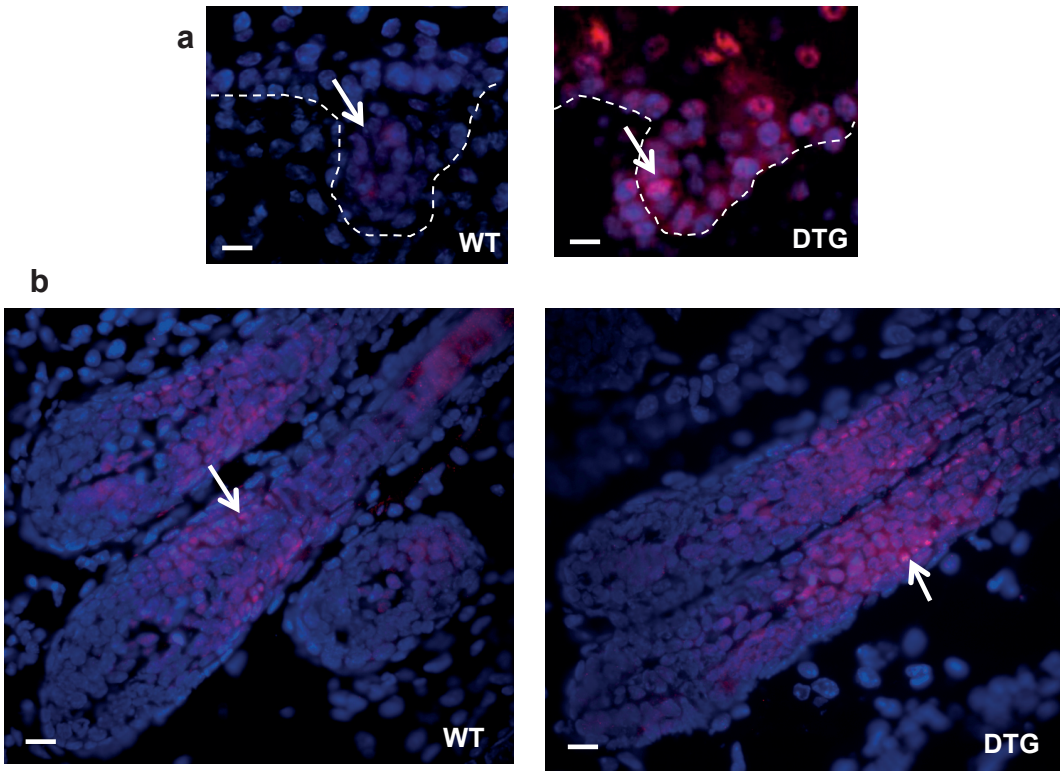

Figure 3.21. Analysis of pSmad 1/5/8 during hair follicle morphogenesis by immunofluorescence (red colour). **(a)** increase in expression of pSmad 1/5/8 in the epithelium of hair follicle placodes of DTG mice compared to WT littermates (stage 2 of hair morphogenesis, embryonic day 17, arrows); **(b)** increase of pSmad 1/5/8 (arrow) immunofluorescence in the inner root sheath and hair shaft of DTG hair follicles compared to WT littermates at postnatal day 8 at anagen-like stage (arrows). Scale bar 50μm.

.

3.12 Overexpression of miR-214 affects key hair follicle regulators during depilation-induced hair cycle

To further validate microarray data, expression of the components of Wnt, Shh, and Bmp signalling pathways was analysed in the hair follicles during different anagen stages.

A reduction in the expression of β-catenin was seen in the developing hair matrix of anagen II hair follicles (day 3 after depilation) and anagen IV hair follicles (day 5 after depilation) in DTG mice compared to WT **(Fig.3.22 a)**. A reduction in β-catenin immunoreactivity was also seen in the hair matrix and dermal papilla in anagen VI hair follicles (day 12 after depilation) in DTG mice compared to WT **(Fig.3.22 a).**

In anagen II hair follicles (day 3 after depilation), no visible difference in Lef-1 expression was seen between WT and DTG **(Fig.3.22 b)**. Lef-1 expression was markedly reduced in the hair matrix and dermal papilla of anagen IV hair follicles (day 5 after depilation). There was also a marked reduction of Lef-1 immunoreactivity in the hair matrix and dermal papillae of anagen VI (day 12 after depilation) hair follicles in DTG mice compared to WT **(Fig 3.22 b)**.

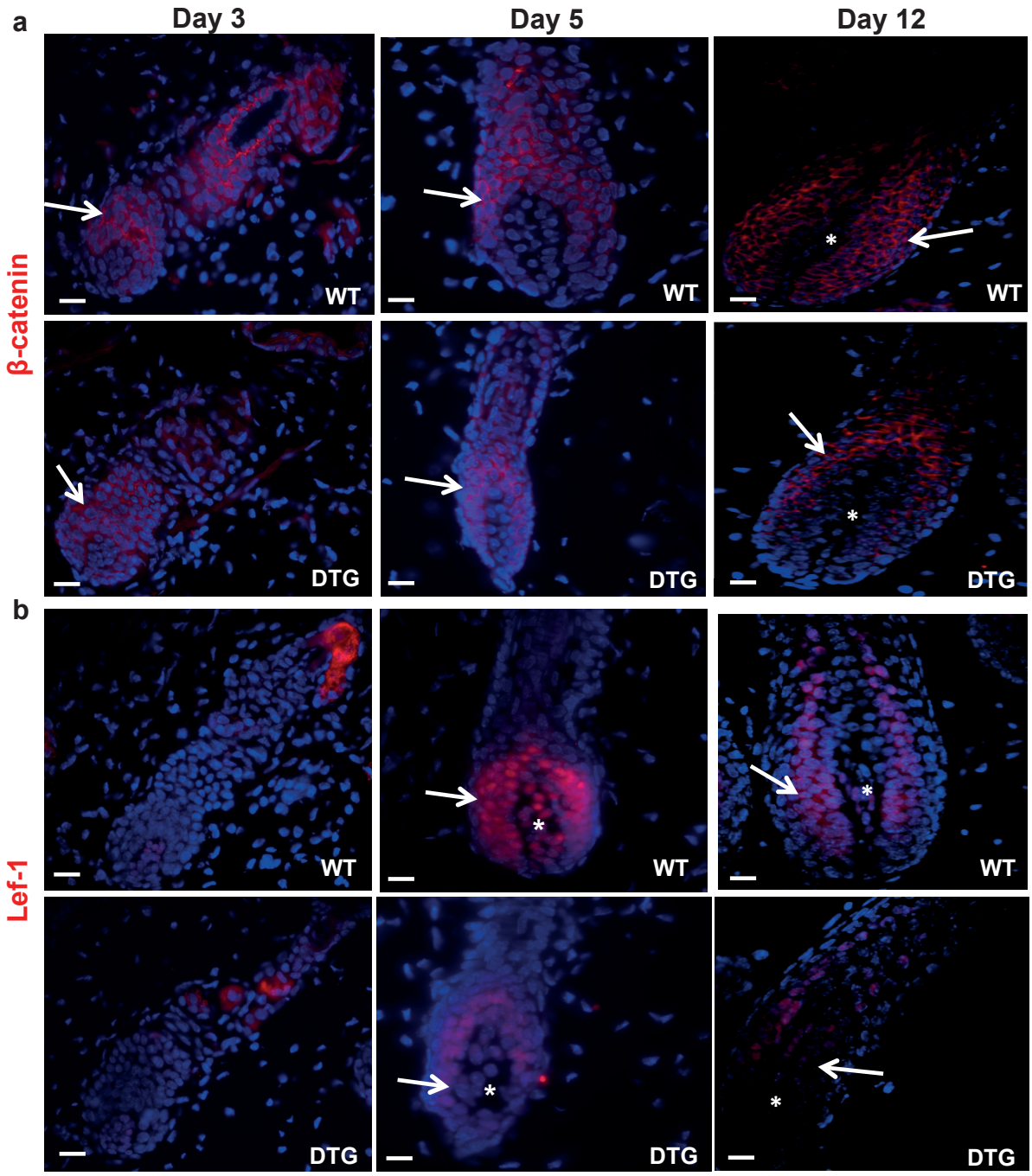

Figure 3.22. Expression of the mediators of Wnt signalling pathway during depilation-induced hair cycle. (a) Immunofluorescence analysis of β-catenin (red colour): reduced β-catenin expression in the hair matrix of anagen II follicles (day 3 after depilation, arrow) and anagen IV (day 5 after depilation, arrow) DTG hair follicles; decrease in β-catenin immunoreactivity in the hair matrix (arrow) and dermal papilla (asterisk) in anagen VI hair follicles in DTG mice (day 12 after depilation); **(b)** immunodetection of Lef-1 (red colour): no noticeable difference in expression of Lef-1 anagen II hair follicles (day 3 after depilation); marked decrease in the expression of Lef-1 in the hair matrix (arrows) and dermal papilla (asterisk) in hair follicles of DTG mice in anagen IV and VI hair follicles (days 5 and 12, respectively). Scale bar 50μm.

Consistent with data obtained above, activity of Shh pathway was reduced in the skin of DTG mice during hair cycle. Immunodetection of Shh in anagen II follicles (day 3 of after depilation) hair cycle showed no visible difference in expression between WT and DTG **(Fig 3.23 a).** However, qRT-PCR analysis confirmed a significant reduction of Gli-1 transcript levels in anagen II DTG skin **(Fig 3.23 b).** The difference in Shh expression became visible in anagen IV transgenic hair follicles (day 5 after depilation) revealed a reduction in expression in the hair matrix of DTG hair follicles compared to WT **(Fig. 3.23 c)**. In anagen VI hair follicles, Shh expression was decreased at both protein and mRNA levels **(Fig. 3.23 d-e),** whilst no significant difference in Gli-1 expression between WT and DTG mice was detected at this time point **(Fig. 3.23 d).**

Expression of pSmad 1/5/8 was increased in the transgenic hair follicles during the hair cycle **(Fig 3.24).** Increased immunoreactivity of pSmad 1/5/8 was seen in anagen II hair follicles (day 3 after depilation) **(Fig 3.24 a)** and anagen IV hair follicles (day 5 after depilation) **(Fig 3.24 b)** in DTG mice compared to WT. In anagen VI, the expression of pSmad 1/5/8 was further increased in the inner root sheath and hair shaft of transgenic follicles (day 12 after depilation) versus WT littermates **(Fig. 3.24 c).**

Consistent with the microarray data, expression of Cyclin D1 was reduced in the hair matrix of anagen VI transgenic follicles **(Fig 3.25 a).** In addition, significant increase in the transcript levels of cyclin-dependent kinase inhibitors Cdkn2a and Cdkn2d was detected in DTG skin at day 5 and at day 12 of depilation-induced hair cycle **(Fig 3.25 b, c).**

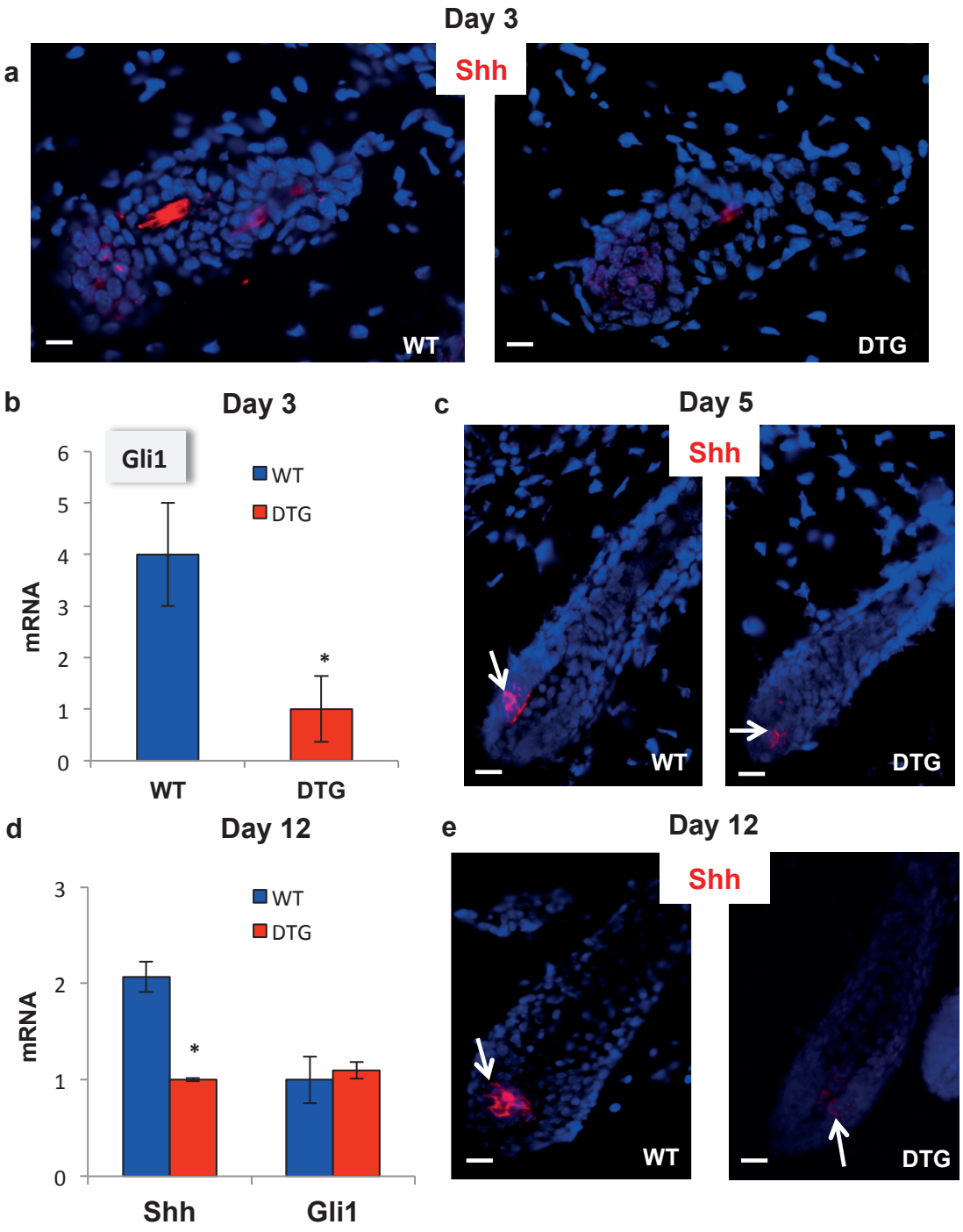

Figure. 3.23 Analysis of Shh signalling during depilation-induced hair cycle. (a) immunofluorescence analysis of Shh in anagen II hair follicles at day 3 of depilation-induced hair cycle: no visible difference in Shh expression between WT and DTG **(b)** qRT-PCR analysis of Gli1 in skin at day 3 (anagen II) after depilation: significant decrease in Gli-1 mRNA in DTG mice compared to WT; **(c)** reduced Shh immunoreactivity in the hair matrix (arrow) of anagen IV hair follicles (day 5 after depilation) in DTG mice compared to WT; **(d)** qRT-PCR: significant decrease in Shh transcript levels, whilst no difference in expression of Gli1 in DTG mice compared to WT in skin at day 12 after depilation (anagen VI); **(e)** reduced Shh immunoreactivity in the hair matrix of anagen VI DTG hair follicles compared to WT mice (arrows, day 12 post depilation); (mean ± SD, *P value<0.05, unpaired Student's t-test, n=3). Scale bar 50µm.

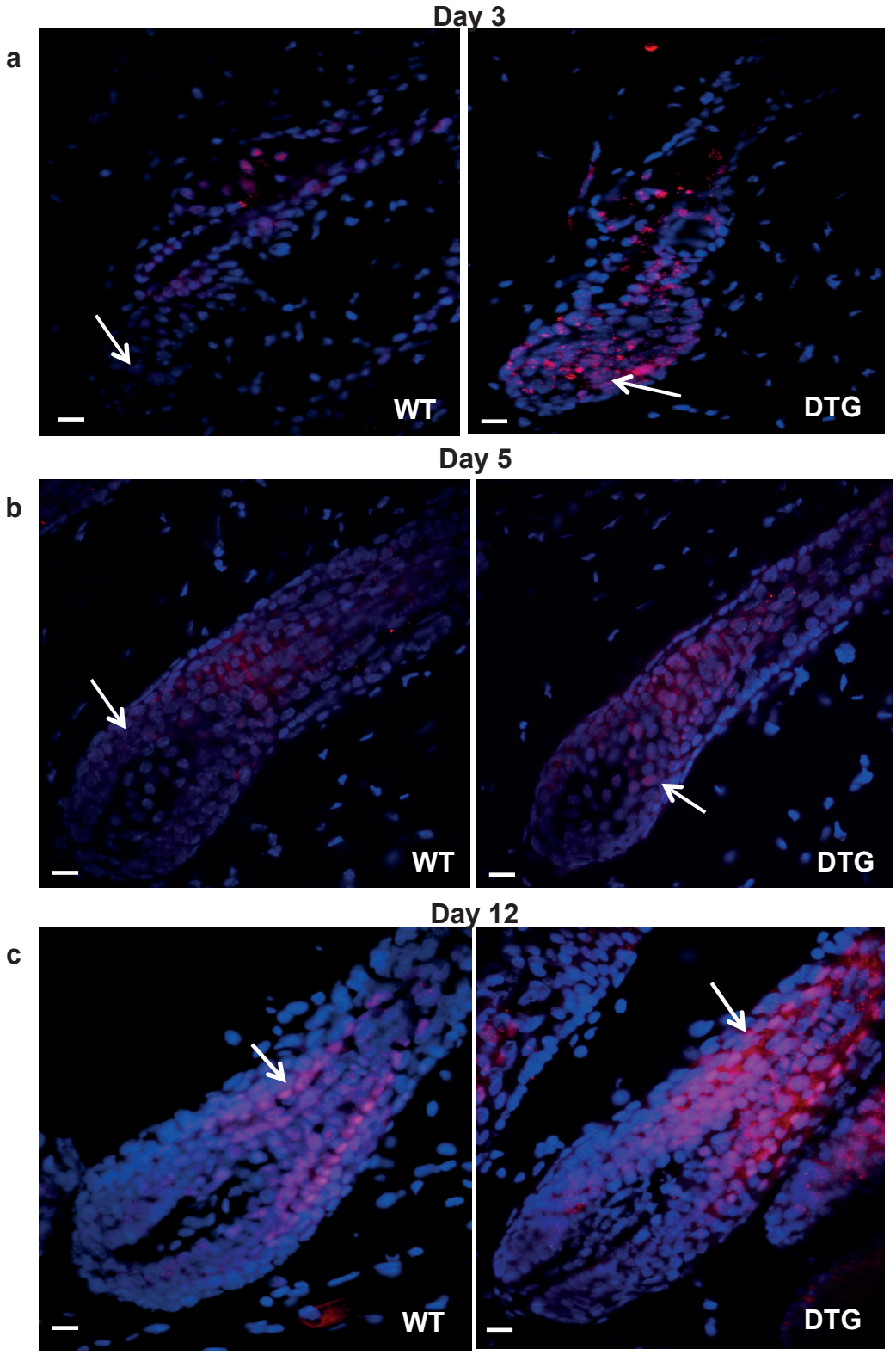

Figure. 3.24. Analysis of pSmad 1/5/8 during depilation-induced hair cycle by immunofluorescence (red colour). (a) increased pSmad 1/5/8 immunoreactivity in anagen II hair follicles DTG mice compared to WT at day 3 after depilation (arrow); **(b)** increase in pSmad 1/5/8 in anagen IV hair follicles (day 5 post depilation; arrow) of DTG mice compared to WT littermates; **(c)** increased expression of pSmad 1/5/8 in the inner root sheath and hair shaft (arrow) in the anagen VI hair follicle of DTG mice compared to WT (day 12 after depilation). Scale bar 50µm.

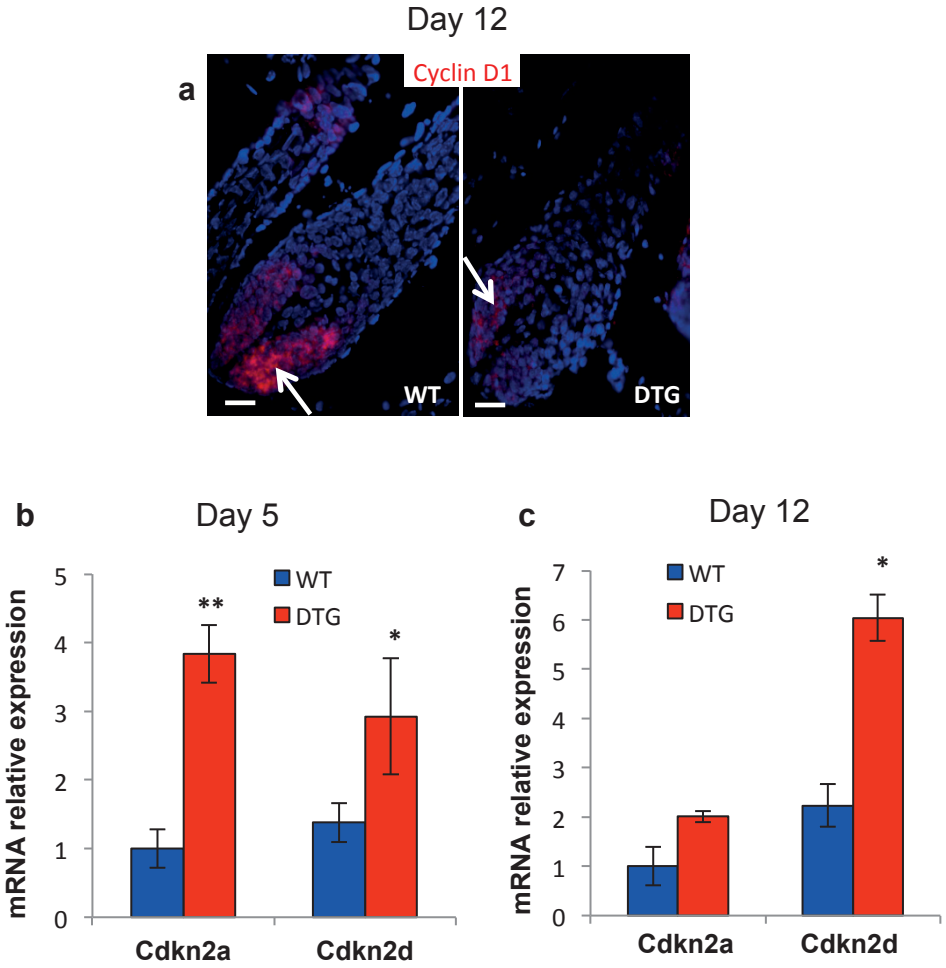

Figure 3.25 Analysis of proliferation during depilation induced hair cycle. (a) Immunofluorescence of Cyclin D1 (red colour) in anagen VI hair follicles at day 12 of depilation-induced hair cycle: decreased expression of Cyclin D1 in the hair matrix of DTG follicles compared to WT littermates (arrow); **(b)** qRT-PCR analysis of Cdkn2a and Cdkn2d in anagen IV skin (day 5 after depilation): significant increase in the expression of Cdkn2a and Cdkn2d in DTG mice compared to WT littermates; **(c)** qRT-PCR analysis of Cdkn2a and Cdkn2d in anagen VI skin (day 12 post depilation): significant increase in Cdkn2a and Cdkn2d transcript levels in DTG mice compared to WT littermates (mean ± SD *P value<0.05, **P<0.02, unpaired Student's t-test). Scale bar 50µm.

To investigate the possible effects of miR-214 on the hair follicle stem cells during depilation-induced hair cycle, analysis of Sox9 expression was performed **(Fig 3.26)**. A reduction in Sox9 expression in the developing outer root sheath of anagen II follicles (day 3 after depilation) **(Fig 3.26 a)** and anagen IV hair follicles (day 5 after depilation) **(Fig 3.26 b)** was observed in DTG mice compared to WT. A visible decrease in the number of Sox9 positive cells was also seen in the outer root sheath of anagen VI hair follicles (day 12 after depilation) **(Fig 3.26 c)** in DTG mice compared to WT. Quantitative analysis of Sox9 positive cells in the outer root sheath of anagen VI hair follicles confirmed a significant reduction in the number of Sox9 positive cells in transgenic hair follicles compared to WT **(Fig 3.26 d).** This suggests that miR-214 overexpression could inhibit a supply of progenitor cells from the bulge for the hair matrix.

These data suggest that miR-214 exerts inhibitory effects on hair follicle cycling, at least in part, via regulating the activity of key signalling pathways (Wnt, Hedgehog, Bmp and Edar) in keratinocytes, as well as via modulation of the Wnt signalling in dermal papilla fibroblasts.

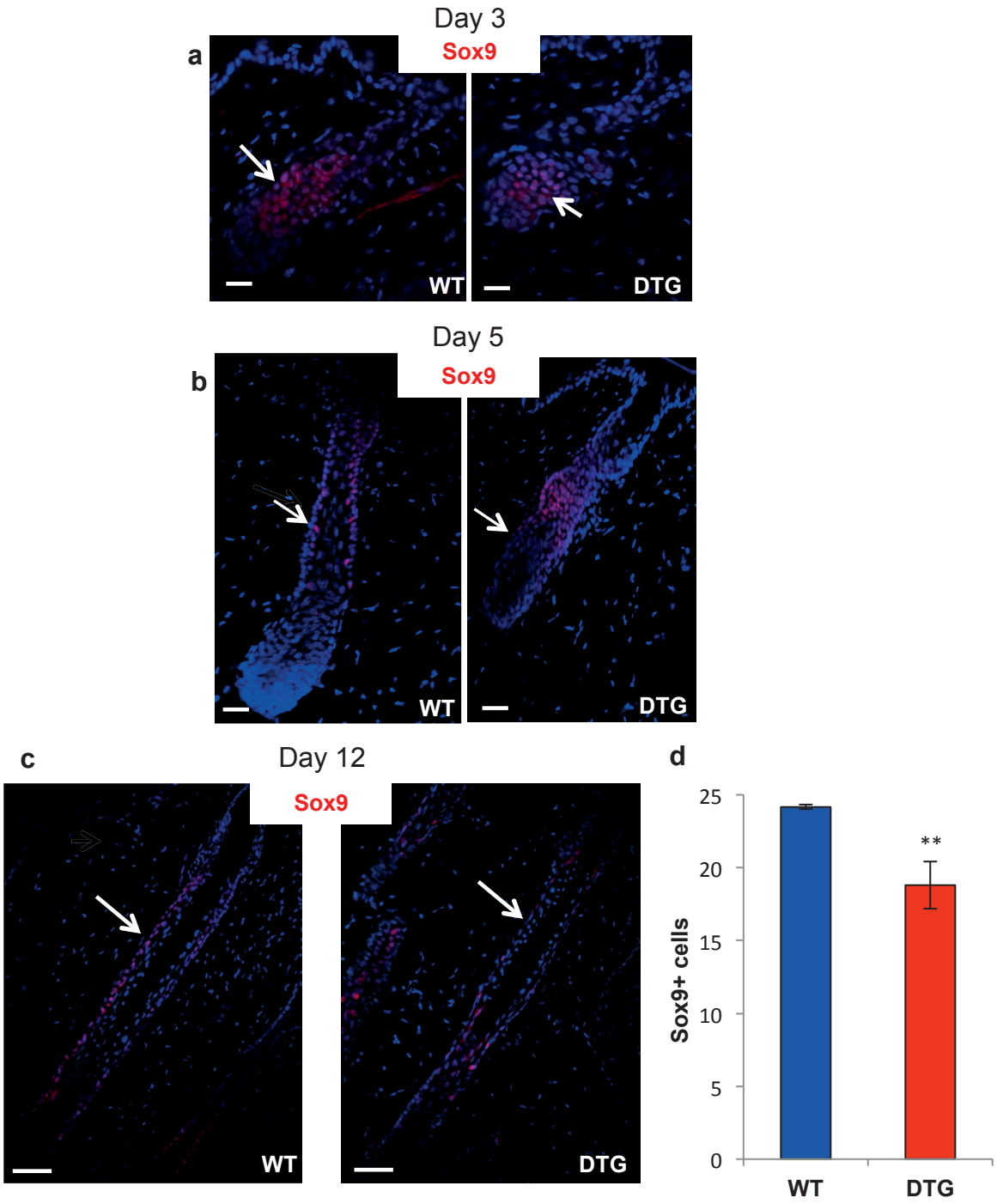

Figure. 3.26 Analysis of the stem cell marker Sox9 during depilation-induced hair cycle by immunofluorescence (red colour).
(a-b) visible reduction in the number of Sox9 positive cells in the developing outer root sheath of anagen IV and VI hair follicles in DTG mice versus WT littermates (arrows, day 3 and 5 post depilation, respectively); **(c-d)** significant decrease in the number of Sox9 positive cells in the outer root sheath of DTG anagen VI hair follicles compared to WT littermates (day 12 after depilation). (mean ± SD, **P value<0.02, unpaired student's t-test). Scale bar 50µm.

3.13 β-catenin is a direct target of miR-214 in keratinocytes

To identify the direct targets of miR-214 in keratinocytes, gene expression profiling results were linked with four databases for prediction of microRNA targets, including PITA, miRanda, miRDB, and TargetScan (**Fig. 3.27 a**). The largest number of possible miR-214 target genes was predicted by PITA and miRanda (192 and 78, respectively). TargetScan and miRDB showed only 18 and 11 possible target genes, respectively. Intersections of PITA, miRanda, miRDB predictions identified 9 common genes that could possibly be direct targets of miR-214, which includes *β-catenin* and *Shh* (**Table 3**). However, overlapping of all four databases further revealed only 3 predicted target genes for miR-214, which expression was altered in DTG keratinocytes, including *β-catenin,* but not *Shh* **(Table 3)**.

PITA, miRanda, miRDB	PITA, miRanda, miRDB, TargetScan
Ctnnb1	Ctnnb1
Dctd	Lhx6
Idh1	Map6d1
Lhx6	
Map6d1	
Pcdh20	
Ppp2r4	
Sdf2l1	
Shh	

Table 3. Overlap of miR-214 predicted targets. Target prediction databases were linked to gene expression profiling to identify direct targets of miR-214 in keratinocytes. Overlap of 3 databases identified 9 common targets (genes of

interest in red highlight), whereas the overlap of all four databases further revealed only 3 predicted targets.

To validate the results of bioinformatic analysis and explore whether *β-catenin* and *Shh* 3'UTR carry functional binding sites for miR-214 (**Fig. 3.27 b, d**), luciferase reporter assay was performed. Co-transfection of HaCaT cells with miR-214 mimic and the *β-catenin* 3'UTR reporter construct caused significant reduction in luciferase activity, compared to the corresponding control, whilst this effect was not detected when *β-catenin* 3'UTR was mutated (**Fig. 3.27 c**), thus confirming that *β-catenin* is a direct target of miR-214. Luciferase reporter assay did not confirm the direct interactions between miR-214 and 3'UTR of *Shh* suggesting that decrease of its expression in the hair follicles after miR-214 overexpression is mediated by other factors (**Fig. 3.27 e**).

To further validate miR-214-*β-catenin* interactions, the effect of miR-214 on the β-catenin/Tcf-dependent transcription activity was evaluated by using TOPflash reporter assay. A significant induction in TOPflash reporter activity, without any effect on FOPflash activity (negative control), was detected in HaCaT cells treated with a synthetic Wnt agonist 6-bromoindirubin-3'-oxime (BIO) (Sato et al., 2004; Tseng et al., 2006), whereas transfection of cells with miR-214 mimic significantly diminished TOPflash activity-induced by BIO (**Fig. 3.27 f**). This result suggested that miR-214 controls *β-catenin* expression by direct binding to its 3'UTR and that β-catenin represents a genuine target of miR-214.

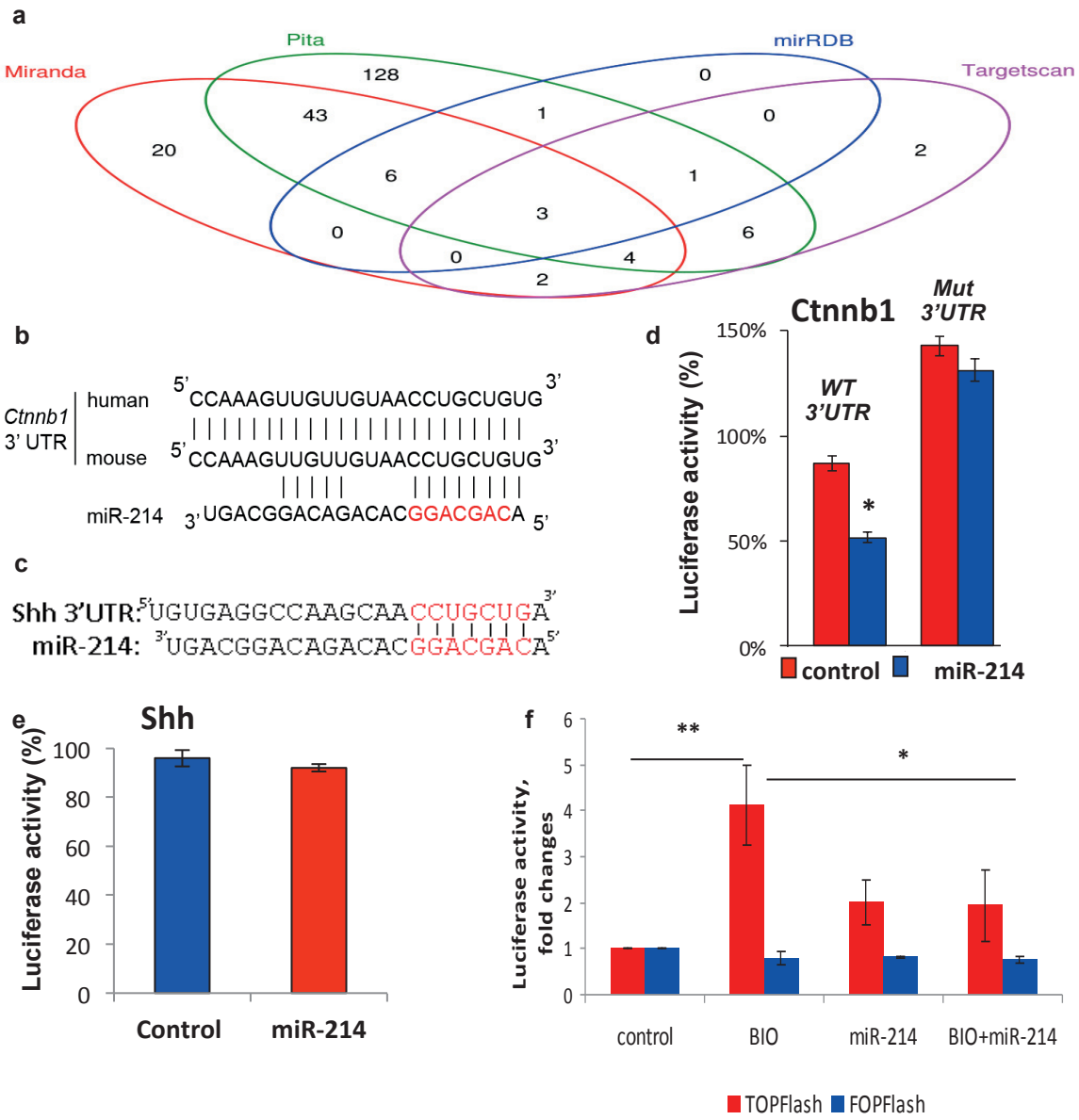

Figure. 3.27. **β-catenin is a direct target of miR-214 (a)** A venn diagram depicting the overlap of four databases for prediction of microRNA targets (PITA, miRanda, miRDB and Targetscan) with gene expression profiling of the epithelium of neonatal DTG mice after 48 hours Doxycycline treatment. Only downregulated genes (<1.5 fold) were included; **(b)** predicted interactions between miR-214 and Ctnnb1: alignment of mouse and human sequences in the 3'-UTR of Ctnnb1 mRNA; **(c)** predicted interactions between miR-214 and Shh: alignment of mouse sequences in the 3'-UTR of Shh; **(d)** significant reduction in luciferase activity due to co-transfection with miR-214 mimic and the Ctnnb1 3'UTR constructs encompassing putative miR-214 target site; no changes in luciferase activity was detected when the potential miRNA binding site was mutated (mut-3'UTR); **(e)** no changes in luciferase activity due to co-transfection with miR-214 mimic and the Shh 3'UTR constructs encompassing putative miR-214 target site; **(f)** TOPflash reporter assay: significant induction in TOPflash reporter activity in HaCaTcells by BIO, which was diminished by miR-214 mimic. No changes in FOPflash activity in any experimental group (mean ± SD, *P value<0.05, **P<0.02, unpaired Student's t-test)

3.14 Activation of Wnt signalling rescues skin phenotype in miR-214 transgenic mice

To explore the functional links between miR-214 and *β-catenin* in vivo, miR-214 trangene was induced since embryonic day 10.5 followed by the subcutaneous injections of Wnt agonist BIO on five consecutive days after birth. Immunofluorescence analysis revealed that pharmacological activation of Wnt signalling resulted in restoration of β-catenin expression on postnatal day 5.5 (P5.5) in DTG mice to the level seen in WT mice (**Fig. 3.28 a**).

Furthermore, BIO treatment lead to induction of new hair follicles in DTG mice postnatally, which resulted in appearance of hair follicles at early stages of morphogenesis (stages 2-3) in DTG mice followed by restoration of their total number to the levels seen in P5.5 WT controls (**Fig. 3.28 b**). To validate the visible difference, quantitative analysis was performed which revealed a significant reduction in the number of hair follicles in DTG compared to WT littermate at P5.5 (**Fig. 3.28 c**). No such difference was found in the number of hair follicles between WT and DT after 5 days of BIO treatment In addition (**Fig. 3.28 d).** Pharmacological Wnt activation resulted in an increase of the hair bulb diameter in the hair follicles at advanced stages (stages 6-7) of morphogenesis in DTG mice, while no increase of hair bulb size was seen in WT mice treated with BIO (**Fig. 3.28 e**). These observations demonstrate that activation of Wnt signalling in DTG mice rescues the effects of miR-214 overexpression in vivo confirming further that miR-214 indeed interfere with the Wnt pathway activity in the developing and postnatal skin.

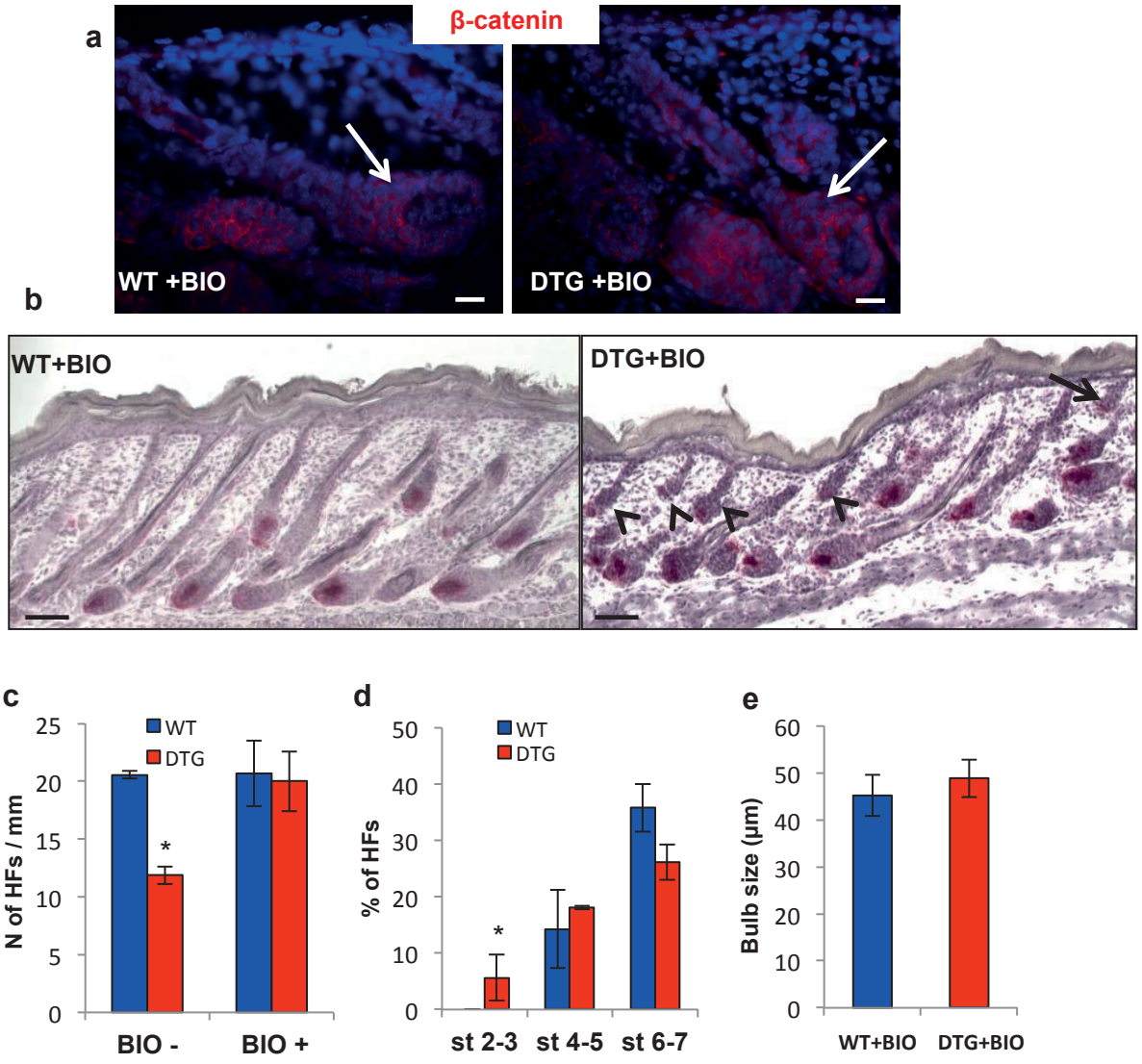

Figure. 3.28. Wnt agonist BIO rescues the phenotype caused by miR-214 overexpression. (a) Immunofluorescence analysis of β-catenin in hair follicles at P5.5 after treatment with Wnt agonist BIO; no difference in expression of β-catenin between WT and DTG; **(b)** Representative microphotographs of histology of back skin of WT and DTG mice after 5 days of BIO treatment at P5.5, arrows show hair follicles at stages 2-3 of hair morphogenesis; **(c)** quantitative analysis revealed a significant reduction in the number of hair follicles in DTG compared to WT littermate at P5.5; no difference was found in the number of hair follicles between WT and DT after 5 days of BIO treatment; **(d)** Quantitative analysis of hair follicles at different stages of morphogenesis in skin of WT and DTG mice after 5 days of BIO treatment revealed a significantly increased number of the hair follicles at the stages 2-3 of morphogenesis in DTG skin versus WT littermates; **(e)** histomorphometric analysis of hair bulb diameter measured across the widest part (line of Auber) in stage 6-7 hair follicles: no difference between WT and DTG (mean ± SD, *P value<0.05, unpaired Student's t-test). Scale bar 50µm.

4.0 DISCUSSION

4.1 miR-214 is expressed in distinct cell populations during hair follicle development and cycling

Complex programmes of gene activation and silencing are involved in skin development and homeostasis. One of the most fascinating appendages of the skin is the hair follicle, which continually regenerates throughout a lifetime. In addition to transcription factor-mediated and epigenetic regulatory mechanisms, programmes of the gene activation and silencing governing hair follicle development and cycling are controlled by miRNAs (Botchkareva, 2012; Yi and Fuchs, 2011). MiRNA-dependent control of gene expression plays a fundamental role in the balancing and fine-tuning of lineage-specific differentiation programs in many organs including skin (Aberdam et al., 2008; Andl et al., 2006; Flynt and Lai, 2008; Yi et al., 2006).

miR-214 is involved in numerous cellular processes such as proliferation, migration, differentiation and apoptosis (Yang et al., 2013; Yin et al., 2010; Zhang et al., 2014) and has shown to be vital in determining cell fate in several cell types (Decembrini et al., 2009; Flynt et al., 2007; Juan et al., 2009). In zebrafish, miR-214 was shown to regulate muscle cell fate decision through regulation of Hh signalling (Flynt et al., 2007). The deletion of Dnm3os (Dynamin3-opposite strand), which contains the murine miR-214 locus leads to several developmental abnormalities (Watanabe et al., 2008). In mouse skeletal muscle, miR-214 targets Ezh2 (Enhancer of zest homologue 2), a Polycomb group protein, to regulate muscle cell differentiation (Juan et al., 2009). Ezh2 performs the epigenetic modification of trimethylation of histone H3 at lysine 27 (H3K27me3) and represses gene transcription. It has been shown that Ezh2 is regulated during myogenesis and prevents muscle differentiation by imposing

H3K27me3 on muscle-specific genes. In order for appropriate muscle gene activation, it is vital to remove Ezh2 and its associated methylation (Caretti et al., 2004). Hence, the repression of Ezh2 by miR-214 is essential for initiating muscle differentiation (Juan et al., 2009).The dynamic regulation of miRNA is exemplified in mouse skeletal muscle, where transcription of miR-214 is regulated by a double-negative feedback loop in which miR-214 is repressed by Ezh2 and activated by myoD/myogenin (Juan et al., 2009). The expression of the miR-214 gene is developmentally regulated by Twist-1, a key transcriptional factor controlling epithelial-mesenchymal transitions (Lee et al., 2009), which is crucial for normal development and tissue repair. It has also been demonstrated that miR-214 plays an important role in controlling the development of the nervous system, teeth, the pancreas, and bone formation (Chen et al., 2010; Joglekar et al., 2007; Sehic et al., 2011; Wang et al., 2013b)

Yi et al showed that miR-214 is one of the most highly expressed miRNAs in the hair follicle during development (Yi et al., 2006), however, its role in the control of skin and hair follicle development and homeostasis is unknown.

This project identified a novel role for miR-214 in the control of skin and hair follicle development and demonstrated that: i) miR-214 shows spatial-temporal changes of the expression patterns in the skin during hair follicle morphogenesis and cycling, ii) inducible overexpression of miR-214 in keratinocytes inhibits cell proliferation, results in a formation of fewer hair follicles with decreased size of the hair bulb, which produce thinner hairs, iii) miR-214 regulates the balance in the activities of multiple signalling pathways, including Wnt, Shh, Edar, and Bmp in developing and postnatal skin, and iv) β-catenin serves as a direct miR-214 target in keratinocytes.

During skin development and postnatal growth, miR-214 expression predominates in differentiating populations of keratinocytes committed either to epidermal or hair follicle cell fates (suprabasal epidermal or hair matrix keratinocytes, respectively), while its expression in the progenitor cell populations of the basal epidermal layer or hair follicle outer root sheath appears to be considerably lower. The difference in expression suggests that miR-214 may play a role in the differentiation of epidermal keratinocytes and possibly involved in determining cell fate during morphogenesis. The abundant expression of miR-214 in the growing hair matrix also suggests that miR-214 is essential for the control of keratinocyte proliferation and differentiation.

In telogen hair follicles, miR-214 was highly expressed in the secondary hair germ. The telogen-anagen transition is promoted by Wnt and FGF signalling, which provide stimulatory signals to the hair follicle stem cells and/or their progeny residing in the hair follicle bulge and secondary hair germ, whereas Bmp signalling functions as an anagen inhibitor antagonising the activity of the FGF and Wnt pathways during telogen (Botchkarev et al., 2001a; Enshell-Seijffers et al., 2010; Greco et al., 2009; Plikus et al., 2008). Thus miR-214 may be involved in regulating these signalling pathways during telogen quiescence and the transition from telogen to anagen.

In mid- and late-anagen stages of the hair cycle, miR-214 was expressed in the bulge of hair follicles, the hair matrix and the inner and outer root sheath. The contrast in expression of miR-214 in differentiating keratinocytes and progenitor cell populations in the basal layer and outer root sheath suggests that miR-214 may play a role in balancing the switch between proliferation and differentiation possibly by maintaining ‘stemness’ in keratinocytes. This is supported by the

low level miR-214 expression in stem cell rich areas such as the bulge in anagen hair follicle, in contrast to higher expression in the hair matrix.

Therefore it was hypothesised that since the spatio-temporal expression of miR-214 in distinct cell populations in the skin and hair follicle coincides with the components of several of the above mentioned signalling pathways, it may therefore function to regulate them.

In this project a transgenic mouse model was employed to further elucidate the role of miR-214 in skin and hair follicle development and cycling.

4.2 K14-driven overexpression of miR-214 negatively affects hair follicle induction

K14-driven miR-214 overexpression in the progenitor cell populations of the epidermis and hair follicle resulted in DTG mice that exhibited a ‘rough’ fur coat in comparison to WT mice which showed an appearance of a ‘smooth’ fur coat. The overexpression of miR-214 led to approximately 30% fewer hair follicles forming in the dorsal skin of mice due to a reduction in the number of both primary and secondary hair follicles.

Skin and hair follicle morphogenesis is controlled by coordinated activities of the Wnt, Hedgehog, Edar, Shh, Bmp, FGF, Notch and other signalling pathways. (Andl et al., 2002; Chiang et al., 1999; Eivers et al., 2008; Enshell-Seijffers et al., 2010; Huelsken et al., 2001; Jiang et al., 1999; Mikkola, 2011; Sick et al., 2006; St-Jacques et al., 1998; Zhang et al., 2009; Zhou et al., 1995). Among these pathways, Wnt signalling operates as the most powerful regulator of skin development and controls cell proliferation in epithelial cells of the epidermis

and hair follicle matrix as well as mesenchymal cells of the dermal papilla. In addition it regulates differentiation of hair matrix keratinocytes as well as the morphogen-producing activity of dermal papilla cells (Andl et al., 2002; Choi et al., 2013; Enshell-Seijffers et al., 2010; Fu and Hsu, 2013; Huelsken et al., 2001; Jiang et al., 1999; Sick et al., 2006; Tsai et al., 2014; Zhou et al., 1995).

The present study demonstrates that miR-214 contributes to regulation of the activity of Wnt signalling pathway in developing skin by targeting its key component β-catenin. Bioinformatic analysis validated by the reporter assays suggested that miR-214 directly targets *β-catenin* in keratinocytes. The immunofluorescence analysis of β-catenin and its transcriptional cofactor Lef-1, showed markedly decreased expression in the epidermis and hair follicle placodes during hair morphogenesis, indicating that miR-214 is involved in regulating the induction of hair follicles, at least in part through modulating Wnt signalling. In developing hair follicles, Wnt signalling pathway operates as activator of the placode formation, while BMP signalling inhibits this process and, together with Wnt inhibitors Dkk1/2/4 promotes the inter-placode cell fate in the epidermal progenitor cells (Andl et al., 2002; Botchkarev et al., 1999a; Jiang et al., 1999; Sick et al., 2006).

The reduced number of hair follicles in miR-214 overexpressing mice is consistent with a study by Huelsken et al, who showed that when β-catenin is absent during skin development, stem cells fail to differentiate into follicular keratinocytes but instead adopt an epidermal fate. Furthermore, the phenotypic properties seen in the skin of DTG mice which included a decrease of epidermal proliferation and epidermal thickness, a proportional decrease in number of all types of the hair follicles and retardation of their morphogenesis,

decrease of the size of hair bulbs and formation of thinner hair shafts compared to WT controls, is consistent with skin phenotype of mice with conditional ablation of β-catenin either in keratinocytes or in the dermal papilla fibroblasts (Enshell-Seijffers et al., 2010; Huelsken et al., 2001; Tsai et al., 2014).

Tsai et al showed that Wnt signalling in dermal condensates is required for hair follicle formation (Tsai et al., 2014). The ablation of β-catenin led to the number of primary guard hair follicle becoming strongly reduced and by embryonic day 18, most guard hair follicles were absent, suggesting that active Wnt signalling in dermal condensates is important for hair follicle formation to proceed after induction. Enshell-Seijffers et al showed that β-catenin activity in the dermal papilla regulates a number of other signalling pathways, including the FGF pathway that can mediate the inductive effects of the dermal papilla on the hair follicle epithelium (Enshell-Seijffers et al., 2010). In addition, the findings of the current study are in the line with the phenotypic properties seen in transgenic mice overexpressing β-catenin in skin keratinocytes, which produced extra hair follicles, a thicker fur coat, with uncontrolled proliferation eventually leading to the formation of tumours (Gat et al., 1998).

As Edar is only expressed in the epidermis, studies have suggested that the Eda signalling pathway is important for placode patterning, affecting the induction of primary and zigzag hair follicles, but not necessary for initial placode formation (Botchkarev and Fessing, 2005; Schmidt-Ullrich et al., 2006; Zhang et al., 2009). However, Edar signalling promotes hair follicle placode formation via stimulation of expression of Shh (Pummila et al., 2007), which operates as a potent stimulator of keratinocyte proliferation in the developing hair follicle (Chiang et al., 1999; St-Jacques et al., 1998). Immunofluorescence

analysis of Edar and Shh showed reduced expression in hair follicle placodes of DTG mice. Given that Wnt signalling operates as upstream of Edar and Hedgehog pathways in the control of formation of the hair follicle placodes (Schmidt-Ullrich et al., 2006; Zhang et al., 2009) these data suggest that the decrease of Edar and Shh expression seen in the hair follicle placodes, is an indirect affect caused by downregulation of Wnt signalling.

In addition to activators, the skin also contains inhibitors of hair follicle induction, in particular BMP signalling has shown to have an inhibitory effect on hair follicle induction (Botchkarev et al., 1999a). Expression of pSmad 1/5/8, an indicator of BMP activity, was increased in the hair follicle placodes and inter-follicular epidermis of DTG mice, indicating that miR-214 overexpression results in activation of BMP signalling. As Edar pathway has been shown to promote the placode cell fate, at least in part, by inhibiting the activity of BMP signalling (Eivers et al., 2008; Plouhinec et al., 2011), the reduction of Edar expression and increase in BMP activity in DTG may also contribute to partially inihibited induction of hair follicle placodes and may promote inter-placode cell fate.

The transcription factor Lhx2 has been shown to be crucial for hair follicle development (Rhee et al., 2006), however immunofluorescence analysis revealed no noticeable difference between WT and DTG littermates during hair follicle development. Thus, indicating that the phenotypic properties seen in DTG during hair follicle induction are independent of Lhx2 regulation.

These data collectively indicate that miR-214 regulates the activity of epidermal keratinocytes and is involved in the induction of hair follicles through direct targeting of Wnt/β-catenin signalling, and indirectly targeting Edar, Shh and BMP pathways.

4.3. K14-driven overexpression of miR-214 modulates hair follicle morphogenesis

Although the rate of hair follicle morphogenesis was not significantly affected and all hair follicles at postnatal day 8 reached anagen-like stage, they were significantly shorter and hair bulbs were significantly smaller in DTG mice. In addition to changes seen in the hair follicle epithelium, the significant reduction in the number of dermal papilla cells was observed in DTG mice during postnatal growth. It is consistent with recently published data demonstrating that decrease of the hair bulb size is associated with reduced cellularity of the dermal papilla (Choi et al., 2013).

Recent data suggest that activity of the Wnt signalling pathways considerably vary in distinct skin compartments: low levels of activity are required for maintenance of epidermal proliferation, medium level signalling is required for maintenance of epithelial-mesenchymal interactions in the hair bulb to promote active hair growth phase, while high activity promotes hair shaft differentiation (Choi et al., 2013). In addition to decreased expression of β-catenin and Lef-1 in the hair matrix, levels of these proteins were reduced in the dermal papilla of DTG hair follicles. This suggests that overexpression of miR-214 in the hair follicle keratinocytes has an effect on dermal papilla fibroblasts as a result of epithelial-mesenchymal interactions. Overexpression of miR-214 resulted in the decreased transcript levels of IGF-I expressed by the dermal papilla. IGF-I acts as a mitogen in the epidermis and hair follicle and is crucial for proper hair shaft differentiation (Weger and Schlake, 2005). The withdrawal of IGF-I from the medium of *in vitro* cultures of human hair follicles in the anagen phase induced premature entry into a catagen-like phase of the hair cycle (Philpott et al.,

1994). Transgenic expression of *IGF-I* in the interfollicular epidermis causes epidermal hyperplasia (Bol et al., 1997). Reduced expression of IGF-1 in postnatal skin of DTG mice may additionally contribute to reduced keratinocyte proliferation and altered hair shaft differentiation.

The changes in cellularity and gene expression in the dermal papilla of DTG mice suggest altered epithelial-mesenchymal interactions. Given that miRNAs are capable of exerting paracrine effects on distantly located cellular targets (Zhu and Fan, 2011), additional studies need to clarify whether miR-214 overexpression in keratinocytes could directly influence cell number and gene expression in dermal papilla fibroblasts, or other paracrine factors released from keratinocytes affect traffic of connective tissue progenitor cells to populate dermal papilla and/or their activity in the hair follicles of DTG mice.

Wnt signalling pathway is a potent regulator of cell proliferation (Gat et al., 1998; MacDonald et al., 2009; Van Mater et al., 2003) and many of the effects of miR-214 on skin and hair follicle development are most likely associated with interference with cell cycle regulation: in fact, short-term activation of miR-214 in the epidermis suppressed the expressions of several cyclins and cyclin dependent kinases, including *cyclin B, cyclin D1, cyclin D2* and *cdk1*, in addition to significant downregulation of β-catenin. Consistent with these observations, substantial upregulation in cyclin-dependent kinase inhibitors Cdkn2a and Cdkn2d was still detected in fully developed follicles (postnatal day 8) of the DTG mice, suggesting the activation of the anti-proliferative program in response to increased levels of miR-214 in the keratinocytes. These data are consistent with studies in which β-catenin has been shown to upregulate cyclin D1 expression (Shtutman et al., 1999; Tetsu and McCormick, 1999). This is

also in line with the results obtained in other models and demonstrating that miR-214 expression is substantially decreased in cutaneous squamous cell carcinoma (Yamane et al., 2013) and that the anti-proliferative effects of miR-214 in myoblast cell line is achieved via targeting Nras (Liu et al., 2010).

However, reduced proliferation seen in the epidermis and hair follicles in DTG mice could partly be a result of altered activity of Shh signalling. In fact, decreased expression of Shh and its signal tranducer Smo was found in the epithelium of DTG mice at postnatal day 2. Shh signalling is required for post hair placode initiation growth by promoting the proliferation of follicular epithelial cells by transcriptional activation of cyclin D1 and cyclin D2 in the developing hair follicles (Chiang et al., 1999; Mill et al., 2003; Schmidt-Ullrich et al., 2006; St-Jacques et al., 1998). This is also consistent with the downregulation of *cyclin D* and *cyclin D2* in the epithelium of DTG mice. In addition, immunofluorescence analysis of Shh revealed a decrease in expression in the epithelium of DTG hair follicles during hair follicle morphogenesis. However, experimental validation of bioinformatic prediction analysis demonstrated that *Shh* does not serve as a direct miR-214 target in keratinocytes. Given that Wnt signalling operates as upstream of Edar and Hedgehog pathways these data suggest that the downregulation of the Edar and Shh expressions seen in the epithelium of DTG hair follicles during morphogenesis mice most likely represent the indirect effects linked to the miR-214-mediated decrease of the Wnt pathway activity in keratinocytes.

The phenotypic properties of DTG mice were not only associated with downregulation of Wnt activity but also an upregulation of BMP activity. The

reduced proliferative activity, hair bulb diameter and hair follicle length of DTG hair follicles is consistent with a previous study by Sharov et al. who demonstrated that hair shaft diameter depends on size of the hair bulb and the proliferative activity of the matrix keratinocytes (Sharov et al., 2006). The inhibition of BMP activity led to the development of larger hair bulbs and thicker hair diameter (Sharov et al., 2006). This is consistent with the findings in this study, in which reduced bulb size and keratinocyte proliferation, was associated with an increase in BMP activity. The expression levels of BMP inhibitor Sostdc1 was reduced in the epithelium of DTG mice in addition to increased immunoreactivity of pSmad 1/5/8 during hair follicle morphogenesis.

The expression of Lef-1 was also decreased during hair follicle morphogenesis, and after short term activation of miR-214 in mouse epithelium. Lef-1, which is the transcriptional cofactor for β-catenin, is required for hair follicle growth. Elevation of Lef-1 expression in the keratinocytes of the hair matrix has been shown to be vital for commitment of keratinocytes for hair shaft differentiation (DasGupta and Fuchs, 1999). Therefore, reduced hair shaft thickness could additionally be attributed to the reduction in the levels Lef-1. In addition Lef-1 has been shown to be vital in determining hair follicle patterning (Zhou et al., 1995), which could also partly contribute to the reduced number of hair follicle seen in DTG mice. These data demonstrate that the phenotypic property of hair follicles in DTG mice is also partly due to altered activity of Lef-1 as a downstream result of β-catenin downregulation.

These data collectively indicate that through the direct targeting of β-catenin, miR-214 directly affects Wnt signalling and indirectly affects Eda, Shh and BMP signalling, during hair follicle morphogenesis.

The dorsal skin of mice produces four different types of hair follicles (guard, awl, auchene and zigzag) that produce hair shafts which vary in shape and structure (Schlake, 2007). In this study we found that the percentage of the different hair shafts produced was similar in WT and DTG mice after miR-214 overexpression, although they were found to be significantly thinner in DTG mice in comparison to WT. Even though hair shafts were thinner in DTG mice they were not significantly shorter in length compared to WT. In addition, the expression of Sox2 was similar in the dermal papilla of WT and DTG mice during postnatal growth and during the hair cycle. The lack of difference in Sox2 expression and hair follicle types between WT and DTG is consistent with a study by Driskell et al who demonstrated that Sox2 is involved in specifying hair follicle type in mammalian epidermis (Driskell et al., 2009).

Immunodetection of the stem cell marker Lhx2 showed decreased expression in the hair follicles of DTG mice at postnatal day 8, indicating that miR-214 affects the activity of hair follicle stem cells. Spatio-temporal expression of miR-214 was seen in the stem cell rich regions; the bulge of fully developed hair follicles during postnatal growth and anagen hair follicles, the secondary hair germ in telogen hair follicles and also in the outer root sheath, where stem cell progeny migrate to the hair matrix. These data together, could lead one to speculate that by co-ordinately fine-tuning the expression of a large number of proteins, miR-214 may be acting as a rheostat to regulate decisions involving the switch from stemness and commitment.

In the hair lineage, quiescent bulge stem cells are known to be activated by external Wnt promoting and BMP inhibitory signals. As stem cell progeny move down along the outer root sheath, they are thought to progressively adjust their fate from that of stem cells to committed progenitors. Eventually, these cells pass a point of no return and end up as transiently-amplifying matrix cells (Hsu et al., 2011). This is consistent with the findings of this study in which β-catenin serves as a direct target of miR-214 and deregulates Wnt and BMP activity, together with reduced migration of stem cell progeny from the bulge to the matrix. However, the potential involvement of miR-214 in regulation of the activity of distinct hair follicle stem cell populations residing in the bulge and also secondary hair germ during hair cycle need to further investigated (Hsu et al., 2011; Huelsken et al., 2001; Rompolas and Greco, 2014).

4.4 Overexpression of miR-214 modulates the expression of key signalling pathways during the hair cycle

After transgene induction during the telogen phase, hair follicles were depilated to induce anagen. The progression of the hair cycle in DTG mice was significantly retarded, in addition to reduced proliferation, thinner hair bulbs and shorter hair follicles, similar to phenotypic properties seen during development.

The activation of stem cells from a quiescent state leading to proliferation and differentiation is a complex process, which remains to be fully elucidated. Pathways which have been shown to be critical to these processes are the Wnt and BMP (Blanpain et al., 2004; DasGupta and Fuchs, 1999; Kobielak et al., 2007) Similar to postnatal hair follicle development, the overexpression of miR-

214 results in decreased expression of the components of Wnt, Shh pathways and increased activity of BMP during the hair cycle.

The immunoreactivity of β-catenin and Lef-1 was found to be reduced in the epithelium and also the dermal papilla of DTG anagen hair follicles. A recent study by Choi et al showed that β-catenin is required within bulge and secondary hair germ cells for anagen initiation, with the deletion of β-catenin in bulge and secondary hair germ cells preventing follicles from progressing through anagen (Choi et al., 2013). BMP signalling has also been shown to repress bulge cell proliferation and the loss of BMP signalling results in premature bulge cell activation (Blanpain et al., 2004; Kobielak et al., 2007).This is consistent with the delay in anagen progression seen in DTG mice, as miR-214 is expressed in the secondary hair germ in telogen hair follicles, these data indicate that the downregulation of β-catenin by miR-214 and subsequently activation of BMP in the secondary hair germ causes a delay in anagen progression in DTG mice.

As miR-214 is highly expressed in the hair bulb, it indicates that it is also involved in regulating hair differentiation and anagen progression by directly targeting β-catenin. This is consistent with previous studies which showed that Wnt/β-catenin signalling is also required for the differentiation of matrix keratinocytes in generating the hair shaft (DasGupta and Fuchs, 1999; Merrill et al., 2001).

Shh promotes epidermal proliferation (Zhou et al., 2006) and in adult mice is essential for anagen onset and proper hair cycling (Sato et al., 1999; Wang et al., 2000). Although Shh expression was similar in early anagen, the expression

of Gli-1 which is an effector of Shh signalling was significantly downregulated, indicating that miR-214 indirectly affects several components of Shh signalling. In late anagen hair follicles, expression of Shh and its target gene Cyclin D1 was reduced in DTG matrix, whereas transcript levels of Cdkn2a and Cdkn2d were increased. This indicates that reduced proliferation and small hair bulbs in DTG mice can be additionally attributed to decreased Shh activity.

The data from this study suggests that decrease of hair follicle size in DTG mice could be associated with the decreased proliferation in the hair matrix, as well as with miR-214 effects on the migration of the progenitor cells from the bulge alongside the outer root sheath towards hair matrix. In fact, hair follicles of DTG mice contained significantly fewer numbers of Sox9 positive cells in the outer root sheath. Sox9 is a transcriptional regulator which is expressed in the hair follicle stem cells and their outer root sheath progenies and is required for guiding stem cell progenies to the hair matrix (Vidal et al., 2005). Therefore, reduced number of Sox9 positive cells in the hair follicle of transgenic mice suggests the inhibitory action of miR-214 on stem cells and their progenies, contributes to the formation of the smaller hair bulbs. However, these effects could also be associated with decreased β−catenin expression, because β−catenin is an upstream regulator controlling Sox9 expression in the intestinal epithelium and neural crest cell (Blache et al., 2004; Liu et al., 2013).

In addition, Dlx3 which is involved in hair follicle differentiation and cycling (Hwang et al., 2008) showed decreased immunoreactivity in the hair follicles of DTG mice. This is consistent with the findings of this study as Dlx3 is positioned downstream of Wnt signalling in regulating hair follicle differentiation (Hwang et

al., 2008). This indicates another indirect effect of altered Wnt signalling caused by miR-214 overexpression in keratinocytes.

4.5 Phenotype of DTG mice hair follicles is rescued by pharmacological activation of Wnt

Importantly, key features of the skin phenotype in miR-214 overexpressing mice (decrease in the number of hair follicles and hair bulb size) were rescued by pharmacological activation of Wnt pathway *in vivo*. The induction of hair follicles during postnatal growth in DTG mice after pharmacological activation of Wnt pathway, in addition to similar hair bulb size of DTG and WT mice further supports the links between miR-214 and activity of Wnt pathway in the skin. These data are also consistent with data published previously and showing miR-214 targeting of β-catenin in hepatocellular carcinoma cells (Wang et al., 2012b). This also supports the hypothesis that miR-214 serves as a rheostat rather than a master regulator; however further analysis would need to be carried out to see whether the phenotype of DTG mice is fully reversible and whether indirect targets are affected.

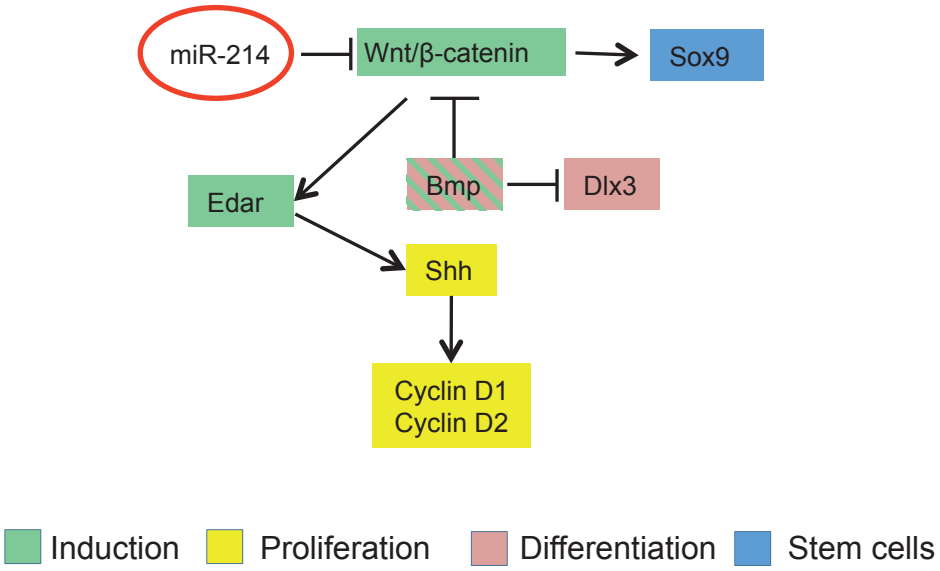

Figure 4.1. Effects of miR-214 on key signalling pathways in hair follicle growth
The scheme illustrates the mechanisms of the effects of miR-214 overexpression in keratinocytes. The targeting of β-catenin, the key component of Wnt signalling, by miR-214, leads to downstream effects on several signalling pathways that includes Bmp, Edar and Shh.

Conclusions

In this project, a novel role for miR-214 in the control of skin and hair follicle development and postnatal physiological regeneration was determined. Based on the data obtained in this study the following conclusions can be made:

(i) miR-214 exhibits discrete expression patterns in the epidermis and hair follicles in developing and postnatal skin. miR-214 is highly expressed in the epithelial stem cells and their lineage-committed progenies during hair follicle development and cycling: miR-214 is expressed in the compartment containing stem cells at predominantly quiescent state (secondary hair germ of telogen hair follicle), while it shows strong expression in highly proliferative compartments (epidermis, hair matrix of anagen hair follicle) during active hair growth.

(ii) Keratinocyte specific overexpression of miR-214 during skin embryogenesis results in the partial inhibition of hair follicle induction and formation of the hair follicles reduced in size, which produce thinner hair.

(iii) Keratinocyte specific overexpression of miR-214 in telogen skin causes retardation in the anagen progression and growth of smaller-sized hair follicles.

(iv) Inhibitory effects of miR-214 on hair follicle development and cycling are associated with supressed activity of stem cells, reduced proliferation in the hair matrix, and altered differentiation.

(v) Overexpression of miR-214 induces complex changes in gene expression programs in keratinocytes, including inhibition of the

number of cyclins and cyclin dependent kinases and the essential components of Wnt, Edar, Shh and Bmp signalling pathways.

(vi) miR-214 directly targets β-catenin in keratinocytes, therefore it directly regulates the activity of Wnt/β-catenin signalling pathways and cell-cycle-associated machinery in epithelial stem cells and their lineage-committed progenies.

(vii) miR-214 may act as one of the upstream effectors of the signalling cascades which governed hair follicle morphogenesis and cycling.

Taken together, the data obtained in this project suggest that miR-214 operates as a key determinant that controls the activity of Wnt signalling pathway by targeting β-catenin expression in the developing and postnatal skin and hair follicles (**Figure 4.1**). As Wnt signalling plays a crucial role in the control of stem cell activity in many organs during development and regeneration, while its uncontrolled activation results in tumorigenesis (Chan et al., 1999; Malanchi et al., 2008), these data provide an important foundation for further analysis of the role of miR-214 as regulator of Wnt pathway activity in many areas of research including stem cell and cancer biology, regenerative medicine and ageing.

Future Work

The following studies could be helpful to further unravel the role of miR-214 in controlling skin and hair follicle homeostasis:

- Further explore the role of miR-214 during spontaneous and depilation-induced hair cycle
- Determine whether miR-214 has a direct effect on epithelial stem cells.
- To delineate the role of miR-214 in the control of injury-associated gene expression programmes in epithelial stem cells and their progenies during wound healing.
- To define how modulation of miR-214 levels in skin affects the initiation and the progression of non-melanoma skin cancers such as basal cell carcinoma (BCC) and squamous cell carcinoma (SCC).
- To explore the role for miR-214 in skin and hair follicle aging and whether miR-214 contributes to the age-associated alterations in skin repair after injury.
- Explore whether miR-214 antagonists could potentially be used as therapeutic agents for hair disorders such as alopecia or hirsutism.
- Investigate whether miR-214 is implicated in disorders caused by abnormal Wnt signalling such as bowel cancer.

References

Abbott, A. L., Alvarez-Saavedra, E., Miska, E. A., Lau, N. C., Bartel, D. P., Horvitz, H. R., and Ambros, V. (2005). The let-7 MicroRNA family members mir-48, mir-84, and mir-241 function together to regulate developmental timing in Caenorhabditis elegans. Dev Cell *9*, 403-414.

Aberdam, D., Candi, E., Knight, R. A., and Melino, G. (2008). miRNAs, 'stemness' and skin. Trends Biochem Sci *33*, 583-591.

Ahmed, M. I., Mardaryev, A. N., Lewis, C. J., Sharov, A. A., and Botchkareva, N. V. (2011). MicroRNA-21 is an important downstream component of BMP signalling in epidermal keratinocytes. J Cell Sci *124*, 3399-3404.

Alonso, L., and Fuchs, E. (2003). Stem cells of the skin epithelium. Proc Natl Acad Sci U S A *100 Suppl 1*, 11830-11835.

Alonso, L., and Fuchs, E. (2006). The hair cycle. J Cell Sci *119*, 391-393.

Alonso, L. C., and Rosenfield, R. L. (2003). Molecular genetic and endocrine mechanisms of hair growth. Horm Res *60*, 1-13.

Ambros, V. (2004). The functions of animal microRNAs. Nature *431*, 350-355.

Ambros, V., Lee, R. C., Lavanway, A., Williams, P. T., and Jewell, D. (2003). MicroRNAs and other tiny endogenous RNAs in C. elegans. Curr Biol *13*, 807-818.

Amelio, I., Lena, A. M., Bonanno, E., Melino, G., and Candi, E. (2013). miR-24 affects hair follicle morphogenesis targeting Tcf-3. Cell Death Dis *4*, e922.

Amelio, I., Lena, A. M., Viticchie, G., Shalom-Feuerstein, R., Terrinoni, A., Dinsdale, D., Russo, G., Fortunato, C., Bonanno, E., Spagnoli, L. G.*, et al.* (2012). miR-24 triggers epidermal differentiation by controlling actin adhesion and cell migration. J Cell Biol *199*, 347-363.

Andl, T., Ahn, K., Kairo, A., Chu, E. Y., Wine-Lee, L., Reddy, S. T., Croft, N. J., Cebra-Thomas, J. A., Metzger, D., Chambon, P.*, et al.* (2004). Epithelial Bmpr1a regulates differentiation and proliferation in postnatal hair follicles and is essential for tooth development. Development *131*, 2257-2268.

Andl, T., Murchison, E. P., Liu, F., Zhang, Y., Yunta-Gonzalez, M., Tobias, J. W., Andl, C. D., Seykora, J. T., Hannon, G. J., and Millar, S. E. (2006). The miRNA-processing enzyme dicer is essential for the morphogenesis and maintenance of hair follicles. Curr Biol *16*, 1041-1049.

Andl, T., Reddy, S. T., Gaddapara, T., and Millar, S. E. (2002). WNT signals are required for the initiation of hair follicle development. Dev Cell *2*, 643-653.

Antonini, D., Russo, M. T., De Rosa, L., Gorrese, M., Del Vecchio, L., and Missero, C. (2010). Transcriptional repression of miR-34 family contributes to p63-mediated cell cycle progression in epidermal cells. J Invest Dermatol *130*, 1249-1257.

Aravin, A. A., Hannon, G. J., and Brennecke, J. (2007). The Piwi-piRNA pathway provides an adaptive defense in the transposon arms race. Science *318*, 761-764.

Auber, L. (1956). Producing wool-fibers, with special reference to keratinization. Trans Roy Soc Edin *62*, 191-254.

Aubin-Houzelstein, G. (2012). Notch signaling and the developing hair follicle. Adv Exp Med Biol *727*, 142-160.

Bak, R. O., and Mikkelsen, J. G. (2014). miRNA sponges: soaking up miRNAs for regulation of gene expression. Wiley Interdiscip Rev RNA *5*, 317-333.

Baroni, A., Buommino, E., De Gregorio, V., Ruocco, E., Ruocco, V., and Wolf, R. (2012). Structure and function of the epidermis related to barrier properties. Clin Dermatol *30*, 257-262.

Bartel, D. P. (2004). MicroRNAs: genomics, biogenesis, mechanism, and function. Cell *116*, 281-297.

Bartel, D. P. (2009). MicroRNAs: target recognition and regulatory functions. Cell *136*, 215-233.

Bazzi, H., Fantauzzo, K. A., Richardson, G. D., Jahoda, C. A., and Christiano, A. M. (2007). The Wnt inhibitor, Dickkopf 4, is induced by canonical Wnt signaling during ectodermal appendage morphogenesis, Vol 305).

Bernstein, E., Kim, S. Y., Carmell, M. A., Murchison, E. P., Alcorn, H., Li, M. Z., Mills, A. A., Elledge, S. J., Anderson, K. V., and Hannon, G. J. (2003). Dicer is essential for mouse development. Nat Genet *35*, 215-217.

Bitgood, M. J., and McMahon, A. P. (1995). Hedgehog and Bmp genes are coexpressed at many diverse sites of cell-cell interaction in the mouse embryo. Dev Biol *172*, 126-138.

Blache, P., van de Wetering, M., Duluc, I., Domon, C., Berta, P., Freund, J. N., Clevers, H., and Jay, P. (2004). SOX9 is an intestine crypt transcription factor, is regulated by the Wnt pathway, and represses the CDX2 and MUC2 genes. J Cell Biol *166*, 37-47.

Blanpain, C., and Fuchs, E. (2006). Epidermal stem cells of the skin. Annu Rev Cell Dev Biol *22*, 339-373.

Blanpain, C., and Fuchs, E. (2009). Epidermal homeostasis: a balancing act of stem cells in the skin. Nat Rev Mol Cell Biol *10*, 207-217.

Blanpain, C., Lowry, W. E., Geoghegan, A., Polak, L., and Fuchs, E. (2004). Self-renewal, multipotency, and the existence of two cell populations within an epithelial stem cell niche. Cell *118*, 635-648.

Blume-Peytavi, U., and Hahn, S. (2008). Medical treatment of hirsutism. Dermatol Ther *21*, 329-339.

Bol, D. K., Kiguchi, K., Gimenez-Conti, I., Rupp, T., and DiGiovanni, J. (1997). Overexpression of insulin-like growth factor-1 induces hyperplasia, dermal abnormalities, and spontaneous tumor formation in transgenic mice. Oncogene *14*, 1725-1734.

Bommer, G. T., Gerin, I., Feng, Y., Kaczorowski, A. J., Kuick, R., Love, R. E., Zhai, Y., Giordano, T. J., Qin, Z. S., Moore, B. B.*, et al.* (2007). p53-mediated activation of miRNA34 candidate tumor-suppressor genes. Curr Biol *17*, 1298-1307.

Borchert, G. M., Lanier, W., and Davidson, B. L. (2006). RNA polymerase III transcribes human microRNAs. Nat Struct Mol Biol *13*, 1097-1101.

Botchkarev, V. A., Botchkareva, N. V., Albers, K. M., Chen, L. H., Welker, P., and Paus, R. (2000). A role for p75 neurotrophin receptor in the control of apoptosis-driven hair follicle regression. Faseb J *14*, 1931-1942.

Botchkarev, V. A., Botchkareva, N. V., Nakamura, M., Huber, O., Funa, K., Lauster, R., Paus, R., and Gilchrest, B. A. (2001a). Noggin is required for induction of the hair follicle growth phase in postnatal skin. Faseb J *15*, 2205-2214.

Botchkarev, V. A., Botchkareva, N. V., Roth, W., Nakamura, M., Chen, L. H., Herzog, W., Lindner, G., McMahon, J. A., Peters, C., Lauster, R.*, et al.* (1999a). Noggin is a mesenchymally derived stimulator of hair-follicle induction. Nat Cell Biol *1*, 158-164.

Botchkarev, V. A., Botchkareva, N. V., Sharov, A. A., Funa, K., Huber, O., and Gilchrest, B. A. (2002). Modulation of BMP signaling by noggin is required for induction of the secondary (nontylotrich) hair follicles. J Invest Dermatol *118*, 3-10.

Botchkarev, V. A., Botchkareva, N. V., Welker, P., Metz, M., Lewin, G. R., Subramaniam, A., Bulfone-Paus, S., Hagen, E., Braun, A., Lommatzsch, M.*, et al.* (1999b). A new role for neurotrophins: involvement of brain-derived neurotrophic factor and neurotrophin-4 in hair cycle control. Faseb J *13*, 395-410.

Botchkarev, V. A., and Fessing, M. Y. (2005). Edar signaling in the control of hair follicle development. J Investig Dermatol Symp Proc *10*, 247-251.

Botchkarev, V. A., Komarova, E. A., Siebenhaar, F., Botchkareva, N. V., Sharov, A. A., Komarov, P. G., Maurer, M., Gudkov, A. V., and Gilchrest, B. A. (2001b). p53 Involvement in the control of murine hair follicle regression. Am J Pathol *158*, 1913-1919.

Botchkarev, V. A., and Paus, R. (2003). Molecular biology of hair morphogenesis: development and cycling. J Exp Zool B Mol Dev Evol *298*, 164-180.

Botchkarev, V. A., Yaar, M., Gilchrest, B. A., and Paus, R. (2003). p75 Neurotrophin receptor antagonist retards apoptosis-driven hair follicle involution (catagen). J Invest Dermatol *120*, 168-169.

Botchkareva, N. V. (2012). MicroRNA/mRNA regulatory networks in the control of skin development and regeneration. Cell Cycle *11*, 468-474.

Botchkareva, N. V., Ahluwalia, G., and Shander, D. (2006). Apoptosis in the hair follicle. J Invest Dermatol *126*, 258-264.

Botchkareva, N. V., Botchkarev, V. A., Chen, L. H., Lindner, G., and Paus, R. (1999). A role for p75 neurotrophin receptor in the control of hair follicle morphogenesis. Dev Biol *216*, 135-153.

Botchkareva, N. V., Khlgatian, M., Longley, B. J., Botchkarev, V. A., and Gilchrest, B. A. (2001). SCF/c-kit signaling is required for cyclic regeneration of the hair pigmentation unit. Faseb J *15*, 645-658.

Botchkareva, N. V., Randall V. A. (2009). The Biology of Hair Growth, Vol 1: William Andrew).

Breving, K., and Esquela-Kerscher, A. (2010). The complexities of microRNA regulation: mirandering around the rules. Int J Biochem Cell Biol *42*, 1316-1329.

Brownell, I., Guevara, E., Bai, C. B., Loomis, C. A., and Joyner, A. L. (2011). Nerve-derived sonic hedgehog defines a niche for hair follicle stem cells capable of becoming epidermal stem cells. Cell Stem Cell *8*, 552-565.

Bueno, M. J., Gomez de Cedron, M., Laresgoiti, U., Fernandez-Piqueras, J., Zubiaga, A. M., and Malumbres, M. (2010). Multiple E2F-induced microRNAs prevent replicative stress in response to mitogenic signaling. Mol Cell Biol *30*, 2983-2995.

Byrne, C., Tainsky, M., and Fuchs, E. (1994). Programming gene expression in developing epidermis. Development *120*, 2369-2383.

Candi, E., Rufini, A., Terrinoni, A., Dinsdale, D., Ranalli, M., Paradisi, A., De Laurenzi, V., Spagnoli, L. G., Catani, M. V., Ramadan, S.*, et al.* (2006). Differential roles of p63 isoforms in epidermal development: selective genetic complementation in p63 null mice. Cell Death Differ *13*, 1037-1047.

Caretti, G., Di Padova, M., Micales, B., Lyons, G. E., and Sartorelli, V. (2004). The Polycomb Ezh2 methyltransferase regulates muscle gene expression and skeletal muscle differentiation. Genes Dev *18*, 2627-2638.

Chan, E. F., Gat, U., McNiff, J. M., and Fuchs, E. (1999). A common human skin tumour is caused by activating mutations in beta-catenin. Nat Genet *21*, 410-413.

Chang, H. Y., Chi, J. T., Dudoit, S., Bondre, C., van de Rijn, M., Botstein, D., and Brown, P. O. (2002). Diversity, topographic differentiation, and positional memory in human fibroblasts. Proc Natl Acad Sci U S A *99*, 12877-12882.

Chang, T. C., Wentzel, E. A., Kent, O. A., Ramachandran, K., Mullendore, M., Lee, K. H., Feldmann, G., Yamakuchi, M., Ferlito, M., Lowenstein, C. J.*, et al.* (2007). Transactivation of miR-34a by p53 broadly influences gene expression and promotes apoptosis. Mol Cell *26*, 745-752.

Chen, C., Ridzon, D. A., Broomer, A. J., Zhou, Z., Lee, D. H., Nguyen, J. T., Barbisin, M., Xu, N. L., Mahuvakar, V. R., Andersen, M. R.*, et al.* (2005). Real-time quantification of microRNAs by stem-loop RT-PCR. Nucleic Acids Res *33*, e179.

Chen, C. H., Sakai, Y., and Demay, M. B. (2001). Targeting expression of the human vitamin D receptor to the keratinocytes of vitamin D receptor null mice prevents alopecia. Endocrinology *142*, 5386-5389.

Chen, D., Jarrell, A., Guo, C., Lang, R., and Atit, R. (2012). Dermal beta-catenin activity in response to epidermal Wnt ligands is required for fibroblast proliferation and hair follicle initiation. Development *139*, 1522-1533.

Chen, H., Shalom-Feuerstein, R., Riley, J., Zhang, S. D., Tucci, P., Agostini, M., Aberdam, D., Knight, R. A., Genchi, G., Nicotera, P.*, et al.* (2010). miR-7 and

miR-214 are specifically expressed during neuroblastoma differentiation, cortical development and embryonic stem cells differentiation, and control neurite outgrowth in vitro. Biochem Biophys Res Commun *394*, 921-927.

Chen, P. Y., and Meister, G. (2005). microRNA-guided posttranscriptional gene regulation. Biol Chem *386*, 1205-1218.

Chendrimada, T. P., Gregory, R. I., Kumaraswamy, E., Norman, J., Cooch, N., Nishikura, K., and Shiekhattar, R. (2005). TRBP recruits the Dicer complex to Ago2 for microRNA processing and gene silencing. Nature *436*, 740-744.

Cheng, A. M., Byrom, M. W., Shelton, J., and Ford, L. P. (2005). Antisense inhibition of human miRNAs and indications for an involvement of miRNA in cell growth and apoptosis. Nucleic Acids Res *33*, 1290-1297.

Chiang, C., Swan, R. Z., Grachtchouk, M., Bolinger, M., Litingtung, Y., Robertson, E. K., Cooper, M. K., Gaffield, W., Westphal, H., Beachy, P. A., and Dlugosz, A. A. (1999). Essential role for Sonic hedgehog during hair follicle morphogenesis. Dev Biol *205*, 1-9.

Choi, Y. S., Zhang, Y., Xu, M., Yang, Y., Ito, M., Peng, T., Cui, Z., Nagy, A., Hadjantonakis, A. K., Lang, R. A.*, et al.* (2013). Distinct functions for Wnt/beta-catenin in hair follicle stem cell proliferation and survival and interfollicular epidermal homeostasis. Cell Stem Cell *13*, 720-733.

Corcoran, D. L., Pandit, K. V., Gordon, B., Bhattacharjee, A., Kaminski, N., and Benos, P. V. (2009). Features of mammalian microRNA promoters emerge from polymerase II chromatin immunoprecipitation data. PLoS One *4*, e5279.

Costin, G. E., and Hearing, V. J. (2007). Human skin pigmentation: melanocytes modulate skin color in response to stress. Faseb J *21*, 976-994.

Cotsarelis, G. (2006). Epithelial stem cells: a folliculocentric view. J Invest Dermatol *126*, 1459-1468.

Cotsarelis, G., Botchkarev, V.A. (2012). Biology of Hair Follicles, Vol 8: McGraw Hill).

Cotsarelis, G., Sun, T. T., and Lavker, R. M. (1990). Label-retaining cells reside in the bulge area of pilosebaceous unit: implications for follicular stem cells, hair cycle, and skin carcinogenesis. Cell *61*, 1329-1337.

Cui, C. Y., Kunisada, M., Piao, Y., Childress, V., Ko, M. S., and Schlessinger, D. (2010). Dkk4 and Eda regulate distinctive developmental mechanisms for subtypes of mouse hair. PLoS One *5*, e10009.

Cullen, B. R. (2004). Transcription and processing of human microRNA precursors. Mol Cell *16*, 861-865.

DasGupta, R., and Fuchs, E. (1999). Multiple roles for activated LEF/TCF transcription complexes during hair follicle development and differentiation. Development *126*, 4557-4568.

Decembrini, S., Bressan, D., Vignali, R., Pitto, L., Mariotti, S., Rainaldi, G., Wang, X., Evangelista, M., Barsacchi, G., and Cremisi, F. (2009). MicroRNAs couple cell fate and developmental timing in retina. Proc Natl Acad Sci U S A *106*, 21179-21184.

Denli, A. M., Tops, B. B., Plasterk, R. H., Ketting, R. F., and Hannon, G. J. (2004). Processing of primary microRNAs by the Microprocessor complex. Nature *432*, 231-235.

Diederichs, S., and Haber, D. A. (2007). Dual role for argonautes in microRNA processing and posttranscriptional regulation of microRNA expression. Cell *131*, 1097-1108.

Driskell, R. R., Giangreco, A., Jensen, K. B., Mulder, K. W., and Watt, F. M. (2009). Sox2-positive dermal papilla cells specify hair follicle type in mammalian epidermis. Development *136*, 2815-2823.

du Cros, D. L. (1993). Fibroblast growth factor and epidermal growth factor in hair development. J Invest Dermatol *101*, 106S-113S.

Eckert, R. L., Adhikary, G., Balasubramanian, S., Rorke, E. A., Vemuri, M. C., Boucher, S. E., Bickenbach, J. R., and Kerr, C. (2013). Biochemistry of epidermal stem cells. Biochim Biophys Acta *1830*, 2427-2434.

Eckert, R. L., Crish, J. F., and Robinson, N. A. (1997). The epidermal keratinocyte as a model for the study of gene regulation and cell differentiation. Physiol Rev *77*, 397-424.

Eivers, E., Fuentealba, L. C., and De Robertis, E. M. (2008). Integrating positional information at the level of Smad1/5/8. Curr Opin Genet Dev *18*, 304-310.

Elias, P. M. (2005). Stratum corneum defensive functions: an integrated view. J Invest Dermatol *125*, 183-200.

Elliott, K., Stephenson, T. J., and Messenger, A. G. (1999). Differences in hair follicle dermal papilla volume are due to extracellular matrix volume and cell number: implications for the control of hair follicle size and androgen responses. J Invest Dermatol *113*, 873-877.

Ellis, T., Gambardella, L., Horcher, M., Tschanz, S., Capol, J., Bertram, P., Jochum, W., Barrandon, Y., and Busslinger, M. (2001). The transcriptional repressor CDP (Cutl1) is essential for epithelial cell differentiation of the lung and the hair follicle. Genes Dev *15*, 2307-2319.

Enshell-Seijffers, D., Lindon, C., Kashiwagi, M., and Morgan, B. A. (2010). beta-catenin activity in the dermal papilla regulates morphogenesis and regeneration of hair. Dev Cell *18*, 633-642.

Fire, A., Xu, S., Montgomery, M. K., Kostas, S. A., Driver, S. E., and Mello, C. C. (1998). Potent and specific genetic interference by double-stranded RNA in Caenorhabditis elegans. Nature *391*, 806-811.

Flanagan, S. P. (1966). 'Nude', a new hairless gene with pleiotropic effects in the mouse. Genet Res *8*, 295-309.

Flynt, A. S., and Lai, E. C. (2008). Biological principles of microRNA-mediated regulation: shared themes amid diversity. Nat Rev Genet *9*, 831-842.

Flynt, A. S., Li, N., Thatcher, E. J., Solnica-Krezel, L., and Patton, J. G. (2007). Zebrafish miR-214 modulates Hedgehog signaling to specify muscle cell fate. Nat Genet *39*, 259-263.

Foitzik, K., Lindner, G., Mueller-Roever, S., Maurer, M., Botchkareva, N., Botchkarev, V., Handjiski, B., Metz, M., Hibino, T., Soma, T.*, et al.* (2000). Control of murine hair follicle regression (catagen) by TGF-beta1 in vivo. Faseb J *14*, 752-760.

Foitzik, K., Paus, R., Doetschman, T., and Dotto, G. P. (1999). The TGF-beta2 isoform is both a required and sufficient inducer of murine hair follicle morphogenesis. Dev Biol *212*, 278-289.

Folgueras, A. R., Guo, X., Pasolli, H. A., Stokes, N., Polak, L., Zheng, D., and Fuchs, E. (2013). Architectural niche organization by LHX2 is linked to hair follicle stem cell function. Cell Stem Cell *13*, 314-327.

Fuchs, E. (1990). Epidermal differentiation: the bare essentials. J Cell Biol *111*, 2807-2814.

Fuchs, E. (2007). Scratching the surface of skin development. Nature *445*, 834-842.

Fuchs, E. (2008). Skin stem cells: rising to the surface. J Cell Biol *180*, 273-284.

Fuchs, E. (2009). Finding one's niche in the skin. Cell Stem Cell *4*, 499-502.

Fuchs, E., and Green, H. (1980). Changes in keratin gene expression during terminal differentiation of the keratinocyte. Cell *19*, 1033-1042.

Fuchs, E., and Horsley, V. (2008). More than one way to skin. Genes Dev *22*, 976-985.

Fuchs, E., and Raghavan, S. (2002). Getting under the skin of epidermal morphogenesis. Nat Rev Genet *3*, 199-209.

Gat, U., DasGupta, R., Degenstein, L., and Fuchs, E. (1998). De Novo hair follicle morphogenesis and hair tumors in mice expressing a truncated beta-catenin in skin. Cell *95*, 605-614.

Godwin, A. R., and Capecchi, M. R. (1998). Hoxc13 mutant mice lack external hair. Genes Dev *12*, 11-20.

Greco, V., Chen, T., Rendl, M., Schober, M., Pasolli, H. A., Stokes, N., Dela Cruz-Racelis, J., and Fuchs, E. (2009). A two-step mechanism for stem cell activation during hair regeneration. Cell Stem Cell *4*, 155-169.

Gregory, R. I., Yan, K. P., Amuthan, G., Chendrimada, T., Doratotaj, B., Cooch, N., and Shiekhattar, R. (2004). The Microprocessor complex mediates the genesis of microRNAs. Nature *432*, 235-240.

Grimson, A., Farh, K. K., Johnston, W. K., Garrett-Engele, P., Lim, L. P., and Bartel, D. P. (2007). MicroRNA targeting specificity in mammals: determinants beyond seed pairing. Mol Cell *27*, 91-105.

Guo, L., Yu, Q. C., and Fuchs, E. (1993). Targeting expression of keratinocyte growth factor to keratinocytes elicits striking changes in epithelial differentiation in transgenic mice. Embo J *12*, 973-986.

Haase, A. D., Jaskiewicz, L., Zhang, H., Laine, S., Sack, R., Gatignol, A., and Filipowicz, W. (2005). TRBP, a regulator of cellular PKR and HIV-1 virus expression, interacts with Dicer and functions in RNA silencing. EMBO Rep *6*, 961-967.

Han, J., Lee, Y., Yeom, K. H., Kim, Y. K., Jin, H., and Kim, V. N. (2004). The Drosha-DGCR8 complex in primary microRNA processing. Genes Dev *18*, 3016-3027.

Han, J., Lee, Y., Yeom, K. H., Nam, J. W., Heo, I., Rhee, J. K., Sohn, S. Y., Cho, Y., Zhang, B. T., and Kim, V. N. (2006). Molecular basis for the recognition of primary microRNAs by the Drosha-DGCR8 complex. Cell *125*, 887-901.

Handjiski, B. K., Eichmuller, S., Hofmann, U., Czarnetzki, B. M., and Paus, R. (1994). Alkaline phosphatase activity and localization during the murine hair cycle. Br J Dermatol *131*, 303-310.

Hansen, L. A., Alexander, N., Hogan, M. E., Sundberg, J. P., Dlugosz, A., Threadgill, D. W., Magnuson, T., and Yuspa, S. H. (1997). Genetically null mice reveal a central role for epidermal growth factor receptor in the differentiation of the hair follicle and normal hair development. Am J Pathol *150*, 1959-1975.

Hansen, T. B., Jensen, T. I., Clausen, B. H., Bramsen, J. B., Finsen, B., Damgaard, C. K., and Kjems, J. (2013). Natural RNA circles function as efficient microRNA sponges. Nature *495*, 384-388.

Hardy, M. H. (1992). The secret life of the hair follicle. Trends Genet *8*, 55-61.

Harkey, M. R. (1993). Anatomy and physiology of hair. Forensic Sci Int *63*, 9-18.

He, L., He, X., Lowe, S. W., and Hannon, G. J. (2007). microRNAs join the p53 network--another piece in the tumour-suppression puzzle. Nat Rev Cancer *7*, 819-822.

Headon, D. J., Emmal, S. A., Ferguson, B. M., Tucker, A. S., Justice, M. J., Sharpe, P. T., Zonana, J., and Overbeek, P. A. (2001). Gene defect in ectodermal dysplasia implicates a death domain adapter in development. Nature *414*, 913-916.

Headon, D. J., and Overbeek, P. A. (1999). Involvement of a novel Tnf receptor homologue in hair follicle induction. Nat Genet *22*, 370-374.

Healy, B. (2005). Skin deep. As the body's largest organ, skin is a powerful yet unappreciated veneer. US News World Rep *139*, 66-68.

Hebert, J. M., Rosenquist, T., Gotz, J., and Martin, G. R. (1994). FGF5 as a regulator of the hair growth cycle: evidence from targeted and spontaneous mutations. Cell *78*, 1017-1025.

Higgins, C. A., Westgate, G. E., and Jahoda, C. A. (2009). From telogen to exogen: mechanisms underlying formation and subsequent loss of the hair club fiber. J Invest Dermatol *129*, 2100-2108.

Hirai, H., Roussel, M. F., Kato, J. Y., Ashmun, R. A., and Sherr, C. J. (1995). Novel INK4 proteins, p19 and p18, are specific inhibitors of the cyclin D-dependent kinases CDK4 and CDK6. Mol Cell Biol *15*, 2672-2681.

Hirai, Y., Nose, A., Kobayashi, S., and Takeichi, M. (1989). Expression and role of E- and P-cadherin adhesion molecules in embryonic histogenesis. II. Skin morphogenesis. Development *105*, 271-277.

Horne, K. A., Jahoda, C. A., and Oliver, R. F. (1986). Whisker growth induced by implantation of cultured vibrissa dermal papilla cells in the adult rat. J Embryol Exp Morphol *97*, 111-124.

Horsley, V., Aliprantis, A. O., Polak, L., Glimcher, L. H., and Fuchs, E. (2008). NFATc1 balances quiescence and proliferation of skin stem cells. Cell *132*, 299-310.

Horsley, V., O'Carroll, D., Tooze, R., Ohinata, Y., Saitou, M., Obukhanych, T., Nussenzweig, M., Tarakhovsky, A., and Fuchs, E. (2006). Blimp1 defines a progenitor population that governs cellular input to the sebaceous gland. Cell *126*, 597-609.

Hsieh, J. C., Sisk, J. M., Jurutka, P. W., Haussler, C. A., Slater, S. A., Haussler, M. R., and Thompson, C. C. (2003). Physical and functional interaction between the vitamin D receptor and hairless corepressor, two proteins required for hair cycling. J Biol Chem *278*, 38665-38674.

Hsu, Y. C., Pasolli, H. A., and Fuchs, E. (2011). Dynamics between stem cells, niche, and progeny in the hair follicle. Cell *144*, 92-105.

Huelsken, J., Vogel, R., Erdmann, B., Cotsarelis, G., and Birchmeier, W. (2001). beta-Catenin controls hair follicle morphogenesis and stem cell differentiation in the skin. Cell *105*, 533-545.

Hutvagner, G., and Simard, M. J. (2008). Argonaute proteins: key players in RNA silencing. Nat Rev Mol Cell Biol *9*, 22-32.

Hwang, J., Mehrani, T., Millar, S. E., and Morasso, M. I. (2008). Dlx3 is a crucial regulator of hair follicle differentiation and cycling. Development *135*, 3149-3159.

Iida, M., Ihara, S., and Matsuzaki, T. (2007). Hair cycle-dependent changes of alkaline phosphatase activity in the mesenchyme and epithelium in mouse vibrissal follicles. Dev Growth Differ *49*, 185-195.

Inamatsu, M., Tochio, T., Makabe, A., Endo, T., Oomizu, S., Kobayashi, E., and Yoshizato, K. (2006). Embryonic dermal condensation and adult dermal papilla induce hair follicles in adult glabrous epidermis through different mechanisms. Dev Growth Differ *48*, 73-86.

Iseki, S., Araga, A., Ohuchi, H., Nohno, T., Yoshioka, H., Hayashi, F., and Noji, S. (1996). Sonic hedgehog is expressed in epithelial cells during development of whisker, hair, and tooth. Biochem Biophys Res Commun *218*, 688-693.

Ito, M., Kizawa, K., Hamada, K., and Cotsarelis, G. (2004). Hair follicle stem cells in the lower bulge form the secondary germ, a biochemically distinct but functionally equivalent progenitor cell population, at the termination of catagen. Differentiation *72*, 548-557.

Ito, M., Yang, Z., Andl, T., Cui, C., Kim, N., Millar, S. E., and Cotsarelis, G. (2007). Wnt-dependent de novo hair follicle regeneration in adult mouse skin after wounding. Nature *447*, 316-320.

Jahoda, C. A., Horne, K. A., and Oliver, R. F. (1984). Induction of hair growth by implantation of cultured dermal papilla cells. Nature *311*, 560-562.

Jahoda, C. A., and Oliver, R. F. (1984). Vibrissa dermal papilla cell aggregative behaviour in vivo and in vitro. J Embryol Exp Morphol *79*, 211-224.

Jahoda, C. A., Oliver, R. F., Reynolds, A. J., Forrester, J. C., Gillespie, J. W., Cserhalmi-Friedman, P. B., Christiano, A. M., and Horne, K. A. (2001). Trans-species hair growth induction by human hair follicle dermal papillae. Exp Dermatol *10*, 229-237.

Jahoda, C. A., Oliver, R. F., Reynolds, A. J., Forrester, J. C., and Horne, K. A. (1996). Human hair follicle regeneration following amputation and grafting into the nude mouse. J Invest Dermatol *107*, 804-807.

Jahoda, C. A., and Reynolds, A. J. (1993). Dermal-epidermal interactions--follicle-derived cell populations in the study of hair-growth mechanisms. J Invest Dermatol *101*, 33S-38S.

Jahoda, C. A., Reynolds, A. J., and Oliver, R. F. (1993). Induction of hair growth in ear wounds by cultured dermal papilla cells. J Invest Dermatol *101*, 584-590.

Jaks, V., Barker, N., Kasper, M., van Es, J. H., Snippert, H. J., Clevers, H., and Toftgard, R. (2008). Lgr5 marks cycling, yet long-lived, hair follicle stem cells. Nat Genet *40*, 1291-1299.

Jamora, C., DasGupta, R., Kocieniewski, P., and Fuchs, E. (2003). Links between signal transduction, transcription and adhesion in epithelial bud development. Nature *422*, 317-322.

Jave-Suarez, L. F., Winter, H., Langbein, L., Rogers, M. A., and Schweizer, J. (2002). HOXC13 is involved in the regulation of human hair keratin gene expression. J Biol Chem *277*, 3718-3726.

Jiang, T. X., Liu, Y. H., Widelitz, R. B., Kundu, R. K., Maxson, R. E., and Chuong, C. M. (1999). Epidermal dysplasia and abnormal hair follicles in

transgenic mice overexpressing homeobox gene MSX-2. J Invest Dermatol *113*, 230-237.

Joglekar, M. V., Parekh, V. S., and Hardikar, A. A. (2007). New pancreas from old: microregulators of pancreas regeneration. Trends Endocrinol Metab *18*, 393-400.

Jones-Rhoades, M. W., Bartel, D. P., and Bartel, B. (2006). MicroRNAS and their regulatory roles in plants. Annu Rev Plant Biol *57*, 19-53.

Juan, A. H., Kumar, R. M., Marx, J. G., Young, R. A., and Sartorelli, V. (2009). Mir-214-dependent regulation of the polycomb protein Ezh2 in skeletal muscle and embryonic stem cells. Mol Cell *36*, 61-74.

Karlsson, L., Bondjers, C., and Betsholtz, C. (1999). Roles for PDGF-A and sonic hedgehog in development of mesenchymal components of the hair follicle. Development *126*, 2611-2621.

Kaufman, C. K., Zhou, P., Pasolli, H. A., Rendl, M., Bolotin, D., Lim, K. C., Dai, X., Alegre, M. L., and Fuchs, E. (2003). GATA-3: an unexpected regulator of cell lineage determination in skin. Genes Dev *17*, 2108-2122.

Kim, B. K., Lee, H. Y., Choi, J. H., Kim, J. K., Yoon, J. B., and Yoon, S. K. (2012). Hairless plays a role in formation of inner root sheath via regulation of Dlx3 gene. J Biol Chem *287*, 16681-16688.

Kimura-Ueki, M., Oda, Y., Oki, J., Komi-Kuramochi, A., Honda, E., Asada, M., Suzuki, M., and Imamura, T. (2012). Hair cycle resting phase is regulated by cyclic epithelial FGF18 signaling. J Invest Dermatol *132*, 1338-1345.

Kobayashi, K., Rochat, A., and Barrandon, Y. (1993). Segregation of keratinocyte colony-forming cells in the bulge of the rat vibrissa. Proc Natl Acad Sci U S A *90*, 7391-7395.

Kobielak, K., Stokes, N., de la Cruz, J., Polak, L., and Fuchs, E. (2007). Loss of a quiescent niche but not follicle stem cells in the absence of bone morphogenetic protein signaling. Proc Natl Acad Sci U S A *104*, 10063-10068.

Koch, P. J., Mahoney, M. G., Cotsarelis, G., Rothenberger, K., Lavker, R. M., and Stanley, J. R. (1998). Desmoglein 3 anchors telogen hair in the follicle. J Cell Sci *111 (Pt 17)*, 2529-2537.

Kolarsick P. A. J., K. M. A., Goodwin C. (2011). Anatomy and physiology of the skin. , Vol 3).

Kollar, E. J. (1970). The induction of hair follicles by embryonic dermal papillae. J Invest Dermatol *55*, 374-378.

Kopan, R., and Weintraub, H. (1993). Mouse notch: expression in hair follicles correlates with cell fate determination. J Cell Biol *121*, 631-641.

Koster, M. I., and Roop, D. R. (2004). The role of p63 in development and differentiation of the epidermis. J Dermatol Sci *34*, 3-9.

Koster, M. I., and Roop, D. R. (2007). Mechanisms regulating epithelial stratification. Annu Rev Cell Dev Biol *23*, 93-113.

Krause, K., and Foitzik, K. (2006). Biology of the hair follicle: the basics. Semin Cutan Med Surg *25*, 2-10.

Krol, J., Loedige, I., and Filipowicz, W. (2010). The widespread regulation of microRNA biogenesis, function and decay. Nat Rev Genet *11*, 597-610.

Kwack, M. H., Kim, M. K., Kim, J. C., and Sung, Y. K. (2012). Dickkopf 1 promotes regression of hair follicles. J Invest Dermatol *132*, 1554-1560.

Lagos-Quintana, M., Rauhut, R., Lendeckel, W., and Tuschl, T. (2001). Identification of novel genes coding for small expressed RNAs. Science *294*, 853-858.

Langbein, L., and Schweizer, J. (2005). Keratins of the human hair follicle. Int Rev Cytol *243*, 1-78.

Langbein, L., Spring, H., Rogers, M. A., Praetzel, S., and Schweizer, J. (2004). Hair keratins and hair follicle-specific epithelial keratins. Methods Cell Biol *78*, 413-451.

Laurikkala, J., Pispa, J., Jung, H. S., Nieminen, P., Mikkola, M., Wang, X., Saarialho-Kere, U., Galceran, J., Grosschedl, R., and Thesleff, I. (2002). Regulation of hair follicle development by the TNF signal ectodysplasin and its receptor Edar. Development *129*, 2541-2553.

Lee, R. C., Feinbaum, R. L., and Ambros, V. (1993). The C. elegans heterochronic gene lin-4 encodes small RNAs with antisense complementarity to lin-14. Cell *75*, 843-854.

Lee, S. H., Jeong, S. K., and Ahn, S. K. (2006). An update of the defensive barrier function of skin. Yonsei Med J *47*, 293-306.

Lee, Y., Ahn, C., Han, J., Choi, H., Kim, J., Yim, J., Lee, J., Provost, P., Radmark, O., Kim, S., and Kim, V. N. (2003). The nuclear RNase III Drosha initiates microRNA processing. Nature *425*, 415-419.

Lee, Y. B., Bantounas, I., Lee, D. Y., Phylactou, L., Caldwell, M. A., and Uney, J. B. (2009). Twist-1 regulates the miR-199a/214 cluster during development. Nucleic Acids Res *37*, 123-128.

Legue, E., and Nicolas, J. F. (2005). Hair follicle renewal: organization of stem cells in the matrix and the role of stereotyped lineages and behaviors. Development *132*, 4143-4154.

Lena, A. M., Shalom-Feuerstein, R., Rivetti di Val Cervo, P., Aberdam, D., Knight, R. A., Melino, G., and Candi, E. (2008). miR-203 represses 'stemness' by repressing DeltaNp63. Cell Death Differ *15*, 1187-1195.

Levy, C., Khaled, M., Robinson, K. C., Veguilla, R. A., Chen, P. H., Yokoyama, S., Makino, E., Lu, J., Larue, L., Beermann, F.*, et al.* (2010). Lineage-specific transcriptional regulation of DICER by MITF in melanocytes. Cell *141*, 994-1005.

Levy, V., Lindon, C., Harfe, B. D., and Morgan, B. A. (2005). Distinct stem cell populations regenerate the follicle and interfollicular epidermis. Dev Cell *9*, 855-861.

Lewis, B. P., Burge, C. B., and Bartel, D. P. (2005). Conserved seed pairing, often flanked by adenosines, indicates that thousands of human genes are microRNA targets. Cell *120*, 15-20.

Lewis, C. J., Mardaryev, A. N., Poterlowicz, K., Sharova, T. Y., Aziz, A., Sharpe, D. T., Botchkareva, N. V., and Sharov, A. A. (2014). Bone morphogenetic protein signaling suppresses wound-induced skin repair by inhibiting keratinocyte proliferation and migration. J Invest Dermatol *134*, 827-837.

Li, L., and Clevers, H. (2010). Coexistence of quiescent and active adult stem cells in mammals. Science *327*, 542-545.

Li, L., Mignone, J., Yang, M., Matic, M., Penman, S., Enikolopov, G., and Hoffman, R. M. (2003). Nestin expression in hair follicle sheath progenitor cells. Proc Natl Acad Sci U S A *100*, 9958-9961.

Lichti, U., Anders, J., and Yuspa, S. H. (2008). Isolation and short-term culture of primary keratinocytes, hair follicle populations and dermal cells from newborn mice and keratinocytes from adult mice for in vitro analysis and for grafting to immunodeficient mice. Nat Protoc *3*, 799-810.

Lim, L. P., Lau, N. C., Garrett-Engele, P., Grimson, A., Schelter, J. M., Castle, J., Bartel, D. P., Linsley, P. S., and Johnson, J. M. (2005). Microarray analysis shows that some microRNAs downregulate large numbers of target mRNAs. Nature *433*, 769-773.

Lin, J. Y., and Fisher, D. E. (2007). Melanocyte biology and skin pigmentation. Nature *445*, 843-850.

Lin, M. H., Leimeister, C., Gessler, M., and Kopan, R. (2000). Activation of the Notch pathway in the hair cortex leads to aberrant differentiation of the adjacent hair-shaft layers. Development *127*, 2421-2432.

Lindner, G., Botchkarev, V. A., Botchkareva, N. V., Ling, G., van der Veen, C., and Paus, R. (1997). Analysis of apoptosis during hair follicle regression (catagen). Am J Pathol *151*, 1601-1617.

Liu, J., Luo, X. J., Xiong, A. W., Zhang, Z. D., Yue, S., Zhu, M. S., and Cheng, S. Y. (2010). MicroRNA-214 promotes myogenic differentiation by facilitating exit from mitosis via down-regulation of proto-oncogene N-ras. J Biol Chem *285*, 26599-26607.

Liu, J. A., Wu, M. H., Yan, C. H., Chau, B. K., So, H., Ng, A., Chan, A., Cheah, K. S., Briscoe, J., and Cheung, M. (2013). Phosphorylation of Sox9 is required for neural crest delamination and is regulated downstream of BMP and canonical Wnt signaling. Proc Natl Acad Sci U S A *110*, 2882-2887.

Lo Celso, C., Prowse, D. M., and Watt, F. M. (2004). Transient activation of beta-catenin signalling in adult mouse epidermis is sufficient to induce new hair follicles but continuous activation is required to maintain hair follicle tumours. Development *131*, 1787-1799.

Lowry, W. E., Blanpain, C., Nowak, J. A., Guasch, G., Lewis, L., and Fuchs, E. (2005). Defining the impact of beta-catenin/Tcf transactivation on epithelial stem cells. Genes Dev *19*, 1596-1611.

Lumpkin, E. A., and Caterina, M. J. (2007). Mechanisms of sensory transduction in the skin. Nature *445*, 858-865.

Lund, E., Guttinger, S., Calado, A., Dahlberg, J. E., and Kutay, U. (2004). Nuclear export of microRNA precursors. Science *303*, 95-98.

Lyle, S., Christofidou-Solomidou, M., Liu, Y., Elder, D. E., Albelda, S., and Cotsarelis, G. (1998). The C8/144B monoclonal antibody recognizes cytokeratin 15 and defines the location of human hair follicle stem cells. J Cell Sci *111 (Pt 21)*, 3179-3188.

MacDonald, B. T., Tamai, K., and He, X. (2009). Wnt/beta-catenin signaling: components, mechanisms, and diseases. Dev Cell *17*, 9-26.

Malanchi, I., Peinado, H., Kassen, D., Hussenet, T., Metzger, D., Chambon, P., Huber, M., Hohl, D., Cano, A., Birchmeier, W., and Huelsken, J. (2008). Cutaneous cancer stem cell maintenance is dependent on beta-catenin signalling. Nature *452*, 650-653.

Mardaryev, A. N., Ahmed, M. I., Vlahov, N. V., Fessing, M. Y., Gill, J. H., Sharov, A. A., and Botchkareva, N. V. (2010). Micro-RNA-31 controls hair cycle-associated changes in gene expression programs of the skin and hair follicle. Faseb Journal *24*, 3869-3881.

Margadant, C., Charafeddine, R. A., and Sonnenberg, A. (2010). Unique and redundant functions of integrins in the epidermis. FASEB J *24*, 4133-4152.

Matoltsy, A. G., and Matoltsy, M. N. (1970). The chemical nature of keratohyalin granules of the epidermis. J Cell Biol *47*, 593-603.

Matsuzaki, T., and Yoshizato, K. (1998). Role of hair papilla cells on induction and regeneration processes of hair follicles. Wound Repair Regen *6*, 524-530.

McElwee, K. J., Kissling, S., Wenzel, E., Huth, A., and Hoffmann, R. (2003). Cultured peribulbar dermal sheath cells can induce hair follicle development and contribute to the dermal sheath and dermal papilla. J Invest Dermatol *121*, 1267-1275.

McGrath, J. A., and Uitto, J. (2010). Anatomy and Organization of Human Skin, Eighth Edition (eds T. Burns, S. Breathnach, N. Cox and C. Griffiths), edn (Wiley-Blackwell, Oxford, UK).

Mecklenburg, L., Tobin, D. J., Muller-Rover, S., Handjiski, B., Wendt, G., Peters, E. M., Pohl, S., Moll, I., and Paus, R. (2000). Active hair growth (anagen) is associated with angiogenesis. J Invest Dermatol *114*, 909-916.

Mendell, J. T. (2008). miRiad roles for the miR-17-92 cluster in development and disease. Cell *133*, 217-222.

Menon, G. K., Cleary, G. W., and Lane, M. E. (2012). The structure and function of the stratum corneum. Int J Pharm *435*, 3-9.

Merrill, B. J., Gat, U., DasGupta, R., and Fuchs, E. (2001). Tcf3 and Lef1 regulate lineage differentiation of multipotent stem cells in skin. Genes Dev *15*, 1688-1705.

Mikkola, M. L. (2007). Genetic basis of skin appendage development. Semin Cell Dev Biol *18*, 225-236.

Mikkola, M. L. (2011). The Edar subfamily in hair and exocrine gland development. Adv Exp Med Biol *691*, 23-33.

Mikkola, M. L., and Millar, S. E. (2006). The mammary bud as a skin appendage: unique and shared aspects of development. J Mammary Gland Biol Neoplasia *11*, 187-203.

Mikkola, M. L., Pispa, J., Pekkanen, M., Paulin, L., Nieminen, P., Kere, J., and Thesleff, I. (1999). Ectodysplasin, a protein required for epithelial morphogenesis, is a novel TNF homologue and promotes cell-matrix adhesion. Mech Dev *88*, 133-146.

Mill, P., Mo, R., Fu, H., Grachtchouk, M., Kim, P. C., Dlugosz, A. A., and Hui, C. C. (2003). Sonic hedgehog-dependent activation of Gli2 is essential for embryonic hair follicle development. Genes Dev *17*, 282-294.

Millar, S. E. (2002). Molecular mechanisms regulating hair follicle development. J Invest Dermatol *118*, 216-225.

Miller, J., Djabali, K., Chen, T., Liu, Y., Ioffreda, M., Lyle, S., Christiano, A. M., Holick, M., and Cotsarelis, G. (2001). Atrichia caused by mutations in the vitamin D receptor gene is a phenocopy of generalized atrichia caused by mutations in the hairless gene. J Invest Dermatol *117*, 612-617.

Milner, Y., Sudnik, J., Filippi, M., Kizoulis, M., Kashgarian, M., and Stenn, K. (2002). Exogen, shedding phase of the hair growth cycle: characterization of a mouse model. J Invest Dermatol *119*, 639-644.

Mizumoto, N., and Takashima, A. (2004). CD1a and langerin: acting as more than Langerhans cell markers. J Clin Invest *113*, 658-660.

Moll, R., Divo, M., and Langbein, L. (2008). The human keratins: biology and pathology. Histochem Cell Biol *129*, 705-733.

Morris, R. J., Liu, Y., Marles, L., Yang, Z., Trempus, C., Li, S., Lin, J. S., Sawicki, J. A., and Cotsarelis, G. (2004). Capturing and profiling adult hair follicle stem cells. Nat Biotechnol *22*, 411-417.

Morrison, K. M., Miesegaes, G. R., Lumpkin, E. A., and Maricich, S. M. (2009). Mammalian Merkel cells are descended from the epidermal lineage. Dev Biol *336*, 76-83.

Muller-Rover, S., Handjiski, B., van der Veen, C., Eichmuller, S., Foitzik, K., McKay, I. A., Stenn, K. S., and Paus, R. (2001). A comprehensive guide for the accurate classification of murine hair follicles in distinct hair cycle stages. J Invest Dermatol *117*, 3-15.

Muller-Rover, S., Rossiter, H., Lindner, G., Peters, E. M., Kupper, T. S., and Paus, R. (1999). Hair follicle apoptosis and Bcl-2. J Investig Dermatol Symp Proc *4*, 272-277.

Myung, P., and Ito, M. (2012). Dissecting the bulge in hair regeneration. J Clin Invest *122*, 448-454.

Myung, P. S., Takeo, M., Ito, M., and Atit, R. P. (2013). Epithelial Wnt ligand secretion is required for adult hair follicle growth and regeneration. J Invest Dermatol *133*, 31-41.

Nakajima, T., Inui, S., Fushimi, T., Noguchi, F., Kitagawa, Y., Reddy, J. K., and Itami, S. (2013). Roles of MED1 in quiescence of hair follicle stem cells and maintenance of normal hair cycling. J Invest Dermatol *133*, 354-360.

Nehls, M., Pfeifer, D., Schorpp, M., Hedrich, H., and Boehm, T. (1994). New member of the winged-helix protein family disrupted in mouse and rat nude mutations. Nature *372*, 103-107.

Nguyen, H., Merrill, B. J., Polak, L., Nikolova, M., Rendl, M., Shaver, T. M., Pasolli, H. A., and Fuchs, E. (2009). Tcf3 and Tcf4 are essential for long-term homeostasis of skin epithelia. Nat Genet *41*, 1068-1075.

Nguyen, H., Rendl, M., and Fuchs, E. (2006). Tcf3 governs stem cell features and represses cell fate determination in skin. Cell *127*, 171-183.

Nowak, J. A., Polak, L., Pasolli, H. A., and Fuchs, E. (2008). Hair follicle stem cells are specified and function in early skin morphogenesis. Cell Stem Cell *3*, 33-43.

Ohyama, M., Terunuma, A., Tock, C. L., Radonovich, M. F., Pise-Masison, C. A., Hopping, S. B., Brady, J. N., Udey, M. C., and Vogel, J. C. (2006). Characterization and isolation of stem cell-enriched human hair follicle bulge cells. J Clin Invest *116*, 249-260.

Oliver, R. F., and Jahoda, C. A. (1988). Dermal-epidermal interactions. Clin Dermatol *6*, 74-82.

Oshima, H., Rochat, A., Kedzia, C., Kobayashi, K., and Barrandon, Y. (2001). Morphogenesis and renewal of hair follicles from adult multipotent stem cells. Cell *104*, 233-245.

Oshimori, N., and Fuchs, E. (2012). Paracrine TGF-beta signaling counterbalances BMP-mediated repression in hair follicle stem cell activation. Cell Stem Cell *10*, 63-75.

Otberg, N., Finner, A. M., and Shapiro, J. (2007). Androgenetic alopecia. Endocrinol Metab Clin North Am *36*, 379-398.

Ozsolak, F., Poling, L. L., Wang, Z., Liu, H., Liu, X. S., Roeder, R. G., Zhang, X., Song, J. S., and Fisher, D. E. (2008). Chromatin structure analyses identify miRNA promoters. Genes Dev *22*, 3172-3183.

Paladini, R. D., Saleh, J., Qian, C., Xu, G. X., and Rubin, L. L. (2005). Modulation of hair growth with small molecule agonists of the hedgehog signaling pathway. J Invest Dermatol *125*, 638-646.

Palmer, H. G., Anjos-Afonso, F., Carmeliet, G., Takeda, H., and Watt, F. M. (2008). The vitamin D receptor is a Wnt effector that controls hair follicle differentiation and specifies tumor type in adult epidermis. PLoS One *3*, e1483.

Panteleyev, A. A., Botchkareva, N. V., Sundberg, J. P., Christiano, A. M., and Paus, R. (1999). The role of the hairless (hr) gene in the regulation of hair follicle catagen transformation. Am J Pathol *155*, 159-171.

Panteleyev, A. A., Jahoda, C. A., and Christiano, A. M. (2001). Hair follicle predetermination. J Cell Sci *114*, 3419-3431.

Panteleyev, A. A., Paus, R., and Christiano, A. M. (2000). Patterns of hairless (hr) gene expression in mouse hair follicle morphogenesis and cycling. Am J Pathol *157*, 1071-1079.

Pasquinelli, A. E., Reinhart, B. J., Slack, F., Martindale, M. Q., Kuroda, M. I., Maller, B., Hayward, D. C., Ball, E. E., Degnan, B., Muller, P.*, et al.* (2000). Conservation of the sequence and temporal expression of let-7 heterochronic regulatory RNA. Nature *408*, 86-89.

Paus, R., and Cotsarelis, G. (1999). The biology of hair follicles. N Engl J Med *341*, 491-497.

Paus, R., and Foitzik, K. (2004). In search of the "hair cycle clock": a guided tour. Differentiation *72*, 489-511.

Paus, R., Foitzik, K., Welker, P., Bulfone-Paus, S., and Eichmuller, S. (1997). Transforming growth factor-beta receptor type I and type II expression during murine hair follicle development and cycling. J Invest Dermatol *109*, 518-526.

Paus, R., Muller-Rover, S., Van Der Veen, C., Maurer, M., Eichmuller, S., Ling, G., Hofmann, U., Foitzik, K., Mecklenburg, L., and Handjiski, B. (1999). A comprehensive guide for the recognition and classification of distinct stages of hair follicle morphogenesis. J Invest Dermatol *113*, 523-532.

Petiot, A., Conti, F. J., Grose, R., Revest, J. M., Hodivala-Dilke, K. M., and Dickson, C. (2003). A crucial role for Fgfr2-IIIb signalling in epidermal development and hair follicle patterning. Development *130*, 5493-5501.

Philpott, M. P., Sanders, D. A., and Kealey, T. (1994). Effects of insulin and insulin-like growth factors on cultured human hair follicles: IGF-I at physiologic

concentrations is an important regulator of hair follicle growth in vitro. J Invest Dermatol *102*, 857-861.

Plikus, M. V., Mayer, J. A., de la Cruz, D., Baker, R. E., Maini, P. K., Maxson, R., and Chuong, C. M. (2008). Cyclic dermal BMP signalling regulates stem cell activation during hair regeneration. Nature *451*, 340-344.

Plouhinec, J. L., Zakin, L., and De Robertis, E. M. (2011). Systems control of BMP morphogen flow in vertebrate embryos. Curr Opin Genet Dev *21*, 696-703.

Polakovicova, S., Seidenberg, H., Mikusova, R., Polak, S., and Pospisilova, V. (2011). Merkel cells--review on developmental, functional and clinical aspects. Bratisl Lek Listy *112*, 80-87.

Poliseno, L., Salmena, L., Zhang, J., Carver, B., Haveman, W. J., and Pandolfi, P. P. (2010). A coding-independent function of gene and pseudogene mRNAs regulates tumour biology. Nature *465*, 1033-1038.

Potter, C. S., Peterson, R. L., Barth, J. L., Pruett, N. D., Jacobs, D. F., Kern, M. J., Argraves, W. S., Sundberg, J. P., and Awgulewitsch, A. (2006). Evidence that the satin hair mutant gene Foxq1 is among multiple and functionally diverse regulatory targets for Hoxc13 during hair follicle differentiation. J Biol Chem *281*, 29245-29255.

Potter, G. B., Beaudoin, G. M., 3rd, DeRenzo, C. L., Zarach, J. M., Chen, S. H., and Thompson, C. C. (2001). The hairless gene mutated in congenital hair loss disorders encodes a novel nuclear receptor corepressor. Genes Dev *15*, 2687-2701.

Powell, B. C., Passmore, E. A., Nesci, A., and Dunn, S. M. (1998). The Notch signalling pathway in hair growth. Mech Dev *78*, 189-192.

Proksch, E., Brandner, J. M., and Jensen, J. M. (2008). The skin: an indispensable barrier. Exp Dermatol *17*, 1063-1072.

Proweller, A., Tu, L., Lepore, J. J., Cheng, L., Lu, M. M., Seykora, J., Millar, S. E., Pear, W. S., and Parmacek, M. S. (2006). Impaired notch signaling promotes de novo squamous cell carcinoma formation. Cancer Res *66*, 7438-7444.

Prussin, C., and Metcalfe, D. D. (2006). 5. IgE, mast cells, basophils, and eosinophils. J Allergy Clin Immunol *117*, S450-456.

Pummila, M., Fliniaux, I., Jaatinen, R., James, M. J., Laurikkala, J., Schneider, P., Thesleff, I., and Mikkola, M. L. (2007). Ectodysplasin has a dual role in

ectodermal organogenesis: inhibition of Bmp activity and induction of Shh expression. Development *134*, 117-125.

Ramalingam, P., Palanichamy, J. K., Singh, A., Das, P., Bhagat, M., Kassab, M. A., Sinha, S., and Chattopadhyay, P. (2014). Biogenesis of intronic miRNAs located in clusters by independent transcription and alternative splicing. RNA *20*, 76-87.

Randall, V. A. (2008). Androgens and hair growth. Dermatol Ther *21*, 314-328.

Reddy, S., Andl, T., Bagasra, A., Lu, M. M., Epstein, D. J., Morrisey, E. E., and Millar, S. E. (2001). Characterization of Wnt gene expression in developing and postnatal hair follicles and identification of Wnt5a as a target of Sonic hedgehog in hair follicle morphogenesis. Mech Dev *107*, 69-82.

Rein, H. (1924). Experimentelle studien über Elektroendosmose an überlebender menschlicher Hau Ztschr f Biol 125–140.

Reinhart, B. J., and Bartel, D. P. (2002). Small RNAs correspond to centromere heterochromatic repeats. Science *297*, 1831.

Reinhart, B. J., Slack, F. J., Basson, M., Pasquinelli, A. E., Bettinger, J. C., Rougvie, A. E., Horvitz, H. R., and Ruvkun, G. (2000). The 21-nucleotide let-7 RNA regulates developmental timing in Caenorhabditis elegans. Nature *403*, 901-906.

Rendl, M., Lewis, L., and Fuchs, E. (2005). Molecular dissection of mesenchymal-epithelial interactions in the hair follicle. PLoS Biol *3*, e331.

Reynolds, A. J., and Jahoda, C. A. (1991). Inductive properties of hair follicle cells. Ann N Y Acad Sci *642*, 226-241; discussion 241-222.

Reynolds, A. J., and Jahoda, C. A. (1992). Cultured dermal papilla cells induce follicle formation and hair growth by transdifferentiation of an adult epidermis. Development *115*, 587-593.

Reynolds, A. J., Lawrence, C., Cserhalmi-Friedman, P. B., Christiano, A. M., and Jahoda, C. A. (1999). Trans-gender induction of hair follicles. Nature *402*, 33-34.

Rhee, H., Polak, L., and Fuchs, E. (2006). Lhx2 maintains stem cell character in hair follicles. Science *312*, 1946-1949.

Riedl, S. J., and Shi, Y. (2004). Molecular mechanisms of caspase regulation during apoptosis. Nat Rev Mol Cell Biol *5*, 897-907.

Ro, S., Park, C., Young, D., Sanders, K. M., and Yan, W. (2007). Tissue-dependent paired expression of miRNAs. Nucleic Acids Res *35*, 5944-5953.

Rogers, G. E. (2004). Hair follicle differentiation and regulation. Int J Dev Biol *48*, 163-170.

Romani, N., Brunner, P. M., and Stingl, G. (2012). Changing views of the role of Langerhans cells. J Invest Dermatol *132*, 872-881.

Rompolas, P., and Greco, V. (2014). Stem cell dynamics in the hair follicle niche. Semin Cell Dev Biol *25-26C*, 34-42.

Rosenquist, T. A., and Martin, G. R. (1996). Fibroblast growth factor signalling in the hair growth cycle: expression of the fibroblast growth factor receptor and ligand genes in the murine hair follicle. Dev Dyn *205*, 379-386.

Sakai, Y., and Demay, M. B. (2000). Evaluation of keratinocyte proliferation and differentiation in vitamin D receptor knockout mice. Endocrinology *141*, 2043-2049.

Sato, N., Leopold, P. L., and Crystal, R. G. (1999). Induction of the hair growth phase in postnatal mice by localized transient expression of Sonic hedgehog. J Clin Invest *104*, 855-864.

Sato, N., Meijer, L., Skaltsounis, L., Greengard, P., and Brivanlou, A. H. (2004). Maintenance of pluripotency in human and mouse embryonic stem cells through activation of Wnt signaling by a pharmacological GSK-3-specific inhibitor. Nat Med *10*, 55-63.

Schlake, T. (2005). FGF signals specifically regulate the structure of hair shaft medulla via IGF-binding protein 5. Development *132*, 2981-2990.

Schlake, T. (2007). Determination of hair structure and shape. Semin Cell Dev Biol *18*, 267-273.

Schlake, T., Schorpp, M., Maul-Pavicic, A., Malashenko, A. M., and Boehm, T. (2000). Forkhead/winged-helix transcription factor Whn regulates hair keratin gene expression: molecular analysis of the nude skin phenotype. Dev Dyn *217*, 368-376.

Schmidt-Ullrich, R., and Paus, R. (2005). Molecular principles of hair follicle induction and morphogenesis. Bioessays *27*, 247-261.

Schmidt-Ullrich, R., Tobin, D. J., Lenhard, D., Schneider, P., Paus, R., and Scheidereit, C. (2006). NF-kappaB transmits Eda A1/EdaR signalling to activate Shh and cyclin D1 expression, and controls post-initiation hair placode down growth. Development *133*, 1045-1057.

Schmittgen, T. D., Lee, E. J., Jiang, J., Sarkar, A., Yang, L., Elton, T. S., and Chen, C. (2008). Real-time PCR quantification of precursor and mature microRNA. Methods *44*, 31-38.

Schneider, M. R., Schmidt-Ullrich, R., and Paus, R. (2009). The hair follicle as a dynamic miniorgan. Curr Biol *19*, R132-142.

Schwarz, D. S., Hutvagner, G., Du, T., Xu, Z., Aronin, N., and Zamore, P. D. (2003). Asymmetry in the assembly of the RNAi enzyme complex. Cell *115*, 199-208.

Sehic, A., Risnes, S., Khuu, C., Khan, Q. E., and Osmundsen, H. (2011). Effects of in vivo transfection with anti-miR-214 on gene expression in murine molar tooth germ. Physiol Genomics *43*, 488-498.

Selbach, M., Schwanhausser, B., Thierfelder, N., Fang, Z., Khanin, R., and Rajewsky, N. (2008). Widespread changes in protein synthesis induced by microRNAs. Nature *455*, 58-63.

Senoo, M., Pinto, F., Crum, C. P., and McKeon, F. (2007). p63 Is essential for the proliferative potential of stem cells in stratified epithelia. Cell *129*, 523-536.

Sethupathy, P., Megraw, M., and Hatzigeorgiou, A. G. (2006). A guide through present computational approaches for the identification of mammalian microRNA targets. Nat Methods *3*, 881-886.

Shang, L., Pruett, N. D., and Awgulewitsch, A. (2002). Hoxc12 expression pattern in developing and cycling murine hair follicles. Mech Dev *113*, 207-210.

Sharov, A. A., Sharova, T. Y., Mardaryev, A. N., Tommasi di Vignano, A., Atoyan, R., Weiner, L., Yang, S., Brissette, J. L., Dotto, G. P., and Botchkarev, V. A. (2006). Bone morphogenetic protein signaling regulates the size of hair follicles and modulates the expression of cell cycle-associated genes. Proc Natl Acad Sci U S A *103*, 18166-18171.

Shtutman, M., Zhurinsky, J., Simcha, I., Albanese, C., D'Amico, M., Pestell, R., and Ben-Ze'ev, A. (1999). The cyclin D1 gene is a target of the beta-catenin/LEF-1 pathway. Proc Natl Acad Sci U S A *96*, 5522-5527.

Sick, S., Reinker, S., Timmer, J., and Schlake, T. (2006). WNT and DKK determine hair follicle spacing through a reaction-diffusion mechanism. Science *314*, 1447-1450.

Siomi, H., and Siomi, M. C. (2010). Posttranscriptional regulation of microRNA biogenesis in animals. Mol Cell *38*, 323-332.

Slominski, A., Tobin, D. J., Shibahara, S., and Wortsman, J. (2004). Melanin pigmentation in mammalian skin and its hormonal regulation. Physiol Rev *84*, 1155-1228.

Slominski, A., and Wortsman, J. (2000). Neuroendocrinology of the skin. Endocr Rev *21*, 457-487.

Slominski, A., Wortsman, J., Plonka, P. M., Schallreuter, K. U., Paus, R., and Tobin, D. J. (2005). Hair follicle pigmentation. J Invest Dermatol *124*, 13-21.

Smyth, G. K., Michaud, J., and Scott, H. S. (2005). Use of within-array replicate spots for assessing differential expression in microarray experiments. Bioinformatics *21*, 2067-2075.

Snippert, H. J., Haegebarth, A., Kasper, M., Jaks, V., van Es, J. H., Barker, N., van de Wetering, M., van den Born, M., Begthel, H., Vries, R. G.*, et al.* (2010). Lgr6 marks stem cells in the hair follicle that generate all cell lineages of the skin. Science *327*, 1385-1389.

Sorrell, J. M., and Caplan, A. I. (2004). Fibroblast heterogeneity: more than skin deep. J Cell Sci *117*, 667-675.

St-Jacques, B., Dassule, H. R., Karavanova, I., Botchkarev, V. A., Li, J., Danielian, P. S., McMahon, J. A., Lewis, P. M., Paus, R., and McMahon, A. P. (1998). Sonic hedgehog signaling is essential for hair development. Curr Biol *8*, 1058-1068.

Stenn, K. (2005). Exogen is an active, separately controlled phase of the hair growth cycle. J Am Acad Dermatol *52*, 374-375.

Stenn, K. S., and Paus, R. (2001). Controls of hair follicle cycling. Physiol Rev *81*, 449-494.

Sundberg, J. P., Rourk, M. H., Boggess, D., Hogan, M. E., Sundberg, B. A., and Bertolino, A. P. (1997). Angora mouse mutation: altered hair cycle, follicular dystrophy, phenotypic maintenance of skin grafts, and changes in keratin expression. Vet Pathol *34*, 171-179.

Tanaka, T., Narisawa, Y., Misago, N., and Hashimoto, K. (1998). The innermost cells of the outer root sheath in human anagen hair follicles undergo specialized keratinization mediated by apoptosis. J Cutan Pathol *25*, 316-321.

Teta, M., Choi, Y. S., Okegbe, T., Wong, G., Tam, O. H., Chong, M. M., Seykora, J. T., Nagy, A., Littman, D. R., Andl, T., and Millar, S. E. (2012). Inducible deletion of epidermal Dicer and Drosha reveals multiple functions for miRNAs in postnatal skin. Development *139*, 1405-1416.

Tetsu, O., and McCormick, F. (1999). Beta-catenin regulates expression of cyclin D1 in colon carcinoma cells. Nature *398*, 422-426.

Tkatchenko, A. V., Visconti, R. P., Shang, L., Papenbrock, T., Pruett, N. D., Ito, T., Ogawa, M., and Awgulewitsch, A. (2001). Overexpression of Hoxc13 in differentiating keratinocytes results in downregulation of a novel hair keratin gene cluster and alopecia. Development *128*, 1547-1558.

Tobin, D. J. (2006). Biochemistry of human skin--our brain on the outside. Chem Soc Rev *35*, 52-67.

Trempus, C. S., Morris, R. J., Bortner, C. D., Cotsarelis, G., Faircloth, R. S., Reece, J. M., and Tennant, R. W. (2003). Enrichment for living murine keratinocytes from the hair follicle bulge with the cell surface marker CD34. J Invest Dermatol *120*, 501-511.

Trempus, C. S., Morris, R. J., Ehinger, M., Elmore, A., Bortner, C. D., Ito, M., Cotsarelis, G., Nijhof, J. G., Peckham, J., Flagler, N.*, et al.* (2007). CD34 expression by hair follicle stem cells is required for skin tumor development in mice. Cancer Res *67*, 4173-4181.

Tsai, S. Y., Sennett, R., Rezza, A., Clavel, C., Grisanti, L., Zemla, R., Najam, S., and Rendl, M. (2014). Wnt/beta-catenin signaling in dermal condensates is required for hair follicle formation. Dev Biol *385*, 179-188.

Tseng, A. S., Engel, F. B., and Keating, M. T. (2006). The GSK-3 inhibitor BIO promotes proliferation in mammalian cardiomyocytes. Chem Biol *13*, 957-963.

Tsuruta, D., Hashimoto, T., Hamill, K. J., and Jones, J. C. (2011). Hemidesmosomes and focal contact proteins: functions and cross-talk in keratinocytes, bullous diseases and wound healing. J Dermatol Sci *62*, 1-7.

Tumbar, T., Guasch, G., Greco, V., Blanpain, C., Lowry, W. E., Rendl, M., and Fuchs, E. (2004). Defining the epithelial stem cell niche in skin. Science *303*, 359-363.

Valladeau, J., Ravel, O., Dezutter-Dambuyant, C., Moore, K., Kleijmeer, M., Liu, Y., Duvert-Frances, V., Vincent, C., Schmitt, D., Davoust, J.*, et al.* (2000). Langerin, a novel C-type lectin specific to Langerhans cells, is an endocytic receptor that induces the formation of Birbeck granules. Immunity *12*, 71-81.

van der Vlist, M., and Geijtenbeek, T. B. (2010). Langerin functions as an antiviral receptor on Langerhans cells. Immunol Cell Biol *88*, 410-415.

van Genderen, C., Okamura, R. M., Farinas, I., Quo, R. G., Parslow, T. G., Bruhn, L., and Grosschedl, R. (1994). Development of several organs that

require inductive epithelial-mesenchymal interactions is impaired in LEF-1-deficient mice. Genes Dev *8*, 2691-2703.

Van Keymeulen, A., Mascre, G., Youseff, K. K., Harel, I., Michaux, C., De Geest, N., Szpalski, C., Achouri, Y., Bloch, W., Hassan, B. A., and Blanpain, C. (2009). Epidermal progenitors give rise to Merkel cells during embryonic development and adult homeostasis. J Cell Biol *187*, 91-100.

Van Mater, D., Kolligs, F. T., Dlugosz, A. A., and Fearon, E. R. (2003). Transient activation of beta -catenin signaling in cutaneous keratinocytes is sufficient to trigger the active growth phase of the hair cycle in mice. Genes Dev *17*, 1219-1224.

Van Neste, D., and Tobin, D. J. (2004). Hair cycle and hair pigmentation: dynamic interactions and changes associated with aging. Micron *35*, 193-200.

Vidal, V. P., Chaboissier, M. C., Lutzkendorf, S., Cotsarelis, G., Mill, P., Hui, C. C., Ortonne, N., Ortonne, J. P., and Schedl, A. (2005). Sox9 is essential for outer root sheath differentiation and the formation of the hair stem cell compartment. Curr Biol *15*, 1340-1351.

Vogt, A., McElwee, K. J., and Blume-Peytavi, U. (2008). Biology of the Hair Follicle.

Walsh, J. G., Cullen, S. P., Sheridan, C., Luthi, A. U., Gerner, C., and Martin, S. J. (2008). Executioner caspase-3 and caspase-7 are functionally distinct proteases. Proc Natl Acad Sci U S A *105*, 12815-12819.

Wang, B., Fallon, J. F., and Beachy, P. A. (2000). Hedgehog-regulated processing of Gli3 produces an anterior/posterior repressor gradient in the developing vertebrate limb. Cell *100*, 423-434.

Wang, D., Zhang, Z., O'Loughlin, E., Lee, T., Houel, S., O'Carroll, D., Tarakhovsky, A., Ahn, N. G., and Yi, R. (2012a). Quantitative functions of Argonaute proteins in mammalian development. Genes Dev *26*, 693-704.

Wang, D., Zhang, Z., O'Loughlin, E., Wang, L., Fan, X., Lai, E. C., and Yi, R. (2013a). MicroRNA-205 controls neonatal expansion of skin stem cells by modulating the PI(3)K pathway. Nat Cell Biol *15*, 1153-1163.

Wang, X., Chen, J., Li, F., Lin, Y., Zhang, X., Lv, Z., and Jiang, J. (2012b). MiR-214 inhibits cell growth in hepatocellular carcinoma through suppression of beta-catenin. Biochem Biophys Res Commun *428*, 525-531.

Wang, X., Guo, B., Li, Q., Peng, J., Yang, Z., Wang, A., Li, D., Hou, Z., Lv, K., Kan, G.*, et al.* (2013b). miR-214 targets ATF4 to inhibit bone formation. Nat Med *19*, 93-100.

Wang, Y., Medvid, R., Melton, C., Jaenisch, R., and Blelloch, R. (2007). DGCR8 is essential for microRNA biogenesis and silencing of embryonic stem cell self-renewal. Nat Genet *39*, 380-385.

Watanabe, T., Sato, T., Amano, T., Kawamura, Y., Kawamura, N., Kawaguchi, H., Yamashita, N., Kurihara, H., and Nakaoka, T. (2008). Dnm3os, a non-coding RNA, is required for normal growth and skeletal development in mice. Dev Dyn *237*, 3738-3748.

Weger, N., and Schlake, T. (2005). Igf-I signalling controls the hair growth cycle and the differentiation of hair shafts. J Invest Dermatol *125*, 873-882.

Woo, W. M., Zhen, H. H., and Oro, A. E. (2012). Shh maintains dermal papilla identity and hair morphogenesis via a Noggin-Shh regulatory loop. Genes Dev *26*, 1235-1246.

Wu, D. D., Irwin, D. M., and Zhang, Y. P. (2008). Molecular evolution of the keratin associated protein gene family in mammals, role in the evolution of mammalian hair. BMC Evol Biol *8*, 241.

Xing, Y. Z., Wang, R. M., Yang, K., Guo, H. Y., Deng, F., Li, Y. H., Ye, J. X., He, L., Lian, X. H., and Yang, T. (2013). Adenovirus-mediated Wnt5a expression inhibits the telogen-to-anagen transition of hair follicles in mice. Int J Med Sci *10*, 908-914.

Yamaguchi, Y., and Hearing, V. J. (2009). Physiological factors that regulate skin pigmentation. Biofactors *35*, 193-199.

Yamane, K., Jinnin, M., Etoh, T., Kobayashi, Y., Shimozono, N., Fukushima, S., Masuguchi, S., Maruo, K., Inoue, Y., Ishihara, T.*, et al.* (2013). Down-regulation of miR-124/-214 in cutaneous squamous cell carcinoma mediates abnormal cell proliferation via the induction of ERK. J Mol Med (Berl) *91*, 69-81.

Yang, T. S., Yang, X. H., Wang, X. D., Wang, Y. L., Zhou, B., and Song, Z. S. (2013). MiR-214 regulate gastric cancer cell proliferation, migration and invasion by targeting PTEN. Cancer Cell Int *13*, 68.

Yi, R., and Fuchs, E. (2010). MicroRNA-mediated control in the skin. Cell Death Differ *17*, 229-235.

Yi, R., and Fuchs, E. (2011). MicroRNAs and their roles in mammalian stem cells. J Cell Sci *124*, 1775-1783.

Yi, R., O'Carroll, D., Pasolli, H. A., Zhang, Z., Dietrich, F. S., Tarakhovsky, A., and Fuchs, E. (2006). Morphogenesis in skin is governed by discrete sets of differentially expressed microRNAs. Nat Genet *38*, 356-362.

Yi, R., Pasolli, H. A., Landthaler, M., Hafner, M., Ojo, T., Sheridan, R., Sander, C., O'Carroll, D., Stoffel, M., Tuschl, T., and Fuchs, E. (2009). DGCR8-dependent microRNA biogenesis is essential for skin development. Proc Natl Acad Sci U S A *106*, 498-502.

Yi, R., Poy, M. N., Stoffel, M., and Fuchs, E. (2008). A skin microRNA promotes differentiation by repressing 'stemness'. Nature *452*, 225-229.

Yi, R., Qin, Y., Macara, I. G., and Cullen, B. R. (2003). Exportin-5 mediates the nuclear export of pre-microRNAs and short hairpin RNAs. Genes Dev *17*, 3011-3016.

Yin, G., Chen, R., Alvero, A. B., Fu, H. H., Holmberg, J., Glackin, C., Rutherford, T., and Mor, G. (2010). TWISTing stemness, inflammation and proliferation of epithelial ovarian cancer cells through MIR199A2/214. Oncogene *29*, 3545-3553.

Yu, J., Peng, H., Ruan, Q., Fatima, A., Getsios, S., and Lavker, R. M. (2010). MicroRNA-205 promotes keratinocyte migration via the lipid phosphatase SHIP2. Faseb Journal *24*, 3950-3959.

Yu, J., Ryan, D. G., Getsios, S., Oliveira-Fernandes, M., Fatima, A., and Lavker, R. M. (2008). MicroRNA-184 antagonizes microRNA-205 to maintain SHIP2 levels in epithelia. Proc Natl Acad Sci U S A *105*, 19300-19305.

Yuhki, M., Yamada, M., Kawano, M., Iwasato, T., Itohara, S., Yoshida, H., Ogawa, M., and Mishina, Y. (2004). BMPR1A signaling is necessary for hair follicle cycling and hair shaft differentiation in mice. Development *131*, 1825-1833.

Zeng, Y., Yi, R., and Cullen, B. R. (2005). Recognition and cleavage of primary microRNA precursors by the nuclear processing enzyme Drosha. Embo J *24*, 138-148.

Zhang, L., Stokes, N., Polak, L., and Fuchs, E. (2011). Specific microRNAs are preferentially expressed by skin stem cells to balance self-renewal and early lineage commitment. Cell Stem Cell *8*, 294-308.

Zhang, Y., Tomann, P., Andl, T., Gallant, N. M., Huelsken, J., Jerchow, B., Birchmeier, W., Paus, R., Piccolo, S., Mikkola, M. L.*, et al.* (2009). Reciprocal

requirements for EDA/EDAR/NF-kappaB and Wnt/beta-catenin signaling pathways in hair follicle induction. Dev Cell *17*, 49-61.

Zhang, Z. C., Li, Y. Y., Wang, H. Y., Fu, S., Wang, X. P., Zeng, M. S., Zeng, Y. X., and Shao, J. Y. (2014). Knockdown of miR-214 promotes apoptosis and inhibits cell proliferation in nasopharyngeal carcinoma. PLoS One *9*, e86149.

Zhou, J. X., Jia, L. W., Liu, W. M., Miao, C. L., Liu, S., Cao, Y. J., and Duan, E. K. (2006). Role of sonic hedgehog in maintaining a pool of proliferating stem cells in the human fetal epidermis. Hum Reprod *21*, 1698-1704.

Zhou, P., Byrne, C., Jacobs, J., and Fuchs, E. (1995). Lymphoid enhancer factor 1 directs hair follicle patterning and epithelial cell fate. Genes Dev *9*, 700-713.

Zhu, H., and Fan, G. C. (2011). Extracellular/circulating microRNAs and their potential role in cardiovascular disease. Am J Cardiovasc Dis *1*, 138-149.

Appendix

Genes that show 2-fold down-regulation in the keratinocytes of K14rtTA/TRE-miR-214 mice versus WT mice

Accession Number	Gene Name	Symbol	Fold Change
	Adhesion/Extracellular matrix		
NM_011302	retinoschisis (X-linked, juvenile) 1	Rs1	5.25
NM_178596	gap junction protein, delta 3	Gjd3	4.73
NM_010708	lectin, galactose binding, soluble 9, transcript variant 1	Lgals9	4.27
NM_010327	glycoprotein Ib, beta polypeptide, transcript variant 2	Gp1bb	3.93
NM_010577	integrin alpha 5	Itga5	3.73
NM_181277	collagen, type XIV, alpha 1	Col14a1	3.15
NM_001081249	versican, transcript variant 1	Vcan	2.90
NM_020486	basal cell adhesion molecule	Bcam	2.77
NM_021334	integrin alpha X	Itgax	2.72
NM_146007	collagen, type VI, alpha 2	Col6a2	2.68
NM_010386	histocompatibility 2, class II, locus DMa	H2-DMa	2.64
NM_013565	integrin alpha 3	Itga3	2.58
NM_011150	lectin, galactoside-binding, soluble, 3 binding protein	Lgals3bp	2.56
NM_023051	calsyntenin 1	Clstn1	2.50
NM_007992	fibulin 2, transcript variant 1	Fbln2	2.44
NM_178685	protocadherin 20	Pcdh20	2.43
NM_010181	fibrillin 2	Fbn2	2.35
NM_001082960	integrin alpha M, transcript variant 1	Itgam	2.32
NM_013552	hyaluronan mediated motility receptor (RHAMM)	Hmmr	2.18
NM_010180	fibulin 1	Fbln1	2.01
	Cell Cycle/Apoptosis		
NM_018754	stratifin	Sfn	3.34
NM_177372	DNA replication helicase 2 homolog	Dna2	3.28
NM_007631	cyclin D1*	Ccnd1	3.76
NM_008564	minichromosome maintenance deficient 2 mitotin	Mcm2	2.91
NM_028131	centromere protein N	Cenpn	2.88
NM_010059	DMC1 dosage suppressor of mck1 homolog, meiosis-specific homologous recombination	Dmc1	2.78
NM_028222	cyclin-dependent kinase inhibitor 3	Cdkn3	2.72
NM_008014	protein phosphatase 1G (formerly 2C), magnesium-dependent, gamma isoform	Ppm1g	2.65
NM_027263	apoptosis-inducing, TAF9-like domain 1	Apitd1	2.60
NM_001012273	baculoviral IAP repeat-containing 5, transcript variant 3	Birc5	2.51
NM_198654	NSL1, MIND kinetochore complex component, homolog	Nsl1	2.50
NM_011015	origin recognition complex, subunit 1, transcript variant A	Orc1	2.43

NM_027954	synaptonemal complex central element protein 2, transcript variant 2	Syce2	2.42
NM_019499	MAD2 mitotic arrest deficient-like 1	Mad2l1	2.33
NM_022654	leucine-rich and death domain containing	Lrdd	2.33
NM_008566	minichromosome maintenance deficient 5, cell division cycle 46	Mcm5	2.29
NM_026560	cell division cycle associated 8	Cdca8	2.28
NM_009828	cyclin A2	Ccna2	2.27
NM_198605	spindle and kinetochore associated complex subunit 3	Ska3	2.26
NM_001042421	kinetochore associated 1	Kntc1	2.25
NM_146235	excision repair cross-complementing rodent repair deficiency complementation group 6 like	Ercc6l	2.23
NM_001159930	centromere protein L , transcript variant 1	Cenpl	2.19
NM_007900	ect2 oncogene, transcript variant 1	Ect2	2.18
NM_007659	cyclin-dependent kinase 1*	Cdk1	2.64
NM_013929	SIVA1, apoptosis-inducing factor, transcript variant 1	Siva1	2.15
NM_011049	cyclin-dependent kinase 16	Cdk16	2.15
NM_172301	cyclin B1*	Ccnb1	2.36
NM_001014976	extra spindle poles-like 1	Espl1	2.15
NM_025995	F-box protein 5	Fbxo5	2.14
NM_011799	cell division cycle 6, transcript variant 1	Cdc6	2.07
NM_027290	minichromosome maintenance deficient 10	Mcm10	2.05
NM_025866	cell division cycle associated 7	Cdca7	2.05
NM_016681	checkpoint kinase 2	Chek2	2.04
NM_175554	claspin	Clspn	2.03
NM_008567	minichromosome maintenance deficient 6	Mcm6	2.03
NM_007630	cyclin B2	Ccnb2	2.02
NM_010790	maternal embryonic leucine zipper kinase	Melk	2.01
NM_009829	Cyclin D2*	Ccnd2	1.49
Chromatin remodelling			
NM_178215	histone cluster 2, H3b	Hist2h3b	4.50
NM_007928	MAP/microtubule affinity-regulating kinase 2, transcript variant 1	Mark2	4.42
NM_175654	histone cluster 1, H4d	Hist1h4d	4.24
NM_178211	histone cluster 1, H4k	Hist1h4k	4.04
NM_178210	histone cluster 1, H4j	Hist1h4j	4.00
NM_178208	histone cluster 1, H4c	Hist1h4c	3.91
NM_175652	histone cluster 4, H4	Hist4h4	3.84
NM_001080819	AT rich interactive domain 1A	Arid1a	3.77
NM_030609	histone cluster 1, H1a	Hist1h1a	3.51
NM_026785	ubiquitin-conjugating enzyme E2C	Ube2c	3.39
NM_020034	histone cluster 1, H1b	Hist1h1b	3.39
NM_015787	histone cluster 1, H1e	Hist1h1e	3.28
NM_033596	histone cluster 2, H4	Hist2h4	3.17
NM_016957	high mobility group nucleosomal binding domain 2	Hmgn2	3.13
NM_001195421	histone cluster 1, H4m	Hist1h4m	3.01
NM_013548	histone cluster 1, H3f	Hist1h3f	2.90
NM_145073	histone cluster 1, H3g	Hist1h3g	2.84
NM_010931	ubiquitin-like, containing PHD and RING finger domains, 1, transcript variant 1	Uhrf1	2.72
NM_175653	histone cluster 1, H3c	Hist1h3c	2.66
NM_178856	GINS complex subunit 2 (Psf2 homolog)	Gins2	2.66

NM_012012	exonuclease 1	Exo1	2.62
NM_001204973	bromodomain containing 2 , transcript variant 2	Brd2	2.56
NM_021790	centromere protein K, transcript variant 1	Cenpk	2.55
NM_175663	histone cluster 1, H2ba	Hist1h2ba	2.54
NM_011234	RAD51 homolog	Rad51	2.53
NM_020022	replication factor C (activator 1) 2	Rfc2	2.51
NM_178183	histone cluster 1, H2ak	Hist1h2ak	2.46
NM_008210	H3 histone, family 3A	H3f3a	2.40
NM_011623	topoisomerase (DNA) II alpha	Top2a	2.38
NM_001163775	TAO kinase 2, transcript variant 2	Taok2	2.37
NM_181586	sirtuin 6 (silent mating type information regulation 2, homolog) 6 , transcript variant 1	Sirt6	2.35
NM_198160	SWI/SNF related, matrix associated, actin dependent regulator of chromatin, subfamily c, member 2, transcript variant 3	Smarcc2	2.35
NM_024184	ASF1 anti-silencing function 1 homolog B	Asf1b	2.33
NM_028039	establishment of cohesion 1 homolog 2	Esco2	2.33
NM_145946	Fanconi anemia, complementation group I	Fanci	2.31
NM_178200	histone cluster 1, H2bm	Hist1h2bm	2.24
NM_009030	retinoblastoma binding protein 4	Rbbp4	2.23
NM_008894	polymerase (DNA directed), delta 2, regulatory subunit	Pold2	2.20
NM_008228	histone deacetylase 1	Hdac1	2.20
NM_013883	sex comb on midleg homolog 1, transcript variant 1	Scmh1	2.18
NM_020004	K(lysine) acetyltransferase 2A, transcript variant 1	Kat2a	2.16
NM_011121	polo-like kinase 1	Plk1	2.16
NM_146208	nei like 3	Neil3	2.16
NM_134083	regulator of chromosome condensation and BTB (POZ) domain containing protein 2 , transcript variant 2	Rcbtb2	2.13
NM_008892	polymerase (DNA directed), alpha 1	Pola1	2.11
NM_029797	meiotic nuclear divisions 1 homolog	Mnd1	2.10
NM_013550	histone cluster 1, H3a	Hist1h3a	2.10
NM_010722	lamin B2	Lmnb2	2.09
NM_026632	replication protein A3	Rpa3	2.08
NM_153141	coactivator-associated arginine methyltransferase 1, transcript variant 2	Carm1	2.07
NM_023294	NDC80 homolog, kinetochore complex component	Ndc80	2.05
NM_172453	PIF1 5'-to-3' DNA helicase homolog	Pif1	2.05
NM_009013	RAD51 associated protein 1	Rad51ap1	2.03
NM_008017	structural maintenance of chromosomes 2	Smc2	1.98
	Cytoskeleton		
NM_011072	profilin 1	Pfn1	3.96
NM_010669	keratin 6B	Krt6b	3.94
NM_009451	tubulin, beta 4A class IVA	Tubb4a	3.93
NM_001163637	janus kinase and microtubule interacting protein 2	Jakmip2	3.39
NM_009449	tubulin, alpha 3B	Tuba3b	3.34
NM_008445	kinesin family member 3C	Kif3c	2.92
NM_130857	keratin associated protein 19-3	Krtap19-3	2.92
NM_183296	keratin associated protein 16-3	Krtap16-3	2.92
NM_016879	keratin 85	Krt85	2.90

NM_011526	transgelin	Tagln	2.88
NM_001163615	keratin associated protein 20-2	Krtap20-2	2.81
NM_130870	keratin associated protein 16-1	Krtap16-1	2.81
NM_175272	neuron navigator 2, transcript variant 1	Nav2	2.76
NM_001113406	keratin associated protein 11-1	Krtap11-1	2.70
NM_019445	formin 2	Fmn2	2.68
NM_148934	tubulin polyglutamylase complex subunit 1	Tpgs1	2.64
NM_010672	keratin associated protein 6-1	Krtap6-1	2.64
NM_028621	keratin associated protein 21-1	Krtap21-1	2.62
NM_019641	stathmin 1	Stmn1	2.60
NM_027771	keratin associated protein 7-1	Krtap7-1	2.58
NM_130873	keratin associated protein 19-4	Krtap19-4	2.57
NM_010626	kinesin family member 7	Kif7	2.50
NM_009931	collagen, type IV, alpha 1	Col4a1	2.42
NM_001024716	TRIO and F-actin binding protein, transcript variant 1	Triobp	2.41
NM_010662	keratin 13	Krt13	2.38
NM_026552	actin related protein 2/3 complex, subunit 4, transcript variant 1	Arpc4	2.37
NM_013928	schwannomin interacting protein 1, transcript variant 4	Schip1	2.34
NM_172946	keratin 222	Krt222	2.32
NM_011654	tubulin, alpha 1B	Tuba1b	2.29
NM_001166157	keratin 81	Krt81	2.29
NM_017470	dynein, axonemal, light chain 4	Dnalc4	2.29
NM_027800	keratin associated protein 2-4	Krtap2-4	2.28
NM_010676	keratin associated protein 19-5	Krtap19-5	2.27
NM_212483	keratin 42	Krt42	2.26
NM_198599	MAP6 domain containing 1	Map6d1	2.25
NM_197945	ProSAPiP1 protein	Prosapip1	2.24
NM_145575	caldesmon 1	Cald1	2.20
NM_017464	neural precursor cell expressed, developmentally down-regulated gene 9, transcript variant 2	Nedd9	2.19
NM_019670	diaphanous homolog 3	Diap3	2.18
NM_080728	myosin, heavy polypeptide 7, cardiac muscle, beta	Myh7	2.16
NM_134471	kinesin family member 2C	Kif2c	2.14
NM_009768	basigin, transcript variant 1	Bsg	2.14
NM_028390	anillin, actin binding protein	Anln	2.13
NM_001191018	keratin associated protein 22-2	Krtap22-2	2.11
NM_133851	nucleolar and spindle associated protein 1, transcript variant 1	Nusap1	2.05
NM_178926	vimentin-type intermediate filament associated coiled-coil protein, transcript variant 1	Vmac	2.01
NM_010675	keratin associated protein 8-1	Krtap8-1	1.98
	Metabolism		
NM_016956	hemoglobin, beta adult minor chain	Hbb-b2	14.97
NM_001080943	zinc finger, DHHC-type containing 22	Zdhhc22	13.25
NM_009653	aminolevulinic acid synthase 2, erythroid, transcript variant 1	Alas2	8.62
NM_008220	hemoglobin, beta adult major chain	Hbb-b1	8.30
NM_008218	hemoglobin alpha, adult chain 1	Hba-a1	6.67
NM_139142	solute carrier family 6 (neurotransmitter transporter), member 20A	Slc6a20a	5.09

NM_018763	carbohydrate sulfotransferase 2	Chst2	4.81
NM_001082975	short chain dehydrogenase/reductase family 39U, member 1	Sdr39u1	4.59
NM_009464	uncoupling protein 3 (mitochondrial, proton carrier)	Ucp3	4.46
NM_001033270	solute carrier family 4, sodium bicarbonate cotransporter, member 7	Slc4a7	4.43
NM_011671	uncoupling protein 2 (mitochondrial, proton carrier)	Ucp2	4.41
NM_027093	NADH dehydrogenase (ubiquinone) complex I, assembly factor 5	Ndufaf5	4.39
NM_001104531	cytochrome P450, family 2, subfamily d, polypeptide 11	Cyp2d11	4.17
NM_019698	aldehyde dehydrogenase 18 family, member A1, nuclear gene encoding mitochondrial protein, transcript variant 1	Aldh18a1	3.95
NM_010066	DNA methyltransferase (cytosine-5) 1 , transcript variant 2	Dnmt1	3.94
NM_001083955	hemoglobin alpha, adult chain 2	Hba-a2	3.58
NM_010596	potassium voltage-gated channel, shaker-related subfamily, member 7	Kcna7	3.47
NM_007817	cytochrome P450, family 2, subfamily f, polypeptide 2	Cyp2f2	3.46
NM_010359	glutathione S-transferase, mu 3	Gstm3	3.37
NM_175403	malectin	Mlec	3.34
NM_134118	trans-2,3-enoyl-CoA reductase , transcript variant 1	Tecr	3.31
NM_007807	cytochrome b-245, beta polypeptide	Cybb	3.31
NM_177186	solute carrier family 35, member E2	Slc35e2	3.26
NM_013784	phosphatidylinositol glycan anchor biosynthesis, class N	Pign	3.22
NM_009034	retinol binding protein 2, cellular	Rbp2	3.15
NM_011371	ST6 (alpha-N-acetyl-neuraminyl-2,3-beta-galactosyl-1,3)-N-acetylgalactosaminide alpha-2,6-sialyltransferase 1	St6galnac1	3.15
NM_016966	3-phosphoglycerate dehydrogenase	Phgdh	3.09
NM_009181	ST8 alpha-N-acetyl-neuraminide alpha-2,8-sialyltransferase 2	St8sia2	3.03
NM_026969	Sec31 homolog A	Sec31a	2.98
NM_001243052	branched chain aminotransferase 2, mitochondrial, transcript variant 2	Bcat2	2.94
NM_027790	dehydrogenase/reductase member 2	Dhrs2	2.91
NM_133189	calcium channel, voltage-dependent, gamma subunit 7	Cacng7	2.85
NM_144845	UDP glycosyltransferases 3 family, polypeptide A2	Ugt3a2	2.84
NM_008525	aminolevulinate, delta-, dehydratase	Alad	2.84
NM_178788	dCMP deaminase (Dctd), transcript variant 1	Dctd	2.81
NM_011961	procollagen lysine, 2-oxoglutarate 5-dioxygenase 2, transcript variant 2	Plod2	2.79
NM_001033175	ceroid-lipofuscinosis, neuronal 6	Cln6	2.78
NM_213733	aminopeptidase-like 1	Npepl1	2.76
NM_030601	chloride channel calcium activated 2	Clca2	2.72
NM_207161	2'-deoxynucleoside 5'-phosphate N-hydrolase 1	Dnph1	2.69
NM_009437	thiosulfate sulfurtransferase, mitochondrial	Tst	2.68
NM_009723	ATPase, Ca++ transporting, plasma membrane 2, transcript variant 1	Atp2b2	2.67
NM_019435	NADH dehydrogenase (ubiquinone) 1 beta	Ndufb11	2.65

	subcomplex, 11		
NM_009374	transglutaminase 3	Tgm3	2.62
NM_146198	solute carrier family 5 (sodium/glucose cotransporter), member 11	Slc5a11	2.59
NM_025412	pyrroline-5-carboxylate reductase-like	Pycrl	2.55
NM_033617	ATPase, H+ transporting, lysosomal V0 subunit B	Atp6v0b	2.53
NM_145603	carboxylesterase 2C	Ces2c	2.51
NM_008631	metallothionein 4	Mt4	2.46
NM_009272	spermidine synthase	Srm	2.41
NM_001044308	calcium channel, voltage-dependent, alpha 1I subunit	Cacna1i	2.40
NM_009662	arachidonate 5-lipoxygenase	Alox5	2.38
NM_009104	ribonucleotide reductase M2	Rrm2	2.38
NM_001163359	fidgetin-like 1, transcript variant 1	Fignl1	2.34
NM_009804	catalase	Cat	2.32
NM_010497	isocitrate dehydrogenase 1 (NADP+), soluble, transcript variant 2	Idh1	2.32
NM_008826	phosphofructokinase, liver, B-type	Pfkl	2.31
NM_009127	stearoyl-Coenzyme A desaturase 1	Scd1	2.28
NM_172371	solute carrier family 16 (monocarboxylic acid transporters), member 13	Slc16a13	2.28
NM_054094	acyl-CoA synthetase medium-chain family member 1	Acsm1	2.27
NM_025408	alkaline ceramidase 3	Acer3	2.26
NM_001271544	solute carrier family 4, sodium bicarbonate cotransporter, member 9, transcript variant 1	Slc4a9	2.26
NM_026764	glutathione S-transferase, mu 4 , transcript variant 1	Gstm4	2.25
NM_010274	glycerol phosphate dehydrogenase 2, mitochondrial (Gpd2), transcript variant 2	Gpd2	2.24
NM_010358	glutathione S-transferase, mu 1	Gstm1	2.22
NM_008278	hydroxyprostaglandin dehydrogenase 15	Hpgd	2.22
NM_020581	angiopoietin-like 4	Angptl4	2.21
NM_172117	ectonucleoside triphosphate diphosphohydrolase 6	Entpd6	2.15
NM_026678	biliverdin reductase A	Blvra	2.15
NM_080440	solute carrier family 8 (sodium/calcium exchanger), member 3, transcript variant 2	Slc8a3	2.15
NM_030262	protein O-fucosyltransferase 2	Pofut2	2.13
NM_172773	solute carrier family 17 (anion/sugar transporter), member 5	Slc17a5	2.12
NM_178696	solute carrier family 25, member 44, transcript variant 1	Slc25a44	2.11
NM_001040699	myotubularin related protein 7	Mtmr7	2.11
NM_177382	cytochrome P450, family 2, subfamily r, polypeptide 1	Cyp2r1	2.11
NM_007838	dolichyl-di-phosphooligosaccharide-protein glycotransferase	Ddost	2.10
NM_172609	translocase of outer mitochondrial membrane 22 homolog	Tomm22	2.08
NM_007621	carbonyl reductase 2	Cbr2	2.08
NM_013541	glutathione S-transferase, pi 1	Gstp1	2.07
NM_011962	procollagen-lysine, 2-oxoglutarate 5-dioxygenase 3	Plod3	2.07
NM_016666	aryl-hydrocarbon receptor-interacting protein	Aip	2.06
NM_007646	CD38 antigen	Cd38	2.05
NM_028638	glutamate decarboxylase-like 1	Gadl1	2.05

NM_007379	ATP-binding cassette, sub-family A, member 2	Abca2	2.04
NM_178086	fatty acid 2-hydroxylase	Fa2h	2.02
NM_019501	prenyl (solanesyl) diphosphate synthase, subunit 1	Pdss1	2.01
NM_008212	hydroxyacyl-Coenzyme A dehydrogenase	Hadh	2.01
NM_026947	enoyl-Coenzyme A delta isomerase 3	Eci3	2.00
NM_138665	sarcosine dehydrogenase	Sardh	2.00
NM_011977	solute carrier family 27 (fatty acid transporter), member 1	Slc27a1	2.00
	Others		
NM_001201391	hemoglobin subunit beta-1-like	Beta-s	29.45
NM_023900	pleckstrin homology domain containing, family J member 1	Plekhj1	5.60
NM_011174	proline rich protein HaeIII subfamily 1	Prh1	5.44
NM_021384	radical S-adenosyl methionine domain containing 2	Rsad2	4.67
NM_138602	PRA1 domain family 2	Praf2	4.14
NM_001042451	synuclein, alpha, transcript variant 1	Snca	4.05
NM_013877	calcium binding protein 5	Cabp5	3.98
NM_201518	fibronectin leucine rich transmembrane protein 2	Flrt2	3.83
NM_177994	R3H domain containing 4	R3hdm4	3.80
NM_001205102	leucine-rich repeat, immunoglobulin-like and transmembrane domains 3	Lrit3	3.76
NM_018803	synaptotagmin X	Syt10	3.74
NM_029000	GTPase, very large interferon inducible 1, transcript variant 1	Gvin1	3.73
NM_207105	histocompatibility 2, class II antigen A, beta 1	H2-Ab1	3.62
NM_080846	HIG1 domain family, member 1B	Higd1b	3.60
NM_001033478	family with sequence similarity 47, member E, transcript variant 1	Fam47e	3.53
NM_001081418	glioma tumor suppressor candidate region gene 1	Gltscr1	3.53
NM_145981	phytanoyl-CoA hydroxylase interacting protein	Phyhip	3.26
NM_021898	testis specific gene A8	Tsga8	3.11
NM_134122	nurim (nuclear envelope membrane protein)	Nrm	3.06
NM_001163614	achaete-scute complex homolog 4	Ascl4	3.04
NM_020583	interferon-stimulated protein, transcript variant 1	Isg20	2.98
NM_173862	family with sequence similarity 83, member A	Fam83a	2.94
NM_175427	family with sequence similarity 163, member B	Fam163b	2.91
NM_001082545	stefin A2	Stfa2	2.77
NM_183187	family with sequence similarity 107, member A	Fam107a	2.76
NM_001142642	fibrosin-like 1, transcript variant 1	Fbrsl1	2.76
NM_001199631	FK506 binding protein 8, transcript variant 3	Fkbp8	2.75
NM_172756	ankyrin repeat and LEM domain containing 1	Ankle1	2.75
NM_133859	olfactomedin-like 3	Olfml3	2.72
NM_001025576	coiled-coil domain containing 141	Ccdc141	2.71
NM_025620	RAB15 effector protein	Rep15	2.70
NM_010807	MARCKS-like 1	Marcksl1	2.63
NM_001081406	leucine rich repeat protein 1	Lrr1	2.51
NM_018884	PDZ domain containing RING finger 3	Pdzrn3	2.50
NM_183170	MPV17 mitochondrial membrane protein-like 2	Mpv17l2	2.44
NM_172116	Parkinson disease 7 domain containing 1	Pddc1	2.42
NM_133719	meteorin, glial cell differentiation regulator	Metrn	2.41

NM_030694	interferon induced transmembrane protein 2	Ifitm2	2.38
NM_145361	BTB (POZ) domain containing 2	Btbd2	2.37
NM_009185	Scl/Tal1 interrupting locus	Stil	2.37
NM_016737	stress-induced phosphoprotein 1	Stip1	2.35
NM_001163721	small integral membrane protein 1 , transcript variant 1	Smim1	2.35
NM_032543	ring finger protein 123	Rnf123	2.35
NM_018771	GIPC PDZ domain containing family, member 1	Gipc1	2.34
NM_025378	interferon induced transmembrane protein 3	Ifitm3	2.32
NM_029377	lin-37 homolog	Lin37	2.30
NM_001199337	apolipoprotein O, transcript variant 2	Apoo	2.29
NM_133831	glioma tumor suppressor candidate region gene 2	Gltscr2	2.27
NM_010219	FK506 binding protein 4	Fkbp4	2.27
NM_138682	leucine rich repeat containing 4	Lrrc4	2.26
NM_026457	spermatid associated, transcript variant 2	Spert	2.25
NM_013515	stomatin	Stom	2.24
NM_053113	eosinophil-associated, ribonuclease A family, member 11	Ear11	2.21
NM_177028	O-acyltransferase like	Oacyl	2.18
NM_011627	trophoblast glycoprotein, transcript variant 1	Tpbg	2.17
NM_146244	ribosomal protein S6 kinase-like 1	Rps6kl1	2.16
NM_133187	family with sequence similarity 198, member B	Fam198b	2.14
NM_001025610	membrane-spanning 4-domains, subfamily A, member 7, transcript variant 2	Ms4a7	2.13
NM_172488	laccase (multicopper oxidoreductase) domain containing 1	Lacc1	2.13
NM_175118	dual specificity phosphatase 28	Dusp28	2.12
NM_080595	EMI domain containing 1	Emid1	2.11
NM_144556	leucine-rich repeat LGI family, member 4	Lgi4	2.11
NM_019661	YKT6 homolog	Ykt6	2.10
NM_021294	diazepam binding inhibitor-like 5	Dbil5	2.09
NM_016663	synaptotagmin III, transcript variant 1	Syt3	2.08
NM_178919	lipase maturation factor 2	Lmf2	2.08
NM_011073	perforin 1 (pore forming protein)	Prf1	2.07
NM_145390	transportin 2 (importin 3, karyopherin beta 2b), transcript variant 1	Tnpo2	2.07
NM_009538	pleiomorphic adenoma gene-like 1	Plagl1	2.05
NM_026938	transmembrane protein 160	Tmem160	2.05
NM_010129	epithelial membrane protein 3, transcript variant 1	Emp3	2.04
NM_010590	ajuba LIM protein	Ajuba	2.03
NM_146156	PDLIM1 interacting kinase 1 like, transcript variant 1	Pdik1l	2.03
NM_001195088	transmembrane channel-like gene family 8, transcript variant A	Tmc8	2.03
NM_183194	gasdermin C3	Gsdmc3	2.01
NM_027984	epsin 3	Epn3	2.00
	Protein folding		
NM_024172	HSPA (heat shock 70kDa) binding protein, cytoplasmic cochaperone 1	Hspbp1	2.47
NM_175199	heat shock protein 12A	Hspa12a	2.03
	Proteolysis		
NM_023635	RAB27A, member RAS oncogene family	Rab27a	5.79

NM_009126	serine (or cysteine) peptidase inhibitor, clade B (ovalbumin), member 3A	Serpinb3a	5.55
NM_201363	serine (or cysteine) peptidase inhibitor, clade B, member 3C	Serpinb3c	4.67
NM_001169153	CD300 antigen like family member F, transcript variant 1	Cd300lf	4.17
NM_145578	ubiquitin-conjugating enzyme E2M, transcript variant 1	Ube2m	3.50
NM_025312	sclerostin domain containing 1*	Sostdc1	4.30
NM_025288	stefin A3	Stfa3	2.99
NM_173869	stefin A2 like 1	Stfa2l1	2.98
NM_001205070	Josephin domain containing 2, transcript variant 1	Josd2	2.94
NM_175188	membrane-associated ring finger (C3HC4) 1, transcript variant 3	March1	2.93
NM_010767	mannan-binding lectin serine peptidase 2, transcript variant 2	Masp2	2.91
NM_011187	proteasome (prosome, macropain) subunit, beta type 7	Psmb7	2.80
NM_145420	ubiquitin-conjugating enzyme E2D 1	Ube2d1	2.74
NM_008604	membrane metallo endopeptidase	Mme	2.65
NM_178738	protease, serine, 35	Prss35	2.60
NM_007649	CD48 antigen	Cd48	2.58
NM_019461	ubiquitin specific peptidase 27, X chromosome	Usp27x	2.53
NM_198680	serine (or cysteine) peptidase inhibitor, clade B (ovalbumin), member 3B	Serpinb3b	2.50
NM_010612	kinase insert domain protein receptor	Kdr	2.49
NM_010418	hect (homologous to the E6-AP (UBE3A) carboxyl terminus) domain and RCC1 (CHC1)-like domain (RLD) 2	Herc2	2.40
NM_015783	ISG15 ubiquitin-like modifier	Isg15	2.35
NM_133354	SMT3 suppressor of mif two 3 homolog 2	Sumo2	2.26
NM_011595	tissue inhibitor of metalloproteinase 3	Timp3	2.21
NM_001001650	protease, serine, 48	Prss48	2.20
NM_001082543	stefin A1	Stfa1	2.20
NM_023386	receptor transporter protein	Rtp4	2.15
NM_198028	serine (or cysteine) peptidase inhibitor, clade B (ovalbumin), member 10, transcript variant 1	Serpinb10	2.09
NM_008607	matrix metallopeptidase 13	Mmp13	2.09
NM_173754	ubiquitin specific peptidase 43	Usp43	2.04
NM_173052	serine (or cysteine) peptidase inhibitor, clade B, member 1b	Serpinb1b	2.01
	RNA processing		
NM_013932	DEAD (Asp-Glu-Ala-Asp) box polypeptide 25	Ddx25	12.54
NM_012011	eukaryotic translation initiation factor 2, subunit 3, structural gene Y-linked	Eif2s3y	6.25
NM_012008	DEAD (Asp-Glu-Ala-Asp) box polypeptide 3, Y-linked	Ddx3y	5.02
NM_153416	achalasia, adrenocortical insufficiency, alacrimia	Aaas	3.31
NM_011358	serine/arginine-rich splicing factor 2	Srsf2	2.99
NM_025500	mitochondrial ribosomal protein L37	Mrpl37	2.94
NM_018799	eukaryotic translation initiation factor 3, subunit I	Eif3i	2.70
NM_001008422	SR-related CTD-associated factor 1	Scaf1	2.54
NM_011431	elongation factor Tu GTP binding domain containing 2, transcript variant 1	Eftud2	2.42

NM_001166589	eukaryotic translation initiation factor 5A, transcript variant 1	Eif5a	2.41
NM_175001	mitochondrial ribosomal protein L22	Mrpl22	2.35
NM_026080	mitochondrial ribosomal protein S24	Mrps24	2.32
NM_023133	ribosomal protein S19	Rps19	2.26
NM_016805	heterogeneous nuclear ribonucleoprotein U	Hnrnpu	2.24
NM_175235	CUGBP, Elav-like family member 6	Celf6	2.22
NM_177367	gem (nuclear organelle) associated protein 4	Gemin4	2.20
NM_173757	mitochondrial ribosomal protein S27	Mrps27	2.19
NM_019484	Aly/REF export factor 2	Alyref2	2.15
NM_148917	poly(A) binding protein, cytoplasmic 4, transcript variant 2	Pabpc4	2.14
NM_009070	ribonucleic acid binding protein S1, transcript variant 1	Rnps1	2.12
NM_207523	ribosomal protein L23A	Rpl23a	2.12
NM_021288	thymidylate synthase, transcript variant 1	Tyms	2.09
NM_022313	Era (G-protein)-like 1	Eral1	2.08
NM_013507	eukaryotic translation initiation factor 4, gamma 2, transcript variant 1	Eif4g2	2.01
	Signalling		
NM_010100	ectodysplasin-A receptor*	Edar	58.69
NM_009170	sonic hedgehog*	Shh	45.41
NM_176996	smoothened homolog (Drosophila) (Smo)	Smo	36.25
NM_008958	patched homolog 2	Ptch2	25.72
NM_133249	peroxisome proliferative activated receptor, gamma, coactivator 1 beta	Ppargc1b	16.21
NM_009987	chemokine (C-X3-C) receptor 1	Cx3cr1	9.75
ENSMUST00000 029611	lymphoid enhancer binding factor 1*	Lef1	9.68
NM_001033960	RAB GTPase activating protein 1, transcript variant 2	Rabgap1	8.53
NM_007416	adrenergic receptor, alpha 1b	Adra1b	6.07
NM_001042605	CD74 antigen, transcript variant 1	Cd74	5.86
NM_199022	SHC (Src homology 2 domain containing) family, member 4	Shc4	4.08
NM_026864	RAS-like, family 11, member A	Rasl11a	3.99
NM_001272024	sema domain, transmembrane domain (TM), and cytoplasmic domain, (semaphorin) 6C , transcript variant 1	Sema6c	3.85
NM_009835	chemokine (C-C motif) receptor 6, transcript variant 1	Ccr6	3.73
NM_146862	olfactory receptor 763	Olfr763	3.59
NM_001081105	ras homolog gene family, member H	Rhoh	3.57
NM_022324	stromal cell-derived factor 2-like 1	Sdf2l1	3.57
NM_008973	pleiotrophin	Ptn	3.52
NM_011562	teratocarcinoma-derived growth factor 1	Tdgf1	3.47
NM_027242	protein phosphatase 1, regulatory subunit 35	Ppp1r35	3.44
NM_013834	secreted frizzled-related protein 1	Sfrp1	3.36
NM_146457	olfactory receptor 282	Olfr282	3.04
NM_011428	synaptosomal-associated protein 25	Snap25	2.85
NM_028808	purinergic receptor P2Y, G-protein coupled 13	P2ry13	2.84
NM_021885	tubby candidate gene	Tub	2.75
NM_007889	dishevelled 3, dsh homolog	Dvl3	2.71
NM_010275	glial cell line derived neurotrophic factor	Gdnf	2.68
NM_008975	protein tyrosine phosphatase 4a3, transcript variant 2	Ptp4a3	2.64

NM_008086	growth arrest specific 1	Gas1	2.61
NM_029408	IQ motif containing D	Iqcd	2.61
NM_183315	cortexin 1	Ctxn1	2.6
NM_207666	delta-like 2 homolog	Dlk2	2.6
NM_010733	leucine rich repeat protein 3, neuronal, transcript variant 2	Lrrn3	2.58
NM_029057	TBC1 domain family, member 30	Tbc1d30	2.58
NM_177740	RGM domain family, member A	Rgma	2.58
NM_013739	docking protein 3	Dok3	2.54
NM_010517	insulin-like growth factor binding protein 4	Igfbp4	2.52
NM_007479	ADP-ribosylation factor 4	Arf4	2.51
NM_009708	Rho family GTPase 2	Rnd2	2.48
NM_008342	insulin-like growth factor binding protein 2	Igfbp2	2.48
NM_022657	fibroblast growth factor 23	Fgf23	2.46
NM_028804	coiled-coil domain containing 3	Ccdc3	2.44
NM_026814	protein phosphatase 1, regulatory subunit 27	Ppp1r27	2.43
NM_198249	Rho guanine nucleotide exchange factor (GEF) 40 , transcript variant 1	Arhgef40	2.43
NM_008356	interleukin 13 receptor, alpha 2	Il13ra2	2.41
NM_011823	G protein-coupled receptor 34	Gpr34	2.41
NM_010572	insulin receptor substrate 4	Irs4	2.38
NM_145431	notchless homolog 1	Nle1	2.38
NM_145373	secreted and transmembrane 1A	Sectm1a	2.37
NM_027280	naked cuticle 1 homolog, transcript variant 1	Nkd1	2.37
NM_026840	platelet-derived growth factor receptor-like	Pdgfrl	2.34
NM_007955	protein tyrosine phosphatase, receptor type, V	Ptprv	2.31
NM_009750	nerve growth factor receptor (TNFRSF16) associated protein 1, transcript variant 1	Ngfrap1	2.26
NM_145379	MAS-related GPR, member F	Mrgprf	2.26
NM_016719	growth factor receptor bound protein 14	Grb14	2.25
NM_016802	ras homolog gene family, member A	Rhoa	2.25
NM_001033484	IQ motif containing GTPase activating protein 3	Iqgap3	2.25
NM_009109	ryanodine receptor 1, skeletal muscle	Ryr1	2.22
NM_008865	prolactin family 3, subfamily b, member 1	Prl3b1	2.22
NM_146216	Vac14 homolog	Vac14	2.22
NM_009314	tachykinin receptor 2	Tacr2	2.21
NM_016891	protein phosphatase 2 (formerly 2A), regulatory subunit A (PR 65), alpha isoform	Ppp2r1a	2.21
NM_016971	interleukin 22	Il22	2.2
NM_007486	Rho, GDP dissociation inhibitor (GDI) beta (Arhgdib)	Arhgdib	2.19
NM_021476	cysteinyl leukotriene receptor 1	Cysltr1	2.18
NM_011915	Wnt inhibitory factor 1	Wif1	2.18
NM_009216	somatostatin receptor 1	Sstr1	2.18
NM_001011850	olfactory receptor 1505	Olfr1505	2.17
NM_147030	olfactory receptor 1134	Olfr1134	2.14
NM_009028	RAS-like, family 2, locus 9	Rasl2-9	2.13
NM_026446	regulator of G-protein signaling 19	Rgs19	2.13
NM_010273	guanosine diphosphate (GDP) dissociation inhibitor 1	Gdi1	2.11
NM_146356	olfactory receptor 521	Olfr521	2.11
NM_020257	C-type lectin domain family 2, member i	Clec2i	2.1
NM_138748	protein phosphatase 2A, regulatory subunit B (PR 53)	Ppp2r4	2.09
NM_206975	interferon, alpha 14	Ifna14	2.08

NM_023209	PDZ binding kinase	Pbk	2.06
NM_008728	natriuretic peptide receptor 3	Npr3	2.04
NM_007865	delta-like 1	Dll1	2.04
NM_017472	sorting nexin 3	Snx3	2.03
NM_001198766	periostin, osteoblast specific factor, transcript variant 3	Postn	2.02
NM_031875	otoferlin, transcript variant 2	Otof	2.02
NM_175168	PTK7 protein tyrosine kinase 7	Ptk7	2.02
NM_028416	kringle containing transmembrane protein 2	Kremen2	2.02
NM_020259	Hedgehog-interacting protein	Hhip	2.01
NM_008113	Rho GDP dissociation inhibitor (GDI) gamma	Arhgdig	2.01
NM_001033851	copine VIII, transcript variant 2	Cpne8	2
NM_001038018	G protein-coupled receptor kinase 6, transcript variant 1	Grk6	2
NM_029646	interleukin 34, transcript variant 2	Il34	2
NM_001164724	interleukin 33, transcript variant 1	Il33	2
NM_001110320	CD72 antigen, transcript variant 1	Cd72	1.99
NM_027571	purinergic receptor P2Y, G-protein coupled 12	P2ry12	1.99
NM_001165902	beta-catenin*	Ctnnb1	1.4
Transcription			
NM_172495	nuclear receptor coactivator 7, transcript variant 1	Ncoa7	11.61
NM_027395	brain abundant, membrane attached signal protein 1	Basp1	4.75
NM_011640	transformation related protein 53, transcript variant 1	Trp53	3.77
NM_008709	v-myc myelocytomatosis viral related oncogene, neuroblastoma derived	Mycn	3.65
NM_008688	nuclear factor I/C, transcript variant 1	Nfic	3.56
NM_009236	SRY-box containing gene 18	Sox18	3.55
NM_181319	T-box 22, transcript variant 2	Tbx22	3.54
NM_016662	Max dimerization protein 3	Mxd3	3.37
NM_010055	distal-less homeobox 3	Dlx3	3.30
NM_025788	nucleus accumbens associated 1, BEN and BTB (POZ) domain containing	Nacc1	3.02
NM_028016	Nanog homeobox	Nanog	2.94
NM_010466	homeobox C8	Hoxc8	2.87
NM_009089	polymerase (RNA) II (DNA directed) polypeptide A	Polr2a	2.81
NM_009331	transcription factor 7, T cell specific	Tcf7	2.76
NM_170759	zinc finger protein 628 (Zfp628)	Zfp628	2.73
NM_178757	interferon regulatory factor 2 binding protein 1	Irf2bp1	2.68
NM_026776	vacuolar protein sorting 25	Vps25	2.65
NM_026532	nuclear transport factor 2	Nutf2	2.64
NM_009235	SRY-box containing gene 15	Sox15	2.62
NM_146040	cell division cycle associated 7 like	Cdca7l	2.62
NM_008505	LIM domain only 2, transcript variant 1	Lmo2	2.58
NM_001037914	multiciliate cell differentiation	Mcin	2.50
NM_026192	calcium binding and coiled coil domain 1	Calcoco1	2.49
NM_011642	transformation related protein 73, transcript variant 1	Trp73	2.46
NM_001001980	LIM and calponin homology domains 1, transcript variant 1	Limch1	2.39
NM_010919	NK2 transcription factor related, locus 2, transcript variant 1	Nkx2-2	2.37
NM_178609	E2F transcription factor 7	E2f7	2.37
NM_027946	DDB1 and CUL4 associated factor 7	Dcaf7	2.36

NM_001033813	zinc finger protein 872	Zfp872	2.35
NM_011139	POU domain, class 2, transcription factor 3	Pou2f3	2.34
NM_011869	mediator complex subunit 24	Med24	2.33
NM_010835	homeobox, msh-like 1	Msx1	2.32
NM_008269	homeobox B6	Hoxb6	2.24
NM_026937	activating signal cointegrator 1 complex subunit 1 , transcript variant 2	Ascc1	2.23
NM_019574	POZ (BTB) and AT hook containing zinc finger 1, transcript variant 1	Patz1	2.22
NM_001109743	SKI family transcriptional corepressor 2	Skor2	2.22
NM_021501	protein inhibitor of activated STAT 4	Pias4	2.22
NM_001163763	transcription factor 19, transcript variant 1	Tcf19	2.21
NM_027658	hexamethylene bis-acetamide inducible 2 , transcript variant 1	Hexim2	2.17
NM_001034900	zinc finger protein 345	Zfp345	2.15
NM_019776	staphylococcal nuclease and tudor domain containing 1	Snd1	2.12
NM_029281	zinc finger protein 820	Zfp820	2.11
NM_008627	Meis homeobox 3	Meis3	2.09
NM_001168502	zinc finger protein 57, transcript variant 3	Zfp57	2.08
NM_194350	v-maf musculoaponeurotic fibrosarcoma oncogene family, protein A	Mafa	2.06
NM_145836	interferon regulatory factor 2 binding protein-like	Irf2bpl	2.06
NM_011249	retinoblastoma-like 1 (p107), transcript variant 1	Rbl1	2.06
NM_011377	single-minded homolog 2	Sim2	2.04
NM_025945	polymerase (RNA) III (DNA directed) polypeptide D, transcript variant 1	Polr3d	2.04
NM_027434	regulation of nuclear pre-mRNA domain containing 1B	Rprd1b	2.04
NM_008321	inhibitor of DNA binding 3	Id3	2.02
NM_010464	homeobox C13	Hoxc13	2.02
NM_009056	regulatory factor X, 2 (influences HLA class II expression), transcript variant 2	Rfx2	2.01
NM_001013368	E2F transcription factor 8	E2f8	2.01
NM_144799	LIM and cysteine-rich domains 1	Lmcd1	2.00
NM_022435	trans-acting transcription factor 5	Sp5	2.00
NM_008500	LIM homeobox protein 6, transcript variant 1	Lhx6	1.99
NM_007531	prohibitin 2	Phb2	1.99
	Transport		
NM_012037	vesicle amine transport protein 1 homolog	Vat1	2.04
NM_001164679	anoctamin 8	Ano8	2.23
NM_008226	hyperpolarization-activated, cyclic nucleotide-gated K+ 2	Hcn2	3.05

Genes that show 2-fold up-regulation in the epithelium of K14rtTA/TRE-miR-214 mice versus WT mice

Accession Number	Gene Name	Symbol	Fold Change

Adhesion/Extracellular matrix			
NM_018857	mesothelin	Msln	43.81
NM_009856	CD83 antigen	Cd83	3.46
NM_139200	cytohesin 1 interacting protein	Cytip	3.39
NM_027852	retinoic acid receptor responder (tazarotene induced) 2	Rarres2	3.08
NM_001243008	collagen, type VI, alpha 3, transcript variant 1	Col6a3	2.98
NM_009903	claudin 4	Cldn4	2.96
NM_022032	PERP, TP53 apoptosis effector	Perp	2.76
NM_001008424	corneodesmosin	Cdsn	2.67
NM_010516	cysteine rich protein 61	Cyr61	2.56
NM_008013	fibrinogen-like protein 2	Fgl2	2.5
NM_053146	protocadherin beta 21	Pcdhb21	2.37
NM_021893	CD274 antigen	Cd274	2.31
NM_138672	stabilin 1	Stab1	2.3
NM_145158	elastin microfibril interfacer 2	Emilin2	2.25
NM_001093749	myelin protein zero-like 3, transcript variant 2	Mpzl3	2.19
NM_027893	poliovirus receptor-related 4 , transcript variant 1	Pvrl4	2.19
NM_033620	par-3 (partitioning defective 3) homolog, transcript variant 3	Pard3	2.18
NM_016919	collagen, type V, alpha 3	Col5a3	2.17
NM_010814	myelin oligodendrocyte glycoprotein	Mog	2.17
NM_008127	gap junction protein, beta 4	Gjb4	2.16
NM_010291	gap junction protein, beta 5	Gjb5	2.16
NM_011016	orosomucoid 2	Orm2	2.16
NM_001111058	CD33 antigen, transcript variant 1	Cd33	2.15
NM_080437	cadherin, EGF LAG seven-pass G-type receptor 3 (flamingo homolog, Drosophila)	Celsr3	2.13
NM_133743	Ly6/Plaur domain containing 3	Lypd3	2.13
NM_001113368	carcinoembryonic antigen-related cell adhesion molecule 2, transcript variant 1	Ceacam2	2.1
NM_008768	orosomucoid 1	Orm1	2.09
NM_028523	discoidin, CUB and LCCL domain containing 2	Dcbld2	2.08
NM_007993	fibrillin 1	Fbn1	2.08
NM_023420	collagen, type IV, alpha 3 binding protein, transcript variant 1	Col4a3bp	2.05
NM_001081053	integrin, alpha 10	Itga10	2
Cell Cycle/Apoptosis			
NM_009397	tumor necrosis factor, alpha-induced protein 3, transcript variant 1	Tnfaip3	5.11
NM_007570	B cell translocation gene 2, anti-proliferative	Btg2	4.69
NM_011540	titin-cap	Tcap	4.31
NM_013642	dual specificity phosphatase 1	Dusp1	3.28
NM_207677	death effector domain-containing DNA binding protein 2	Dedd2	2.96
NM_009871	cyclin-dependent kinase 5, regulatory subunit 1 (p35)	Cdk5r1	2.63
NM_001162908	sestrin 1, transcript variant 1	Sesn1	2.61
NM_001081156	TMF1-regulated nuclear protein 1	Trnp1	2.61
NM_130886	caspase recruitment domain family, member 14	Card14	2.59
NM_009760	BCL2/adenovirus E1B interacting protein 3	Bnip3	2.46
NM_007609	caspase 4, apoptosis-related cysteine peptidase	Casp4	2.42

NM_008681	N-myc downstream regulated gene 1	Ndrg1	2.32
NM_013469	annexin A11	Anxa11	2.25
NM_025427	regulator of cell cycle	Rgcc	2.17
NM_001103182	lin-9 homolog, transcript variant 1	Lin9	2.14
NM_144899	ADAMTS-like 4	Adamtsl4	2.13
NM_001003920	BR serine/threonine kinase 1, transcript variant 1	Brsk1	2
NM_008795	cyclin-dependent kinase 18	Cdk18	2
	Chromatin remodeling		
NM_001097979	histone cluster 1, H2bq	Hist1h2bq	59.61
NM_178909	WD repeat domain 92	Wdr92	9.88
NM_178196	histone cluster 1, H2bg	Hist1h2bg	5.99
NM_015786	histone cluster 1, H1c	Hist1h1c	4.74
NM_023422	histone cluster 1, H2bc	Hist1h2bc	4.26
BC015270	histone cluster 2, H3c2	Hist2h3c2	3.7
BC059807	chromodomain helicase DNA binding protein 6	Chd6	3.64
NM_199299	PHD finger protein 15	Phf15	3.61
NM_013807	polo-like kinase 3	Plk3	3.51
NM_025519	charged multivesicular body protein 4C	Chmp4c	3.27
NM_001167884	suppressor of variegation 4-20 homolog 1 (Drosophila) , transcript variant 7	Suv420h1	2.69
NM_030082	histone cluster 3, H2ba	Hist3h2ba	2.58
NM_001081315	bromodomain and PHD finger containing, 3	Brpf3	2.49
NM_178218	histone cluster 3, H2a	Hist3h2a	2.4
NM_001109691	PHD finger protein 21A, transcript variant 3	Phf21a	2.34
NM_001128151	cat eye syndrome chromosome region, candidate 2	Cecr2	2.33
NM_001081269	Wolf-Hirschhorn syndrome candidate 1-like 1, transcript variant 2	Whsc1l1	2.24
NM_153421	polyhomeotic-like 3 (Drosophila) , transcript variant 2	Phc3	2.22
NM_010434	homeodomain interacting protein kinase 3, transcript variant 1	Hipk3	2.19
NM_027892	protein phosphatase 1, regulatory (inhibitor) subunit 12A	Ppp1r12a	2.16
NM_026110	PAX3 and PAX7 binding protein 1	Paxbp1	2.14
NM_001017426	KDM1 lysine (K)-specific demethylase 6B	Kdm6b	2.04
NM_001177374	ubiquitin protein ligase E3 component n-recognin 2, transcript variant 2	Ubr2	2.03
NM_011235	RAD51 homolog D	Rad51d	2.02
	Cytoskeleton		
NM_008508	loricrin	Lor	8.18
NM_025420	late cornified envelope 1M	Lce1m	5.51
NM_027762	trichohyalin-like 1	Tchhl1	4.5
NM_001099774	keratin associated protein 17-1	Krtap17-1	3.85
NM_029667	late cornified envelope 1I	Lce1i	3.83
NM_212487	keratin 78	Krt78	3.81
NM_027137	late cornified envelope 1D	Lce1d	3.62
NM_011472	small proline-rich protein 2F	Sprr2f	3.61
NM_001005510	spectrin repeat containing, nuclear envelope 2	Syne2	3.5
NM_013560	heat shock protein 1	Hspb1	3.49
NM_026394	late cornified envelope 1F	Lce1f	3.49
NM_011470	small proline-rich protein 2D	Sprr2d	3.49
NM_033373	keratin 23	Krt23	3.38

NM_011471	small proline-rich protein 2E	Sprr2e	3.23
NM_011619	troponin T2, cardiac, transcript variant 9	Tnnt2	3.19
NM_010664	keratin 18	Krt18	3.14
NM_001252372	myosin binding protein C, slow-type , transcript variant 1	Mybpc1	3.14
NM_008473	keratin 1	Krt1	3.06
NM_028622	late cornified envelope 1C (Lce1c)	Lce1c	2.97
NM_001039376	phosphodiesterase 4D interacting protein (myomegalin), transcript variant 1	Pde4dip	2.88
NM_026822	late cornified envelope 1B	Lce1b	2.84
NM_001271484	CAP-GLY domain containing linker protein family, member 4, transcript variant 4	Clip4	2.79
NM_028044	calponin 3, acidic	Cnn3	2.75
NM_007585	annexin A2	Anxa2	2.74
NM_033175	late cornified envelope 3C	Lce3c	2.72
NM_025501	late cornified envelope 3B	Lce3b	2.64
NM_001018079	late cornified envelope 3F	Lce3f	2.59
NM_026811	late cornified envelope 1E	Lce1e	2.57
NM_001270426	late cornified envelope 3D	Lce3d	2.55
NM_001039472	kinesin family member 21B	Kif21b	2.4
NM_018790	activity regulated cytoskeletal-associated protein	Arc	2.38
NM_028721	nephronophthisis 3 (adolescent), transcript variant 1	Nphp3	2.38
NM_025413	late cornified envelope 1G	Lce1g	2.33
NM_030203	TSPY-like 4	Tspyl4	2.33
NM_145070	huntingtin interacting protein 1 related	Hip1r	2.26
NM_010630	kinesin family member C2	Kifc2	2.24
NM_025984	late cornified envelope 1A1	Lce1a1	2.24
NM_019765	CAP-GLY domain containing linker protein 1	Clip1	2.19
NM_001039594	late cornified envelope 3A	Lce3a	2.18
NM_146120	gelsolin, transcript variant 1	Gsn	2.17
NM_001109657	growth arrest specific 7, transcript variant 2	Gas7	2.14
NM_133357	keratin 75	Krt75	2.11
NM_001254760	late cornified envelope 1K	Lce1k	2.11
NM_019809	PDZ and LIM domain 5, transcript variant 2	Pdlim5	2.08
NM_009450	tubulin, beta 2A class IIA	Tubb2a	2.07
NM_010660	keratin 10	Krt10	2.06
NM_175180	WD repeat domain 44	Wdr44	2.06
NM_178593	RCSD domain containing 1, transcript variant 1	Rcsd1	2.04
NM_198113	slingshot homolog 3	Ssh3	2.03
NM_001163664	troponin T3, skeletal, fast , transcript variant 1	Tnnt3	2.01
	Metabolism		
NM_013743	pyruvate dehydrogenase kinase, isoenzyme 4, nuclear gene encoding mitochondrial protein	Pdk4	5.79
NM_175650	ATPase type 13A5	Atp13a5	5.26
NM_027299	degenerative spermatocyte homolog 2 (Drosophila), lipid desaturase, transcript variant 1	Degs2	5.02
NM_011435	superoxide dismutase 3, extracellular	Sod3	4.95
NM_146118	solute carrier family 25 (mitochondrial carrier, phosphate carrier), member 25, transcript variant 1	Slc25a25	4.52
NM_001111331	Kv channel interacting protein 3, calsenilin , transcript variant 2	Kcnip3	4.38

NM_001199283	solute carrier family 43, member 2, transcript variant 1	Slc43a2	4.33
NM_007409	alcohol dehydrogenase 1 (class I)	Adh1	4.23
NM_001164613	ATPase type 13A4, transcript variant 3	Atp13a4	4.18
NM_001130194	bestrophin 2, transcript variant 1	Best2	4.18
NM_009593	ATP-binding cassette, sub-family G (WHITE), member 1	Abcg1	3.91
NM_026945	alcohol dehydrogenase 6A (class V)	Adh6a	3.68
NM_001177753	6-phosphofructo-2-kinase/fructose-2,6-biphosphatase 3, transcript variant 2	Pfkfb3	3.61
NM_194333	solute carrier family 23 (nucleobase transporters), member 3	Slc23a3	3.52
NM_001098789	NADH dehydrogenase (ubiquinone) 1 alpha subcomplex, 4-like 2	Ndufa4l2	3.45
NM_011031	procollagen-proline, 2-oxoglutarate 4-dioxygenase, alpha II polypeptide , transcript variant 2	P4ha2	3.45
NM_030696	solute carrier family 16 (monocarboxylic acid transporters), member 3	Slc16a3	3.28
NM_001042591	arrestin domain containing 3	Arrdc3	3.27
NM_028784	coagulation factor XIII, A1 subunit, transcript variant 1	F13a1	3.24
NM_028133	EGL nine homolog 3 (C. elegans)	Egln3	3.13
NM_183161	solute carrier family 17, member 9	Slc17a9	3.01
NM_033648	FXYD domain-containing ion transport regulator 4, transcript variant 1	Fxyd4	2.99
NM_001111111	autophagy related 16-like 2	Atg16l2	2.92
NM_001114084	diacylglycerol O-acyltransferase 2-like 6	Dgat2l6	2.88
NM_029415	solute carrier family 10 (sodium/bile acid cotransporter family), member 6	Slc10a6	2.84
NM_007421	adenylosuccinate synthetase like 1	Adssl1	2.74
NM_172883	major facilitator superfamily domain containing 7A	Mfsd7a	2.74
NM_013455	acrosin prepropeptide, transcript variant 1	Acr	2.71
NM_172837	lipase, family member K, transcript variant 2	Lipk	2.7
NM_030558	carbonic anhydrase 15	Car15	2.68
NM_153143	potassium channel tetramerisation domain containing 11	Kctd11	2.67
NM_001267707	solute carrier organic anion transporter family, member 1a5, transcript variant 1	Slco1a5	2.67
NM_007470	apolipoprotein D	Apod	2.66
NM_001195033	abhydrolase domain containing 12B	Abhd12b	2.65
NM_001079865	carboxylesterase 2F	Ces2f	2.65
NM_011198	prostaglandin-endoperoxide synthase 2	Ptgs2	2.65
NM_172524	NIPA-like domain containing 4	Nipal4	2.63
NM_177243	solute carrier family 26, member 9	Slc26a9	2.62
NM_153404	lipase, member H, transcript variant 2	Liph	2.58
NM_019664	potassium inwardly-rectifying channel, subfamily J, member 15 , transcript variant 2	Kcnj15	2.57
NM_001160165	neuraminidase 2, transcript variant 3	Neu2	2.56
NM_009695	apolipoprotein C-II	Apoc2	2.55
NM_011786	arachidonate lipoxygenase 3	Aloxe3	2.53
NM_001039176	elongation of very long chain fatty acids (FEN1/Elo2, SUR4/Elo3, yeast)-like 1, transcript variant 1	Elovl1	2.49
NM_175475	cytochrome P450, family 26, subfamily b, polypeptide 1, transcript variant 1	Cyp26b1	2.46
NM_001081349	solute carrier family 43, member 1, transcript	Slc43a1	2.41

	variant 1		
NM_134006	retinol dehydrogenase 5	Rdh5	2.4
NM_001012434	potassium channel tetramerisation domain containing 14, transcript variant 2	Kctd14	2.39
NM_029688	sulfiredoxin 1 homolog	Srxn1	2.39
NM_001042719	DDHD domain containing 1, transcript variant 3	Ddhd1	2.36
NM_001081421	UDP-N-acetyl-alpha-D-galactosamine:polypeptide N-acetylgalactosaminyltransferase-like 1	Galntl1	2.36
NM_173785	IBA57, iron-sulfur cluster assembly homolog, transcript variant 1	Iba57	2.35
NM_027172	solute carrier protein family 52, member 3 , transcript variant 1	Slc52a3	2.35
NM_009022	aldehyde dehydrogenase family 1, subfamily A2	Aldh1a2	2.32
NM_027868	solute carrier family 41, member 3, transcript variant 1	Slc41a3	2.32
NM_145828	xylosyltransferase II	Xylt2	2.32
NM_021301	solute carrier family 15 (H+/peptide transporter), member 2, transcript variant 1	Slc15a2	2.28
BC047268	phospholipase D2	Pld2	2.27
NM_183220	1-aminocyclopropane-1-carboxylate synthase (non-functional)	Accs	2.24
NM_172692	glucosidase beta 2	Gba2	2.23
NM_053079	solute carrier family 15 (oligopeptide transporter), member 1	Slc15a1	2.23
NM_018830	N-acylsphingosine amidohydrolase 2	Asah2	2.22
NM_018881	flavin containing monooxygenase 2	Fmo2	2.22
NM_013509	enolase 2, gamma neuronal	Eno2	2.21
NM_001163689	patatin-like phospholipase domain containing 2, transcript variant 1	Pnpla2	2.21
NM_026784	phosphomevalonate kinase, transcript variant 1	Pmvk	2.18
NM_026644	1-acylglycerol-3-phosphate O-acyltransferase 4 (lysophosphatidic acid acyltransferase, delta)	Agpat4	2.17
NM_010239	ferritin heavy chain 1, transcript variant 1	Fth1	2.17
NM_008504	granzyme M (lymphocyte met-ase 1)	Gzmm	2.17
NM_145423	solute carrier family 5 (iodide transporter), member 8	Slc5a8	2.17
NM_052993	core 1 synthase, glycoprotein-N-acetylgalactosamine 3-beta-galactosyltransferase, 1	C1galt1	2.16
NM_019779	cytochrome P450, family 11, subfamily a, polypeptide 1	Cyp11a1	2.16
NM_175331	5'-nucleotidase domain containing 3	Nt5dc3	2.16
NM_008131	glutamate-ammonia ligase (glutamine synthetase)	Glul	2.15
NM_009177	ST3 beta-galactoside alpha-2,3-sialyltransferase 1	St3gal1	2.15
NM_001039710	coenzyme Q10 homolog B, transcript variant 1	Coq10b	2.14
NM_027340	lipase, family member N	Lipn	2.13
NM_147219	ATP-binding cassette, sub-family A , member 5	Abca5	2.09
NM_019807	acid phosphatase, prostate , transcript variant 2	Acpp	2.07
NM_172607	nicotinate phosphoribosyltransferase domain containing 1	Naprt1	2.07

NM_029810	5'-nucleotidase, cytosolic II , transcript variant 3	Nt5c2	2.07
NM_027406	aldehyde dehydrogenase 1 family, member L1	Aldh1l1	2.06
NM_153803	galactosidase, beta 1-like 2	Glb1l2	2.06
NM_001159864	potassium channel tetramerisation domain containing 18, transcript variant 1	Kctd18	2.05
NM_001161767	UDP-N-acetyl-alpha-D-galactosamine:polypeptide N-acetylgalactosaminyltransferase 6, transcript variant 1	Galnt6	2.04
NM_145447	major facilitator superfamily domain containing 7C	Mfsd7c	2.04
NM_013820	hexokinase 2	Hk2	2.03
NM_001161765	flavin containing monooxygenase 5, transcript variant 1	Fmo5	2.02
NM_025718	deoxyribonuclease 1-like 2	Dnase1l2	2.02
NM_013850	ATP-binding cassette, sub-family A, member 7	Abca7	2.01
NM_009721	ATPase, Na+/K+ transporting, beta 1 polypeptide	Atp1b1	2.01
	Others		
NM_172051	transmembrane and coiled coil domains 3, transcript variant 1	Tmcc3	7.29
NM_001163502	ELM2 and Myb/SANT-like domain containing 1, transcript variant 1	Elmsan1	6.84
NM_001166173	dermokine, transcript variant 3	Dmkn	5.26
NM_001204959	resistin , transcript variant 2	Retn	5.11
NM_175307	family with sequence similarity 46, member B	Fam46b	4.69
NM_001199210	eva-1 homolog C (C. elegans) , transcript variant 1	Eva1c	4.66
NM_197986	transmembrane protein 140	Tmem140	4
NM_172205	suprabasin, transcript variant 1	Sbsn	3.93
NM_001190436	Finkel-Biskis-Reilly murine sarcoma virus (FBR-MuSV) ubiquitously expressed, transcript variant 3	Fau	3.74
NM_028798	cysteine-rich C-terminal 1	Crct1	3.73
NM_001033411	predicted gene 826	Gm826	3.55
BC090258	interferon induced transmembrane protein 1	Ifitm1	3.24
NM_027511	histidine rich carboxyl terminus 1	Hrct1	3.19
NM_013473	annexin A8	Anxa8	3.16
NM_009778	complement component 3	C3	3.16
NM_145535	syndecan binding protein (syntenin) 2	Sdcbp2	2.91
NM_027585	cyclic nucleotide binding domain containing 2	Cnbd2	2.88
NM_001013749	transmembrane protein 151B	Tmem151b	2.87
NM_172801	otopetrin 2	Otop2	2.85
NM_001033410	predicted gene 757	Gm757	2.79
NM_181397	raftlin lipid raft linker 1	Rftn1	2.78
NM_001163572	transmembrane protein 170B	Tmem170b	2.73
NM_001025572	ankyrin repeat domain 12	Ankrd12	2.58
NM_010220	FK506 binding protein 5	Fkbp5	2.57
NM_173415	nyctalopin	Nyx	2.57
NM_175407	sine oculis-binding protein homolog (Drosophila)	Sobp	2.56
NM_176860	ubiquitin associated and SH3 domain containing, B	Ubash3b	2.56
NM_010732	leucine rich repeat protein 2, neuronal	Lrrn2	2.52
NM_031195	macrophage scavenger receptor 1, transcript	Msr1	2.52

	variant 1		
NM_020578	EH-domain containing 3	Ehd3	2.48
NM_011573	testis expressed gene 264, transcript variant 1	Tex264	2.48
NM_013562	interferon-related developmental regulator 1	Ifrd1	2.4
NM_019576	thrombospondin, type I, domain 1, transcript variant 1	Thsd1	2.39
NM_170684	copine VII	Cpne7	2.38
NM_029116	kelch repeat and BTB (POZ) domain containing 11	Kbtbd11	2.38
NM_010706	lectin, galactose binding, soluble 4	Lgals4	2.37
NM_176834	ring finger protein 208	Rnf208	2.37
NM_011029	ribosomal protein SA	Rpsa	2.36
NM_026146	EPS8-like 1	Eps8l1	2.34
NM_178884	obscurin-like 1	Obsl1	2.33
NM_146008	t-complex 11 (mouse) like 2	Tcp11l2	2.32
NM_026835	membrane-spanning 4-domains, subfamily A, member 6D	Ms4a6d	2.31
NM_001085507	zinc finger and BTB domain containing 34	Zbtb34	2.31
NM_133898	NEDD4 binding protein 2-like 1	N4bp2l1	2.3
NM_001081652	NAC alpha domain containing	Nacad	2.3
NM_001162974	leucine rich repeat containing 51, transcript variant 3	Lrrc51	2.29
NM_001038592	glutaredoxin 2 , transcript variant 1	Glrx2	2.28
NM_001205353	GRAM domain containing 4, transcript variant 2	Gramd4	2.28
NM_144797	meteorin, glial cell differentiation regulator-like	Metrnl	2.28
NM_001159577	ligand of numb-protein X 1, transcript variant 1	Lnx1	2.24
NM_027898	GRAM domain containing 1A	Gramd1a	2.23
NM_001136259	target of myb1 homolog, transcript variant 2	Tom1	2.22
NM_009150	selenium binding protein 1	Selenbp1	2.2
NM_001164557	PDZK1 interacting protein 1 , transcript variant 1	Pdzk1ip1	2.18
NM_145853	two pore channel 1	Tpcn1	2.17
NM_053167	tripartite motif-containing 9 , transcript variant 1	Trim9	2.17
NM_027166	yippee-like 5	Ypel5	2.17
NM_011157	serglycin	Srgn	2.16
NM_026588	syntaxin 19	Stx19	2.16
NM_001168514	mitogen-activated protein kinase 14, transcript variant 4	Mapk14	2.15
NM_178242	trinucleotide repeat containing 18, transcript variant B	Tnrc18	2.14
NM_009441	tetratricopeptide repeat domain 3	Ttc3	2.14
NM_153507	copine II	Cpne2	2.13
NM_013532	leukocyte immunoglobulin-like receptor, subfamily B, member 4	Lilrb4	2.13
NM_001081235	meningioma 1	Mn1	2.13
NM_001024134	tripartite motif-containing 15, transcript variant 2	Trim15	2.13
NM_011123	proteolipid protein (myelin) 1	Plp1	2.12
NM_053166	tripartite motif-containing 7	Trim7	2.12
NM_181073	pleckstrin homology domain containing, family H (with MyTH4 domain) member 1	Plekhh1	2.11
NM_133774	StAR-related lipid transfer (START) domain containing 4	Stard4	2.11
NM_001146022	WD repeat and FYVE domain containing 4	Wdfy4	2.11
NM_001008233	pleckstrin homology domain containing, family	Plekhn1	2.1

	N member 1		
NM_177775	extended synaptotagmin-like protein 3	Esyt3	2.07
NM_026235	La ribonucleoprotein domain family, member 6	Larp6	2.07
NM_019814	HIG1 domain family, member 1A	Higd1a	2.06
NM_177185	ubinuclein 2	Ubn2	2.06
NM_001256057	predicted gene 11570	Gm11570	2.05
NM_172694	multiple EGF-like-domains 9	Megf9	2.05
NM_177632	family with sequence similarity 43, member A	Fam43a	2.04
NM_001146043	G elongation factor, mitochondrial 2, transcript variant 2	Gfm2	2.04
NM_027116	NTPase, KAP family P-loop domain containing 1	Nkpd1	2.04
NM_028950	NOL1/NOP2/Sun domain family member 6, transcript variant 2	Nsun6	2.04
NM_001271727	tripartite motif-containing 2, transcript variant 3	Trim2	2.02
NM_016714	nucleoporin 50	Nup50	2.01
NM_001045483	mitogen-activated protein kinase 1 interacting protein 1, transcript variant 1	Mapk1ip1	2
	Protein folding		
NM_028430	peptidylprolyl isomerase (cyclophilin)-like 6	Ppil6	2.25
NM_018808	DnaJ (Hsp40) homolog, subfamily B, member 1	Dnajb1	2.23
	Proteolysis		
NM_013459	complement factor D (adipsin)	Cfd	11.31
NM_177322	angiotensin II receptor, type 1a	Agtr1a	8.65
NM_011414	secretory leukocyte peptidase inhibitor	Slpi	7.4
NM_008871	serine (or cysteine) peptidase inhibitor, clade E, member 1	Serpine1	6.57
NM_001252569	serine (or cysteine) peptidase inhibitor, clade A, member 1A, transcript variant 2	Serpina1a	3.91
NM_133753	ERBB receptor feedback inhibitor 1	Errfi1	3.83
NM_001199940	serine (or cysteine) peptidase inhibitor, clade A, member 3I	Serpina3i	3.72
NM_015790	icos ligand	Icosl	3.69
NM_010511	interferon gamma receptor 1	Ifngr1	3.56
NM_009247	serine (or cysteine) peptidase inhibitor, clade A, member 1E	Serpina1e	3.47
NM_028660	kallikrein related-peptidase 9	Klk9	3.39
NM_009245	serine (or cysteine) peptidase inhibitor, clade A, member 1C	Serpina1c	3.31
NM_024406	fatty acid binding protein 4, adipocyte	Fabp4	3.12
NM_009776	serine (or cysteine) peptidase inhibitor, clade G, member 1	Serping1	3.09
NM_011113	plasminogen activator, urokinase receptor	Plaur	2.99
NM_009543	ring finger protein 103	Rnf103	2.98
NM_007796	cytotoxic T lymphocyte-associated protein 2 alpha, transcript variant 1	Ctla2a	2.87
NM_009246	serine (or cysteine) peptidase inhibitor, clade A, member 1D	Serpina1d	2.87
NM_027997	serine (or cysteine) peptidase inhibitor, clade A, member 9	Serpina9	2.83
NM_007781	colony stimulating factor 2 receptor, beta 2, low-affinity	Csf2rb2	2.79
NM_178691	YOD1 OTU deubiquitinating enzyme 1 homologue	Yod1	2.71
NM_001025439	calcium/calmodulin-dependent protein kinase	Camk2d	2.62

	II, delta, transcript variant 1		
NM_016845	proacrosin binding protein, transcript variant 1	Acrbp	2.61
NM_026414	aspartic peptidase, retroviral-like 1	Asprv1	2.61
NM_019932	platelet factor 4	Pf4	2.47
NM_001039042	kallikrein related-peptidase 13	Klk13	2.42
NM_007797	cytotoxic T lymphocyte-associated protein 2 beta, transcript variant 1	Ctla2b	2.41
NM_008906	cathepsin A , transcript variant 1	Ctsa	2.41
NM_173749	peptidase domain containing associated with muscle regeneration 1	Pamr1	2.4
NM_001040106	AP2 associated kinase 1, transcript variant 1	Aak1	2.26
NM_178730	transmembrane protease, serine 11f	Tmprss11f	2.23
NM_028894	LON peptidase N-terminal domain and ring finger 3	Lonrf3	2.21
NM_011177	kallikrein related-peptidase 6, transcript variant 1	Klk6	2.2
NM_183284	serine peptidase inhibitor, Kazal type 2	Spink2	2.17
NM_001081115	non-specific cytotoxic cell receptor protein 1 homolog (zebrafish)	Nccrp1	2.13
NM_052976	oligophrenin 1	Ophn1	2.12
NM_178694	zyg-11 related, cell cycle regulator	Zer1	2.11
NM_139147	Rab40b, member RAS oncogene family	Rab40b	2.06
NM_007899	extracellular matrix protein 1, transcript variant 1	Ecm1	2.05
NM_001001803	serine peptidase inhibitor, Kazal type 7 (putative)	Spink7	2.04
	RNA processing		
NM_011756	zinc finger protein 36	Zfp36	4.91
NM_007475	ribosomal protein, large, P0	Rplp0	2.95
BC096413	ribosomal protein L37a	Rpl37a	2.82
NM_001114079	poly(A) binding protein, cytoplasmic 1-like	Pabpc1l	2.8
NM_133819	protein phosphatase 1, regulatory (inhibitor) subunit 15b	Ppp1r15b	2.79
NM_009095	ribosomal protein S5	Rps5	2.62
NM_033541	2'-5' oligoadenylate synthetase 1C	Oas1c	2.43
NM_025963	ribosomal protein S10	Rps10	2.42
NM_026020	ribosomal protein, large P2	Rplp2	2.22
NM_016680	CLK4-associating serine/arginine rich protein, transcript variant L	Clasrp	2.14
NM_053255	elaC homolog 1	Elac1	2.1
NM_025919	ribosomal protein L11	Rpl11	2.1
NM_175937	cytoplasmic polyadenylation element binding protein 2 , transcript variant 1	Cpeb2	2.09
NM_175529	leukocyte receptor cluster (LRC) member 9	Leng9	2.07
NM_011287	ribosomal protein L10A	Rpl10a	2.03
NM_001024837	adenosine deaminase, RNA-specific, B1, transcript variant 2	Adarb1	2.02
	Signalling		
NM_011314	serum amyloid A 2	Saa2	40.51
NM_008176	chemokine (C-X-C motif) ligand 1	Cxcl1	23.24
NM_009117	serum amyloid A 1	Saa1	12.21
NM_011333	chemokine (C-C motif) ligand 2	Ccl2	9.04
NM_008361	interleukin 1 beta	Il1b	8.5
NM_009627	adrenomedullin	Adm	7.04
NM_007707	suppressor of cytokine signaling 3	Socs3	4.9

NM_007913	early growth response 1	Egr1	4.62
NM_015811	regulator of G-protein signaling 1	Rgs1	4.39
NM_011338	chemokine (C-C motif) ligand 9	Ccl9	4.29
NM_177868	forkhead-associated (FHA) phosphopeptide binding domain 1	Fhad1	3.93
NM_013652	chemokine (C-C motif) ligand 4	Ccl4	3.8
NM_015776	microfibrillar associated protein 5	Mfap5	3.58
NM_026577	ADP-ribosylation factor-like 13B	Arl13b	3.55
NM_029083	DNA-damage-inducible transcript 4	Ddit4	3.51
NM_008344	insulin-like growth factor binding protein 6	Igfbp6	3.38
NM_011817	growth arrest and DNA-damage-inducible 45 gamma	Gadd45g	3.37
NM_009615	a disintegrin and metallopeptidase domain 17	Adam17	3.33
NM_009061	regulator of G-protein signaling 2	Rgs2	3.28
NM_017466	chemokine (C-C motif) receptor-like 2	Ccrl2	3.27
NM_020622	family with sequence similarity 3, member B	Fam3b	3.19
NM_009841	CD14 antigen	Cd14	3.17
NM_146491	olfactory receptor 1410	Olfr1410	3.14
NM_011905	toll-like receptor 2	Tlr2	3.14
NM_177137	guanine nucleotide binding protein, alpha stimulating, olfactory type, transcript variant 2	Gnal	3.07
NM_145857	nucleotide-binding oligomerization domain containing 2	Nod2	2.99
NM_172718	small G protein signaling modulator 1, transcript variant 1	Sgsm1	2.99
NM_009017	retinoic acid early transcript beta	Raet1b	2.95
NM_023463	lymphocyte antigen 6 complex, locus G6C	Ly6g6c	2.84
NM_001163262	c-Maf inducing protein, transcript variant 1	Cmip	2.8
NM_027106	arginine vasopressin-induced 1	Avpi1	2.77
NM_010276	GTP binding protein	Gem	2.76
NM_008855	protein kinase C, beta	Prkcb	2.62
NM_021274	chemokine (C-X-C motif) ligand 10	Cxcl10	2.61
NM_001163634	wingless-related MMTV integration site 7B, transcript variant 2	Wnt7b	2.59
NM_178256	RALBP1 associated Eps domain containing protein 2	Reps2	2.58
NM_007706	suppressor of cytokine signaling 2, transcript variant 1	Socs2	2.57
NM_013693	tumor necrosis factor	Tnf	2.52
NM_025540	sarcolipin	Sln	2.46
NM_001081155	Rap1 GTPase-activating protein , transcript variant 1	Rap1gap	2.45
NM_009184	PTK6 protein tyrosine kinase 6	Ptk6	2.44
NM_010592	Jun proto-oncogene related gene d	Jund	2.43
NM_011058	platelet derived growth factor receptor, alpha polypeptide , transcript variant 1	Pdgfra	2.42
NM_010831	salt inducible kinase 1	Sik1	2.39
NM_008773	purinergic receptor P2Y, G-protein coupled 2	P2ry2	2.37
NM_025404	ADP-ribosylation factor-like 4D	Arl4d	2.36
NM_022019	dual specificity phosphatase 10	Dusp10	2.36
NM_008343	insulin-like growth factor binding protein 3	Igfbp3	2.33
NM_001130409	PTK2 protein tyrosine kinase 2, transcript variant 2	Ptk2	2.32
NM_001081212	insulin receptor substrate 2	Irs2	2.31
NM_178111	transformation related protein 53 inducible nuclear protein 2	Trp53inp2	2.3
NM_178258	interleukin 22 receptor, alpha 2	Il22ra2	2.28

NM_013584	leukemia inhibitory factor receptor, transcript variant 1	Lifr	2.28
NM_198703	WNK lysine deficient protein kinase 1, transcript variant 1	Wnk1	2.28
NM_001035533	A kinase (PRKA) anchor protein 2, transcript variant 1	Akap2	2.25
NM_018883	calcium/calmodulin-dependent protein kinase kinase 1, alpha	Camkk1	2.24
NM_021306	endothelin converting enzyme-like 1	Ecel1	2.24
NM_010559	interleukin 6 receptor, alpha	Il6ra	2.22
NM_175445	Ras association (RalGDS/AF-6) domain family member 2	Rassf2	2.22
NM_011530	transporter 2, ATP-binding cassette, sub-family B (MDR/TAP)	Tap2	2.16
NM_139307	vasorin	Vasn	2.16
NM_010950	numb-like	Numbl	2.15
NM_133924	sorting nexin family member 21	Snx21	2.12
NM_001025250	vascular endothelial growth factor A, transcript variant 1	Vegfa	2.1
NM_007557	bone morphogenetic protein 7	Bmp7	2.09
NM_001002842	PML-RAR alpha-regulated adaptor molecule 1 (Pram1), transcript variant 1	Pram1	2.09
BC122879	nebulette	Nebl	2.05
NM_080843	suppressor of cytokine signaling 4	Socs4	2.02
NM_146322	olfactory receptor 187	Olfr187	2.01
NM_178710	salt inducible kinase 2	Sik2	2.01
NM_001081412	breakpoint cluster region	Bcr	2
	Transcription		
NM_001077364	TSC22 domain family, member 3, transcript variant 1	Tsc22d3	13.68
NM_007498	activating transcription factor 3	Atf3	7.41
NM_008036	FBJ osteosarcoma oncogene B	Fosb	7.34
NM_010444	nuclear receptor subfamily 4, group A, member 1	Nr4a1	7.12
NM_010234	FBJ osteosarcoma oncogene	Fos	6.58
NM_010828	Cbp/p300-interacting transactivator, with Glu/Asp-rich carboxy-terminal domain, 2	Cited2	6.21
NM_007679	CCAAT/enhancer binding protein (C/EBP), delta	Cebpd	5.67
NM_153287	cysteine-serine-rich nuclear protein 1	Csrnp1	4.92
NM_001033324	zinc finger and BTB domain containing 16	Zbtb16	4.28
NM_010591	Jun oncogene	Jun	4.23
NM_016868	hypoxia inducible factor 3, alpha subunit , transcript variant 2	Hif3a	4.01
NM_007914	ets homologous factor	Ehf	3.86
NM_008390	interferon regulatory factor 1, transcript variant 1	Irf1	3.81
NM_001113333	cryptochrome 2 (photolyase-like) , transcript variant 2	Cry2	3.67
NM_010638	Kruppel-like factor 9	Klf9	3.46
NM_010907	nuclear factor of kappa light polypeptide gene enhancer in B cells inhibitor, alpha	Nfkbia	3.39
NM_021897	transformation related protein 53 inducible nuclear protein 1, transcript variant 1	Trp53inp1	3.39
NM_010755	v-maf musculoaponeurotic fibrosarcoma oncogene family, protein F	Maff	3.33
NM_008452	Kruppel-like factor 2	Klf2	3.14

NM_027477	zinc finger protein 398 , transcript variant 1	Zfp398	3.06
NM_013874	D4, zinc and double PHD fingers family 1	Dpf1	3
NM_010235	fos-like antigen 1	Fosl1	2.99
NM_009821	runt related transcription factor 1, transcript variant 4	Runx1	2.97
NM_017373	nuclear factor, interleukin 3, regulated	Nfil3	2.94
NM_030612	nuclear factor of kappa light polypeptide gene enhancer in B cells inhibitor, zeta , transcript variant 1	Nfkbiz	2.88
NM_010056	distal-less homeobox 5, transcript variant 1	Dlx5	2.79
NM_009565	zinc finger and BTB domain containing 7B	Zbtb7b	2.71
NM_011276	ring finger protein, LIM domain interacting	Rlim	2.7
NM_010499	immediate early response 2	Ier2	2.63
NM_023755	transcription factor CP2-like 1	Tfcp2l1	2.58
NM_027947	zinc finger and BTB domain containing 43, transcript variant 1	Zbtb43	2.57
NM_011498	basic helix-loop-helix family, member e40	Bhlhe40	2.48
NM_009637	AE binding protein 2, transcript variant 3	Aebp2	2.47
NM_153599	cyclin-dependent kinase 8	Cdk8	2.47
NM_020610	nuclear receptor interacting protein 3	Nrip3	2.46
NM_023184	Kruppel-like factor 15	Klf15	2.42
NM_183208	zinc finger, MIZ-type containing 1	Zmiz1	2.4
NM_013519	forkhead box C2	Foxc2	2.39
NM_001029929	zinc finger, MYND-type containing 15	Zmynd15	2.38
NM_010137	endothelial PAS domain protein 1	Epas1	2.37
NM_021397	zinc finger and BTB domain containing 32	Zbtb32	2.37
NM_027264	zinc finger protein 715	Zfp715	2.34
NM_011803	Kruppel-like factor 6	Klf6	2.3
NM_175606	HOP homeobox, transcript variant 1	Hopx	2.29
NM_011753	zinc finger protein 26	Zfp26	2.29
NM_177993	high mobility group box transcription factor 1, transcript variant 2	Hbp1	2.25
NM_011066	period circadian clock 2	Per2	2.22
NM_001100460	zinc finger and BTB domain containing 42	Zbtb42	2.22
NM_009744	B cell leukemia/lymphoma 6	Bcl6	2.19
NM_008554	achaete-scute complex homolog 2 (Drosophila)	Ascl2	2.15
NM_001025577	avian musculoaponeurotic fibrosarcoma (v-maf) AS42 oncogene homolog	Maf	2.15
NM_177660	zinc finger and BTB domain containing 10	Zbtb10	2.15
NM_009884	CCAAT/enhancer binding protein (C/EBP), gamma	Cebpg	2.06
NM_010658	v-maf musculoaponeurotic fibrosarcoma oncogene family, protein B	Mafb	2.04
NM_008270	homeobox B9	Hoxb9	2.03
NM_001009935	thioredoxin interacting protein, transcript variant 1	Txnip	2.03
NM_177790	zinc finger protein 385C	Zfp385c	2.01
NM_001029838	Pbx/knotted 1 homeobox 2 , transcript variant 2	Pknox2	2.01
NM_172643	zinc finger and BTB domain containing 41 homolog	Zbtb41	2.01
NM_031391	general transcription factor II A, 1, transcript variant 1	Gtf2a1	2
	Transport		
NM_008432	potassium channel, subfamily U, member 1	Kcnu1	2.48

NM_020506	exportin 4	Xpo4	2.09
NM_029491	trafficking protein particle complex 8, transcript variant 2	Trappc8	2.04
NM_011324	sodium channel, nonvoltage-gated 1 alpha	Scnn1a	2.03
NM_172476	transmembrane channel-like gene family 7	Tmc7	2.01

*genes validated by qPCR